USGS
science for a changing world

In cooperation with the U.S. Bureau of Reclamation

Documentation of a Groundwater Flow Model (SJRRPGW) for the San Joaquin River Restoration Program Study Area, California

Scientific Investigations Report 2014–5148

U.S. Department of the Interior
U.S. Geological Survey

Cover photo: Picture taken of San Joaquin River Reach 2A (river mile 219) looking downstream in July 2009. Photo taken by Doug Deflitch, U.S. Bureau of Reclamation.

Documentation of a Groundwater Flow Model (SJRRPGW) for the San Joaquin River Restoration Program Study Area, California

By Jonathan A. Traum, Steven P. Phillips, George L. Bennett, Celia Zamora, and Loren F. Metzger

In cooperation with the U.S. Bureau of Reclamation

Scientific Investigations Report 2014–5148

U.S. Department of the Interior
U.S. Geological Survey

U.S. Department of the Interior
SALLY JEWELL, Secretary

U.S. Geological Survey
Suzette M. Kimball, Acting Director

U.S. Geological Survey, Reston, Virginia: 2014

For more information on the USGS—the Federal source for science about the Earth, its natural and living resources, natural hazards, and the environment, visit http://www.usgs.gov or call 1–888–ASK–USGS.

For an overview of USGS information products, including maps, imagery, and publications, visit http://www.usgs.gov/pubprod

To order this and other USGS information products, visit http://store.usgs.gov

Any use of trade, firm, or product names is for descriptive purposes only and does not imply endorsement by the U.S. Government.

Although this information product, for the most part, is in the public domain, it also may contain copyrighted materials as noted in the text. Permission to reproduce copyrighted items must be secured from the copyright owner.

Suggested citation:
Traum, J.A., Phillips, S.P., Bennett, G.L., Zamora, Celia, and Metzger, L.F., 2014, Documentation of a groundwater flow model (SJRRPGW) for the San Joaquin River Restoration Program study area, California: U.S. Geological Survey Scientific Investigations Report 2014–5148, 151 p., *http://dx.doi.org/10.3133/sir20145148*.

ISSN 2328-0328

Conversion Factors

Inch/Pound to SI

Multiply	By	To obtain
	Length	
inch (in)	2.54	centimeter (cm)
foot (ft)	0.3048	meter (m)
mile (mi)	1.609	kilometer (km)
	Area	
acre	4,047	square meter (m^2)
square mile (mi^2)	2.590	square kilometer (km^2)
	Volume	
acre-foot (acre-ft)	1,233	cubic meter (m^3)
	Flow rate	
acre-foot per month (acre-ft/month)	0.0004691	cubic meter per second (m^3/s)
acre-foot per year (acre-ft/yr)	0.00003909	cubic meter per second (m^3/s)
cubic foot per second (ft^3/s)	0.02832	cubic meter per second (m^3/s)
	Hydraulic conductivity	
foot per day (ft/d)	0.3048	meter per day (m/d)
	Hydraulic conductance	
foot squared per day (ft^2/d)	0.09290	meter squared per day (m^2/d)

Temperature in degrees Celsius (°C) may be converted to degrees Fahrenheit (°F) as follows:

°F=(1.8×°C)+32

Temperature in degrees Fahrenheit (°F) may be converted to degrees Celsius (°C) as follows:

°C=(°F-32)/1.8

Vertical coordinate information is referenced to North American Vertical Datum of 1988 (NAVD 88). Elevation, as used in this report, refers to distance above the vertical datum.

Horizontal coordinate information is referenced to the North American Datum 1983 (NAD 83) geographic coordinate system. The projected coordinate system used is State Plane California Zone III in ft.

Abbreviations

CCID	Central California Irrigation District
CVHM	Central Valley Hydrologic Model
CVP	Central Valley Project
DAU	Detailed Analysis Unit
DTW	depth to the water table
DWR	California Department of Water Resources
ET	actual evapotranspiration
ET_o	reference evapotranspiration
Fei	fraction of evaporation of irrigation
Fep	fraction of evaporation of precipitation
FMP2	Farm Process
Ftr	fraction of transpiration
GIRAS	Geographic Information Retrieval and Analysis System
HEC-RAS	Hydrologic Engineering Centers River Analysis System
HUF	Hydrogeologic Unit Flow
IDW	inverse distance weighting
MPG	Mendota Pool Group
NHD	National Hydrography Dataset
NLCD	North American Land Class Data
NWIS	National Water Information System
PAs	Planning Areas
PEST	parameter estimation software
PRISM	Parameter-Elevation Regressions on Independent Slopes Model
Reclamation	U.S. Bureau of Reclamation
SJAxial	San Joaquin Axial
SJDist	San Joaquin Distal
SJProx	San Joaquin Proximal
SJRRP	San Joaquin River Restoration Program
SJRRPGW	San Joaquin River Restoration Program groundwater flow model
SFR2	Streamflow-Routing Package
TPROGS	Transition-Probability Geostatistical Software
USGS	U.S. Geological Survey
WSFans	Westside Fans

Acknowledgments

Many people contributed to the successful development of the San Joaquin River Restoration Program groundwater flow model (SJRRPGW). Claudia Faunt (U.S. Geological Survey) provided valuable technical expertise on model development and also provided data from the Central Valley Hydrologic Model (CVHM) that were used to develop several SJRRPGW input files. Randy Hanson (U.S. Geologicl Survey) and Wolfgang Schmid (University of Arizona), developers of the Farm Process (FMP2) for MODFLOW, provided assistance implementing MODFLOW-FMP2 for the SJRRPGW. John Doherty (Watermark Numerical Computing) developed the BeoPEST software used for SJRRPGW calibration, provided technical support on using BeoPEST, and added features to BeoPEST to support this work. Susan Cundiff (Tetra Tech) developed the stream rating tables used in the SJRRPGW. Steven Predmore (U.S. Geological Survey) and Donald Martin (U.S. Geological Survey) developed custom tools and scripts for pre- and post-processing model datasets. Katrina Harrison (U.S. Bureau of Reclamation), Chris White (Central California Irrigation District), and Chris Montoya (California Department of Water Resources) provided valuable unpublished data used to develop the model. The San Joaquin River Restoration Program (SJRRP) seepage subgroup, which includes staff from Reclamation, staff from California Department of Water Resources (DWR), and Brian Heywood (CDM Smith), provided guidance on the model development.

Contents

Abstract....1
Introduction....1
Purpose and Scope....2
Study Area....2
Hydrogeology....2
General Geologic Setting....2
Sediment-Texture Analysis....4
Sediment-Texture Data....4
Transition-Probability Geostatistical Software Discretization....4
Development of Sediment-Texture Models....6
Hydrologic Setting....8
Surface Water....8
Groundwater....11
Groundwater-Elevation Database....11
Groundwater Elevation and Movement....12
Interaction of Surface Water and Groundwater....19
Land-Surface Data....19
Ground-Surface Elevation....19
Soils....19
Land-Use and Crop Data....19
Crop-Related Data....23
Climate....23
Water Supply and Demand Data....32
Urban and Wildlife Management Areas Water Supply and Demand....32
Model Development....32
Spatial and Temporal Discretization....38
Spatial Discretization....38
Temporal Discretization....38
Simulation of Irrigated Agriculture and Other Land-Surface Processes....38
Subregion Definitions....38
Irrigation Water Demand....38
Irrigation Water Supply....42
Development of Farm Process Datasets....42
Simulation of Surface Water....42
Calculation of Streamflow....42
Interaction of Surface Water and Groundwater....43
Simulation of Groundwater....44
Initial Conditions....44
Boundary Conditions....44
Aquifer Properties....47
Water-Table Simulation....48
Recharge and Discharge....50

Contents–Continued

Model Calibration....51
Calibration Data....51
Calibration Process....51
Parameters Estimated....55
Observation Weights....55
Calibration Results....63
Model Fit to Observations of Groundwater Elevations....63
Groundwater Elevations at Representative Calibration Wells....66
Model Fit to Streamflow Observations....72
Correlation Coefficient....72
Sensitivity Analysis and Parameter Uncertainty....72
Composite Sensitivity....75
Confidence Limits....75
Model Results....77
Simulated Hydrologic Budgets....77
Groundwater Budget....78
Farm Budget....78
Streamflow Budget....90
Maps of Water-Table Elevation....92
Maps of Groundwater and Surface-Water Interaction....92
Model Limitations and Appropriate Use....105
Future Work....106
Model Enhancements....106
Investigate Predictive Uncertainty of Simulated Stream Seepage....106
Sensitivity to Transition-Probability Geostatistical Software Texture Realizations....106
Summary and Conclusions....107
References Cited....108
Appendix A. Crop-Related Data Utilized from the Central Valley Hydrologic Model....111
Appendix B. Information for San Joaquin River Restoration Program Groundwater Model Calibration Wells....119
Appendix C. Calibration Results....127

Figures

1. Map showing study area, San Joaquin Valley, California 3
2. Map showing grid extent, geologic domains, and locations of wells used for the Transition-Probability Geostatistical Software model, San Joaquin Valley, California 5
3. Graphs showing the relation between vertical transition probabilities for each facies and geologic domain measured from borehole data and simulated using Markov chain models, San Joaquin Valley study area, California 7
4. Diagram showing combined model of sediment-texture distribution derived from Transition-Probability Geostatistical Software of four geologic domains in the San Joaquin Valley, California 8
5. Map showing streamflow network in the study area, San Joaquin Valley, California 10
6. Graph showing monthly average stream inflow and outflow to study area, San Joaquin Valley, California 11
7. Graphs showing semi-variogram results corresponding to the kriged depth to water-table maps, San Joaquin Valley, California: *A,* 1981; *B,* 1983; *C,* 1988; *D,* 1991; and *E,* 2006 13
8. Maps showing interpolated depth to water table in study area, San Joaquin Valley, California: *A,* Fall 1981, a Normal-Dry water year; *B,* Fall 1983, a Wet water year; *C,* Fall 1988, a Dry water year; *D,* Fall 1991, a Normal-Dry water year; *E,* Fall 2006, a Wet water year 14
9. Map showing ground-surface elevation in the study area, San Joaquin Valley, California 20
10. Map showing soil classifications in the study area, San Joaquin Valley, California 21
11. Maps showing distribution of crop type in the study area, San Joaquin Valley, California: *A,* 1961–68; *B,* 1968–78; *C,* 1978–93; *D,* 1994–99; *E,* 1999–2003 24
12. Map showing annual average precipitation in the study area, San Joaquin Valley, California 29
13. Graph showing monthly average precipitation and evapotranspiration in the study area, San Joaquin Valley, California 30
14. Map showing annual average evapotranspiration in the study area, San Joaquin Valley, California 31
15. Graph showing annual surface-water deliveries to the study area, San Joaquin Valley, California 33
16. Graph showing monthly average surface deliveries to the study area, San Joaquin Valley, California 33
17. Map showing estimated spatial distribution of urban groundwater pumping in the study area for April 1999–September 2003, San Joaquin Valley, California 34
18. Graphs showing estimated urban groundwater pumping in the study area, San Joaquin Valley, California: *A,* Annual; *B,* Monthly 35
19. Map showing wildlife management areas simulated in the study area, San Joaquin Valley, California 36
20. Map showing San Joaquin River Restoration Program groundwater flow model grid, San Joaquin Valley, California 39
21. Map showing San Joaquin River Restoration Program groundwater flow model subregions, San Joaquin Valley, California 41

Figures–Continued

22. Graph showing streambed elevation along Chowchilla Bypass, San Joaquin Valley, California 43
23. Map showing San Joaquin River Restoration Program groundwater flow model initial groundwater elevation, San Joaquin Valley, California 45
24. Map showing San Joaquin River Restoration Program groundwater flow model division of general-head model boundaries, San Joaquin Valley, California 46
25. Diagrams showing an example of horizontal combination of Transition-Probability Geostatistical Software grid cells onto the San Joaquin River Restoration Program groundwater flow model grid cells, San Joaquin Valley, California 47
26. Diagrams showing an example Hydrogeologic Unit Flow Package combination of vertical Transition-Probability Geostatistical Software texture layers onto the San Joaquin River Restoration Program groundwater flow model layers, San Joaquin Valley, California 48
27. Map showing San Joaquin River Restoration Program groundwater flow model uppermost active layer for each model cell, San Joaquin Valley, California 49
28. Map showing observation wells used in the San Joaquin River Restoration Program groundwater flow model calibration, San Joaquin Valley, California 52
29. Map showing location of streamgages used in the San Joaquin River Restoration Program groundwater flow model calibration, San Joaquin Valley, California 54
30. Graphs showing relation between simulated and observed groundwater elevations: *A,* Histogram of residual groundwater elevations; *B,* Simulated and observed groundwater elevations; *C,* Residual and observed groundwater elevations 64
31. Map showing average residual (simulated – observed) groundwater elevation at observation wells used in the San Joaquin River Restoration Program groundwater flow model calibration, San Joaquin Valley, California 67
32. Representative hydrographs for each San Joaquin River Restoration Program groundwater flow model calibration area comparing simulated and observed groundwater elevations, San Joaquin Valley, California: *A,* Fresno; *B,* Madera Area; *C,* Mendota; *D,* Chowchilla; *E,* Central California Irrigation District (CCID) South – shallow; *F,* CCID South – deep; *G,* Merced; *H,* CCID North 68
33. Graphs showing relation between simulated and observed streamflows: *A,* histogram of residuals between simulated and observed streamflows; *B,* simulated and observed streamflows; *C,* residual and observed streamflows 73
34. Graph showing simulated and observed streamflow downstream from San Joaquin River Reach 5, San Joaquin Valley, California 74
35. Graphs showing relative composite sensitivities of San Joaquin River Restoration Program groundwater flow model parameters, San Joaquin Valley, California: *A,* sensitivity to crop coefficients for each crop type; *B,* sensitivity to irrigation efficiencies for each subregion; *C,* sensitivity to hydraulic parameters 76
36. Graph showing San Joaquin River Restoration Program groundwater flow model annual groundwater budget and cumulative change in groundwater storage, San Joaquin Valley, California 82
37. Map showing San Joaquin River Restoration Program groundwater flow model agricultural water supply by subregion, San Joaquin Valley, California 85

Figures–Continued

38. Map showing San Joaquin River Restoration Program groundwater flow model agricultural water demand by subregion, San Joaquin Valley, California 86
39. Graph showing San Joaquin River Restoration Program groundwater flow model annual average farm budget, San Joaquin Valley, California 89
40. Graphs showing San Joaquin River Restoration Program groundwater flow model annual seepage for San Joaquin River Management Reaches, San Joaquin Valley, California: *A,* Reach 1; *B,* Reach 2; *C,* Reach 3; *D,* Reach 4; *E,* Reach 5 93
41. Maps showing San Joaquin River Restoration Program groundwater flow model-simulated groundwater elevation and depth to water table, San Joaquin Valley, California: *A,* Fall 1981 simulated groundwater elevation; *B,* Fall 1981 simulated depth to water table; *C,* Fall 1983 simulated groundwater elevation; *D,* Fall 1983 simulated depth to water table; *E,* Fall 1988 simulated groundwater elevation; *F,* Fall 1988 simulated depth to water table; *G,* Fall 1991 simulated groundwater elevation; *H,* Fall 1991 simulated depth to water table 96
42. Map showing San Joaquin River Restoration Program groundwater flow model average groundwater and surface-water interaction, San Joaquin Valley, California 104
A-1. Graph showing monthly crop coefficients for each crop utilized in the San Joaquin River Restoration Program groundwater flow model by different land-use types: *A,* agricultural, undeveloped, and other uses; *B,* agricultural uses; *C,* agricultural and other developed uses 112
C-1. Hydrographs showing simulated and observed groundwater elevations at each calibration well in the San Joaquin valley, 1961–2001: *A,* calibration wells 1–8; *B,* calibration wells 9–16; *C,* calibration wells 17–24; *D,* calibration wells 25–32; *E,* calibration wells 33–40; *F,* calibration wells 41–48; *G,* calibration wells 49–56; *H,* calibration wells 57–64; *I,* calibration wells 65–72; *J,* calibration wells 73–80; *K,* calibration wells 81–88; *L,* calibration wells 89–96; *M,* calibration wells 97–104; *N,* calibration wells 105–112; *O,* calibration wells 113–120; *P,* calibration wells 121–128; *Q,* calibration wells 129–133 128
C-2. Hydrographs showing differences between simulated and observed streamflow at all 19 calibration streamgages in the San Joaquin valley, 1940–2005: *A,* San Joaquin River (SJR) near El Nido, Gravelly Ford, and Chowchilla Bypass at Head above Bifurcation; *B,* SJR below Bifurcation, SJR near Mendota, and SJR near Dos Palos; *C,* Eastside bypass near El Nido, SJR near El Nido, and Eastside Bypass below Mariposa Bypass; *D,* Bear Creek below Eastside Canal, SJR near Stevinson, and Salt Slough at Highway 165 near Stevinson; *E,* SJR at Fremont Ford Bridge, Mud Slough near Gustine, and Merced River near Stevinson; *F,* SJR near Newman, Donney Bridge, and Mariposa Bypass near Crane Ranch; *G,* SJR near Crows Landing 145

Tables

1. Proportions and mean lengths used in the Transition-Probability Geostatistical Software model for each geologic domain in the San Joaquin Valley study area, California 6
2. Streamflow data available in study area, San Joaquin Valley, California....9
3. Minimum, maximum, and mean difference between interpolated and known values of depth to water table for a given year, San Joaquin Valley, California....12
4. Land-use data available for the study area, San Joaquin Valley, California 22
5. Crop types in the study area, San Joaquin Valley, California....22
6. MODFLOW packages and processes used in the San Joaquin River Restoration Program groundwater flow model, San Joaquin Valley, California 37
7. San Joaquin River Restoration Program groundwater flow model subregion descriptions, San Joaquin Valley, California....40
8. Example distribution of aquifer texture in the San Joaquin River Restoration Program groundwater flow model, San Joaquin Valley, California 48
9. Percentage of wells screened above the Corcoran Clay, San Joaquin Valley, California 50
10. Streamgages used in the San Joaquin River Restoration Program groundwater flow model calibration, San Joaquin Valley, California....53
11. Prior information used for calibration of the San Joaquin River Restoration Program groundwater flow model model, San Joaquin Valley, California 56
12. San Joaquin River Restoration Program groundwater flow model final parameter values, San Joaquin Valley, California 60
13. Comparison of San Joaquin River Restoration Program groundwater flow model parameter values to values in similar studies, San Joaquin Valley, California....63
14. Components of San Joaquin River Restoration Program groundwater flow model simulated hydrologic budgets, San Joaquin Valley, California....78
15. San Joaquin River Restoration Program groundwater flow model annual average groundwater budget by subregion, San Joaquin Valley, California 79
16. San Joaquin River Restoration Program groundwater flow model annual groundwater budget, San Joaquin Valley, California 80
17. San Joaquin River Restoration Program groundwater flow model monthly average groundwater budget, San Joaquin Valley, California 83
18. San Joaquin River Restoration Program groundwater flow model annual average farm budget by subregion, San Joaquin Valley, California 84
19. San Joaquin River Restoration Program groundwater flow model annual average farm budget, San Joaquin Valley, California 87
20. San Joaquin River Restoration Program groundwater flow model monthly average farm budget, San Joaquin Valley, California 90
21. San Joaquin River Restoration Program groundwater flow model annual average streamflow budget, San Joaquin Valley, California 91
22. San Joaquin River Restoration Program groundwater flow model monthly average streamflow budget, San Joaquin Valley, California 93

Tables–Continued

A-1. Non-time varying crop-related data in study area for each crop type 115
A-2. Fractions of transportation and evaporation of consumptive use for each crop type 116
A-3. Irrigation efficiencies through the simulation period averaged by San Joaquin River Restoration Program groundwater flow model subregion, San Joaquin Valley, California 117
B-1. Well information for selected Central California Irrigation District monitoring wells used in model calibration for the San Joaquin River Restoration Project area, Fresno, Madera, and Merced Counties, California.....120
B-2. Well information for selected wells from the California Department of Water Resources and U.S. Geological Survey databases used in model calibration for the San Joaquin River Restoration Project area, Fresno, Madera, and Merced Counties, California 124

Documentation of a Groundwater Flow Model (SJRRPGW) for the San Joaquin River Restoration Program Study Area, California

By Jonathan A. Traum, Steven P. Phillips, George L. Bennett, Celia Zamora, and Loren F. Metzger

Abstract

To better understand the potential effects of restoration flows on existing drainage problems, anticipated as a result of the San Joaquin River Restoration Program (SJRRP), the U.S. Geological Survey (USGS), in cooperation with the U.S. Bureau of Reclamation (Reclamation), developed a groundwater flow model (SJRRPGW) of the SJRRP study area that is within 5 miles of the San Joaquin River and adjacent bypass system from Friant Dam to the Merced River. The primary goal of the SJRRP is to reestablish the natural ecology of the river to a degree that restores salmon and other fish populations. Increased flows in the river, particularly during the spring salmon run, are a key component of the restoration effort. A potential consequence of these increased river flows is the exacerbation of existing irrigation drainage problems along a section of the river between Mendota and the confluence with the Merced River. Historically, this reach typically was underlain by a water table within 10 feet of the land surface, thus requiring careful irrigation management and (or) artificial drainage to maintain crop health. The SJRRPGW is designed to meet the short-term needs of the SJRRP; future versions of the model may incorporate potential enhancements, several of which are identified in this report.

The SJRRPGW was constructed using the USGS groundwater flow model MODFLOW and was built on the framework of the USGS Central Valley Hydrologic Model (CVHM) within which the SJRRPGW model domain is embedded. The Farm Process (FMP2) was used to simulate the supply and demand components of irrigated agriculture. The Streamflow-Routing Package (SFR2) was used to simulate the streams and bypasses and their interaction with the aquifer system. The 1,300-square mile study area was subdivided into 0.25-mile by 0.25-mile cells. The sediment texture of the aquifer system, which was used to distribute hydraulic properties by model cell, was refined from that used in the CVHM to better represent the natural heterogeneity of aquifer-system materials within the model domain. In addition, the stream properties were updated from the CVHM to better simulate stream-aquifer interactions, and water-budget subregions were refined to better simulate agricultural water supply and demand. External boundary conditions were derived from the CVHM.

The SJRRPGW was calibrated for April 1961 to September 2003 by using groundwater-level observations from 133 wells and streamflow observations from 19 streamgages. The model was calibrated using public-domain parameter estimation software (PEST) in a semi-automated manner. The simulated groundwater-level elevations and trends (including seasonal fluctuations) and surface-water flow magnitudes and trends reasonably matched observed data. The calibrated model is planned to be used to assess the potential effects of restoration flows on agricultural lands and the relative capabilities of proposed SJRRP actions to reduce these effects.

Introduction

More than a century of human development in the San Joaquin Valley has led to a decline in the quantity and diversity of aquatic and riparian habitats along the lower San Joaquin River. The building of Friant Dam during the 1950s and subsequent diversion of water from the San Joaquin River for agricultural irrigation led to the extinction of the spring salmon run and a decline in other native fish populations above the Merced River (McBain and Trush, Inc., 2002). In 2006, following an 18-year lawsuit, the U.S. Departments of the Interior and Commerce, the Natural Resources Defense Council, and the Friant Water Users Authority reached a settlement designed to restore the native fisheries (Natural Resources Defense Council versus Kirk Rodgers, Stipulation of Settlement, 2006). The settlement resulted in the formation of the San Joaquin River Restoration Program (SJRRP), for which Federal funding was approved in 2009 (San Joaquin River Restoration Program, 2012).

The overall goal of the SJRRP is to restore the natural ecology along the San Joaquin River to a degree that restores and maintains salmon and other fish populations. Furthermore, the goal of habitat restoration is to be sought while reducing or avoiding negative water-supply effects to the long-term Central Valley Project contractors in the Friant Division (McBain and Trush, Inc., 2002).

Increased flows in the river, particularly during the spring salmon run, are a key component of the settlement agreement and the restoration effort. One potential consequence of these increased river flows, however, is the exacerbation of existing irrigation drainage problems through increased seepage from the river along presently losing reaches or reduced groundwater discharge to the river along presently gaining reaches. Historically, the San Joaquin River between Mendota and the confluence with the Merced River typically was underlain by a water table within 10 feet (ft) of the land surface. These shallow water-table conditions require a combination of careful irrigation management and artificial drainage to avoid substantial inundation of crop roots and associated effects on crop health.

To better understand the potential effects of restoration flows on these existing drainage problems, the U.S. Geological Survey (USGS), in cooperation with the U.S. Bureau of Reclamation (Reclamation), developed a groundwater flow model (SJRRPGW). This model simulates the groundwater flow system, the surface-water flow system, and the interaction between the two. The SJRRPGW is designed to meet the short-term needs of the SJRRP, which include preliminary evaluations of (1) the groundwater monitoring network; (2) areas most susceptible to developing high water-table conditions during restoration flows; (3) water-table conditions during various future climatic conditions; (4) the relative effectiveness of proposed actions to reduce negative effects on crop; and (5) potential hydrologic effects of various reach-specific projects.

Purpose and Scope

This report documents the development and calibration of the SJRRPGW, which simulates the groundwater and surface-water flow systems and the interaction between the two. The SJRRPGW domain is the area within 5 miles (mi) of a 150-mi reach of the San Joaquin River and adjacent bypass system from Friant Dam to the Merced River (fig. 1). Vertically, the SJRRPGW includes the aquifer system above the Corcoran Clay Member of the Tulare Formation, or about the upper 250 ft of aquifer-system material in the area.

The SJRRPGW was developed as part of a USGS study supporting the SJRRP Seepage Sub-Group. The SJRRPGW was developed to estimate the potential effects of restoration flows on agricultural lands and to evaluate the relative capabilities of proposed SJRRP actions to reduce these effects. In addition, the study seeks to determine areas within the hydraulic influence of the San Joaquin River. These areas will be vulnerable to seepage effects from restoration flows and are most susceptible to developing shallow groundwater conditions that could harm crops. This study also uses the SJRRPGW to estimate historical groundwater conditions in areas without historical observation records. These historical groundwater conditions can be used to evaluate the groundwater-elevation thresholds developed as part of the SJRRP Seepage Management Plan.

The Central Valley Hydrologic model (CVHM) (Faunt, 2009), from which the lateral and lower boundary conditions for the SJRRPGW were derived, has a model-grid spatial resolution that is too low to meet most needs of the SJRRP. For example, many subreaches of the San Joaquin River where the model will be utilized are only a few miles long and would be represented by only a few CVHM cells; the refined SJRRPGW represents these areas in much higher resolution. In addition to the model grid, several other aspects of the hydrologic system were refined spatially and improved within the SJRRPGW, including the sediment-texture distribution, stream and bypass network, water-budget subregions, land use, and surface-water deliveries. The SJRRPGW model is limited to the current timeframe of the CVHM, which is from 1961 to 2003.

Study Area

The study area (fig. 1) is in the San Joaquin Valley in California and overlies portions of Fresno, Madera, Merced, and Stanislaus Counties. Land use is predominantly agricultural, but also includes urban and wildlife management areas. The study area is characterized by Mediterranean-like climate with hot and dry summers and cool and damp winters. Average monthly temperatures range from 55 degrees Fahrenheit (°F) in January to 99 °F in July. The average annual rainfall is 11.4 inches (in.); nearly 90 percent of rainfall occurs between November and April.

Hydrogeology

General Geologic Setting

The Central Valley, situated between the Sierra Nevada to the east and the Coast Ranges to the west, is a northwest-trending structural trough (Bartow, 1991). The Sierra Nevada is composed primarily of pre-Tertiary granitic rocks separated from the Central Valley by a foothill belt of marine sediments and metavolcanic rocks. The Coast Ranges are a complex assemblage of rocks, including marine and continental sediments of Cretaceous to Quaternary age (Burow and others, 2004).

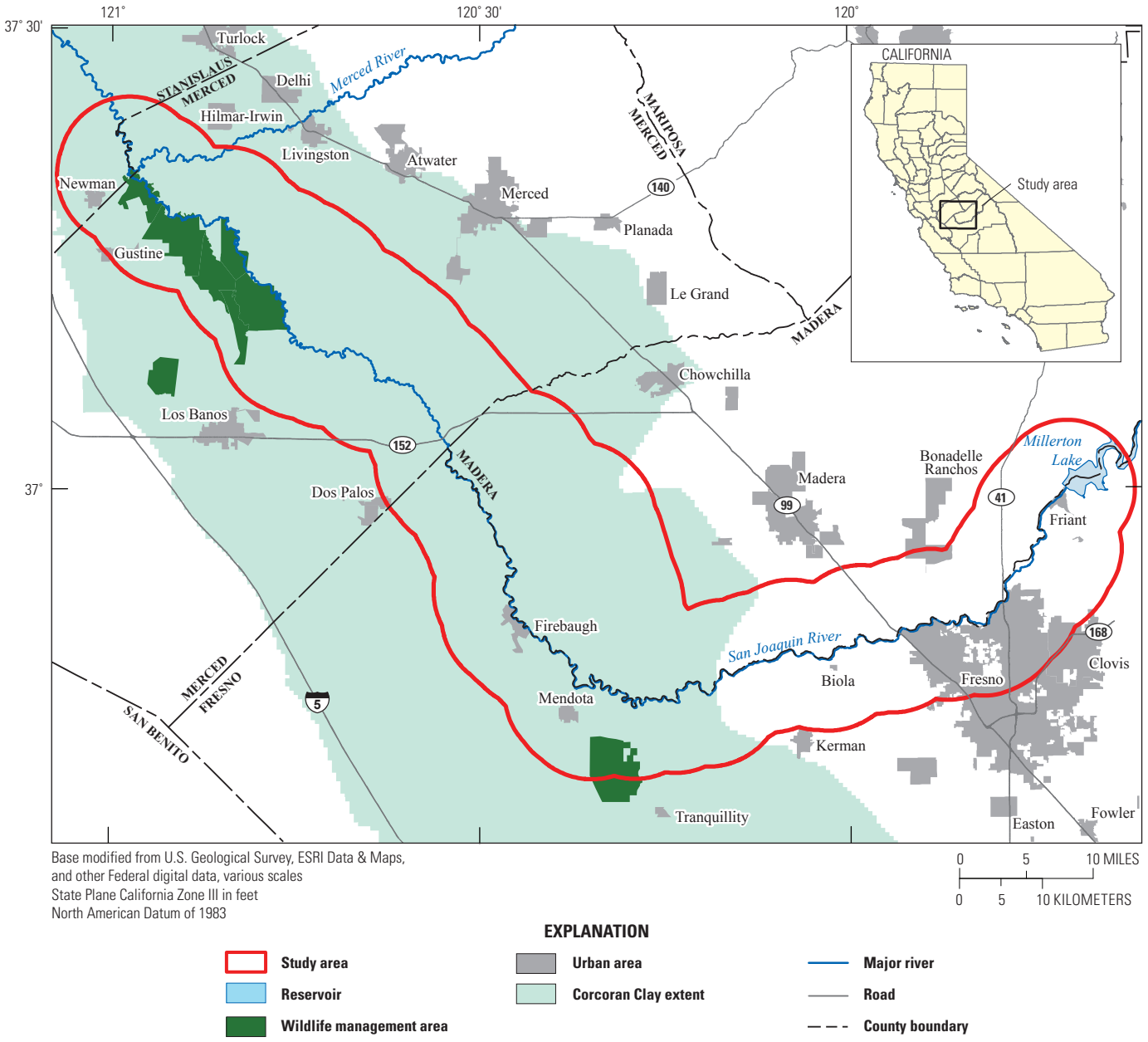

Figure 1. Study area, San Joaquin Valley, California.

The San Joaquin Valley can be divided generally into three physiographic regions—the eastern and western alluvial fans and basin deposits. Alluvial-fan deposits on both sides of the valley are composed predominantly of coarse-grained sediments near the head of each fan that become finer grained toward the valley trough. The sediments in the eastern alluvial fan generally are coarser than those west of the San Joaquin River because the source rocks and watershed characteristics differ. Basin deposits in the region are a combination of coarse-grained channel deposits and fine-grained deposits from flood events (Burow and others, 2004).

The study area is dominated by shallow unconsolidated deposits of gravel, sand, silt, and clay, primarily in the form of alluvium derived from granitic sources to the east and marine sources to the west. Other types of sedimentary deposits in the study area include lacustrine and marsh deposits, dune sands, channel deposits, and flood-basin deposits. Along the valley trough, alluvium derived from the Coast Ranges intermingles with material derived from the Sierra Nevada (Belitz and Heimes, 1990). Sedimentary formations are not clearly delineated in the study area but likely form a sequence of overlapping terrace and alluvial-fan systems (Marchand and Allwardt, 1981) for an area north of the study area. This sequence of deposits indicates cycles of alluviation, soil formation, and channel incision influenced by climatic fluctuations and associated glaciation in the Sierra Nevada (Bartow, 1991).

The Corcoran Clay (fig. 1), which defines the lower extent of most of the study area, is an extensive lacustrine diatomaceous-clay deposit, spanning about two thirds of the San Joaquin Valley. The Corcoran Clay is a Member of the Tulare Formation (Croft, 1972) and has been correlated with the E-clay (Page, 1986). Page (1986) used results of previous work and a limited number of well logs and geophysical logs to map the areal extent of this regional unit. In the study area, the eastern extent of the Corcoran Clay roughly parallels the valley axis of the San Joaquin River. The top of the Corcoran Clay is between 85 and 260 ft below land surface, and the unit has a thickness from 0 to 120 ft (Page, 1986).

Sediment-Texture Analysis

The hydraulic properties of the aquifer system in the study area were estimated on the basis of the distribution of sediment texture, or facies, derived from drillers' logs. The texture distribution was interpolated using a geostatistical approach that determines the probability of transitioning from one facies to another and incorporates factors related to the ways sediments were deposited or their depositional environments (Carle and Fogg, 1996). For this study, these factors included the strike, dip, and mean dimensions of the facies. A number of studies have shown this geostatistical tool, Transition-Probability Geostatistical Software (TPROGS) (Carle, 1999), is valuable for development of geologically plausible subsurface characterizations (Ritzi and others, 1995, 2000; Fogg and others, 1998; Weissmann and Fogg, 1999; Weissmann and others, 1999; Fleckenstein and others, 2006).

The strength of this geostatistical approach is the ability to incorporate geologic interpretation into the modeling process. Lee and others (2007) presented a comparison of modeled geologic heterogeneity in an alluvial-fan setting using two geostatistical simulation techniques—sequential Gaussian and transition probability geostatistics. They showed the sequential Gaussian simulation was unable to capture important geologic characteristics, and the transition probability geostatistical approach was able to create more realistic subsurface simulations.

Sediment-Texture Data

A database of lithologic information from drillers' logs describing boreholes within the study area was created from that developed for the CVHM (Faunt, 2009). From those logs used for the CVHM, 214 were selected for use in this study. An additional 402 drillers' logs from the California Department of Water Resources (DWR) and from a subset of wells installed for the SJRRP were selected to densify the areal coverage and fill gaps where possible. Sediment descriptions on drillers' logs can be ambiguous and variable; therefore, a rating scheme (Faunt, 2009) was used to select the highest quality logs for inclusion in the database. Sediment descriptions from the logs were discretized into 1-ft intervals [0.3 meters (m)], entered into the database, and interpreted as one of four facies—gravel, sand, muddy sand, or clay. The locations of wells used for the TPROGS simulations are well distributed throughout the study area (fig. 2).

Transition-Probability Geostatistical Software Discretization

The grid resolution of the TPROGS model is designed to accommodate the range of mean transition lengths (the mean lengths in three dimensions of each facies) derived from the available texture data. The model cell dimensions are 0.125 mi by 0.125 mi horizontally and 3.28 ft (1 m) thick. The grid, which is flat-lying (unlike that for the SJRRPGW model), consists of 600 rows, 350 columns, and 255 layers, resulting in 53,550,000 nodes. The grid does not include the easternmost part of the study area, from near Fresno to Friant Dam (fig. 2), because borehole data are limited and seepage-related issues are expected to be minor in this area. The lower extent of the TPROGS grid is the top of the Corcoran Clay. About half the TPROGS grid is inactive because of the L-shaped study area. Of the 616 drillers' logs in the database, 550 are within the TPROGS grid.

The study area is divided into four unique depositional environments that were simulated by using four separate TPROGS models (fig. 2). The morphology of the San Joaquin Valley guided the definition of each domain. One domain represents fluvial deposits associated with the San Joaquin River along the valley axis. This domain is flanked by two others representing the distal portions of alluvial fans east and west of the river. Another domain represents the higher-energy depositional environment associated with the proximal (near source) portion of the San Joaquin River alluvial fan.

The first domain, the San Joaquin Proximal (SJProx), is defined as the proximal (near-source) sediments of the San Joaquin River alluvial fan. The domain approximately coincides with subreaches 1A and 1B, or the stretch of the San Joaquin River from Friant Dam to Gravelly Ford (about 12 mi east of Mendota). The second domain, the San Joaquin Distal (SJDist), is defined as the distal (far from source) sediments of the San Joaquin and other eastside alluvial fans; the SJDist domain begins near Gravelly Ford and ends near the confluence with the Merced River. The third domain, the San Joaquin Axial (SJAxial), is the area within 2 mi of the San Joaquin River, beginning near the Chowchilla Bypass Bifurcation Structure (about 8 mi east of Mendota) and ending downstream of the confluence with the Merced River. SJAxial approximates the extent of flood-basin and other fluvial deposits associated with the San Joaquin River. The last domain, the Westside Fans (WSFans), represents the area west of the San Joaquin River composed of alluvial-fan deposits derived from the Coast Ranges. TPROGS models were developed separately for each domain, and the results were merged into a composite sediment-texture model for the study area.

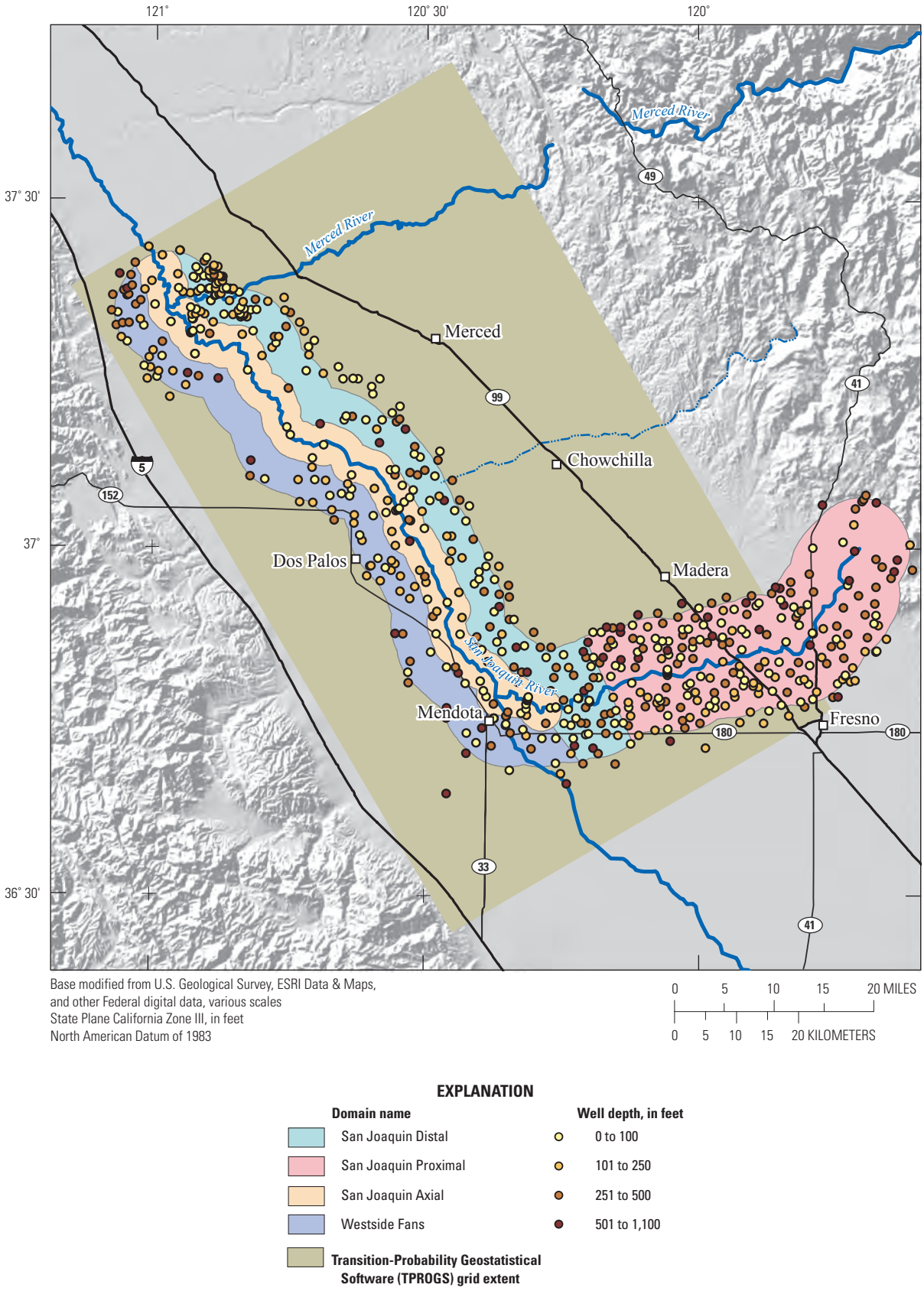

Figure 2. Grid extent, geologic domains, and locations of wells used for the Transition-Probability Geostatistical Software (TPROGS) model, San Joaquin Valley, California.

Development of Sediment-Texture Models

Using TPROGS, the probability of one texture class being vertically adjacent to another and the rate at which one class transitions to another was estimated from drillers' logs. TPROGS calculated the vertical transition probabilities between facies, the mean thickness of each facies, and the proportion of each facies for each of the four domains (Carle, 1999). These values were used in developing z-direction Markov chain models for each of the domains (fig. 3).

The "lag" value shown on the abscissa in figure 3 is the vertical distance over which the probability of transitioning from one facies to another (or to itself) is calculated. The diagonal element for each domain (gravel-gravel, sand-sand, and so on) (fig. 3) represents the auto-transition probability or the transition of a facies to itself; thus, the auto-transition probability is related to the facies thickness. The off-diagonal elements (gravel-sand, gravel-muddy sand, and so on) show the cross-transition probabilities, which are the probability that one facies transitions to another as the lag (in terms of thickness or vertical distance) increases. The spatial correlation tendencies of the various facies with respect to each other is shown in figure 3. For example, sand has the highest probability of being on top of gravel in the SJAxial domain, whereas clay has a higher probability of being above gravels in the WSFans domain.

TPROGS uses the Markov chain models to approximate the transition probabilities and uses these in sequential indicator simulations, which were used for generation of multiple realizations of facies distribution that are equally probable (Carle and Fogg, 1996). The results from this process were smoothed using simulated annealing, which preserves cross-correlations between sediment types that can affect preferential flow (Fogg and others, 1998).

Markov chain models were also developed for the lateral principal directions (x and y); these models are more difficult to develop because information about lengths of horizontal facies is sparse, and boreholes typically are too far apart to make reasonable correlations, particularly in alluvial settings. Different methods have been applied in the region for estimation of lengths of horizontal facies. Weissmann and Fogg (1999), in work done on the Kings River Fan in the San Joaquin Valley, mapped and measured C-horizon soil textures to get estimates of the mean lengths of each of their facies categories. Phillips and others (2007), in work done along the Merced River in the San Joaquin Valley, applied a scaling factor to estimate the lateral mean lengths on the basis of the vertical means lengths. The scaling factor was based on the interpreted horizontal continuity of sediments between wells and previous reports of the sedimentary geology of the area. Lateral mean lengths were interpreted to be 200 times greater in the dip direction and 100 times greater in the strike direction than the facies thicknesses observed in the borehole data. For this study, lateral facies dimensions were derived on the basis of a more physically based approach of Weissmann and Fogg (1999).

The Markov chain model for the SJProx domain was developed using data from 158 wells. Facies proportions, vertical mean lengths, and transition probabilities were calculated using borehole data from these wells (table 1). Lateral mean lengths were adopted from the TPROGS model developed by Weissmann and Fogg (1999) (table 1) for deposits of the Kings River alluvial fan. Although the San Joaquin River alluvial fan is smaller than the Kings River fan, the size of the fan has been constrained by its location in the San Joaquin Valley. Lower subsidence rates and the connection of the San Joaquin River to local base level have limited the overall fan size (Weissmann and others, 2005). However, because the drainage area in the Sierra Nevada above the San Joaquin River alluvial fan is comparable to that for the Kings River, it is reasonable to expect similar characteristics of sediment supply and stream discharge.

Table 1. Proportions and mean lengths used in the Transition-Probability Geostatistical Software (TPROGS) model for each geologic domain in the San Joaquin Valley study area, California.

[Proportion expressed as fraction of 1]

Facies	Proportion	Mean length (meters)		
		X	Y	Z
San Joaquin Proximal (SJProx)				
Gravel	0.03	650	200	4.7
Sand	0.47	1,500	625	4.2
Muddy sand	0.14	800	400	3.9
Clay	0.36	973	439	3.6
San Joaquin Distal (SJDist)				
Gravel	0.01	640	200	4.6
Sand	0.41	1,300	550	3.7
Muddy sand	0.14	820	410	4.0
Clay	0.44	1,171	527	4.3
San Joaquin Axial (SJAxial)				
Gravel	0.03	200	350	3.7
Sand	0.51	330	800	3.9
Muddy sand	0.17	210	430	2.5
Clay	0.29	157	366	2.8
Westside Fans (WSFans)				
Gravel	0.11	750	230	5.6
Sand	0.41	2,150	900	7.5
Muddy sand	0.08	640	540	3.1
Clay	0.41	1,112	492	5.6

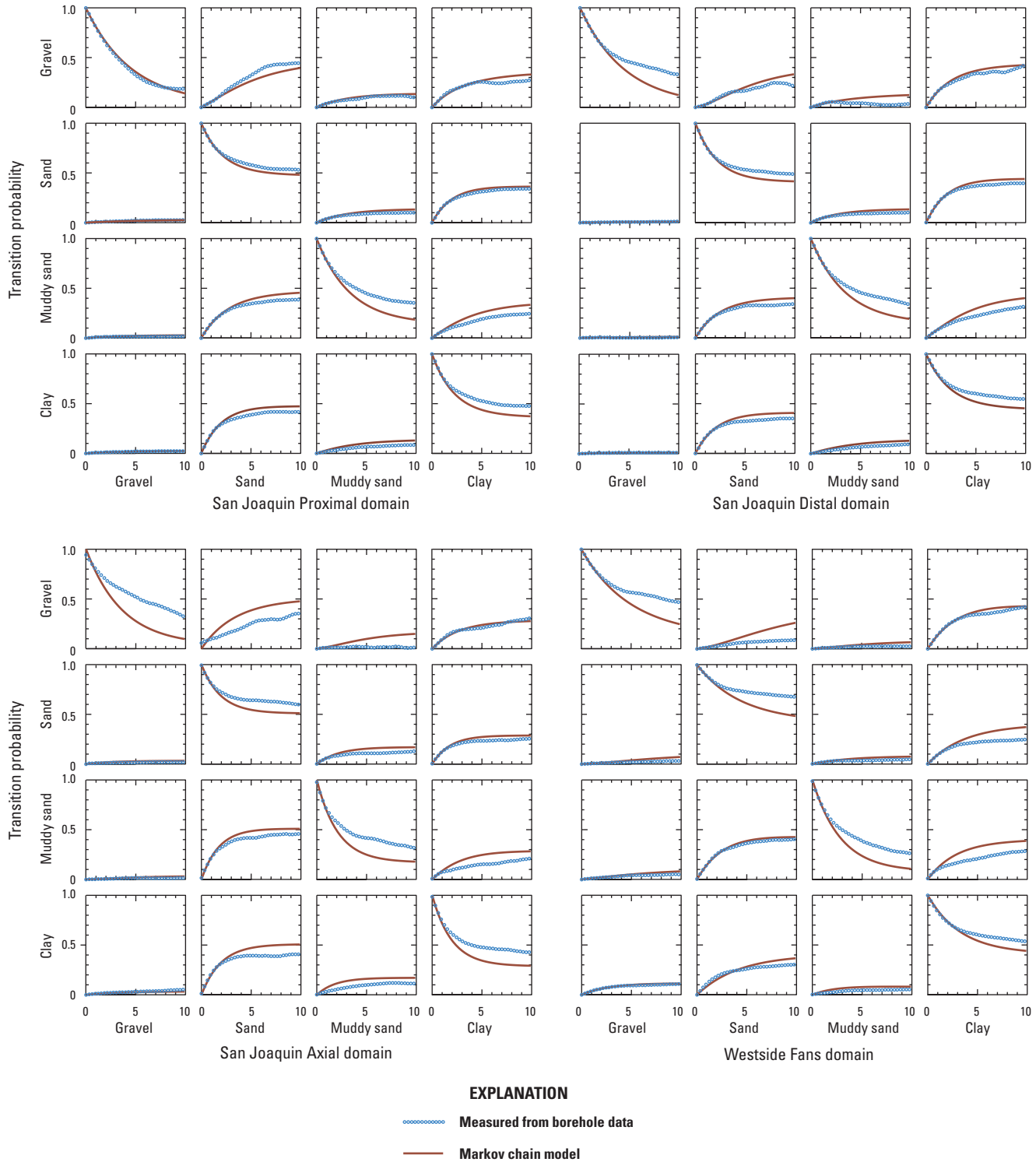

Figure 3. Relation between vertical transition probabilities for each facies and geologic domain measured from borehole data and simulated using Markov chain models, San Joaquin Valley study area, California.

The lateral components of the Markov chain models for the SJDist (196 wells), SJAxial (93 wells), and WSFans (103 wells) domains were developed on the basis of those derived for the SJProx domain. Lateral mean facies lengths were scaled from the SJProx values by the ratio of the vertical mean facies lengths. For example, the mean thickness of clay in SJProx is 11.8 ft and in SJDist is 14.1 ft, or about 20 percent thicker. Accordingly, the lateral mean facies lengths for SJDist were assumed to be about 20 percent greater than those for SJProx. This process was repeated for each of the facies and domains (table 1). The results are similar to those obtained using the method of Phillips and others (2007) but with greater variability from facies to facies.

These three-dimensional Markov chain models of the four domains approximated the transition probabilities used for sequential indicator simulations. The four domains were then merged into a composite realization (fig. 4). A single composite realization represents one of many possible distributions of the defined facies. A key advantage of this method is that the same input can be used to generate hundreds of realizations, which provide the opportunity to explore a wide range of equally probable facies distributions. For this study, a single composite realization was randomly selected to represent the facies distribution in the study area.

Each of the composite realizations honor the overall proportions of hydrofacies determined from well logs in each domain (table 1) and their depositional alignments. For example, the SJAxial domain (fig. 4) contains a greater proportion of the sand facies than the flanking domains because the sediments in this geologic domain were deposited in a direction parallel to the river, orthogonal to the other domains.

Hydrologic Setting

Surface Water

The major surface-water feature in the study area is the San Joaquin River. The study area also contains several other streams as well as flood-control bypass channels and structures. The streamflow network in the study area (fig. 5) was mapped using a combination of aerial photographs and the 1:24,000 National Hydrography Dataset (NHD) (U.S. Geologic Survey, 2011). Reclamation has divided the San Joaquin River into five major planning reaches (fig. 5). Reach 1 extends 37 river miles from Friant Dam to Gravelly Ford. Reach 2 extends 21 river miles from Gravelly Ford to Mendota Dam. Reach 3 extends 25 river miles from Mendota Pool to Sack Dam. Reach 4 extends 56 river miles from Sack Dam to the Eastside Bypass confluence. Reach 5 extends 17 river miles from the Eastside Bypass confluence to the Merced River confluence. Some of these reaches are further divided into subreaches. Note, the area of concern for seepage-related issues is from Mendota to the confluence of the Merced River, representing much of the study area (Reaches 2B through 5).

Inflows for the 10 streams or canals entering the study area (table 2 and fig. 5) were obtained from a variety of sources. Inflow for the San Joaquin River and the North Fork Lower Kings River (also known as James Bypass) were obtained from the USGS National Water Information System (NWIS). Inflow to the Mendota Pool from the Delta-Mendota Canal was obtained from the CALSIM Water Resources Simulation Model (California Department of Water Resources, 2011a). For the other seven locations, inflows were specified

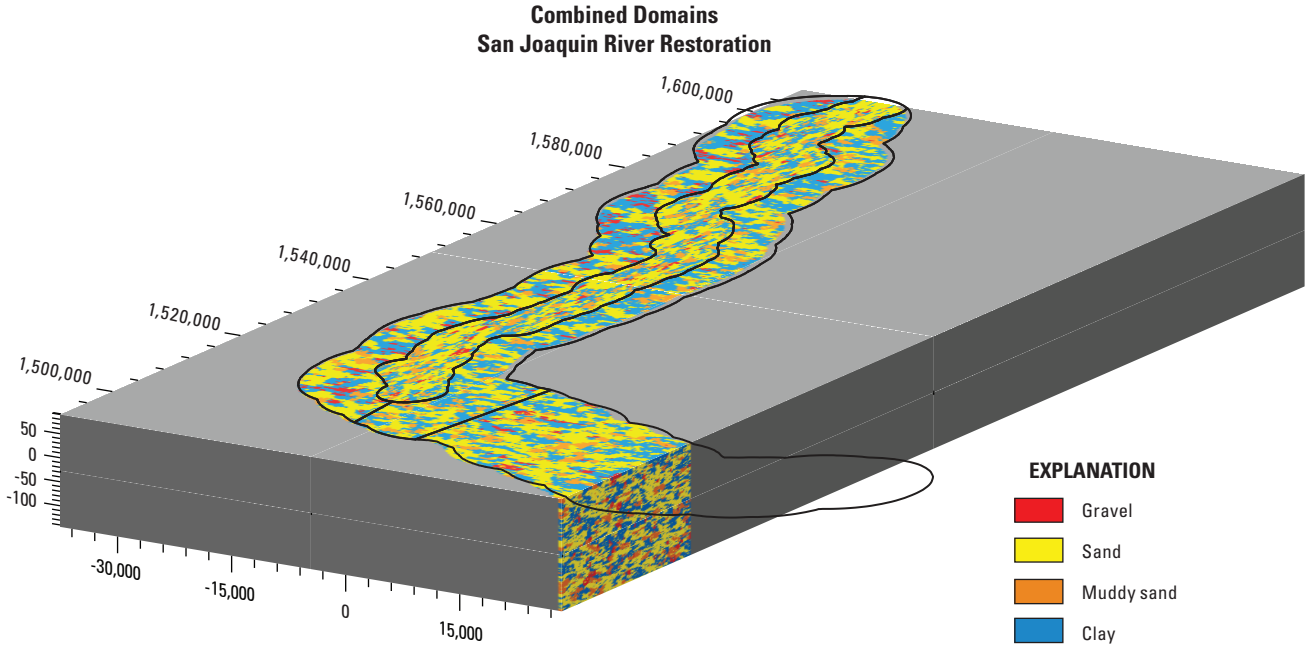

Figure 4. Combined model of sediment-texture distribution derived from Transition-Probability Geostatistical Software (TPROGS) of four geologic domains in the San Joaquin Valley, California.

Table 2. Streamflow data available in study area, San Joaquin Valley, California.

[**Abbreviations:** Calif., California; CALSIM, CALSIM Water Resources Simulation Model; CVHM, Central Valley Hydrologic Model; mm/yyyy, month/year; USGS, U.S. Geological Survey; +, plus; –, minus; —, no data]

Inflow or diversion	Description	Date data available (mm/yyyy)	Type	Source	Source description
Merced River	—	04/1961–09/2003	Stream inflow	CVHM	Segment 72 Reach 33
Bear Creek	—	04/1961–09/2003	Stream inflow	CVHM	Segment 50 Reach 30
Deadmans Creek	—	04/1961–09/2003	Stream inflow	CVHM	Segment 58 Reach 28
Chowchilla River	—	04/1961–09/2003	Stream inflow	CVHM	Segment 46 Reach 24
Fresno River	—	04/1961–09/2003	Stream inflow	CVHM	Segment 35 Reach 26
San Joaquin River	—	10/1940–Present	Stream inflow	USGS streamgage	11251000—San Joaquin River below Friant, Calif.
James Bypass (also known as Kings River or Fresno Slough)	—	10/1947–Present	Stream inflow	USGS streamgage	11253500—James Bypass near San Joaquin, Calif.
Los Banos Creek	—	04/1961–09/2003	Stream inflow	Estimated from CVHM	Assumed same as Orestimba Creek
Orestimba Creek	—	04/1961–09/2003	Stream inflow	CVHM	Segment 80 Reach 60
Mariposa Bifurcation Structure	Diversion from Eastside Bypass into Mariposa Bypass	10/1921–09/2003	Bypass diversion	CALSIM	Node C587A
Sand Slough Bypass Control Structure	Diversion from the San Joaquin River into Eastside Bypass via Sand Slough	10/1921–09/2003	Bypass diversion	CALSIM	Node C609A
Chowchilla Bypass Bifurcation Structure	Diversion from the San Joaquin River into the Chowchilla Bypass	10/1921–09/2003	Bypass diversion	CALSIM	Node C605A (flow that remains in the San Joaquin River below the Bifurcation)
Sack Dam	Diversion from the San Joaquin River into Arroyo Canal	10/1921–09/2003	Irrigation diversion	CALSIM	Node D608B + Node D608C
Mendota Pool	Diversion from Delta Mendota Canal into Mendota Pool	10/1921–09/2003	Canal inflow	CALSIM	Node C708 − Node D607B − Node D607C

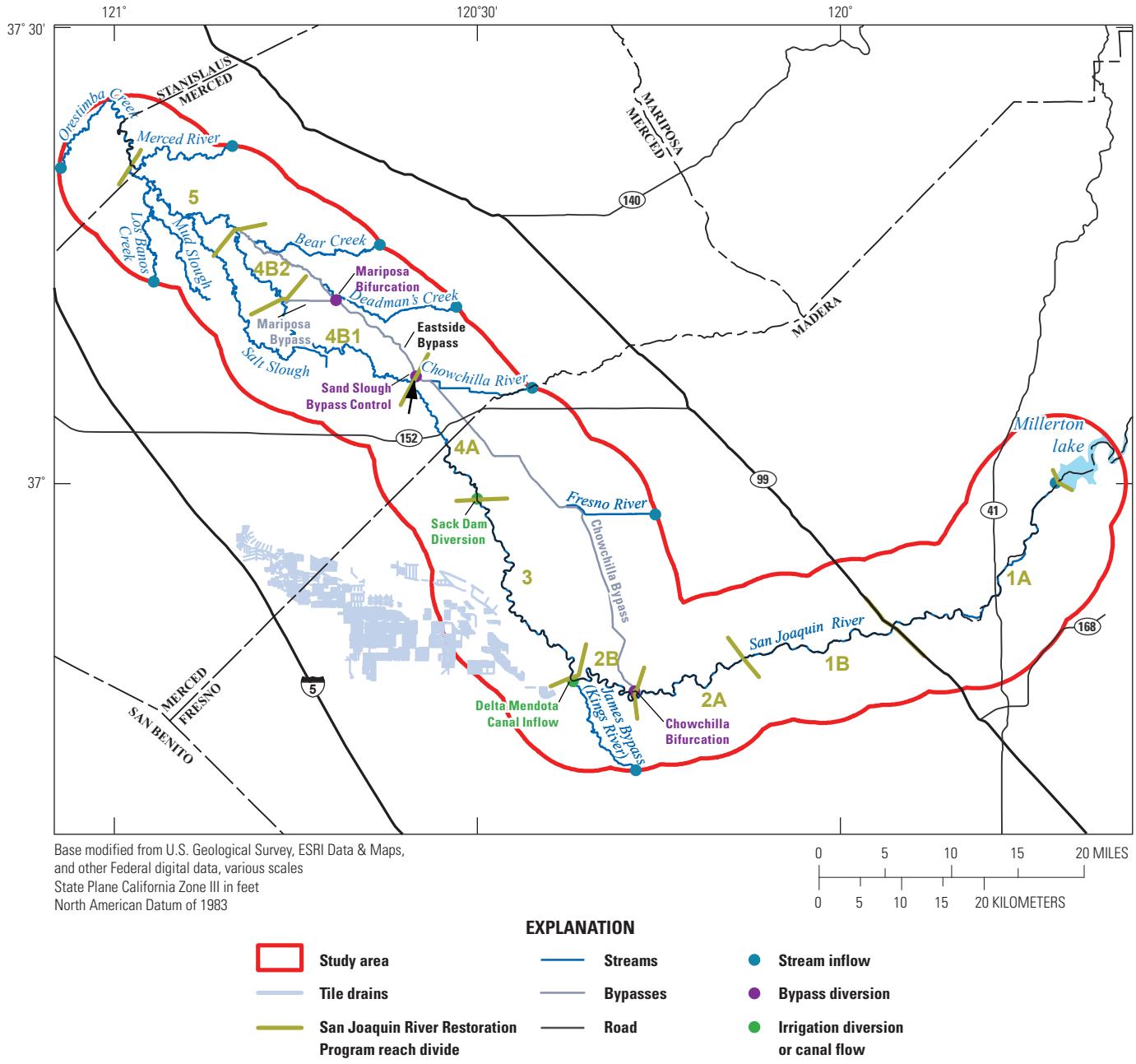

Figure 5. Streamflow network in the study area, San Joaquin Valley, California.

as the simulated flows for these streams from the CVHM at the study-area boundary.

The study area has three major bypass diversion structures—Chowchilla Bypass Bifurcation Structure, Sand Slough Bypass Control Structure, and Mariposa Bifurcation Structure (fig. 5). In addition, there is an irrigation diversion on the San Joaquin River at Sack Dam. Data for these bypasses and the irrigation diversion also were obtained from the CALSIM model (table 2).

The average annual stream inflow to the study area from 1961 to 2003 is approximately 1.4 million acre-feet (acre-ft); 68 percent of this inflow occurs during February through June (fig. 6). The San Joaquin and Merced Rivers contribute 65 percent of the total inflow into the study area.

The average annual stream outflow from the study area can be approximated by the streamgage on the San Joaquin River near Newman, Calif. (USGS site identification number 11274000), which is downstream from the Merced River confluence. The average annual stream outflow from the study area from 1961 to 2003 is also approximately 1.4 million acre-ft.

Groundwater

Groundwater-Elevation Database

A groundwater-level database consisting of almost 90,000 records for 2,800 wells within the SJRRP study area was compiled for the period 1920 through 2009. More than 90 percent of the available records represent the period after 1960. The frequency of water-level measurements for any particular well generally is limited to biannual spring and fall measurements, although monthly, weekly, and daily records are available for a few wells for short periods.

Approximately 18 percent of the wells in the groundwater-level database are classified as observation wells. Wells reportedly used for groundwater withdrawal, including irrigation, domestic, stock, and public supply, account for about 65 percent of the wells. The remaining 17 percent of the wells in the database are classified as either unused production wells or are lacking specific information regarding their intended purpose. Water-level records were obtained from the California Department of Water Resources (DWR) Water Data

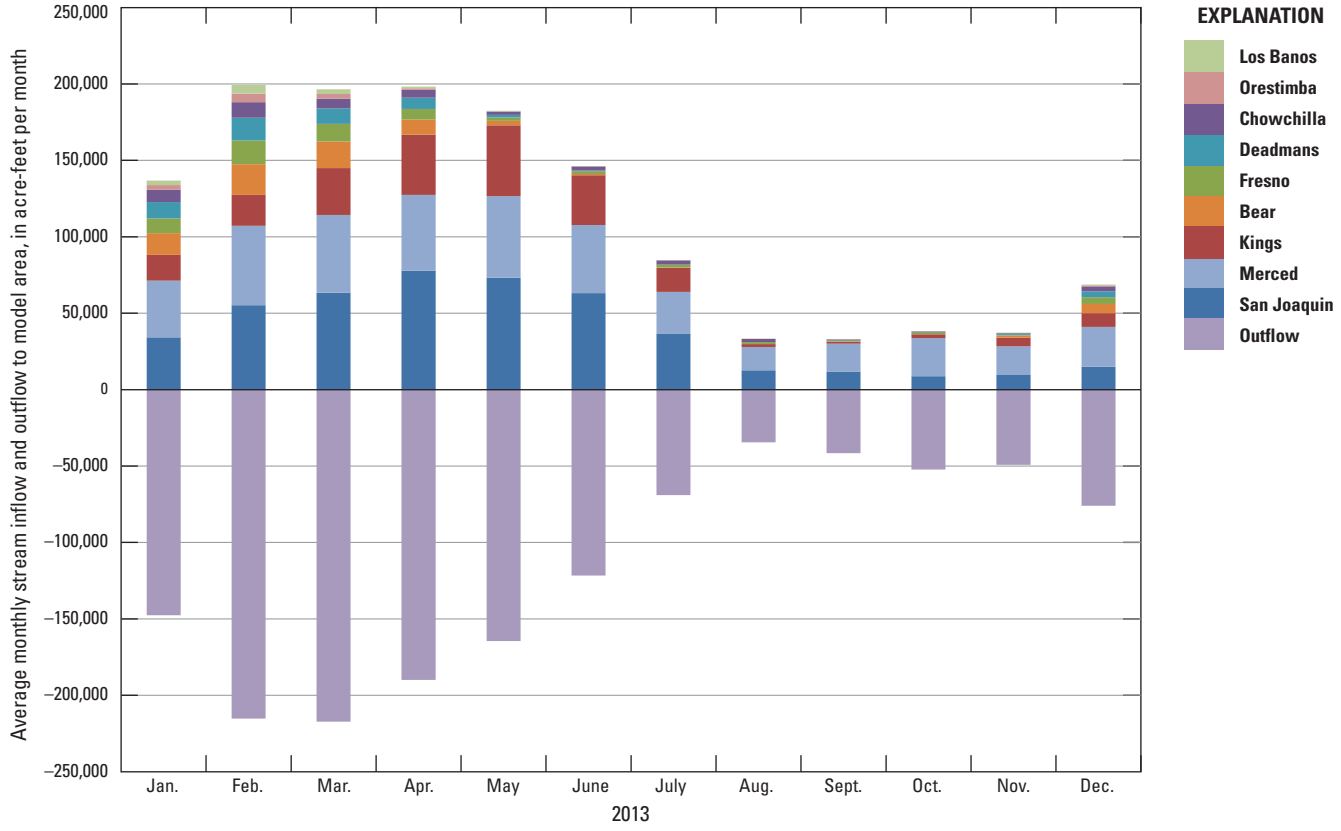

Figure 6. Monthly average stream inflow and outflow to study area, San Joaquin Valley, California.

Library (WDL) online database, the USGS NWIS database, the Mendota Pool Group (MPG), and the Central California Irrigation District (CCID). The database compiled for this project also includes approximately 600 water-level measurements through 2009 that were obtained from 62 SJRRP observation wells installed and monitored by Reclamation beginning in the spring of 2008.

Groundwater Elevation and Movement

The history of hydrologic and associated water-table changes in and around the study area provides useful information on areas vulnerable to shallow water-table conditions. Agricultural development began in the late 1800s but accelerated rapidly post-World War II (Bertoldi and others, 1991). Through the 1960s, most water used for irrigation was groundwater, and this was reflected in a long-term decline of groundwater elevations in some areas (Belitz and Heimes, 1990).

Although groundwater elevations declined throughout much of the region within and surrounding the study area, shallow groundwater conditions persisted in some areas near the San Joaquin River, particularly on the west side (U.S. Bureau of Reclamation, 1962). Part of the explanation for these shallow groundwater areas is that surface water is the primary water supply for irrigation as opposed to groundwater in these areas as well as fine-grained soils in the shallow subsurface. Riparian use of water from the San Joaquin River was the local norm before Friant Dam was constructed and flows in the river diminished; in exchange for the loss of this source of irrigation water, deliveries of surface water from the Sacramento-San Joaquin Delta via the Delta-Mendota Canal were made available, starting in 1951, to the San Joaquin River Water Authority Exchange Contractors, including the CCID, San Luis Canal Company, and Columbia Canal Company (McBain and Trush, Inc., 2002). Agricultural tile drains were installed in the 1950s and 1960s to help manage many of these areas (fig. 5) (J. McGahan, Summers Engineering, written commun, 2002; S. Styles, Irrigation Training and Research Center, written commun., 2002).

Maps of depth to the water table (DTW) for selected years were created by using an ordinary kriging interpolation method. Ordinary kriging takes into account two important aspects of estimation, distance and clustering. The basic technique for ordinary kriging uses a weighted average of neighboring samples (well locations with corresponding DTW data) to estimate unknown values of DTW at neighboring locations. The results were optimized by applying variogram models (Gaussian, exponential, and spherical) known to work well with spatially continuous data and examining the semi-variogram, depicted using a graph that relates the difference between a value at one location and the value at another according to the distance and direction between them. The optimization process resulted in semi-variograms exhibiting a linear behavior near the origin (a straight line could be fit to the first few points on the semi-variogram), and the selection of a spherical variogram model on the basis of the intersection of the straight line and the range of the semi-variogram (Isaaks and Srivastava, 1989).

Semi-variogram models are developed for each dataset to calculate the interpolated DTW (fig. 7). The semivariance depicts how closely the values at a given distance are spatially correlated. This correlation can be inferred from the semi-variograms by examining how well the empirical data fits the variogram model. The distance at which each of the modeled variograms begins to reach an asymptote corresponds to the range of the semi-variogram. The range defines the maximum distance at which spatial correlation between given well locations can be estimated. As expected, spatial correlation distance is less for years with sparse well coverage throughout the study area (2006) and greater for years with greater density of well coverage (1981, 1983, and 1988). For example, in 1983, empirical data fits the model line to a distance of approximately 75,000 ft (approximately 14 mi); in 2006, empirical data fits the model line to less than approximately 50,000 ft (approximately 9 mi).

The minimum, maximum, and mean difference between interpolated and known values of DTW are shown in table 3. The location of the maximum difference in DTW for all years was in Reach 1A, which is an area where the interpolated surface under estimates the local shallow groundwater conditions of a few wells near the San Joaquin River in an area where the regional water table is relatively deep.

The DTW maps (fig. 8) were created for the fall measurement period (September 15 through November 15) for the years having the greatest number of measurements and (or) the greatest interest with respect to particular climatic conditions. The fall period is relatively unaffected by irrigation, is minimally affected by rainfall, generally has the most available water-level data, and approximates the seasonal low. Available

Table 3. Minimum, maximum, and mean difference between interpolated and known values of depth to water table for a given year, San Joaquin Valley, California.

[**Abbreviations**: DTW, depth to water table; ft, feet]

Year	Well count	Minimum DTW difference (ft)	Maximum DTW difference (ft)	Mean DTW difference (ft)
1981	654	0.0	22.5	1.2
1983	837	0.0	9.1	0.4
1988	792	0.0	9.0	0.5
1991	743	0.0	11.0	0.6
1994	789	0.0	7.4	0.6
1999	500	0.0	6.4	0.5
2006	503	0.0	5.9	0.6
2007	302	0.0	5.2	0.5
2008	333	0.0	13.3	1.4
2009	295	0.0	5.6	0.4
2010	289	0.0	41.8	6.8

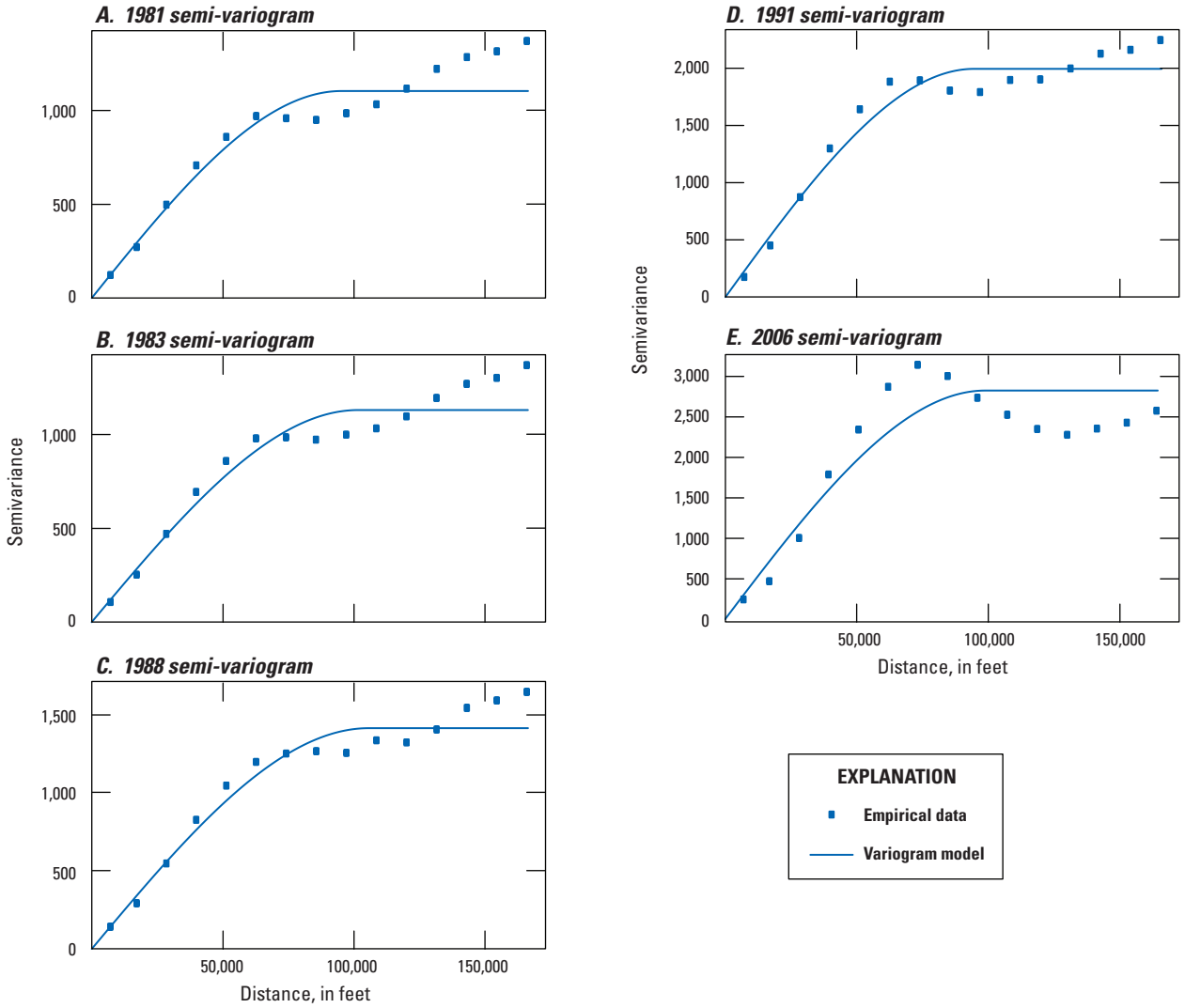

Figure 7. Semi-variogram results corresponding to the kriged depth to water-table maps, San Joaquin Valley, California: *A*, 1981; *B*, 1983; *C*, 1988; *D*, 1991; and *E*, 2006.

water-level data prior to the 1980s are insufficient for mapping DTW below land surface, but data from shallow wells during the 1960s indicate large areas where the DTW was less than 10 ft. These areas were predominantly west of the San Joaquin River. Water-year designations (Critical-Low, Critical-High, Dry, Normal-Dry, Normal-Wet, and Wet) were defined by the SJRRP on the basis of the total annual unimpaired runoff at Friant Dam for the water year (October through September) (Natural Resources Defense Council v. Kirk Rodgers, Stipulation of Settlement, 2006).

Substantial deliveries of surface water to the area west of the study area began during the early 1970s with the completion of the California Aqueduct. Accompanied by a large decrease in groundwater pumping, this caused a dramatic recovery of water levels over much of the west side of the valley (Belitz and Heimes, 1990). Because of sparse availability of data, it is not clear if this recovery to the west had a substantial effect on shallow water levels within the study area. Water levels on the east side, however, continued to decline, and by 1981, water levels were much lower on the east side than on the west side (fig. 8*A*); 1981 was a Normal-Dry year preceded by a Wet year (1980) and Normal-Wet year (1979). Notably, the shallowest groundwater areas in 1981 are primarily very near to and west of the river, with the exception of areas east of the river in Reaches 4 and 5.

Following 1981, two Wet years caused substantial increases in the water table over most of the study area. The DTW in 1983 indicates recovery of water levels along the eastern margin of the study area toward Chowchilla and Madera and considerable growth in the shallow groundwater areas along the west side and parts of the east side along the river and to the north (fig. 8*B*).

Following 1983, there was a range of water-year types; however, a drought started in 1987 with a Dry year. By 1988, also a Dry year, water levels along the eastern margin of the study area had declined, and the area of shallow groundwater had retreated westward; however, the shallow groundwater area remained widespread on the west side (fig. 8*C*).

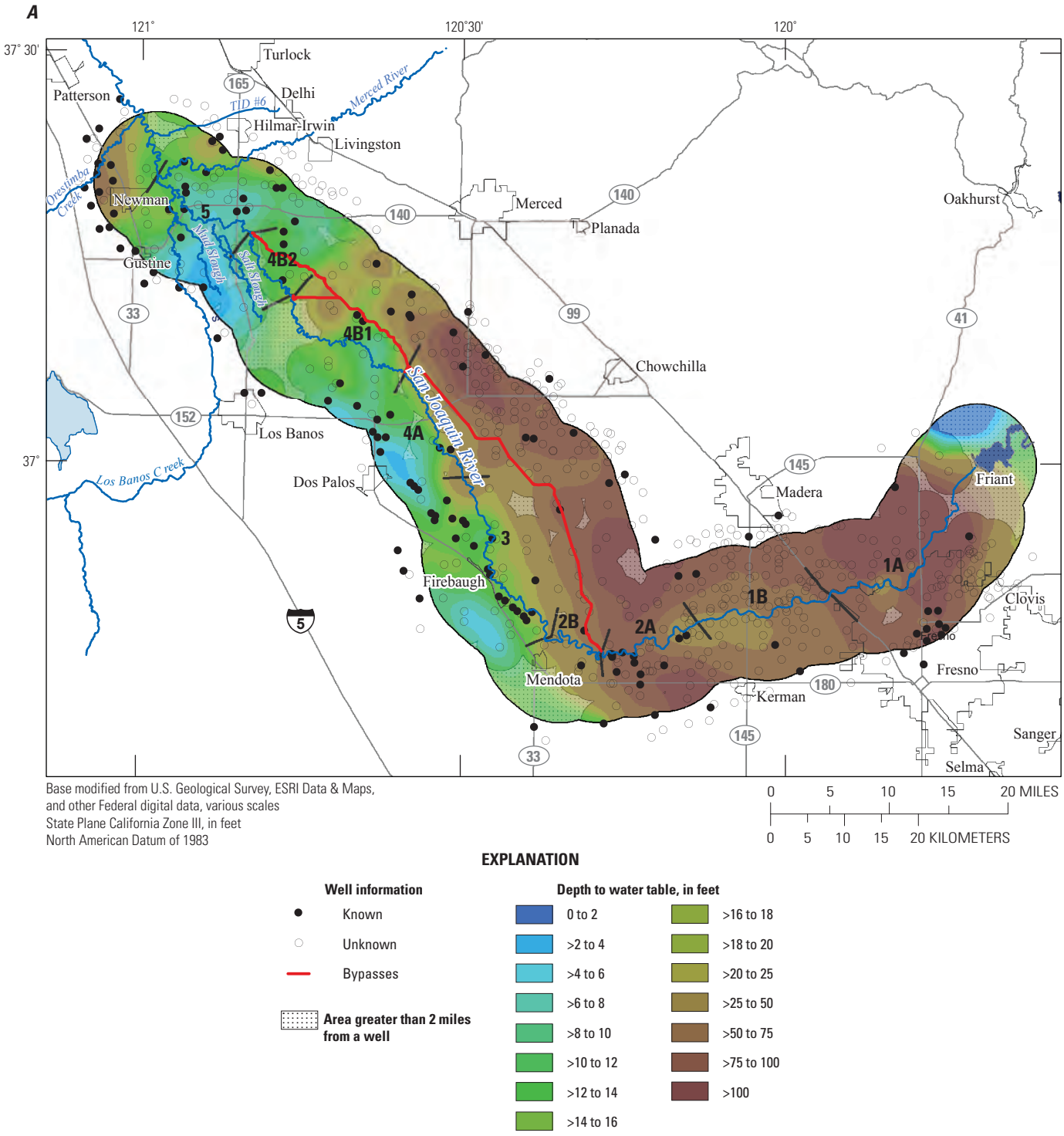

Figure 8. Interpolated depth to water table in study area, San Joaquin Valley, California: *A*, Fall 1981, a Normal-Dry water year; *B*, Fall 1983, a Wet water year; *C*, Fall 1988, a Dry water year; *D*, Fall 1991, a Normal-Dry water year; *E*, Fall 2006, a Wet water year.

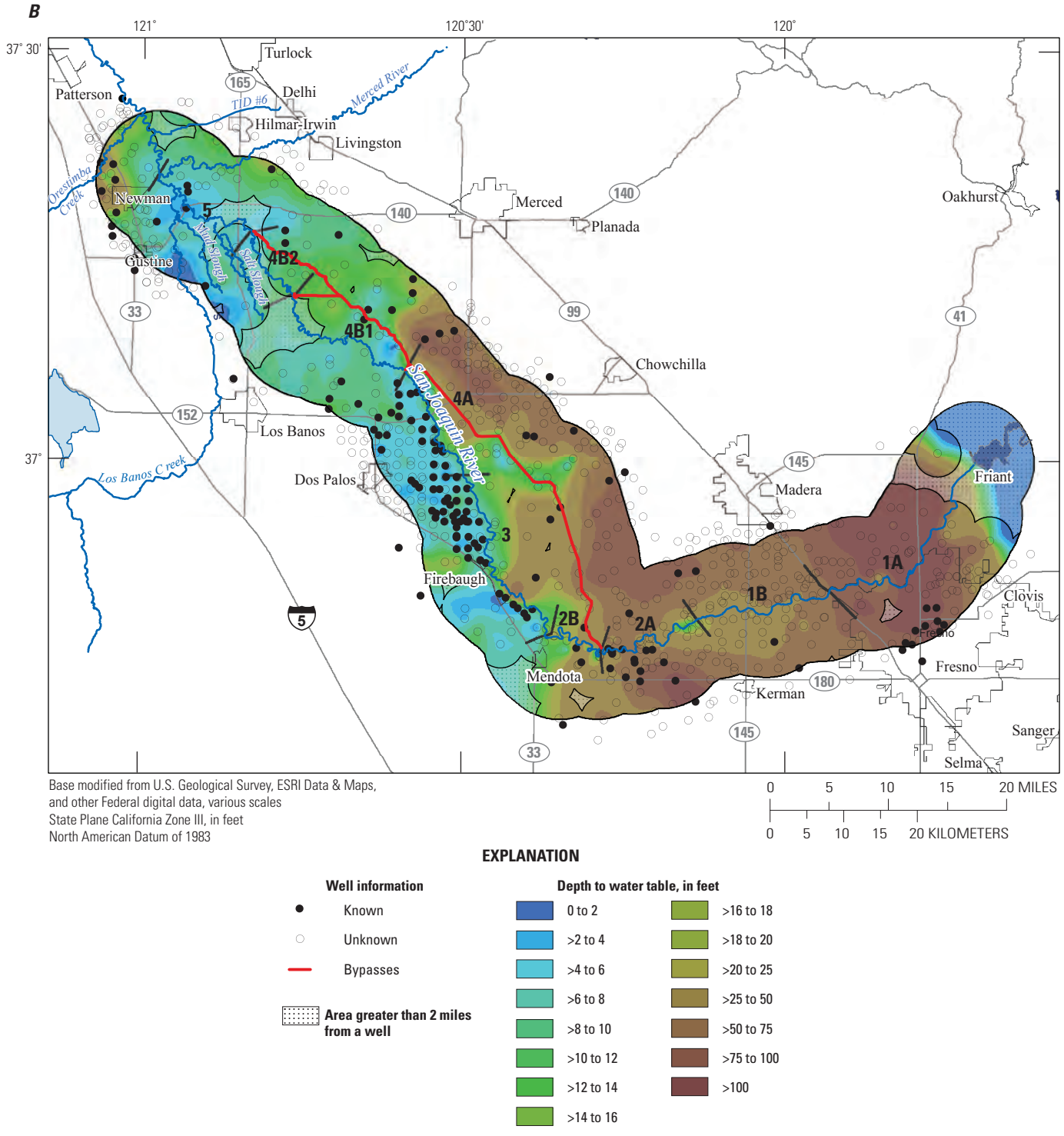

Figure 8. —Continued.

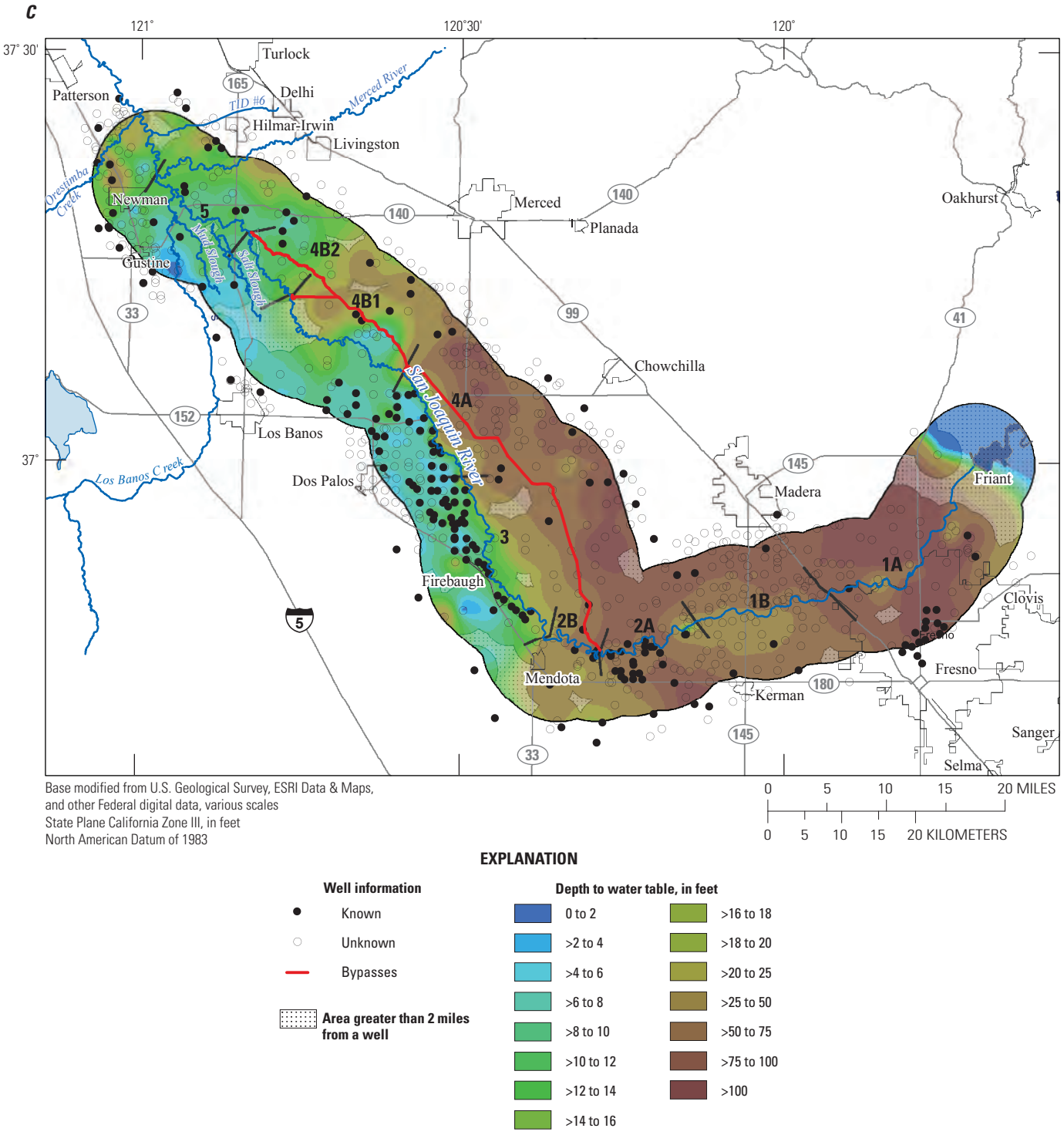

Figure 8. —Continued.

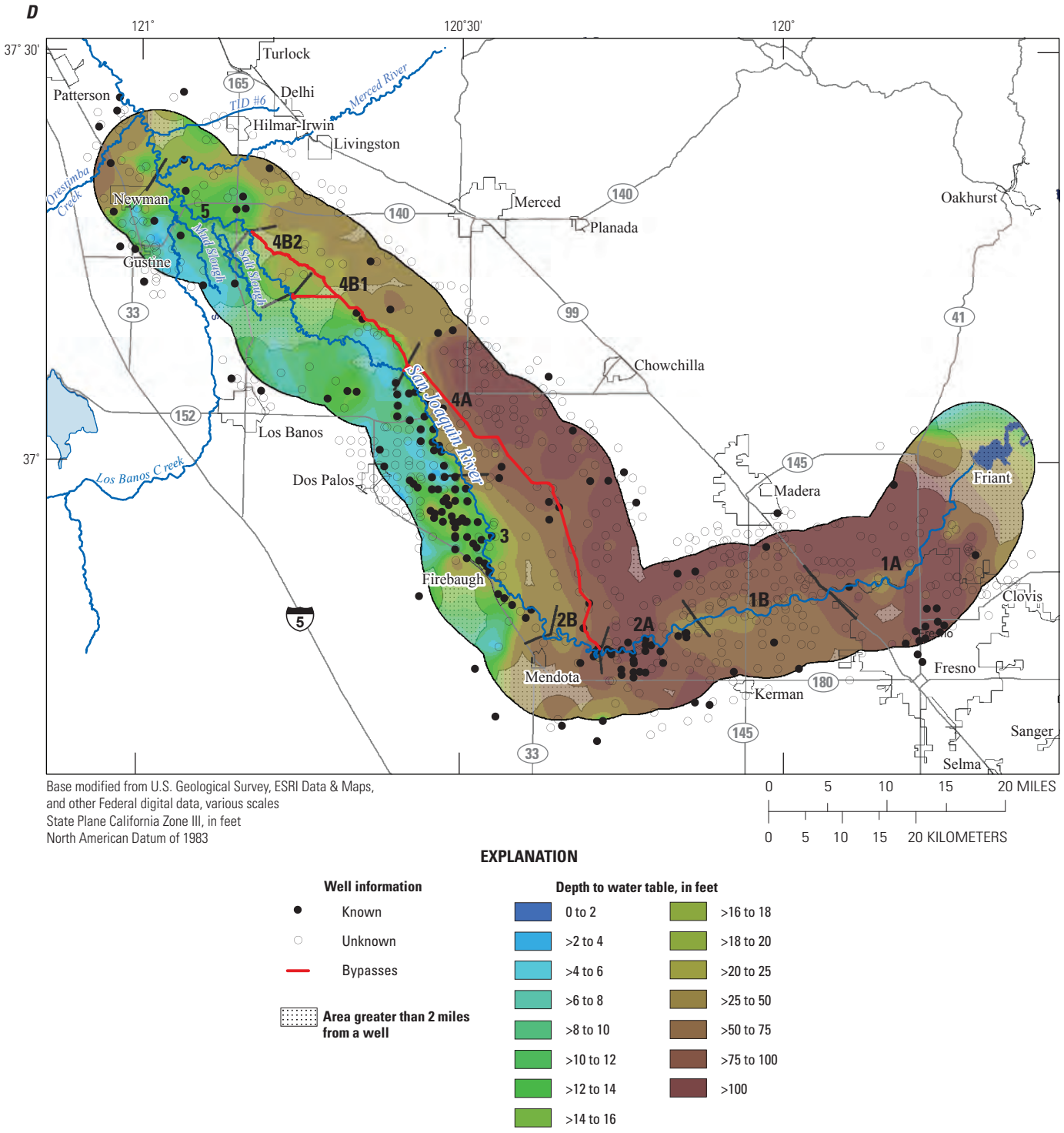

Figure 8. —Continued.

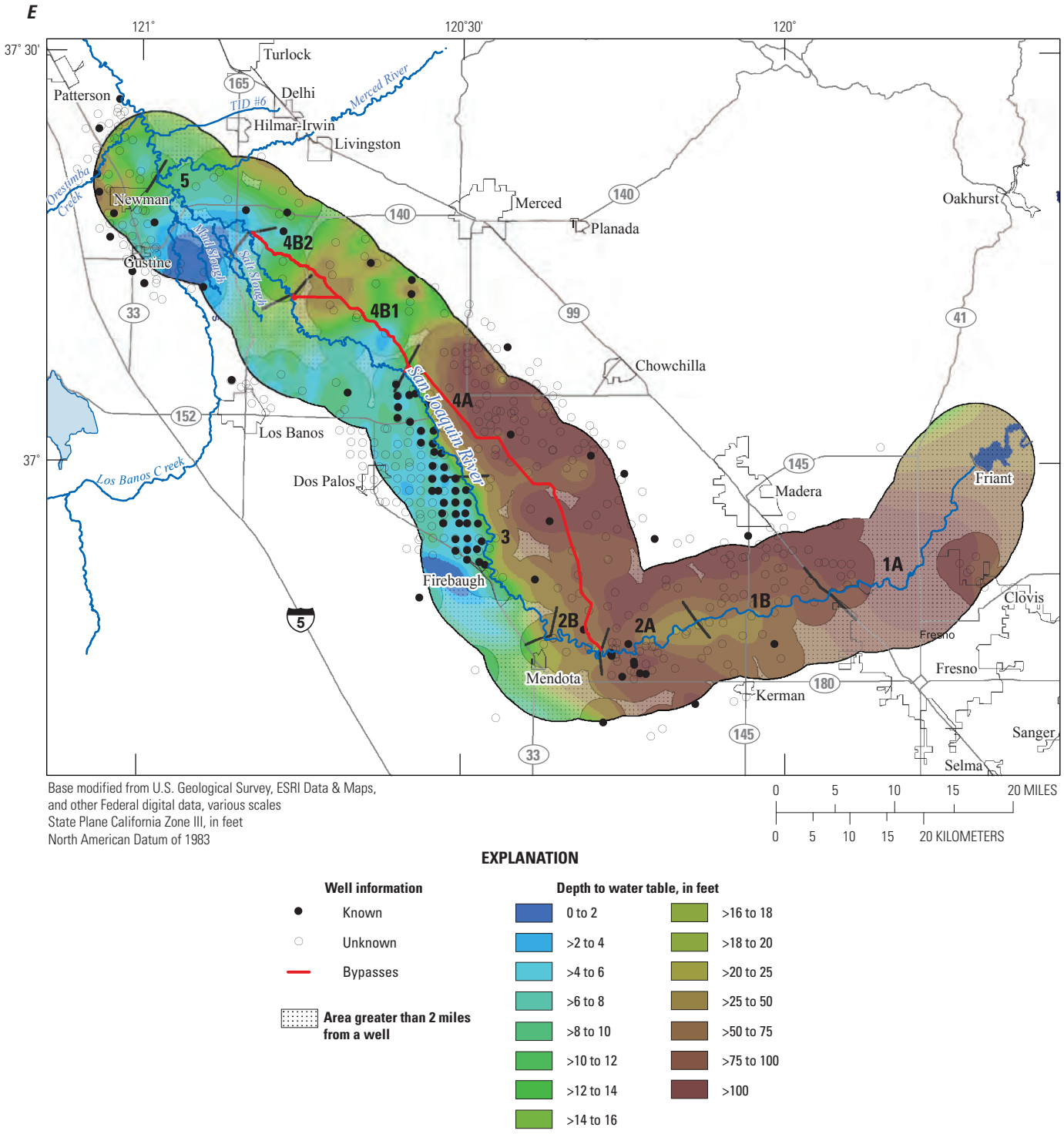

Figure 8. —Continued.

Between 1988 and 1992, the drought continued—all water-year types were Normal-Dry or Dry. Data from 1991, the fifth year of a 6-year drought, show a change in water levels in response to the combination of reduced availability of surface water, increased groundwater pumping, and reduced recharge from precipitation. By 1991, water levels had declined substantially along the eastern margin of the study area, and the areas of shallow groundwater had retreated compared to those prior to the drought (fig. 8*D*).

A Wet year in 2006 was preceded by several Normal-Wet and Normal-Dry years. Although water levels along the eastern margin had remained low, the shallow groundwater areas west of the river and east of the river to the north were fully reestablished (fig. 8*E*).

This brief historical review shows that shallow groundwater areas, particularly west of the San Joaquin River and east of the river along Reaches 4 and 5, have persisted through time with the exception of during drought conditions. Persistent shallow groundwater areas shown to be within the hydraulic influence of the San Joaquin River potentially are vulnerable to seepage effects from restoration flows.

The historic response of shallow groundwater areas to drought and other dry climatic conditions indicates the shallow water table is sensitive to reduced surface-water availability and associated groundwater pumping on both sides of the river, which is consistent with previous findings by Belitz and Phillips (1995) and K.D. Schmidt and Associates (McBain and Trush, Inc., 2002, p. 4–26). This has implications for year-to-year operations of the SJRRP and for groundwater pumping as a potential future response action.

Interaction of Surface Water and Groundwater

Prior to development, gaining conditions existed along the San Joaquin River from approximately Reach 2B to Reach 5 (McBain and Trush, Inc., 2002). Between predevelopment and 1961, the water table in the study area substantially declined, by up to 80 ft in some areas, because of regional groundwater pumping. This pumping changed the predevelopment direction of groundwater flow from toward the San Joaquin River to away from the river toward pumping locations. This changed the San Joaquin River from a gaining stream to a losing stream in many parts of the study area (McBain and Trush, Inc., 2002).

Several previous studies estimated the San Joaquin River gains (or losses) from (or to) the groundwater system in the study area (McBain and Trush, Inc., 2002). Other sources documenting estimates of seepage from the San Joaquin River include expert testimony (Deverel, 2005). Comparison of flow rates in the river between streamgages during the interim flow releases for the SJRRP (*http://www.restoresjr.net/flows/SurfaceWater/index.html*) gives an estimate of seepage between each streamgage.

On the basis of available information, estimates of Reach 1 river losses range from 105 to 250 cubic feet per second (ft^3/s); those for Reach 2 range from 75 to 170 ft^3/s. Reach 3 is typically a losing reach, whereas Reaches 4 and 5 are typically gaining reaches; however, in these reaches, there can be a net river loss or gain depending on the local and regional hydraulic gradients. Near fields with surface-water irrigation, there is typically a net river gain from groundwater during the growing season. In contrast, near fields with groundwater pumping, there is typically a net river loss to groundwater during the growing season. Data collected during interim flow releases in 2009 showed net seepage losses increased during higher flows compared to lower flows, which is to be expected. The data also showed net seepage losses were greatest during the beginning of increased flows and diminished over time.

Land-Surface Data

Land-surface processes can have a substantial effect on the hydrologic conditions near the San Joaquin River. Most notably, agriculture that relies on groundwater for irrigation purposes can have a large influence on the lowering groundwater levels in the study area. Conversely, agriculture that relies on surface water for irrigation purposes can have a large influence on the raising groundwater levels in the study area. The datasets discussed in the following sections, including ground-surface elevation, soils, land-use, and water supply and demand, are important for understanding these potential effects.

Ground-Surface Elevation

The elevation of the ground surface in the study area ranges from about 50 ft along the northernmost part of the San Joaquin River to more than 1,000 ft at the eastern extent of the study area (fig. 9). Ground-surface elevation data were obtained from the USGS National Elevation Dataset (Gesch and others, 2009).

Soils

The soil data utilized in the study area (and the CVHM) were obtained from the State Soil Geographic Database STATSGO (U.S. Department of Agriculture, Natural Resource Conservation Service, 2005). Two soil types are present within the study area—silty clay and sandy loam; the former is the dominant type (fig. 10).

Land-Use and Crop Data

The study area is predominantly an agricultural area; in 2000, 66 percent of the land use in the study area was agriculture, 28 percent was native vegetation, and 6 percent was urban. Major crop types grown in the study area include cotton, vineyards, pasture, orchards, and field crops.

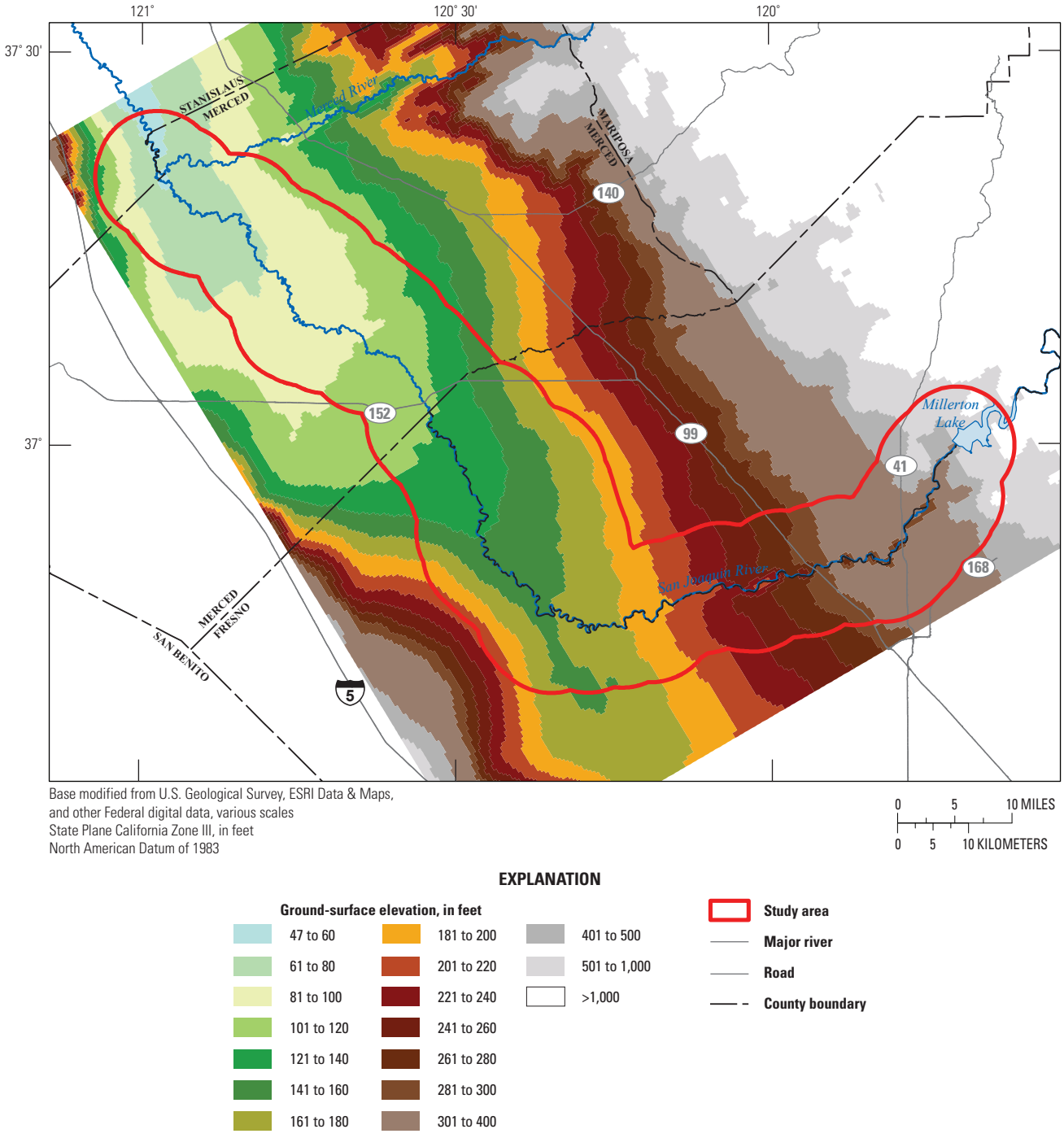

Figure 9. Ground-surface elevation in the study area, San Joaquin Valley, California.

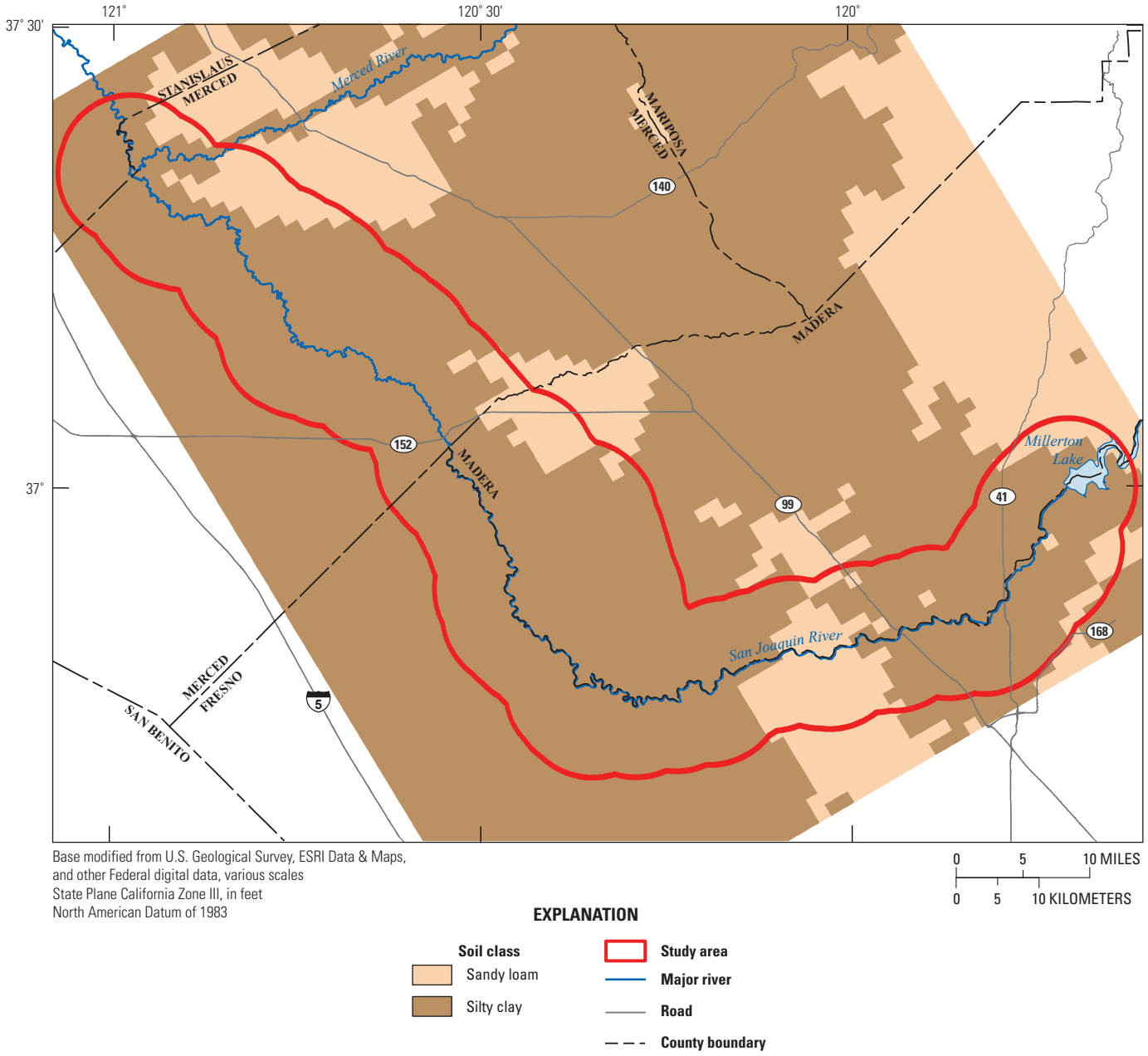

Figure 10. Soil classifications in the study area, San Joaquin Valley, California.

Table 4. Land-use data available for the study area, San Joaquin Valley, California.

[**Abbreviations**: CSU, California State University; CVHM, Central Valley Hydrologic Model; DWR, Department of Water Resources; mm/yyyy, month/year; USGS, U.S. Geological Survey]

Land-use data source	Data provider	Coverages used	Dates used to represent (mm/yyyy)	Same dataset in CVHM
Central Valley Historic Vegetation Mapping Project (CVHVMP)	CSU Chico	1960	04/1961–03/1968	Yes
Geographic Information Retrieval and Analysis System (GIRAS)	USGS	1973	04/1968–03/1978	Yes
North American Land Class Data (NLCD)	USGS	1992	04/1978–03/1993	Yes
County land-use surveys	California DWR	Fresno County 1994, Madera County 1995, Merced County 1995, Stanislaus County 1996	04/1993–03/1999	No
County land-use surveys	California DWR	Fresno County 2000, Madera County 2001, Merced County 2002, Stanislaus County 2004	04/1999–10/2003	No

The source of recent land-use data (mid-1990s and later) was from DWR land-use surveys (California Department of Water Resources, 2011b). Historic land-use surveys were obtained from various sources discussed in following paragraphs; these are the same datasets used in the CVHM (table 4).

The study area includes four counties: Fresno, Madera, Merced, and Stanislaus. The DWR conducts land-use surveys by county approximately every 7 years, and the survey dates for each of these counties commonly differ. Two composite land-use coverages were developed for the study area from the available land-use surveys. One composite coverage (referred to as the 1995 coverage) combines the 1994 Fresno County, 1995 Madera County, 1995 Merced County, and 1996 Stanislaus County surveys. The other composite coverage (referred to as the 2000 coverage) combines the 2000 Fresno County, 2001 Madera County, 2002 Merced County, and 2004 Stanislaus County surveys. The 1995 coverage was assumed to represent the period April 1993 through March 1999, and the 2000 coverage represented the period April 1999 through October 2003.

Three coverages were used to represent the period before April 1993. For April 1961 through March 1968, a land-use coverage derived from a patchwork of sources developed by California State University Chico (2003) was used. For April 1968 through March 1978, Anderson level II classifications from the Geographic Information Retrieval and Analysis System (GIRAS) were used (U.S. Geologic Survey, 1990). For April 1978 through March 1993, North American Land Class Data (NLCD) were used (U.S. Geologic Survey, 1999). These three coverages also were used in the CVHM and are described in that report in detail (Faunt, 2009).

The DWR land-use surveys contain more than 80 different land-use/crop types, hereafter referred to as "crop types." For this study, 15 specific crop types were used (table 5). These crop types are based on the DWR "class" symbol, which is the minimum breakdown of land use provided in

Table 5. Crop types in the study area, San Joaquin Valley, California.

[**Abbreviations**: DWR, Department of Water Resources; N/A, not available]

Crop identification number	Specific land-use/crop types	DWR class symbol
1	Water	NW
2	Urban	U, UR, UC, UI, UL, UV
23	Irrigated native vegetation	NV, NR, NB
3	Non-irrigated native vegetation	NV, NR, NB
8	Idle	I
9	Truck, nursery, and berry crops (Truck)	T
10	Citrus and subtropical (Citrus)	C
11	Field	F
18	Cotton	F—subclass 1
12	Vineyards	V
13	Pasture	P
14	Grain and hay crops (Grain)	G
15	Semiagricultural and incidental to agriculture (Dairies)	S
16	Deciduous fruits and nuts (Orchards)	D
17	Rice	R
	General land-use/crop types	
4	Orchard, groves, and vineyards	N/A
5	Pasture and hay	N/A
6	Row crops	N/A
7	Small grains	N/A
19	Developed	N/A
20	Cropland and pasture	N/A

their surveys. Cotton, which is a subclass of field crops, was separated into its own crop type because it is widespread in the study area, and it typically has different water-use characteristics than other field crops. Native vegetation was also separated into irrigated native vegetation (to represent irrigated wildlife management areas) and non-irrigated native vegetation.

In addition to these 15 specific crops types, 6 general crop-type categories were utilized to accommodate the more historic land-use surveys, which have less detailed crop categories than the DWR surveys (table 5).

Five crop-distribution maps were used in this study (fig. 11*A–E*). The crop distributions for the historic periods were aggregated at 1-mi resolution, consistent with the CVHM grid. Those for the two most recent periods were aggregated at 0.25-mi resolution.

Crop-Related Data

This section briefly defines and describes the crop-related data used in this study; more detailed definitions are provided in Schmid and Hanson (2009). Values for crop-related datasets are provided by the CVHM and are documented in appendix A. Crop coefficients and irrigation efficiencies were adjusted during model calibration.

Crop-related data include the following:

- Root-zone depths.
- Root-uptake coefficients (negative hydrostatic-pressure heads for optimal growth, anoxia, and wilting point).
- Crop coefficients.
- Fractions of transpiration and evaporation.
- Fractions of direct runoff for precipitation.
- Fractions of direct runoff for irrigation.
- Irrigation efficiencies.

Root-zone depths are defined for each crop type and are important for calculating the groundwater uptake by crops. Root-uptake coefficients represent, for each crop type, the relative hydrostatic pressure at which anoxia, optimal growth, and wilting occur. Crops such as rice have a relative hydrostatic pressure greater than zero for anoxia because they grow even when the fields are flooded. Most crops will experience anoxia if the roots are inundated for an extended period. Wilting occurs if the water content in the root zone is too low to sustain the crop for an extended period.

A crop coefficient is the ratio of the actual evapotranspiration (ET) for a crop to the reference evapotranspiration (ET_o) and is used as a scaling factor for calculating actual ET from ET_o. Crop coefficients are defined for each crop type and vary monthly on the basis of the growth stage of the crop.

The fractions of transpiration and evaporation vary linearly with the amount of field area covered by each crop type and sum to 1.0. These fractions vary monthly on the basis of the growth stage of the crop. For example, a bare field will have a fraction of transpiration (Ftr) of 0.0 and a fraction of evaporation of precipitation (Fep) of 1.0. In contrast, a field with a crop canopy covering the entire field will have an Ftr of 1.0 and an Fep of 0.0. The fraction of evaporation of irrigation (Fei) is the portion of the field not covered by the crop canopy that has irrigation water flowing on it (such as an irrigation furrow); it is always less than or equal to Fep (Schmid and Hanson, 2009).

The fraction of direct runoff of precipitation represents the fraction of the total precipitation that runs off directly to the streams and is not available for crop use. Fractions of direct runoff of precipitation are defined for each crop type. The fraction of precipitation available for crop use is equal to 1.0 minus the fraction of direct runoff of precipitation.

The fraction of direct runoff of irrigation represents the fraction of the total irrigation supply (groundwater pumping and surface-water deliveries) that runs off directly to the streams and is not available for crop use. Fractions of direct runoff of irrigation are defined for each crop type. The fraction of irrigation water available for crop use is equal to 1.0 minus the fraction of direct runoff of irrigation.

Irrigation efficiency can be defined in many different ways. For this study, it is defined as the ratio of water utilized (consumptively) by the crop to the water applied to the crop. The fraction of irrigation water that becomes percolation to groundwater is equal to 1.0 minus the irrigation efficiency.

Climate

The long-term average annual precipitation in the study area, from 1961 to 2003, was 11.4 in., ranging spatially from 7 to 18 in. (fig. 12). The vast majority (89 percent) of the precipitation is during November to April (fig. 13). Monthly spatially varying precipitation estimates for the study area during 1961–2003 were obtained from the Parameter-Elevation Regressions on Independent Slopes Model (PRISM) (Climate Source, 2006).

Long-term average annual ET_o in the study area, from 1961 to 2003, is 53.2 in., ranging spatially from 50 to 55 in. (fig. 14). A total of 64 percent of ET_o occurs during the growing season between May and October (fig. 13). Evapotranspiration exceeds rainfall in all months except December and January, which necessitate irrigation in order to grow most crops in the study area. Monthly spatially varying ET_o datasets for the study area were calculated from the temperature data in the PRISM model (Climate Source, 2006) using the Hargreaves-Samani equation (Hargreaves and Samani, 1982).

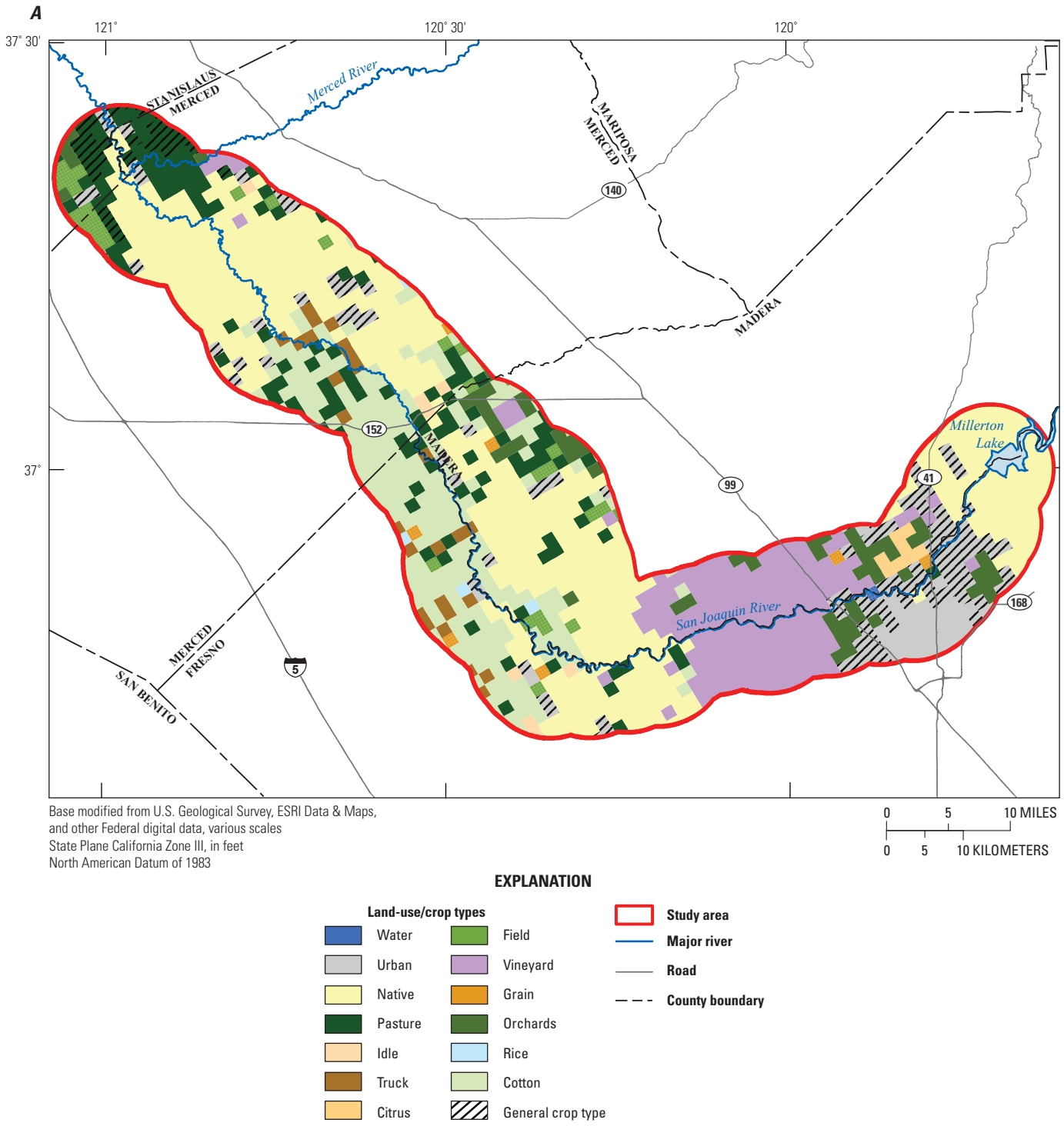

Figure 11. Distribution of crop type in the study area, San Joaquin Valley, California: *A*, 1961–68; *B*, 1968–78; *C*, 1978–93; *D*, 1994–99; *E*, 1999–2003.

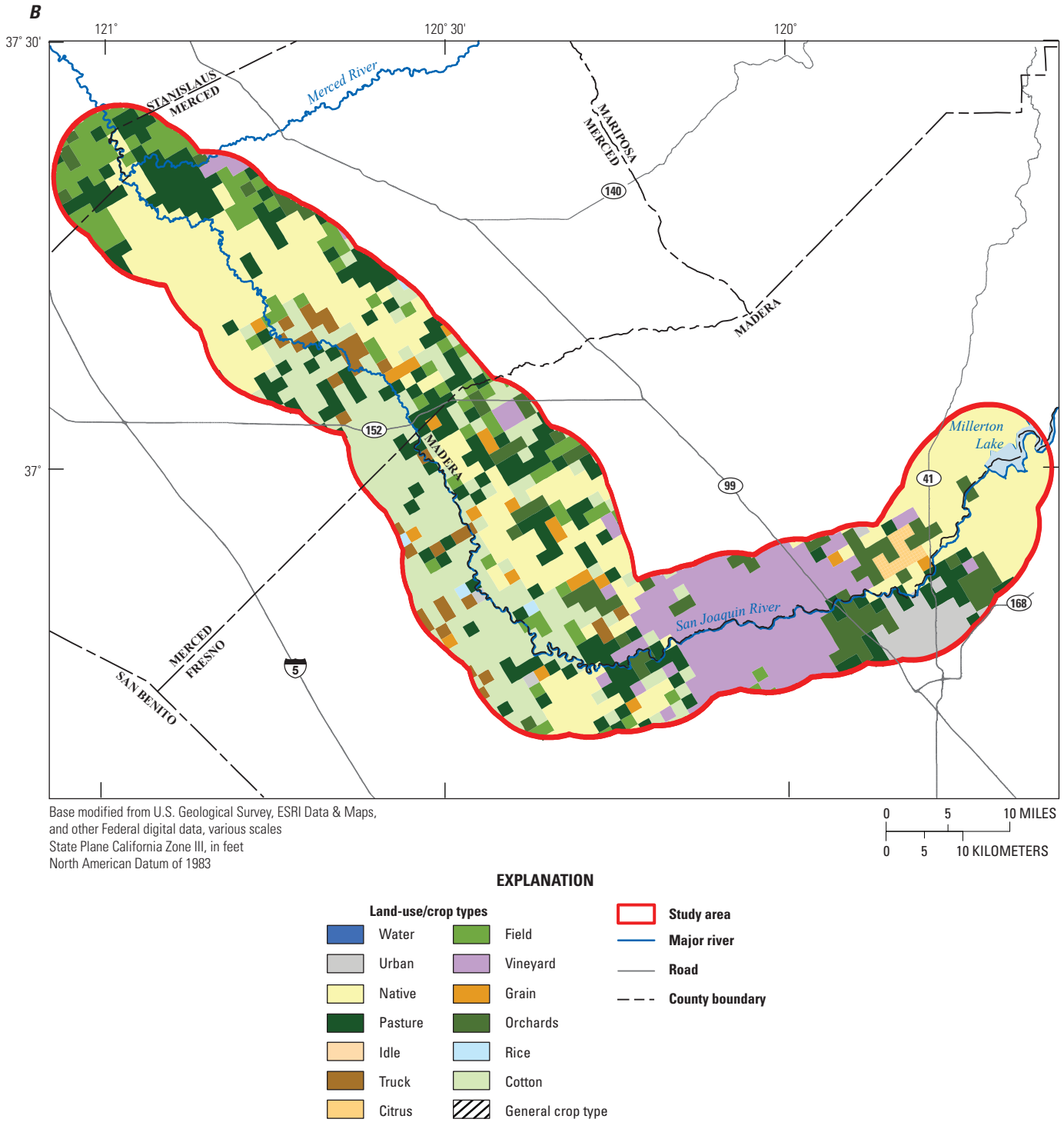

Figure 11. —Continued

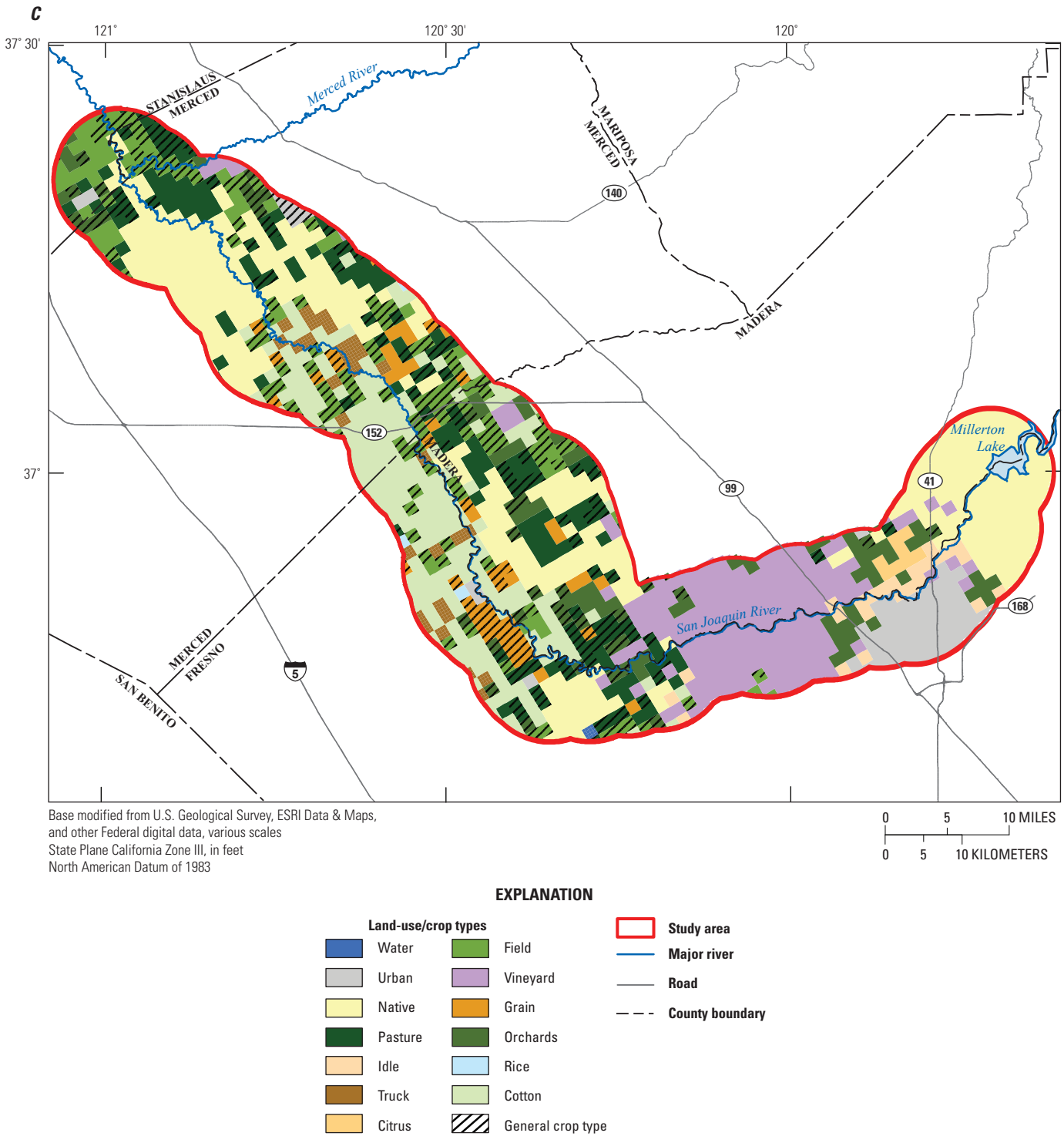

Figure 11. —Continued

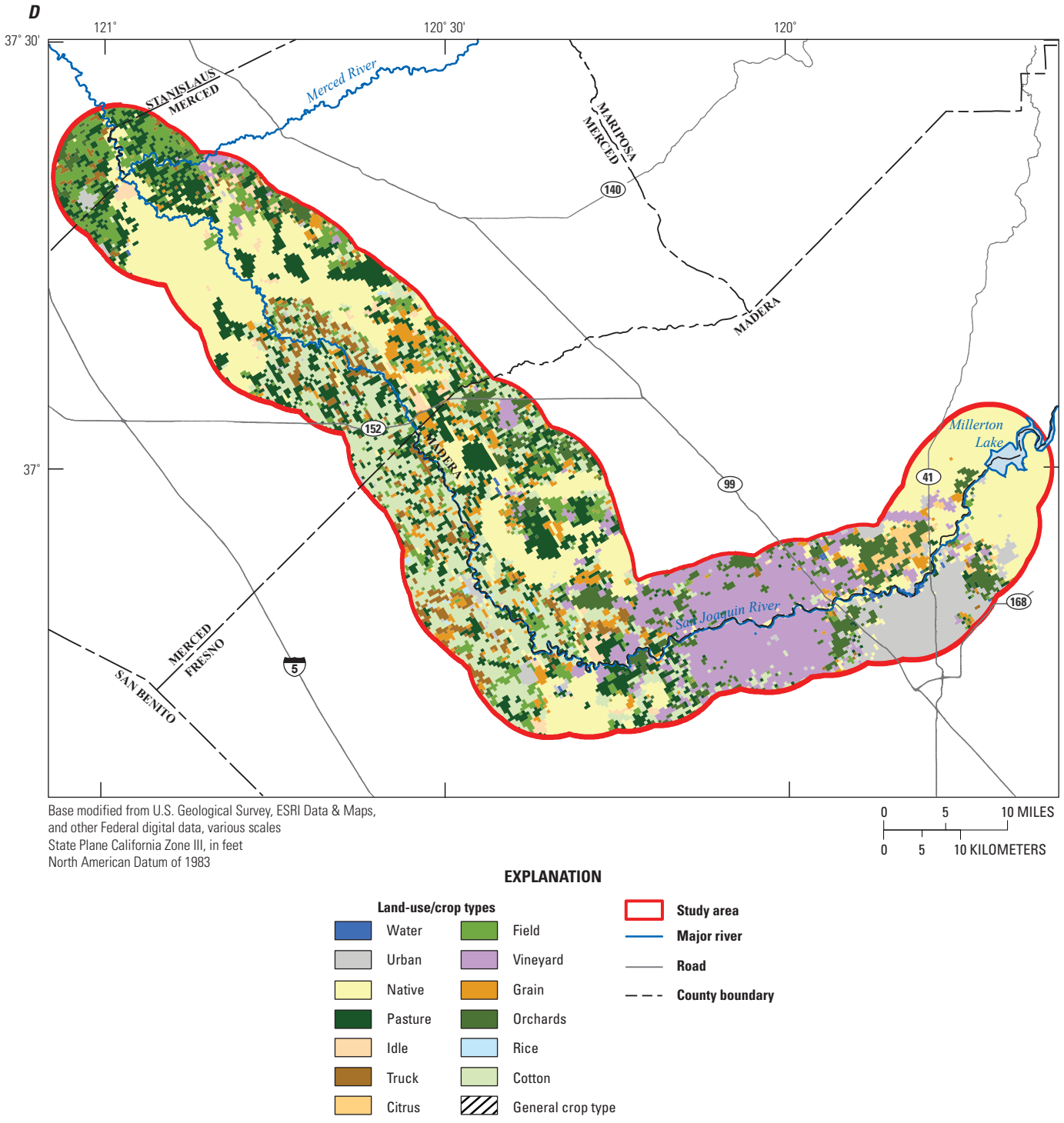

Figure 11. —Continued

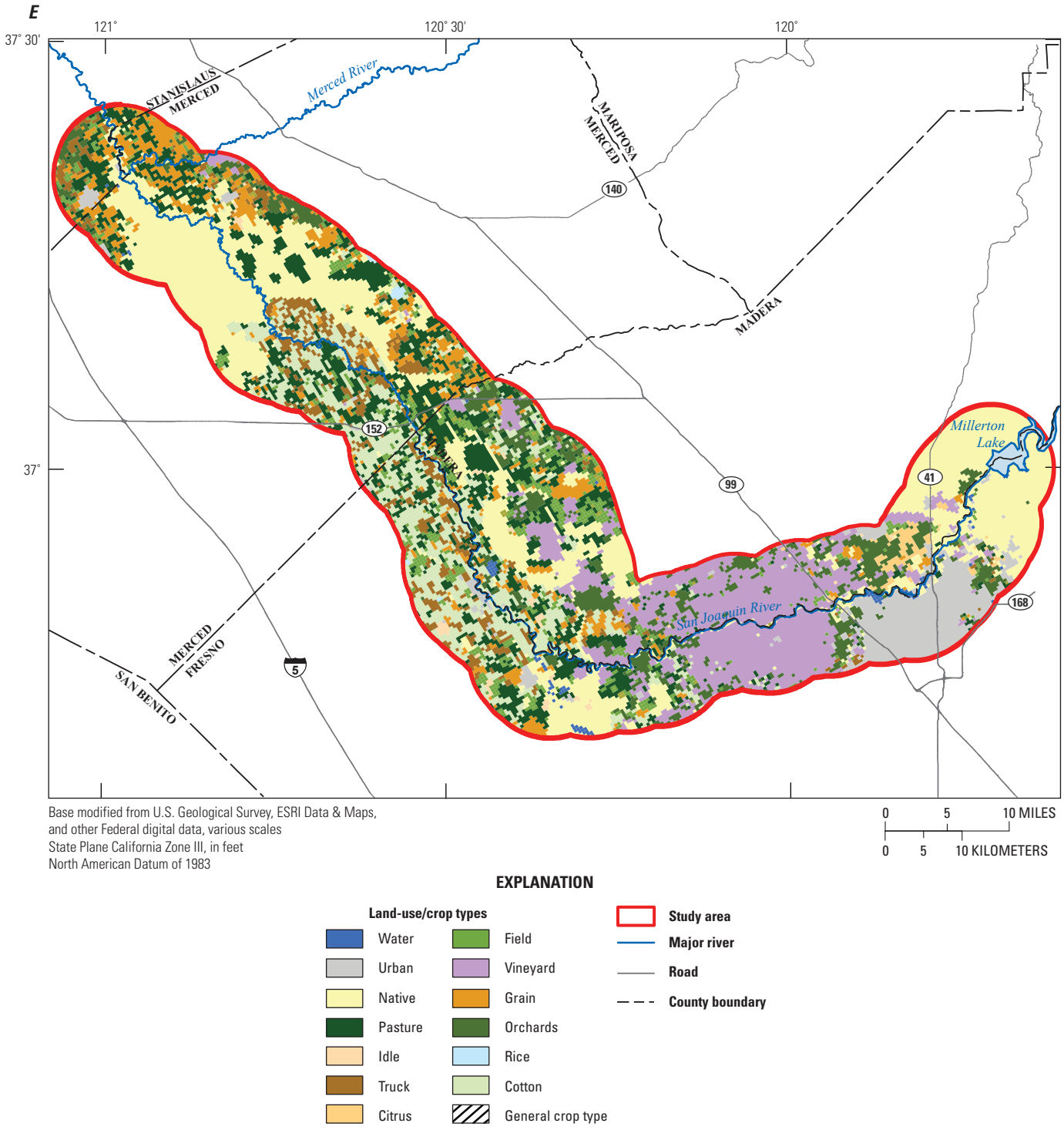

Figure 11. —Continued

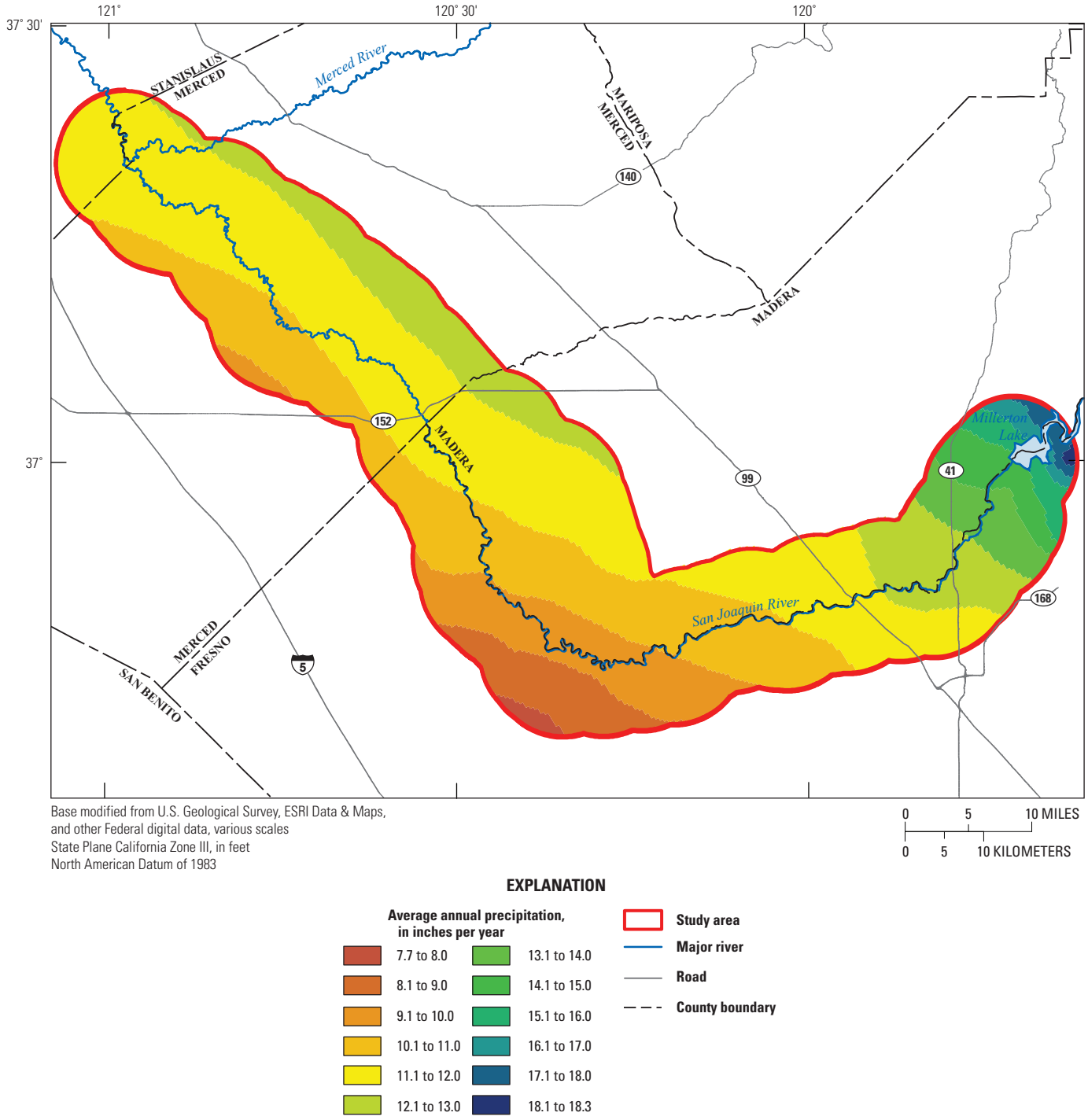

Figure 12. Annual average precipitation in the study area, San Joaquin Valley, California.

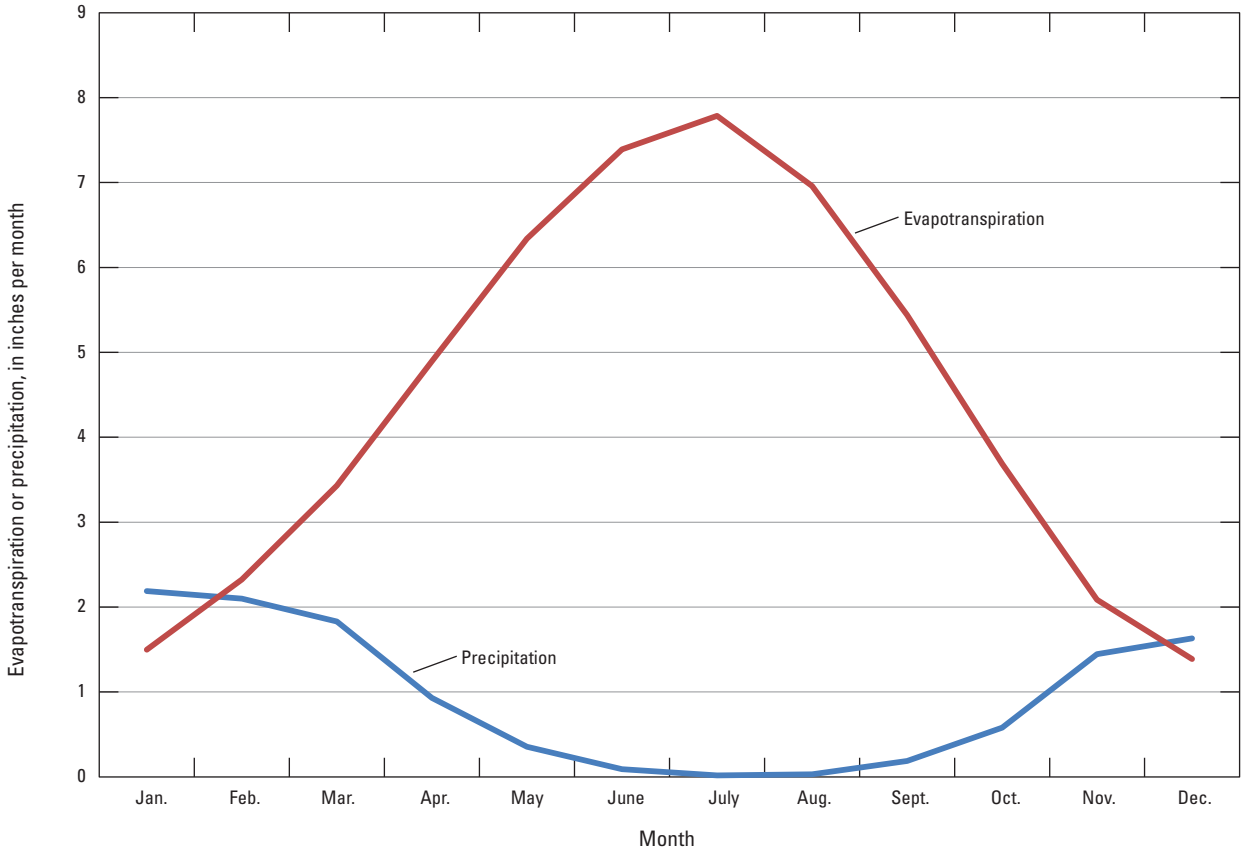

Figure 13. Monthly average precipitation and evapotranspiration (ET_o) in the study area, San Joaquin Valley, California.

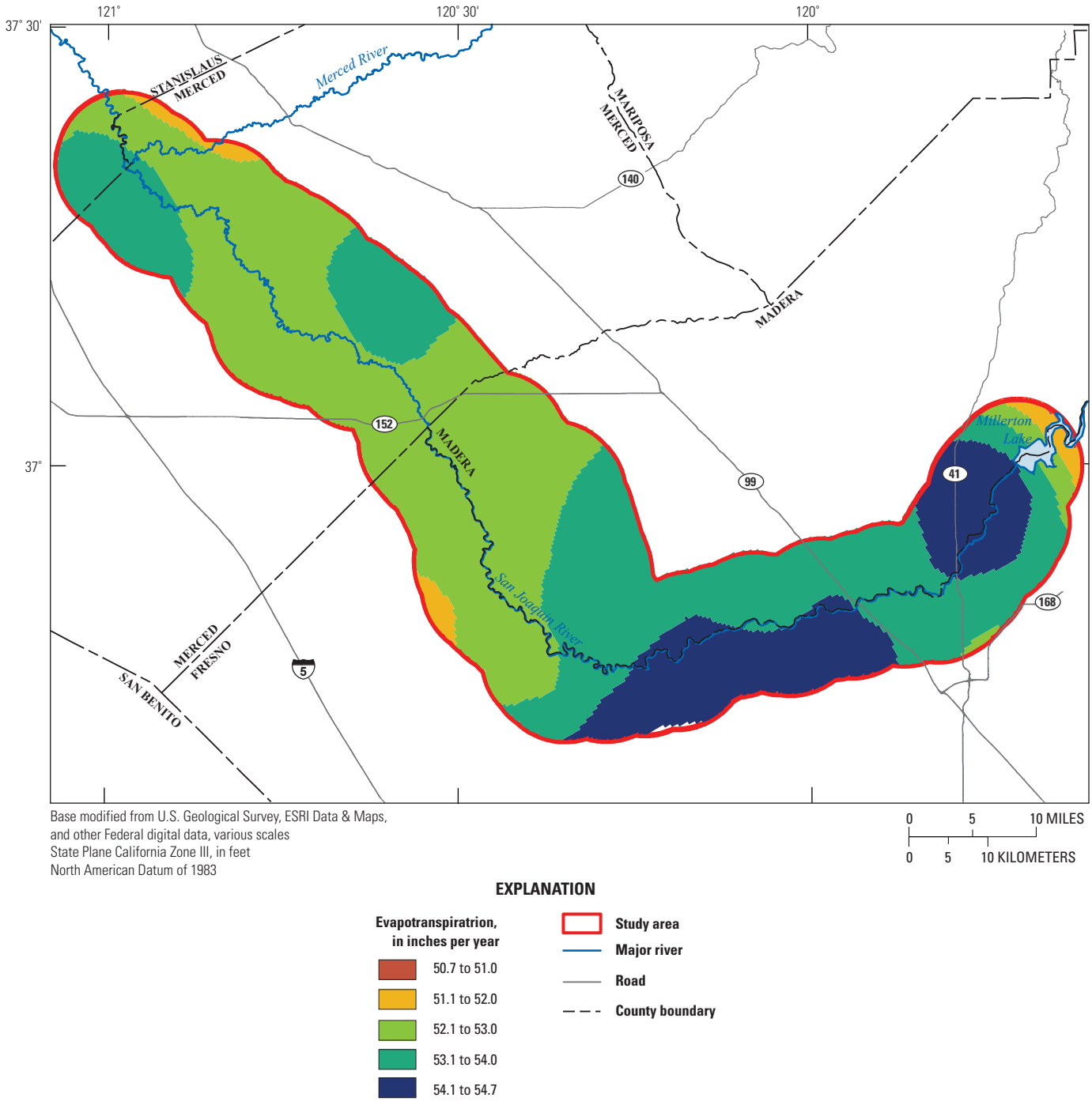

Figure 14. Annual average evapotranspiration in the study area, San Joaquin Valley, California.

Water Supply and Demand Data

Agriculture is the single largest user of water in the study area. Urban areas are small relative to the agricultural area, and their corresponding water use is also small by comparison. The study area also includes several irrigated wildlife management areas. Agriculture in the study area relies on groundwater and surface water for irrigation purposes. The area west of the San Joaquin River irrigates predominantly with surface water, and the area to the east of the San Joaquin River irrigates predominantly with groundwater.

Surface-water deliveries for agriculture are reported by Reclamation and DWR, the Federal and state water providers. Much of the study area west of the San Joaquin River receives surface water through the Federal Central Valley Project (CVP). Monthly deliveries from 1970 to present are well documented by individual water purveyor. CVP delivery records from 1993 to present are available online (U.S. Bureau of Reclamation, Central Valley Operations Office, 2011). CVP delivery records during 1970–92, available in hard-copy format from DWR (California Department of Water Resources, written commun., 2009), were obtained and digitized.

Parts of the study area east of the San Joaquin River receive CVP water via the Madera Canal, for which data are available. Much of the surface water on the east side is derived from local supplies, such as the Kings, San Joaquin, Fresno, and Chowchilla Rivers. Data for deliveries of local surface-water supplies to individual water purveyors generally are not available. To estimate these deliveries, annual surface-water deliveries for 1998–2005, aggregated by DWR into geographic regions called Detailed Analysis Units (DAUs), were obtained from DWR (Chris Montoya, California Department of Water Resources, written commun., 2011). DWR also compiles monthly surface-water delivery data for larger geographic regions called Planning Areas (PAs), which are composed of multiple DAUs. Monthly surface-water deliveries for these PAs during the entire study period (1961–2003) were obtained from DWR (C. Brush, California Department of Water Resources, written commun., 2007) as part of the CVHM study.

Monthly surface-water deliveries to the city of Fresno, city of Clovis, and Fresno Irrigation District were obtained from the annual Kings River Watermaster Reports (Kings River Water Association, 1961–2003). Monthly surface-water deliveries to Gravelly Ford Water District were obtained from CALSIM records (California Department of Water Resources, 2011a).

The aggregated annual surface-water deliveries to the study area from 1961 to 2003 average 860,000 acre-ft, ranging from 410,000 acre-ft in 1977, a drought year, to 1,290,000 acre-ft in 1984 (fig. 15). The largest monthly average surface-water deliveries to the study area during 1961–2003 were during the spring-summer growing season, which coincides with the greatest agricultural demand (fig. 16).

Urban and Wildlife Management Areas Water Supply and Demand

Urban water demand in the study area is driven by municipal water use for the organized communities and by private domestic water use in the rural areas. Municipal water purveyors in the study area include city of Newman, city of Firebaugh, city of Mendota, city of Gustine, city of Dos Palos, Biola Community Services District, community of Bonadelle Ranchos, Pinedale County Water District, city of Fresno, and city of Clovis. Pumping data available for these purveyors (Chris White, Central California Irrigation District, written commun., 2011) were insufficient to develop a complete pumping record for the entire study period. Groundwater pumping for urban water supply was estimated from land-use surveys by assuming an annual pumping rate of 1 acre-ft per acre. The spatial distribution of urban pumping for April 1999–September 2003, for example, coincides with the urban land use for 2000 (fig. 17). By applying this methodology, the total annual estimated urban pumping during the simulation period was estimated (fig. 18*A*); this estimate generally was consistent with the available data. The annual pumping was distributed on a monthly basis (fig. 18*B*) using the monthly distribution of the available data. Rural domestic water use in the study area is supplied though private domestic wells. As with agricultural production wells, little or no data are available for these wells.

The study area contains several wildlife management areas, including North Grasslands Wildlife Areas, Los Banos Wildlife Management Area, San Luis National Wildlife Refuge, and Mendota Wildlife Management Area (fig. 19). These wildlife areas receive surface water though the CVP; data for these deliveries were obtained in the same manner as the CVP agricultural deliveries.

Model Development

Groundwater flow in the SJRRPGW was simulated using MODFLOW-FMP2 (Schmid and Hanson, 2009), which is based on MODFLOW-2005 (Harbaugh, 2005). The Farm Process (FMP2) was used primarily to simulate the supply and demand components of irrigated agriculture. Agricultural pumping data are not available in the study area, so the FMP2 was especially useful for estimating this large component of the groundwater budget. The FMP2 also simulates percolation (below the root zone) of irrigation water and precipitation, a major component of total recharge in the study area. The Hydrogeologic Unit Flow (HUF) Package (Anderman and Hill, 2000) was used to specify the aquifer properties, including hydraulic conductivity, specific yield, and specific storage. The Streamflow-Routing (SFR2) Package (Niswonger and Prudic, 2005) was used to simulate the streams and bypasses in the model and the interaction between these streams and the groundwater system. The Observations Package (Hill and others, 2000) and the HYDMOD Package (Hanson and Leake, 1999) were used to process model results. The MODFLOW packages and processes used in the SJRRPGW are summarized in table 6.

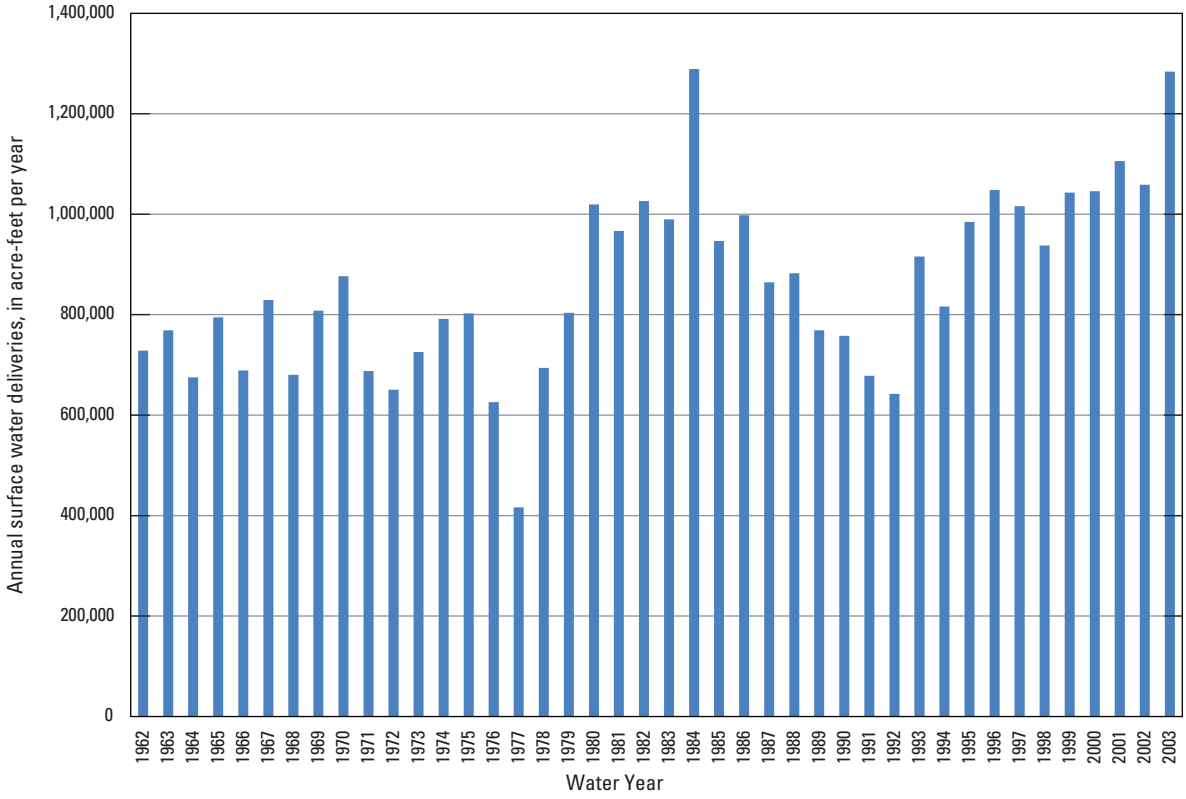

Figure 15. Annual surface-water deliveries to the study area, San Joaquin Valley, California.

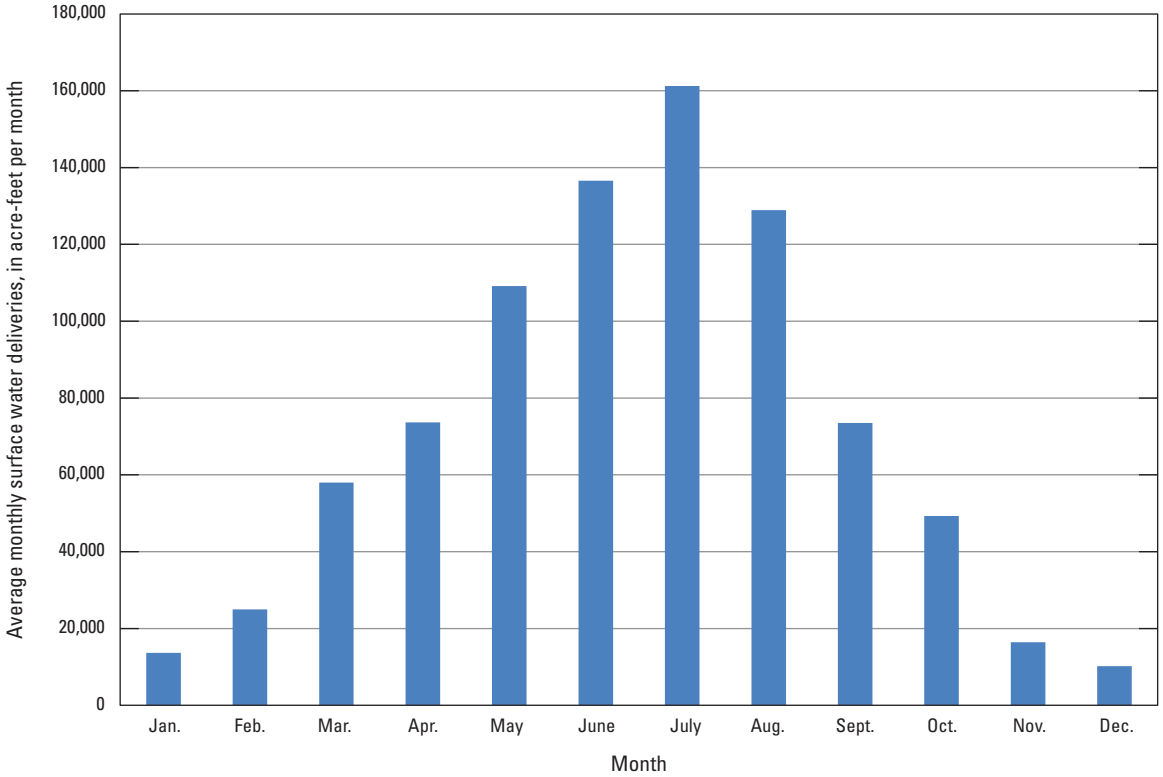

Figure 16. Monthly average surface deliveries to the study area, San Joaquin Valley, California.

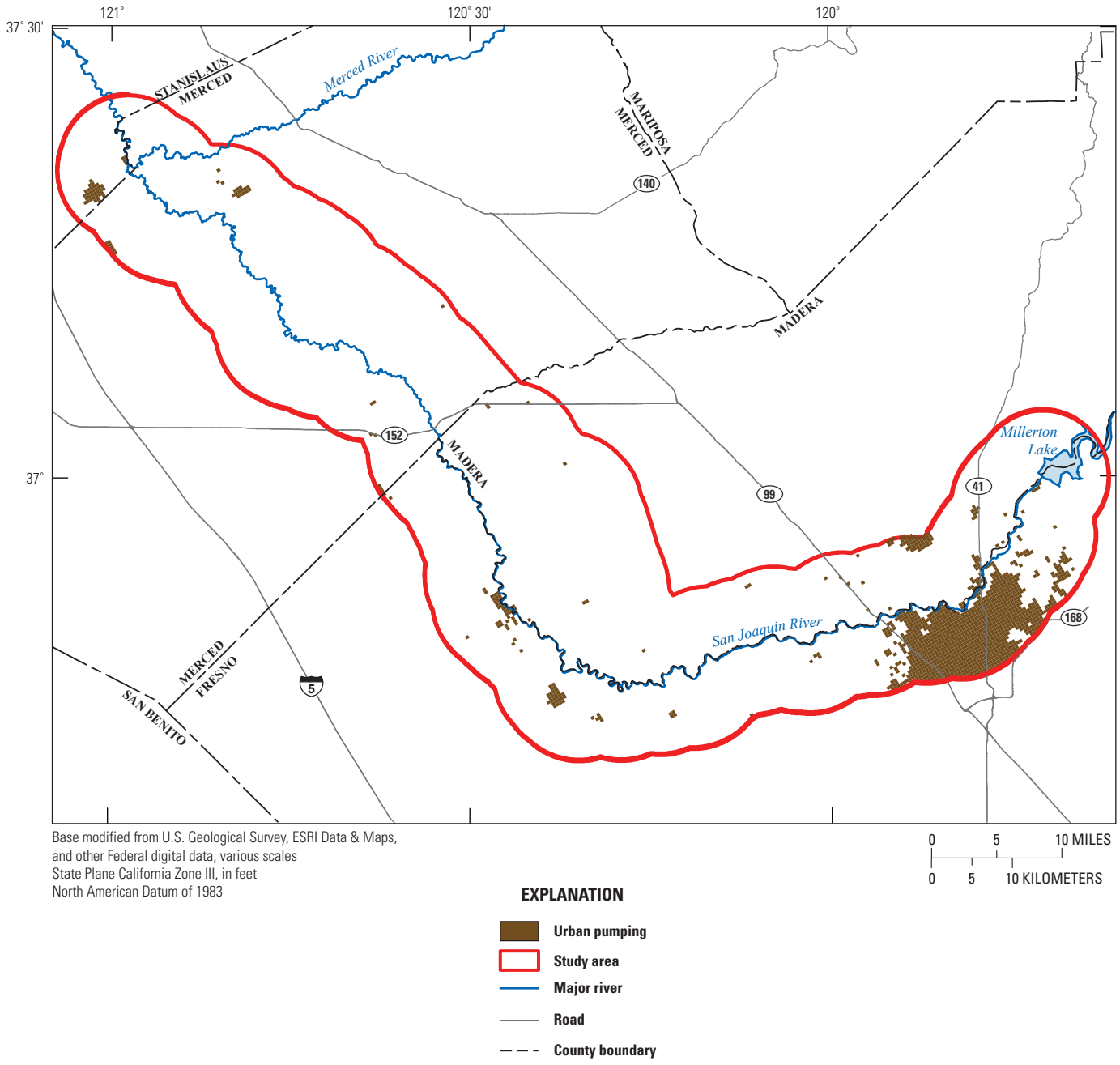

Figure 17. Estimated spatial distribution of urban groundwater pumping in the study area for April 1999–September 2003, San Joaquin Valley, California.

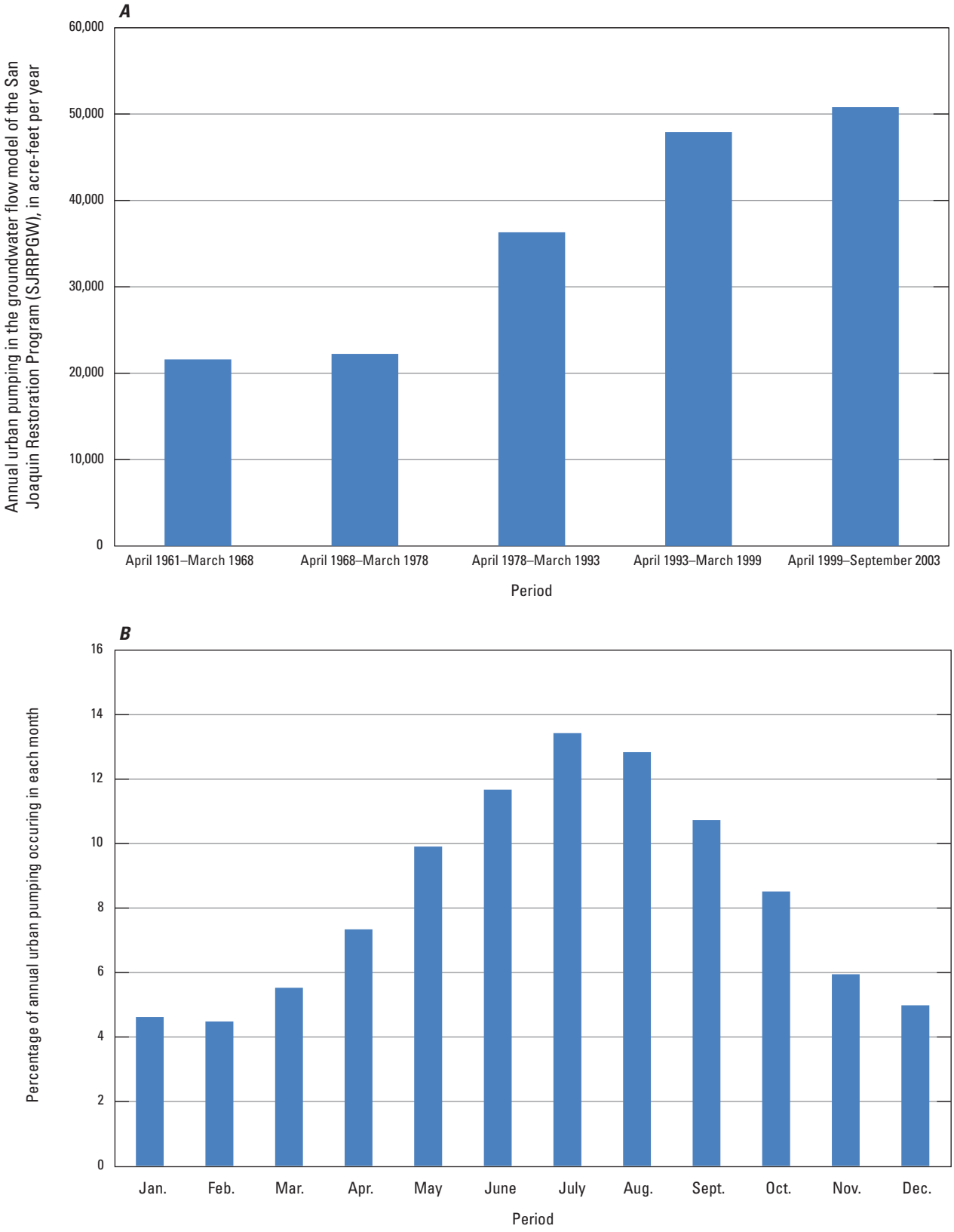

Figure 18. Estimated urban groundwater pumping in the study area, San Joaquin Valley, California: *A*, Annual; *B*, Monthly.

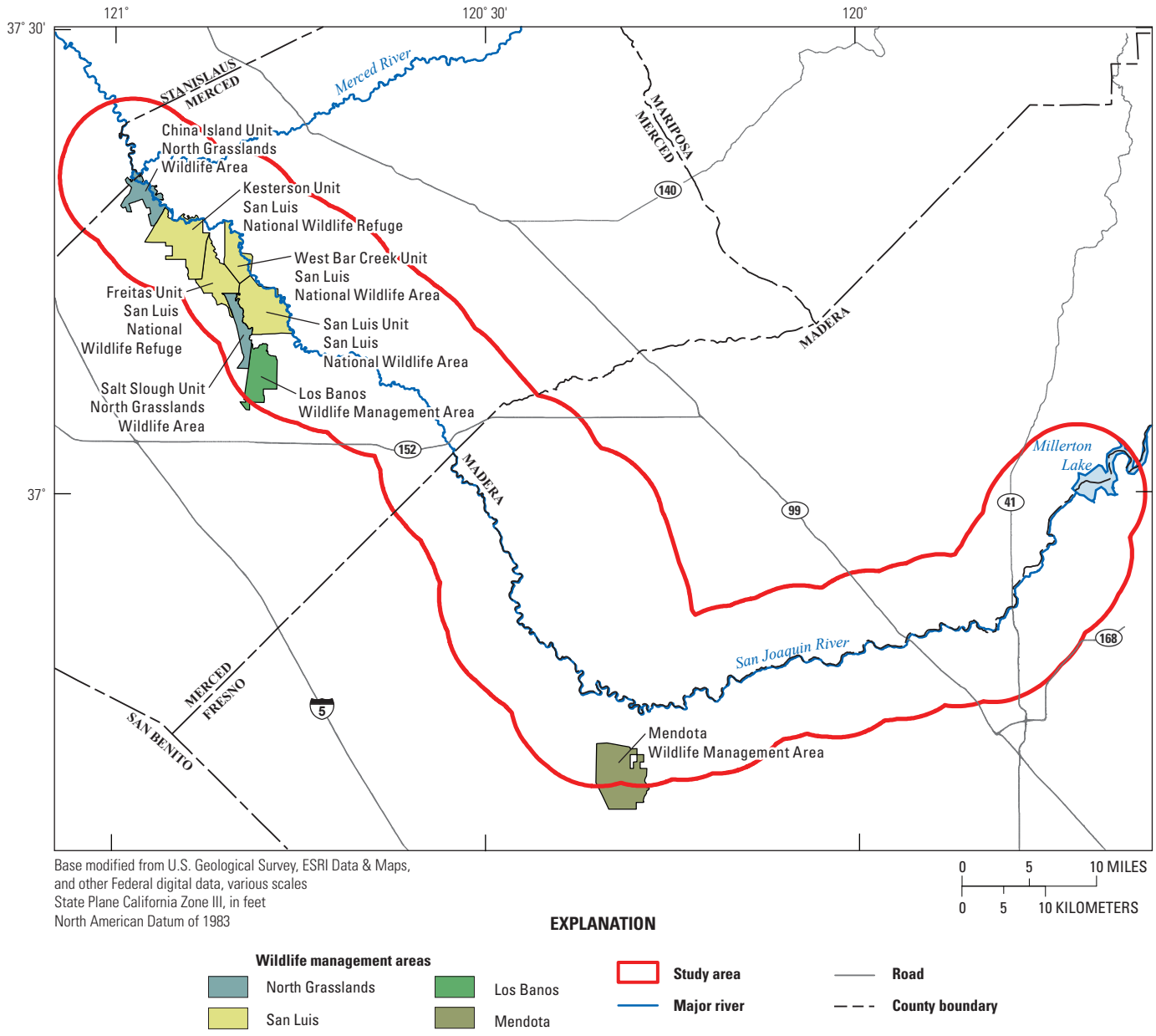

Figure 19. Wildlife management areas simulated in the study area, San Joaquin Valley, California.

Table 6. MODFLOW packages and processes used in the San Joaquin River Restoration Program groundwater flow model (SJRRPGW), San Joaquin Valley, California.

[**Abbreviations**: CVHM, Central Valley Hydrologic Model; TPROGS, Transition-probability geostatistical software; —, no data]

MODFLOW package or process	Acronym	Function	Model input data	Reference
Basic	BAS6	Defining initial conditions and active model layers	Initial groundwater levels, active model cells for each layer	Harbaugh, 2005
Discretization	DIS	Defining spatial and temporal discretization	Grid definition, layer definition, simulation period, stress period and time-step length, ground-surface elevation	Harbaugh, 2005
Farm	FMP2	Simulating the water supply and demand for irrigated land	Subregion definition, soil types, percipitation, evapotranspiration, land use, crop types, crop water-use parameters, surface-water deliveries	Schmid and Hanson, 2009
General-Head Boundary	GHB	Simulating vertical and horizontal boundary flows into and out of the model area	Groundwater elevations at model boundary (from CVHM), boundary conductance	Harbaugh, 2005
Head Observations	HOB	Defining observed groundwater levels used in model calibration	Location of observation wells, dates when observations are avalible	Hill and others, 2000
Hydrologic Unit Flow	HUF2	Defining the properties or aquifer material	Hydraulic conductivity, specific yield, and specific storage for each class of aquifer material	Anderman and Hill, 2000, 2003
Hydmod	HYD	Generating time-series model output for calibration wells and streamgages	Location of streamgages and observation wells	Hanson and Leake, 1999
Name	NAM	Defining the names of the input and output files	—	Harbaugh, 2005
Output Contol	OC	Defining when model output is printed	—	Harbaugh, 2005
Preconditioned Conjugate-Gradient	PCG	Solving the finite difference equations	—	Harbaugh, 2005
Parameter Value	PVAL	Defining model parameters	Model parameters	Harbaugh, 2005
Streamflow Routing	SFR2	Simulating streamflow and the groundwater surface water interactions	Surface hydrology configuration, streamflow, diversions	Niswonger and Prudic, 2005
Zone	ZONE	Defining the aquifer materials	Aquifer texture from TPROGS	Harbaugh, 2005
Well	WEL	Defining urban groundwater pumping	Municipal-well lcoations, municipal	Harbaugh, 2005

Spatial and Temporal Discretization

Spatial Discretization

The study area (fig. 1) is encompassed within a finite-difference grid containing 304 rows and 248 columns with a grid cell size of 0.25 mi by 0.25 mi (fig. 20). The grid is rotated by 34 degrees west of north to coincide with the CVHM grid such that groups of 16 SJRRPGW cells overlay each CVHM cell. Each layer in the grid contains a total of 75,392 cells, of which 21,395 are active, for a total active area of 1,337 mi^2. Some of the active cells in SJRRPGW are outside the CVHM domain (fig. 20). These 1,419 SJRRPGW cells are active for simulating streamflow and certain land-surface processes (such as ET of native vegetation and routing of precipitation to the stream system) but are inactive for simulating groundwater flow, resulting in 19,976 SJRRPGW cells being active for groundwater flow.

The SJRRPGW is vertically discretized into five layers. The top of layer 1 is the mean ground-surface elevation in each cell. Layer 1 elevations were modified where necessary to slope downhill in cells with streams. The bottom of layer 5 coincides with the top of the Corcoran Clay, a low-permeability unit. Layers 1–3 are each 16.7 ft thick; layer 4 is 100 ft thick; and layer 5 is the remaining thickness down to the Corcoran Clay (116 ft average).

The five SJRRPGW layers coincide with the upper three layers of CVHM. Layers 1–3 of the SJRRPGW correspond to layer 1 of the CVHM; layer 4 of the SJRRPGW corresponds to layer 2 of the CVHM; and layer 5 of the SJRRPGW corresponds to CVHM layer 3. This refinement of the shallow part of the aquifer system allows for more accurate representation of near-surface physical features and increases the capability of accurate simulation of the shallow water table.

Temporal Discretization

The SJRRPGW is a transient model that simulates monthly groundwater and surface-water flow from April 1961 through September 2003. This 42.5-year simulation period coincides with that of the CVHM, which is used for SJRRPGW external groundwater elevation and streamflow and boundary conditions. In addition to corresponding to the CVHM, the 1961–2003 period is associated with a range of climatic variability such as the 1976–77 and 1987–92 droughts and the 1982–1984 and 1995–2000 wet periods. Also, several key datasets needed for model development (for example, surface-water deliveries) and calibration (for example, groundwater elevations) are available during the 1961–2003 period.

The simulation period is 510 monthly stress periods; time-varying input data, such as ET_o, rainfall, and stream inflow, are specified as monthly average values for each stress period. The stress periods were further divided into two equal-length time steps, primarily to aid in numerical convergence. Model output such as groundwater elevations, stream stage, and flow components of groundwater, surface water, and irrigated agriculture were calculated for each time step.

Simulation of Irrigated Agriculture and Other Land-Surface Processes

The FMP2 (Schmid and Hanson, 2009) was used to simulate the supply and demand components of irrigated agriculture as well as other land-surface processes. The components and processes simulated include precipitation, surface-water delivery, pumping of groundwater, plant uptake of shallow groundwater, plant evapotranspiration, on-farm efficiencies, precipitation runoff, irrigation runoff, and percolation to groundwater. This report provides an overview of how the FMP2 functions with regard to those components used for the SJRRPGW. For a comprehensive description of the FMP2, including its theoretical and mathematical underpinnings, the FMP2 documentation (Schmid and Hanson, 2009) should be consulted.

Subregion Definitions

The FMP2 simulates key processes on the basis of groups of cells called subregions. The SJRRPGW was divided into 28 subregions (table 7 and fig. 21). Because the dominant land use in the study area is irrigated agriculture, the subregions are defined primarily on the basis of the boundaries of water purveyors in the study area, including water districts, irrigation districts, and municipal service areas. In areas not organized into water or irrigation districts, the subregion boundaries are based on rivers. Because the subregion divisions are based on the boundaries of water purveyors, the divisions also coincide with the available data on surface-water deliveries.

Irrigation Water Demand

For each model cell, the irrigation requirement is a function of crop type and ET_o. For every stress period, each cell is assigned a crop type on the basis of the dominant land use in that cell as shown in the maps of crop distribution (fig. 11*A–E*). The irrigation requirement for a cell is calculated by FMP2 as the product of ET_o and the crop coefficient for the crop type. The irrigation requirement is then increased to account for evaporation of irrigation water. The irrigation demand for a cell is calculated by dividing the irrigation requirement by the irrigation efficiency, which is specified for each crop in each subregion. The total irrigation demand for a subregion is calculated by summing the irrigation demand for each model cell in the subregion. This calculation is done for each model stress period, because the crop type, ET_o, irrigation efficiencies, and some of the crop properties can change with each stress period.

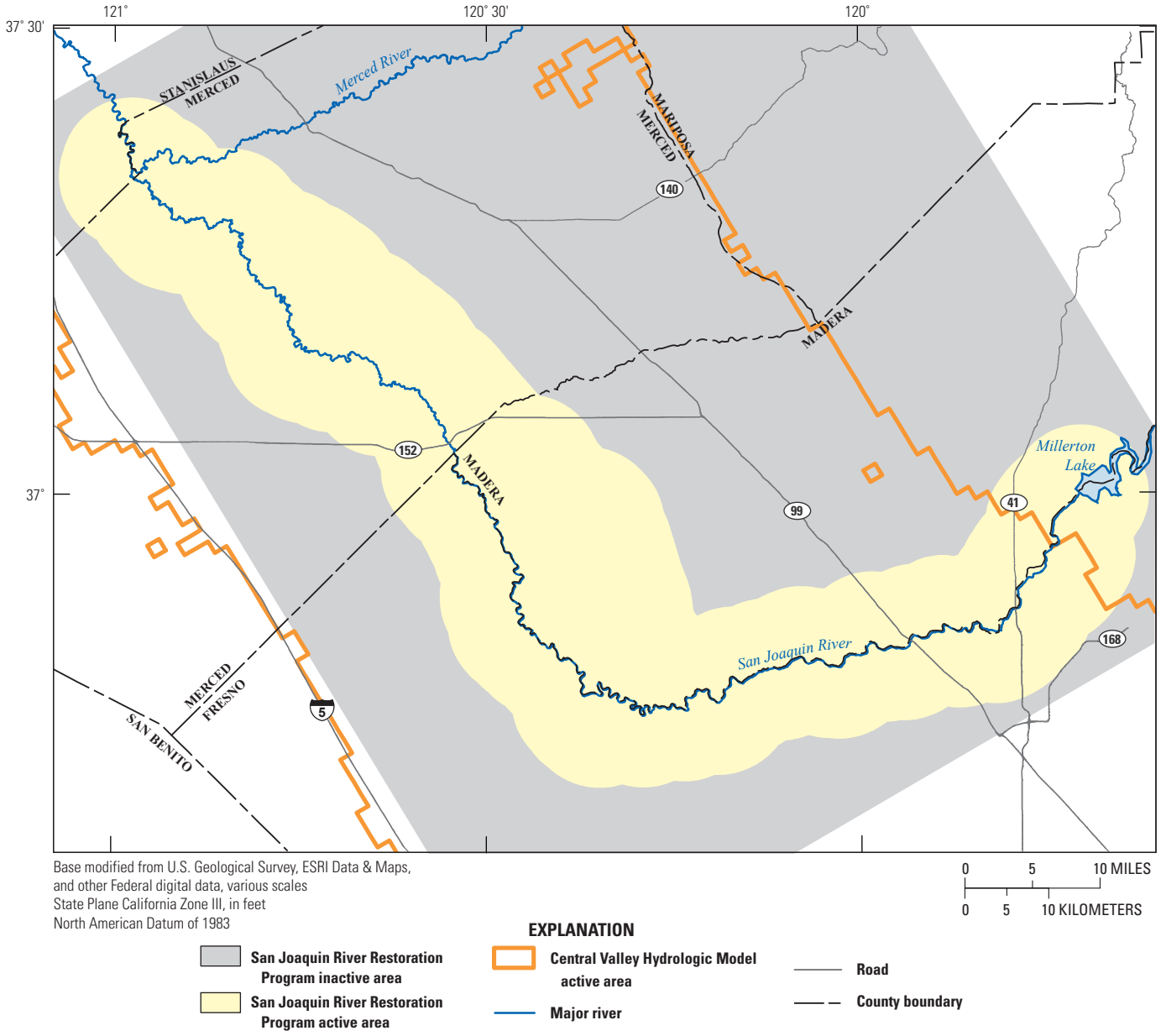

Figure 20. San Joaquin River Restoration Program groundwater flow model (SJRRPGW) grid, San Joaquin Valley, California.

Table 7. San Joaquin River Restoration Program groundwater flow model (SJRRPGW) subregion descriptions, San Joaquin Valley, California.

[**Abbreviations**: I.D., Irrigation District; W.D., Water District]

Subregion number	Subregion name	Simulated area (acres)	Description
1	Turlock I.D.	16,000	Portion of Turlock Irrigation District within the model area.
2	Central California I.D. North	26,000	Portion of Central California irrigation District within the model area and portion of the City of Gustine within the model area .
3	City of Newman	2,000	Municipal Service Area for the City of Newman .
4	Stevenson W.D.	52,000	Bounded on the west by the San Joaquin River Reach 5; on the north by the Merced River; on the east by the model boundary; and on the south by the Bear River. Includes Stevenson Water District.
5	Grasslands W.D.	20,000	Portion of Grasslands Water District within the model area and Los Banos Wildlife Management Area.
6	Wildlife Refuges	36,000	North Grasslands Wildlife Area, Kesterson National Wildlife Area, and San Luis National Wildlife Refuge.
7	Unorganized Merced County	39,000	Bounded on the west by the San Joaquin River Reach 4B2; on the north by the Bear River; on the east by the model boundary; and on the south by Deadmans Creek and Mariposa Slough.
8	Turner Island W.D.	36,000	Bounded on the west by the San Joaquin River Reach 4B1; on the north by Deadmans Creek and Mariposa Slough; on the east by the model boundary and El Nido I.D.; and on the south by the Chowchilla River. Includes Turner Island Water District.
9	San Luis Canal Company	47,000	Portion of San Luis Canal Company within the model area.
10	El Nido I.D.	8,000	El Nido Irrigation District.
11	Chowchilla W.D.	24,000	Portion of Chowchilla Water District within the model area.
12	Unorganized Madera County	31,000	Bounded on the west by the Sierra W.D. and Clayton W.D.; on the north by El Nido I.D.; on the east by Chowchilla W.D. and Madera I.D.; and on the south by the Fresno River.
13	Sierra W.D.	13,000	Sierra Water District (currently inactive).
14	Clayton W.D.	3,000	Clayton Water District.
15	Central California I.D. South	54,000	Portion of Central California irrigation District within the model area; the City of Firebaugh; and Camp 13.
16	Firebaugh Canal Company	20,000	Portion of Firebaugh Canal Company within the model area.
17	Westlands W.D.	27,000	Portion of Westland Water District within the model area; portion of Broadview water district within the model area; and the city of Mendota.
18	Columbia Canal Co.	19,000	Columbia Canal Company.
19	New Stone W.D.	36,000	Bounded on the southwest by Columbia Canal Co.; on the north by the Fresno River, and on the east by the Chowchilla Bypass. Includes New Stone Water District.
20	Farmers W.D.	2,000	Farmers Water District.
21	Allso W.D.	45,000	Bounded on the south by the San Joaquin River Reach 2A; on the west by the Chowchilla Bypass; on the north by the Fresno River; and on the east by the model boundary and Gravelly Ford W.D. Includes Allso Water District.
22	Mendota Wildlife Area	41,000	Bounded on the north by the San Joaquin River Reach 2A, Farmers W.D., and Columbia Canal Co.; on the west by Westlands W.D.; on the south by the model boundary; and on the east by Fresno I.D. Includes a portion of the Mendota Wildlife Management Area in the model area.
23	Gravelly Ford W.D.	8,000	Gravelly Ford Water District.
24	Madera I.D.	48,000	Portion of Madera Irrigation District in model area.
25	Fresno I.D.	44,000	Portion of Fresno Irrigation District in model area and the community of Biola.

Table 7. San Joaquin River Restoration Program groundwater flow model (SJRRPGW) subregion descriptions, San Joaquin Valley, California.—Continued

[**Abbreviations**: I.D., Irrigation District; W.D., Water District]

Subregion number	Subregion name	Simulated area (acres)	Description
26	Bonadelle Ranchos	72,000	Bounded on the southeast by the San Joaquin River Reach 1A, on the west by Madera I.D., and on the north by the model boundary. Includes a portion of the community of Bonadelle Ranchos.
27	City of Fresno	48,000	Portion of the city of Fresno in the model area, portion of the city of Clovis in the model area, and Pinedale County W.D.
28	Foothills	39,000	Bounded on the northwest by the San Joaquin River Reach 1A, on the south by the cities of Fresno and Clovis, on the east by the model boundary.

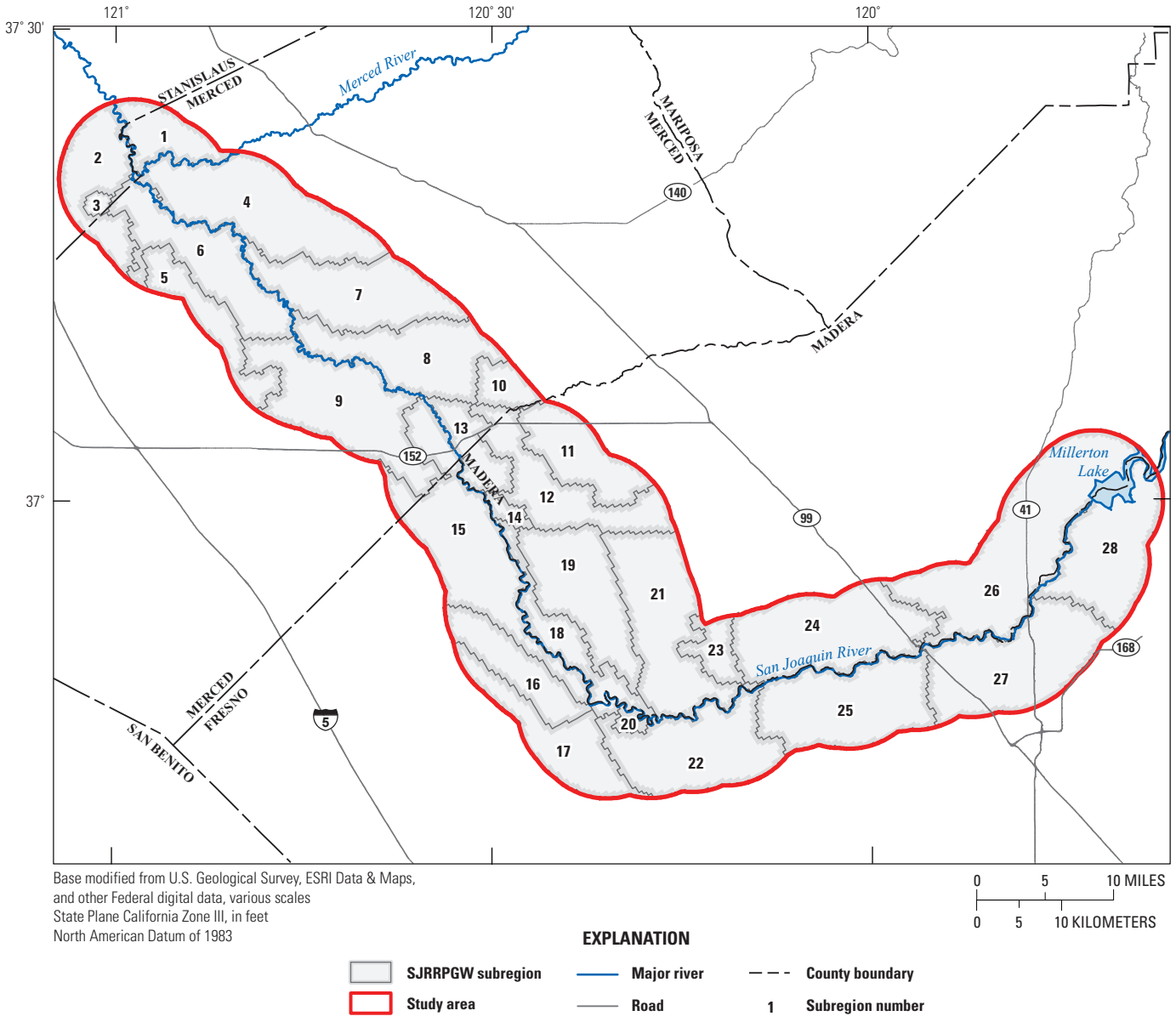

Figure 21. San Joaquin River Restoration Program groundwater flow model (SJRRPGW) subregions, San Joaquin Valley, California.

Irrigation Water Supply

Water to meet the irrigation demand of a subregion is supplied, in this order, by precipitation, root uptake of shallow groundwater, surface-water deliveries, and groundwater production. For each subregion, FMP2 first meets irrigation demand with precipitation, which is reduced by a crop-dependent precipitation runoff factor and then bygroundwater uptake. Next, FMP2 attempts to meet the remaining irrigation demand with surface-water delivery, which also is reduced by a crop-dependent irrigation runoff factor. If any irrigation demand is unmet by surface-water delivery, the FMP2 calculates the groundwater production needed for each subregion to meet the remaining irrigation demand. For non-irrigated crop types, such as native vegetation, the FMP2 reduces the consumptive use of the crop such that the evapotranspiration from the crop does not exceed available water (precipitation and groundwater uptake).

Data on the location and properties of the active agricultural production wells are not available for the study area. For the SJRRPGW, a virtual, or hypothetical, agricultural well was placed in each model cell containing an irrigated crop. The virtual agricultural well extracts groundwater during stress periods when the FMP2 calculates a remaining irrigation demand for that cell. The total monthly groundwater production calculated by FMP2 is distributed evenly to all active agricultural wells in each subregion.

The virtual well approach simulates a total of 19,976 wells, which is more than are estimated to exist in the study area. Thus, each virtual well generally is pumping less water than a typical irrigation well would pump. Therefore, the SJRRPGW tends to underestimate local drawdowns near real irrigation wells and, conversely, tends to overestimate local drawdowns in areas distant from real irrigation wells. However, the virtual well approach reasonably estimates regional drawdowns.

Development of Farm Process Datasets

Ground-surface elevation is used by the FMP2 to route runoff from rainfall and irrigation to the simulated streams and to estimate transpiration of shallow groundwater. *Soils* data are used to define the capillary fringe depth and other parameters that influence transpiration from groundwater. Precipitation data are used to calculate water supply, runoff, and percolation to groundwater associated with rainfall. Values of ET_o and crop coefficients are used with *land-use and crop data* to calculate the potential evapotranspiration for each model cell.

Monthly agricultural surface-water deliveries to each model subregion were determined by aggregating all available data. If data were not available at the scale of the subregion, deliveries were estimated by using the available data at a larger scale, such as a Detailed Analysis Unit (DAU), and multiplying by the fractional area of agricultural land in the DAU that is within the subregion. Similarly, for areas served by water purveyors that are clipped by the model boundary, the surface-water delivery to the portion within the study area was estimated by multiplying the total delivery to the purveyor by the percentage of the agricultural land within the study area.

In addition to irrigated crops, a specific crop type, called irrigated native vegetation, was defined for the wildlife management areas. The crop water-use parameters for irrigated native vegetation are the same as non-irrigated native vegetation, but the crop type is irrigated. As with other irrigated lands, virtual wells were placed in each model cell in the wildlife management areas. This assumption is consistent with the DWR DAU water budgets, which indicate groundwater as a source for some wildlife management areas to provide adequate water supplies to native vegetation to keep it healthy and not stressed (Chris Montoya, California Department of Water Resources, written commun., 2011).

Simulation of Surface Water

The SJRRPGW simulates streamflow and groundwater/surface-water interactions for the major streams and bypasses in the study area using the Streamflow-Routing Package (SFR2) (Niswonger and Prudic, 2005). The streamflow network is simulated using 1,697 stream reaches, each corresponding to an SJRRPGW model cell that underlies the stream network. The stream reaches were grouped into 91 stream segments, such that reaches in each segment had similar hydrologic characteristics. These hydrologic characteristics include the streambed slope and the relation between the stream stage, width, and discharge (stream rating table). For the San Joaquin River, Chowchilla Bypass, Eastside Bypass, and Mariposa Bypass, these characteristics were obtained from a Hydrologic Engineering Centers River Analysis System (HEC-RAS) model of the San Joaquin River (Tetra Tech, 2010). For other simulated streams, these characteristics were obtained from the CVHM datasets (Faunt, 2009).

Measured streambed elevations used to construct the HEC-RAS model were highly variable, and the discretization was much smaller than for the SJRRPGW cells; therefore, a smoothed representation was used for model input. An example of the measured streambed elevations for the Chowchilla Bypass Bifurcation Structure and the simplified streambed elevations used in the SJRRPGW are shown in figure 22. The stream stage-discharge relation for the Chowchilla Bypass is also shown in figure 22. The vertical lines show the segment divisions that were placed where major changes occur in either the streambed slope or the stream rating table.

Calculation of Streamflow

The SFR2 tracks streamflow within the SJRRPGW by routing the flow in each of the stream segments to the next downstream segment. Surface water enters the SJRRPGW at 10 locations where inflow data are available. Nine of these segments are located where the streams enter the model boundary. The 10th inflow is from the Delta Mendota Canal

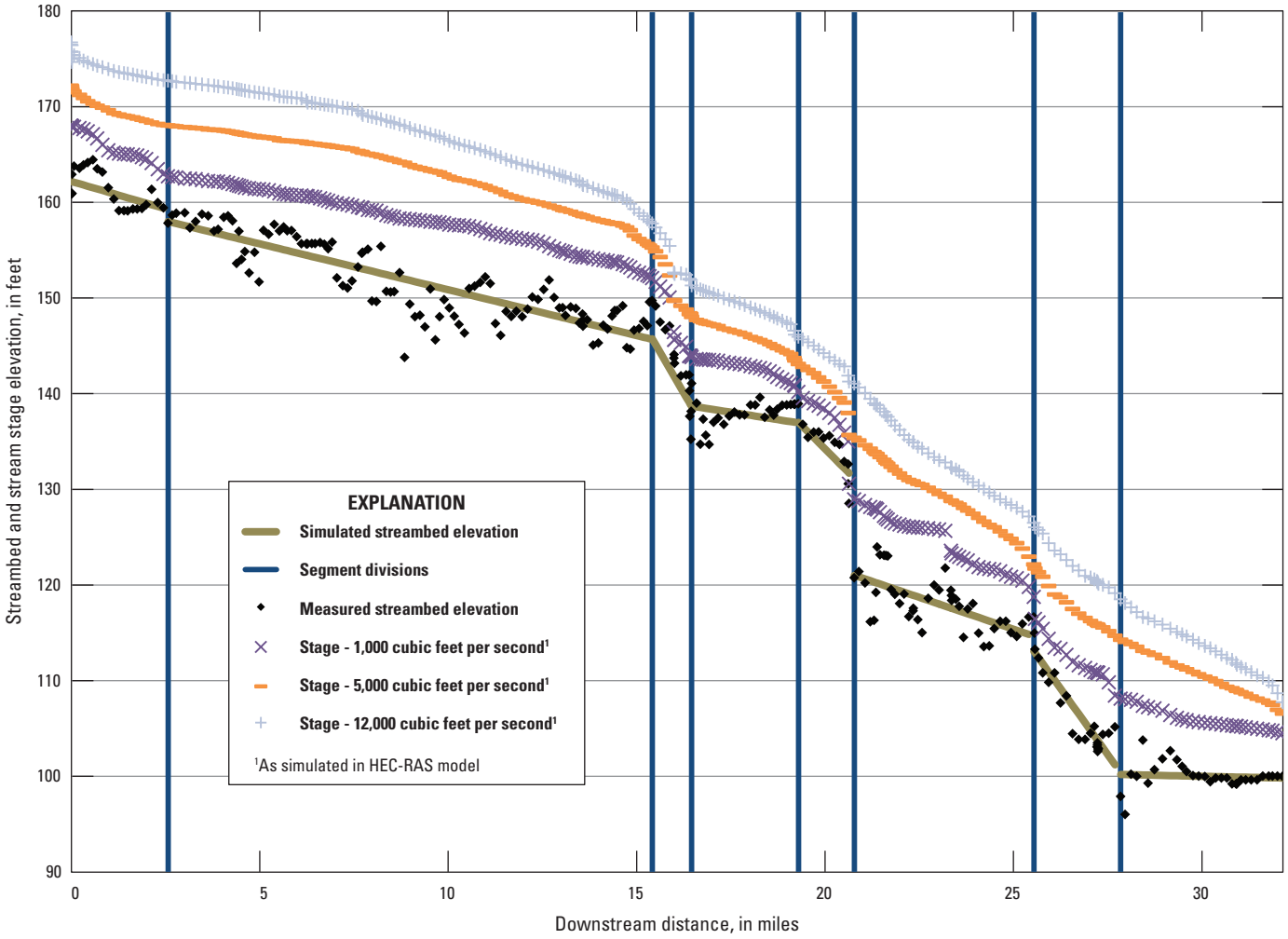

Figure 22. Streambed elevation along Chowchilla Bypass, San Joaquin Valley, California.

at Mendota Pool on the San Joaquin River (segment 35); this inflow is added to the other flows entering the stream segment from within the study area.

Surface water exits the SJRRPGW at the farthest downstream segment on the San Joaquin River (segment 91) and at Sack Dam on the San Joaquin River (segment 45). The Sack Dam diversion is based on historical data and results in some (or all) of the flow being diverted out of the streamflow network.

Many confluences in the SJRRPGW route water from two stream segments to the same downstream segment. There are also three bifurcations where outflow may be divided into two downstream segments, on the basis of historical data. These bifurcations are at Chowchilla Bypass Bifurcation Structure (segment 26), Sand Slough Bypass Control Structure (segment 56), and Mariposa Bifurcation Structure (segment 66) (fig. 5).

Within a stream segment, SFR2 routes the outflow from one reach to the next downstream reach. In each reach, flow can be increased or decreased because of the interaction of surface water and groundwater or can be increased because of runoff of irrigation water or precipitation calculated by the FMP2.

Interaction of Surface Water and Groundwater

SFR2 calculates the stream stage on the basis of the streambed elevation, flow in the stream, and other stream hydraulic characteristics. SFR2 uses this stream stage to calculate the hydraulic gradient between the stream and the model cell representing the top of the aquifer system underlying the stream. If the stream stage is above the head in the cell (positive hydraulic gradient), the stream loses water to the aquifer system; conversely, if the steam stage is below the head in the cell (negative hydraulic gradient), the stream gains water from the aquifer system.

The magnitude of the stream gain or loss is controlled by the magnitude of the hydraulic gradient and the streambed conductance. Streambed conductance is a property of the length of the stream in the cell, the streambed thickness,

the stream width, and the streambed hydraulic conductivity. The stream length within a cell was calculated by overlaying the stream network with the model grid using a geographic information system (GIS) software. The streambed thickness is assumed to be 3.28 ft (1 m). The streambed hydraulic conductivity was initially set to 1 foot per day (ft/d) for all segments, but it was modified during calibration.

Tile Drains (fig. 5) are present in the southwest corner of the model in the eastern portion of the Grasslands Drainage Area. These drains are not simulated in the model because specific information on the drains is not available to the extent that would be needed to include them in the simulation (such as the depth of drain laterals and the time series of flow rates). In addition, most of the drained area is outside the model boundary. The lateral general-head boundary imposed on the SJRRPGW in this area attempts to account for the net effects of tile drainage in the Grasslands Drainage Area on the model. Note, the SFR2 segments that have no inflow component (such as Mud and Salt Slough) gain flow from groundwater and runoff and, thus, act like drains in the simulation.

Simulation of Groundwater

Initial Conditions

Calibration of a steady-state simulation to calculate the initial groundwater elevations was not done for the SJRRPGW because of minimal observations available prior to and during the early period of human development in the area in the late 1800s. Initial groundwater elevations used in the model were estimated by developing a map of the spring 1961 groundwater elevation. Measurements for 611 wells for the period mid-February through early-May 1961 were selected to represent spring conditions. This particular period was selected in order to maximize the number of data points and to avoid measurements of groundwater elevation that coincided with the onset of the growing season. For wells having multiple measurements, the date closest to the middle of that period (last week of March) was selected. Groundwater elevations that indicated possible measurement error or non-static conditions or that appeared to represent dynamic conditions were excluded.

The map of groundwater elevation for spring 1961 was developed using GIS software and the inverse distance weighting (IDW) method of interpolation with a 32.8 ft (10 m) grid. This grid was then overlain onto the SJRRPGW grid for calculating the initial groundwater elevations. Using this method, the computed groundwater-elevation map represents composite groundwater levels aggregated vertically and distributed areally.

The spring 1961 groundwater elevation was used as the initial groundwater elevation for all five model layers. The model was then run for 12 stress periods (1 year). The resulting heads were subsequently used as the spring 1961 starting heads (fig. 23). This method dissipates the head and flow transients in the model caused by the inherent disequilibrium related to the compositely estimated initial heads and establishes vertical head gradients between model layers on the basis of their relative hydrogeologic properties. During calibration, this procedure was periodically repeated as the model parameters changed to ensure the initial conditions were consistent with the final calibrated parameters.

Boundary Conditions

The lateral and lower boundary conditions are simulated using the General-Head Boundary (GHB) Package (Harbaugh, 2005), which calculates head-dependent flows into and out of the study area. The direction and magnitude of this cross-boundary flow is governed by a specified head representing conditions outside the model and a specified conductance value of aquifer materials between the outermost active cell and the specified head location. The heads for the lateral general-head boundaries were specified for each model stress period using the calculated head values from the CVHM in the cells adjacent to the SJRRPGW boundary. The specified lateral or horizontal conductance (C_{bh}) values for the lateral general-head boundaries were estimated using the following equation:

$$C_{bh} = K_h \times \frac{A}{L} \quad (1)$$

where

A is the cross-sectional area of the SJRRPGW cell (0.25 mi * layer thickness),

L is the distance of general head from model boundary (a calibrated parameter), and

K_h is horizontal hydraulic conductivity (a calibrated parameter).

During model calibration, the value of K_h/L was estimated for three sections of the model boundary (fig. 24), as opposed to using K_h/L values based on the CVHM. The purpose for this approach is rooted in the local performance of the CVHM, which matches observed groundwater elevations well along the western side along the valley axis, horizontal GHB zone 1 (fig. 24); less well along the opposite boundary, horizontal GHB zone 2; and poorly in the Fresno area, closer to Friant Dam, horizontal GHB zone 3. Calibrating the conductance values separately for various sections of the boundary (fig. 24) permitted flexibility to strengthen the simulated hydraulic connection between the CVHM and SJRRPGW where the boundary heads matched observed heads and to weaken the simulated connection where the match to observed heads by the CVHM was poor.

The specified general-head value for each cell of the lower boundary was assigned for each model stress period using the calculated head from layer 6 of the CVHM, which represents the aquifer underlying the Corcoran Clay. The specified lower or vertical hydraulic conductance was estimated using equation 1, substituting C_{bv} for C_{bh} and vertical hydraulic conductivity (K_v) for K_h,

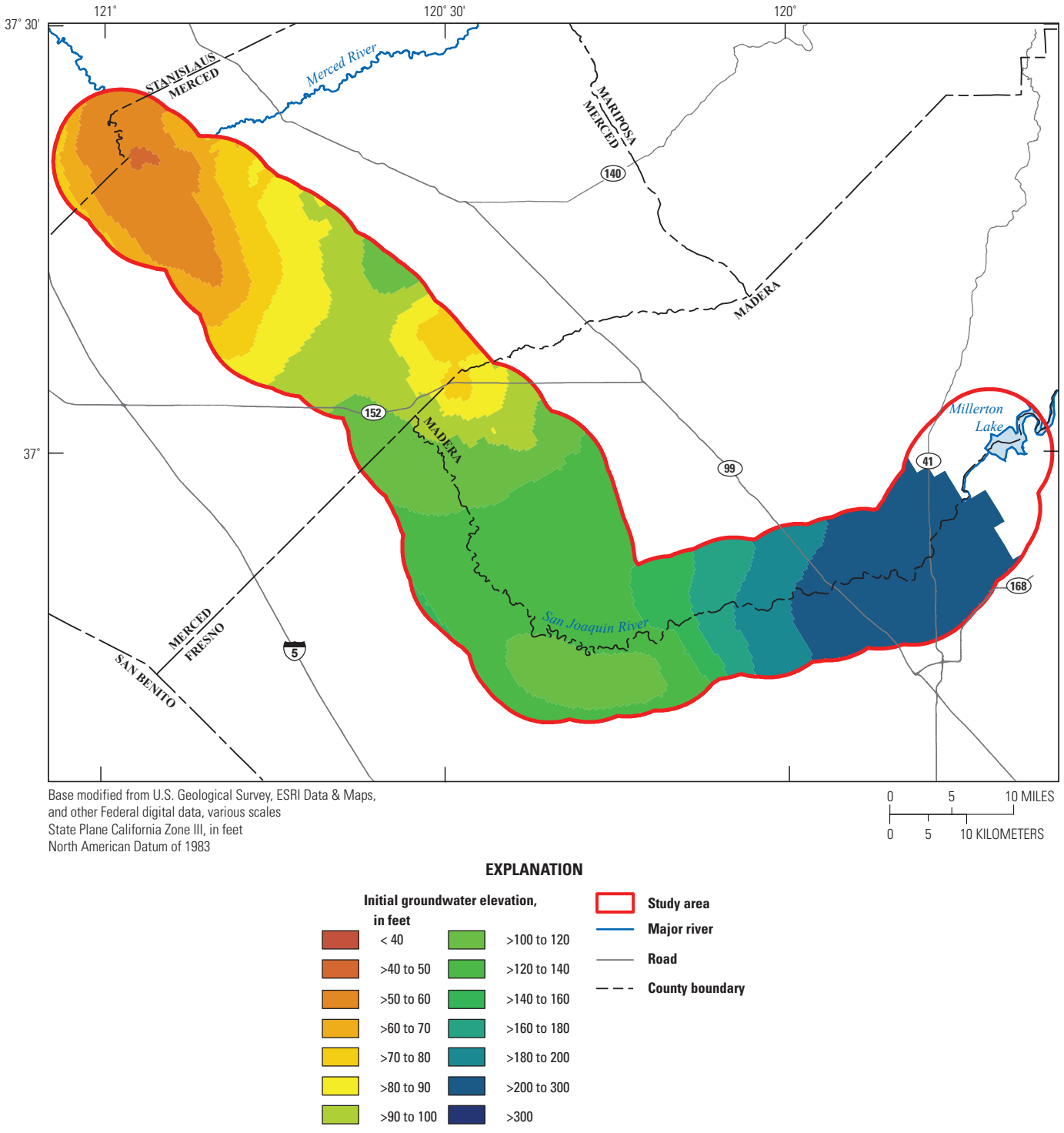

Figure 23. San Joaquin River Restoration Program groundwater flow model (SJRRPGW) initial groundwater elevation, San Joaquin Valley, California.

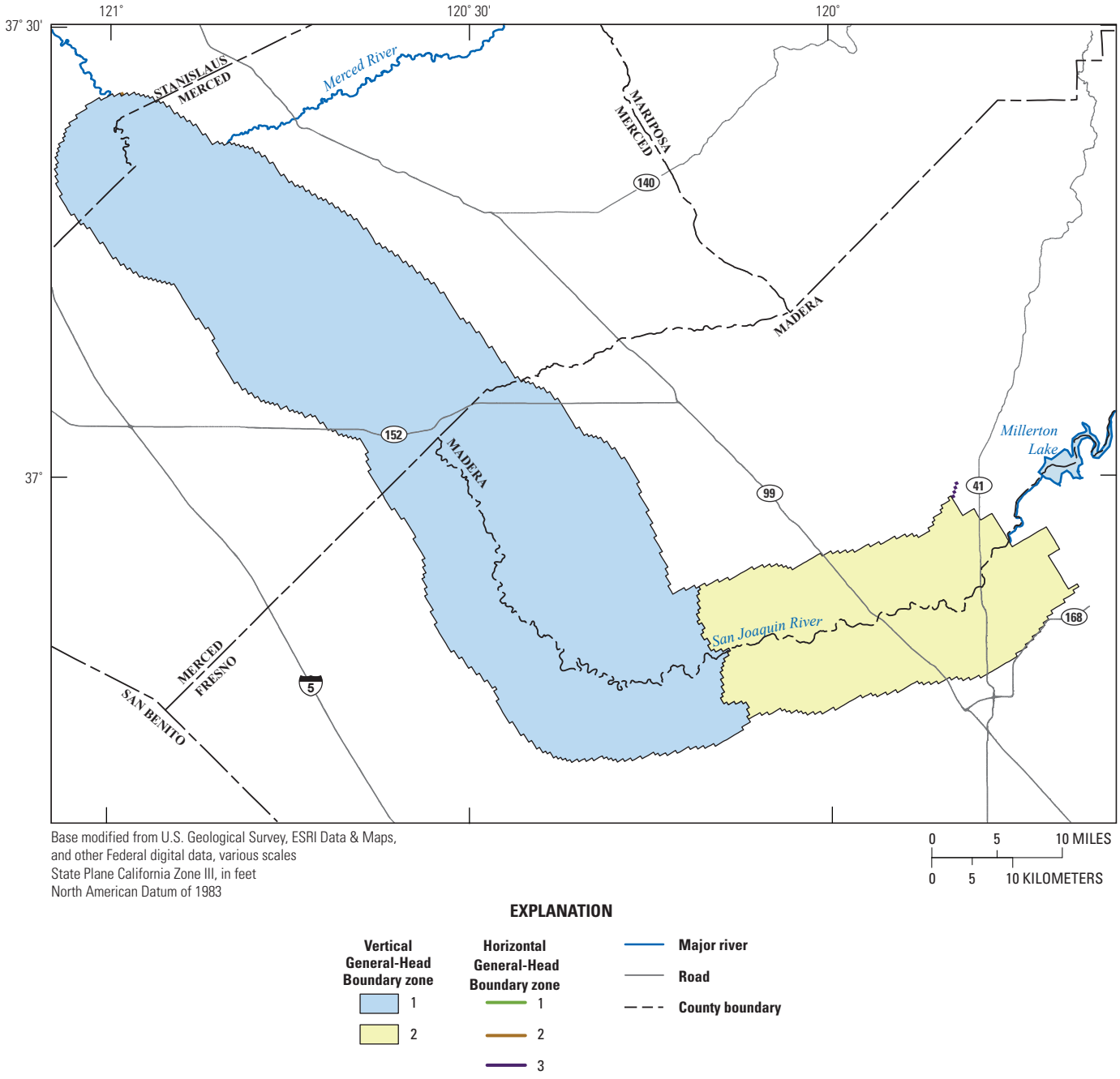

Figure 24. San Joaquin River Restoration Program groundwater flow model (SJRRPGW) division of general-head model boundaries, San Joaquin Valley, California.

where

A is the area of the SJRRPGW cell (0.25 mi * 0.25 mi), and

L is the thickness of Corcoran Clay (estimated by the total thickness of layers 4 and 5 in the CVHM, or a value of 2 ft where the Corcoran Clay is not present).

During model calibration, the value of K_v was estimated for two parts of the model (fig. 24) as described above for the lateral boundaries.

Aquifer Properties

The program TPROGS (Carle, 1999) was used to develop 100 equally probable three-dimensional sediment-texture distributions, or models, of the study area on the basis of data from 616 drillers' logs and various imposed constraints. The first texture model was chosen arbitrarily as representative of the true distribution of sediment texture in the study area.

The cell size of the texture model grid is 0.125 mi by 0.125 mi laterally, and it is oriented to coincide with the SJRRPGW grid such that groups of four texture model cells overlay one SJRRPGW cell. The vertical resolution of the texture model grid is 3.28 ft (1 m), which is much finer than that of the SJRRPGW. Sediment texture was grouped into four classes—gravel, sand, muddy sand, and clay (fig. 4). The texture model grid is a rectangular box shape, whereas the SJRRPGW grid has an irregular top (based on ground-surface elevation) and irregular bottom (based on the top of the Corcoran Clay). The texture model grid extends vertically beyond the top and bottom of SJRRPGW grid; the texture information outside the SJRRPGW grid is not used.

When the texture model and SJRRPGW grids are overlain, the four texture classes and the four texture model grid cells can be combined into 35 possible combinations (256 permutations) horizontally within a SJRRPGW grid cell. These 35 combinations were binned into 5 classes of aquifer materials as follows:

- Gravel—cells (SJRRPGW) with at least 2 gravels and less than 2 muddy sands or clays (7 of the possible 35 combinations).
- Sand—cells with at least 2 sands, less than 2 gravels, and less than 2 muddy sands or clays (6 of the possible 35 combinations).
- Muddy sand—cells with at least 2 muddy sands and less than 2 sands or gravels (7 of the possible 35 combinations).
- Clay—cells with at least 3 clays (4 of the possible 35 combinations).
- Mix—all other combinations (11 of the possible 35 combinations).

An example of a 3 by 3 model-cell section of the SJRRPGW grid illustrating how the texture model cells are combined into the SJRRGW cells is shown in figure 25. A control file that specifies how all 256 permutations are binned into the 5 classes of aquifer materials is available by request with the model archive.

The texture model does not extend all the way to the eastern SJRRPGW model boundary, so a sixth class, called "foothills," is assigned to active model cells that lie outside the texture model boundary. On the basis of these combinations, sand makes up the largest percentage of the SJRRPGW texture, and gravel makes up the least (table 8).

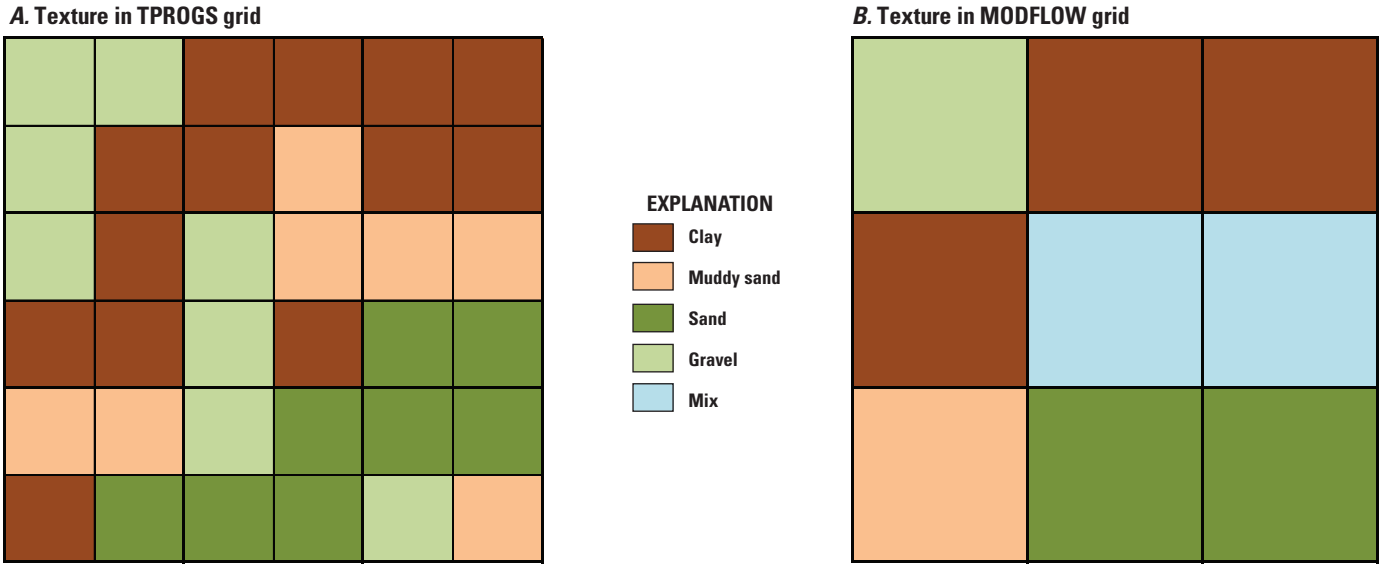

Figure 25. Example of horizontal combination of Transition-Probability Geostatistical Software (TPROGS) grid cells onto the San Joaquin River Restoration Program groundwater flow model (SJRRPGW) grid cells, San Joaquin Valley, California.

Table 8. Example distribution of aquifer texture in the San Joaquin River Restoration Program groundwater flow model (SJRRPGW), San Joaquin Valley, California.

Aquifer texture	Percentage
Gravel	3
Sand	33
Muddy sand	12
Clay	25
Mix	14
Foothills	13

By using the criteria above, the binned texture class was calculated for each 3.28-ft (1-m) vertical increment at the lateral resolution of the SJRRPGW grid. The interpolation of the 255 3.28-ft layers into the thicker SJRRPGW grid layers was accomplished using the HUF Package (Anderman and Hill, 2000). The HUF Package allows the vertical geometry of the 255 layers, which is supplied by the texture model, to be defined separately from the 5 model layers. An example of how the HUF Package combines vertical texture model layers onto the SJRRPGW model layers is shown in figure 26.

Water-Table Simulation

Although the uppermost active model layer in the SJRRPGW represents the water table and unconfined groundwater flow, confined flow is simulated in all the layers, which is a necessary and common approach for avoiding numerical instability and long execution times (Hill and Tiedeman, 2007). Attempts to simulate the upper layer as unconfined resulted in an eight-fold increase in model run time and caused convergence failures during the calibration process.

The HUF SYTP option is used to properly represent unconfined aquifer storage (Anderman and Hill, 2003). The SYTP option allows a unitless value of specific yield to be defined to represent the storage coefficient in all uppermost active cells when all model layers are confined. During the calibration process, if the simulated groundwater elevation in a cell was below the bottom elevation of a cell for the entire simulation, that model cell was manually made inactive such that the saturated thickness of the aquifer is not overestimated (fig. 27).

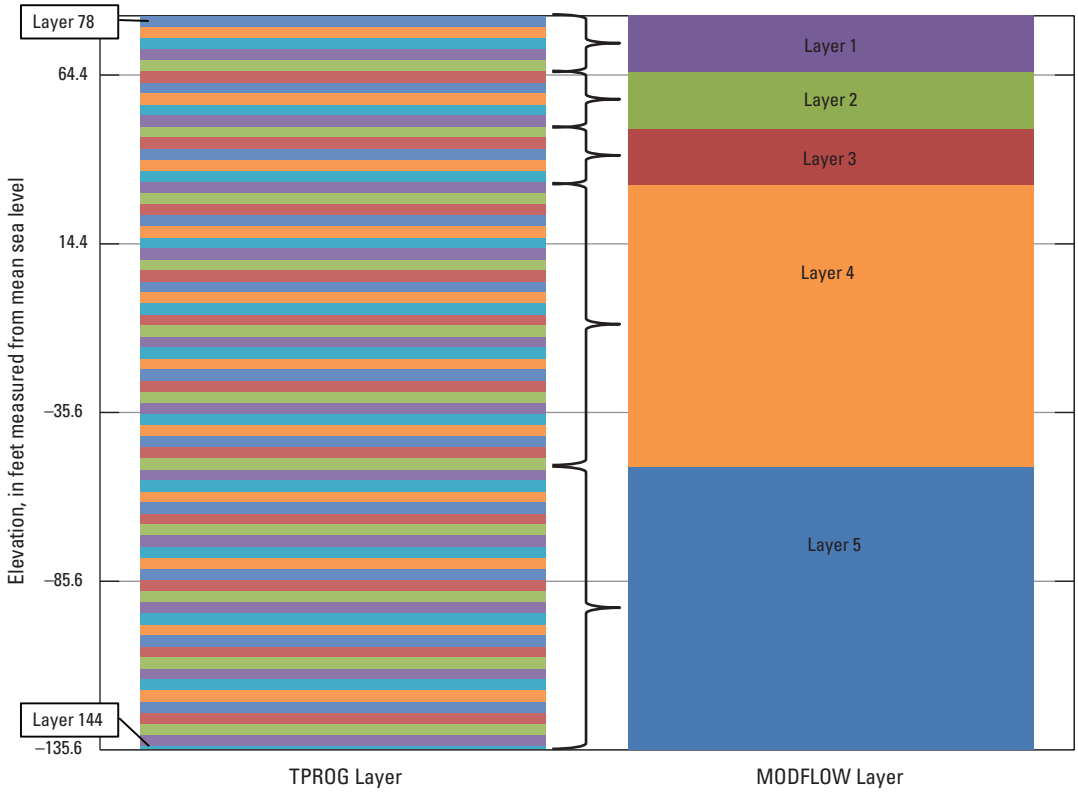

Figure 26. Example Hydrogeologic Unit Flow Package combination of vertical Transition-Probability Geostatistical Software (TPROG) texture layers onto the San Joaquin River Restoration Program groundwater flow model (SJRRPGW) model layers (Row 81, Column 31), San Joaquin Valley, California.

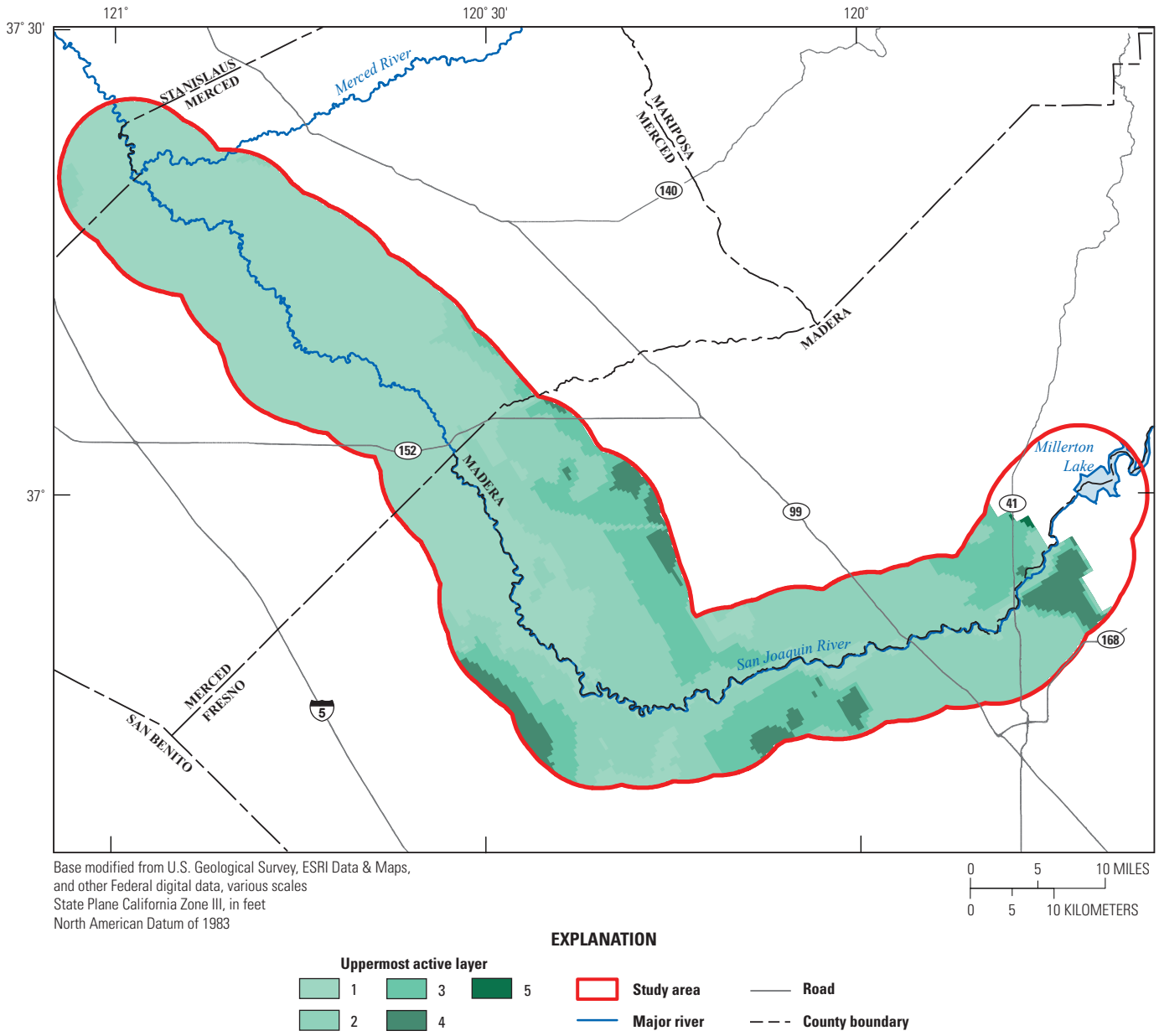

Figure 27. San Joaquin River Restoration Program groundwater flow model (SJRRPGW) uppermost active layer for each model cell, San Joaquin Valley, California.

Recharge and Discharge

Sources of groundwater recharge to the SJRRPGW include percolation of rainfall and irrigation water, leakage from streams, and subsurface inflow through the lateral and bottom boundaries of the SJRRPGW. Groundwater discharge from the SJRRPGW occurs as municipal pumping, agricultural pumping, root uptake of shallow groundwater, outflows to streams, and subsurface outflow through the lateral and bottom boundaries of the SJRRPGW.

Percolation of rainfall and irrigation water is simulated by the FMP2. During the rainy season (and sometimes during the growing season), precipitation may exceed the irrigation requirement in a cell. During the growing season, irrigated land will usually have some excess water applied to account for inefficiency (the irrigation efficiency is less than 100 percent). In both cases, this excess water percolates below the root zone and is simulated as groundwater recharge in the model. Agricultural pumping and root uptake of shallow groundwater also are simulated by the FMP2. Leakage from streams and groundwater discharge to streams are simulated by the SFR2 Package.

Subsurface inflow and outflow through the lateral and bottom boundaries of the SJRRPGW are simulated by the General-Head Boundary (GHB) Package. The heads for the general-head boundaries are specified for each model stress period using the calculated head values from the CVHM in the cells adjacent to the SJRRPGW boundary. For each cell, if the head at the SJRRPGW boundary cell is less than the general head, inflow occurs. If the head at the SJRRPGW boundary cell is greater than the general head, outflow occurs.

Municipal well pumping is simulated in the SJRRPGW by using the standard well package of MODFLOW (Harbaugh, 2005). Pumping is estimated on the basis of the amount of urban acreage and was aggregated by the 28 FMP2 subregions. Some of the deeper municipal wells in the study area are screened below the Corcoran Clay and are not directly included in the SJRRPGW, which simulates only the aquifer above the Corcoran Clay. To account for these deep wells, the total municipal pumping for each subregion is scaled on the basis of the percentage of wells in that subregion screened above the Corcoran Clay (table 9). Pumping beneath the Corcoran Clay is simulated in the CVHM and affected the lower boundary condition of the SJRRPGW model simulated using the GHB Package.

Rural population in the study area is estimated, on the basis of 2010 census block group data (National Historical Geographic Information System, 2011), to be less than 25 percent of the total population. Rural domestic groundwater production is expected to be small compared to municipal groundwater production (which is small relative to agricultural groundwater production). In addition, rural domestic groundwater used indoors is largely returned to the aquifer system through septic systems, and the net rural domestic groundwater extraction is small. Thus, rural water use is not included in the SJRRPGW. Similarly, industrial groundwater pumping in the study area is expected to be small and also is not included in the SJRRPGW.

Table 9. Percentage of wells screened above the Corcoran Clay, San Joaquin Valley, California.

[**Abbreviations**: N/A, not available]

Subregion	Number of wells with screen information	Percentage of wells screened above Corcoran Clay
1	2	50
2	6	100
3	0	N/A—Used 100
4	9	89
5	8	38
6	4	100
7	3	67
8	9	44
9	9	100
10	2	0
11	9	67
12	3	100
13	4	50
14	0	N/A—Used 50
15	5	100
16	4	100
17	19	42
18	2	100
19	6	83
20	4	75
21	2	100
22	21	100
23	1	0
24	3	100
25	3	100
26	3	100
27	8	88
28	1	100

Model Calibration

Hydrologic model calibration can be defined as the process of exploring a range of possible model parameters in order to achieve a set of model parameters for which the respective model results adequately approximate the real hydrologic system. For the SJRRPGW, as with most hydrologic models, the real hydrologic system is represented by a historical set of observed data (such as groundwater elevations and streamflow), which are known and measurable at discrete locations with a degree of uncertainty that is based principally on measurement error. In contrast, the distribution of the parameter values (such as hydraulic conductivity) is largely unknown, except perhaps at a few discrete locations, and can only be constrained by a range of reasonable values that are based on measurements and estimates from previous investigations. In the SJRRPGW, the model parameters adjusted during model calibration include the fllowing:

- Hydraulic conductivity, specific yield, and specific storage.
- Streambed hydraulic conductivity.
- General-head boundary hydraulic conductivity (as described earlier).
- Crop evapotranspiration coefficient.
- Subregion irrigation efficiency.

The goal of calibrating the SJRRPGW was to develop a hydrologically reasonable and representative model that provides a good match to observed historic values and is adequate for use in simulations of past and potential future aquifer-system responses to natural and imposed hydrologic stresses.

Calibration Data

A subset of the approximately 2,800 wells that have recorded groundwater elevations in the study area was selected for model calibration by using the following criteria:

- Availability of construction information for determining the SJRRPGW layer(s) that the well is hydraulically connected to.
- At least 5 years of groundwater-level record.
- At least 15 observations.

On the basis of these criteria, historical data from 133 wells, totaling 10,196 observations, were available for the model calibration. Among measurements from various wells, 78 were inconsistent with the rest of the measurements at those wells and were removed as outliers, resulting in 10,118 observations used for model calibration. For calibration purposes, these observations are treated as independent measurements (though it is likely observations at the same well are correlated). Of the 133 wells, 78 (7,411 observations) were from the DWR or USGS databases, and 55 (2,707 observations) were from the CCID monitoring program. Well construction and other information for the CCID, DWR, and USGS wells are listed in appendix B. The 55 CCID wells are shallow wells on the west side of the San Joaquin River along Reaches 3 and 4A; the median well-screen midpoint for these wells is 12.3 ft below ground surface. The remaining 78 wells are spatially distributed throughout the study area; the median well-screen midpoint for these wells is 198 ft below ground surface. The wells were grouped regionally into seven calibration well groups for the purpose of generating calibration statistics (Fresno, Madera, Mendota, Chowchilla, CCID South, CCID North, and Merced) (fig. 28).

The observations of groundwater elevation were copied into two identical “groups” of data, called “heads” and “drawdown,” that were treated differently in the calibration process. For the heads group, the observed values were compared directly to the simulated values. For the drawdown group, the change from one observed value to the initial observed value was compared to the change in the corresponding simulated values. These groups of data were weighted equally. Calibration of the SJRRPGW to values of heads favors accurate simulation of the overall magnitude of groundwater elevations. Calibration to values of drawdown favors accurate simulation of seasonal fluctuations and long-term trends in groundwater elevations. In many circumstances in groundwater models, it is more effective to match drawdowns than to match the heads themselves to achieve the best overall calibration (Hill and others, 2000).

Data from 19 streamgages were used to calibrate the SJRRPGW. Streamflow data are available daily or sub-daily; however, the model stress periods are monthly, so mean monthly observed streamflow values were calculated for comparison with simulated values. Data are not available from all streamgages for the entire simulation period. Monthly averaging and selection of records resulted in 4,695 mean monthly observations for calibration (table 10 and fig. 29). As with the observed groundwater levels, these observations are treated as independent observations, though it is likely that some observations are correlated. The simulated San Joaquin River flow leaving the study area was calibrated using data from the streamgage on the San Joaquin River near Crows Landing, which is 2 river miles downstream from the downgradient (northwest) model boundary.

Calibration Process

The process of model calibration involves comparison of model output with observed conditions and adjustment of model parameters within reasonable ranges such that simulated conditions adequately represent observed conditions. Prior to calibration, all model parameters were assigned initial values on the basis of previous work in the region (Phillips and others, 2007; Faunt, 2009).

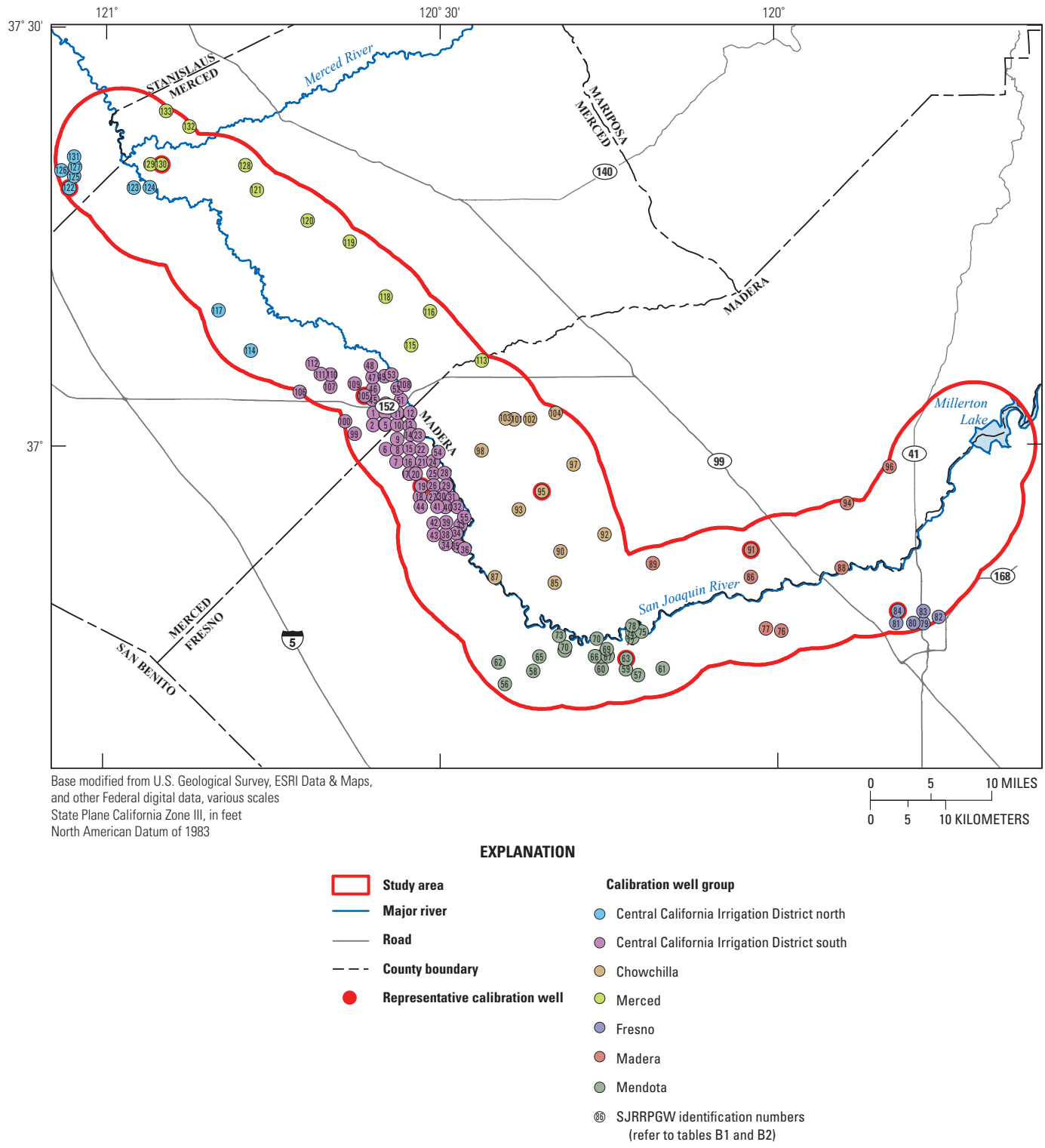

Figure 28. Observation wells used in the San Joaquin River Restoration Program groundwater flow model (SJRRPGW) calibration, San Joaquin Valley, California.

Table 10. Streamgages used in the San Joaquin River Restoration Program groundwater flow model (SJRRPGW) calibration, San Joaquin Valley, California.

[**Abbreviations**: DWR, Department of Water Resources; mm/yyyy, month/year; USBR, U.S. Bureau of Reclamation; USGS, U.S. Geological Survey]

SJRRPGW identification number	Streamgage identification	Streamgage name	Source	First record (mm/yyyy)	Last record[1] (mm/yyyy)	Total number of mean monthly records	Number of records that overlap with model period	Observation site weight for calibration
1	DNB	San Joaquin River at Donney Bridge	DWR	11/1988	09/2007	183	142	0.084
2	11253000	San Joaquin River near Biola	USGS	10/1952	09/1961	108	6	0.408
3	GRF	San Joaquin River at Gravely Ford	DWR	10/1974	09/2007	396	348	0.054
4	SJB	San Joaquin River below Bifurcation	DWR	10/1974	09/2007	292	259	0.062
5	CBP	Chowchilla Bypass at Head above Bifurcation	DWR	10/1974	12/1997	259	259	0.062
6	11254000	San Joaquin River near Mendota	USGS and USBR	10/1950	06/2005	396	327	0.055
7	11256000	San Joaquin River near Dos Palos	USGS and USBR	10/1950	12/1995	222	174	0.076
8	11260000	San Joaquin River near El Nido	USGS	10/1950	12/1995	222	174	0.076
9	ELN	Eastside Bypass near El Nido	DWR	10/1980	09/2007	324	276	0.060
10	EBM	Eastside Bypass below Mariposa Bypass	DWR	10/1980	09/2007	324	276	0.060
11	B00420	Mariposa Bypass near Crane Ranch	DWR	10/1961	09/1994	252	252	0.063
12	B05516	Bear Creek below Eastside Canal	DWR	10/1980	09/2007	324	276	0.060
13	SJS	San Joaquin River near Stevinson	DWR	10/1981	09/2007	312	264	0.062
14	11261100	Salt Slough at Highway 165 near Stevinson	USGS	10/1985	09/2007	252	204	0.070
15	11262900	Mud Slough near Gustine	USGS	10/1985	09/2007	264	216	0.068
16	11261500	San Joaquin River at Fremont Ford Bridge	USGS	10/1950	09/2007	372	198	0.071
17	11272500	Merced River near Stevinson	USGS	10/1940	09/2006	720	438	0.048
18	11274000	San Joaquin River near Newman	USGS	10/1950	09/2007	684	510	0.044
19	11274550	San Joaquin River near Crows Landing	USGS	10/1995	09/2007	144	96	0.102

[1]As of September 2007.

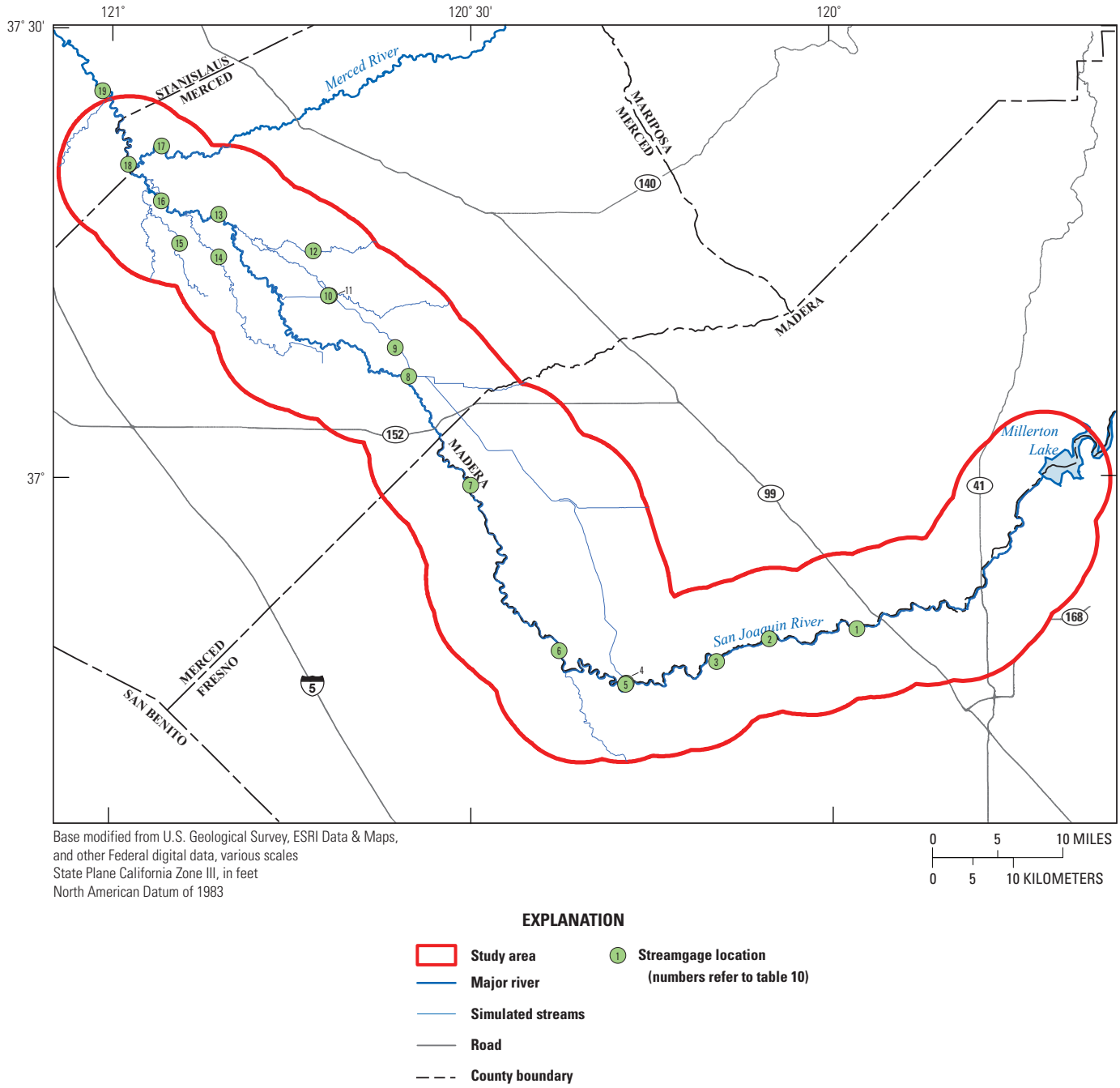

Figure 29. Location of streamgages used in the San Joaquin River Restoration Program groundwater flow model (SJRRPGW) calibration, San Joaquin Valley, California.

Calibration of the SJRRPGW was accomplished in a semiautomated manner by using a public-domain model-independent parameter estimation program (PEST) (Doherty, 2005). PEST was run in "estimation mode;" prior information was used to regularize the parameter values. The use of prior information ensures the estimated parameter values fall within a range that makes physical sense. Two types of prior information were used—direct parameter values to regularize individual parameter values and relations between pairs of parameters to regularize ratios between two parameters values (table 11). The relative and overall weighing of the prior information equation was adjusted as needed during calibration to insure the prior information neither dominated nor failed to influence the objective function.

PEST was used to find the parameter set that minimizes the sum of the squared deviations between each observation and its corresponding simulated value (referred to as the "objective function," Doherty, 200) calculated using:

$$\Phi = \sum_{m} \left(\left(h_m^{sim} - h_m^{obs} \right) w_m \right)^2 \qquad (2)$$

where

Φ is the objective function that PEST is trying to minimize,

h_m^{obs} is the observed value of observation or prior information m,

h_m^{sim} is the simulated value corresponding to observation or prior information m,

w_m is the weight of the m^{th} observation, and

m is the total number of observations and prior information.

A residual is defined as the simulated value at the observation location minus the observed value: ($h_m^{sim} - h_m^{obs}$). A negative residual means the model is simulating the groundwater elevation or streamflow too low, and a positive residual means the model is simulating the groundwater elevation or streamflow too high.

Parameters Estimated

Because of the runtime constraint, calibration of all the crop-related parameters was not feasible. During initial parameter estimation runs, SJRRPGW was determined to be most sensitive to the crop coefficients and the irrigation efficiencies and relatively less sensitive to changes in the other crop-related parameters. Therefore, PEST was used to estimate the crop coefficients and irrigation efficiencies, and the remaining crop-related parameters were fixed at the CVHM values.

Crop coefficients and irrigation efficiencies vary monthly in the model and also vary for each subregion. In addition, irrigation efficiencies also varies by crop type. To retain these monthly variations and longer-term trends determined in the CVHM, scale factors were used to calibrate the entire array of crop coefficients for each of the 21 crops and the entire array of irrigation efficiencies for each of the 28 subregions. PEST also was used to estimate the values for 32 hydraulic parameters, including aquifer properties, streambed hydraulic conductivities, and the hydraulic conductivities of the general-head boundaries. In total, 81 model parameters were calibrated using PEST (table 12). During the calibration process, the 32 hydraulic parameters were log-transformed in order to make the model results vary more linearly with changes in parameter values, which can speed up the parameter estimation process.

Observation Weights

As discussed previously, groundwater elevations and streamflow observations were used for the PEST calibration. One problem with utilizing both observation types in the calibration process is that streamflows and groundwater elevations are of vastly different magnitudes. For example, because the model units are in ft and days, a typical streamflow observation is 86 million cubic ft per day (ft^3/d, or approximately 1,000 ft^3/s), and a typical groundwater elevation is 100 ft. Without weighting, a small difference between an observed and simulated streamflow of 870,000 ft^3/d (approximately 1 ft^3/s) would be "seen by PEST" as being equivalent to a change of 870,000 ft in groundwater elevation.

In order to overcome this unit discrepancy, all the differences between observed and simulated streamflow were weighted such that they represented a percentage change rather than an absolute change. The weights were set so that a 5-percent difference between simulated and observed streamflow would be "seen by PEST" as equivalent to a 1-ft difference between simulated and observed groundwater elevation. For streamflow observations below 100 ft^3/s, it was assumed the flow was 100 ft^3/s for the purpose of calculating the weight. For example, if the observed flow was 0 ft^3/s and the simulated flow was 50 ft^3/s, the difference would be "seen by PEST" as 50 percent.

Because the number of observations at each site varies and in order to prevent sites with a lot of observations from dominating the calibration process, sites with fewer observations were given additional weight so that the weights for individual sites were spatially consistent. The overall weight at each site is shown for streamgages in table 10 and for groundwater wells in appendix B. The overall weight at each observation, which is a product of the site weight and the unit discrepancy weight, is contained in the PEST control file, available in the model files.

Table 11. Prior information used for calibration of the San Joaquin River Restoration Program groundwater flow model (SJRRPGW) model, San Joaquin Valley, California.

[**Abbreviations**: ft/d, feet per day; N/A, not available; 1/d, 1 per day; 1/ft, 1 per foot]

Parameter name	Description	Prior information value	Units	Weight
	Direct parameter values			
HK_Gravel	Horizontal hydraulic conductivity of gravel	500	ft/d	16.6
HK_Sand	Horizontal hydraulic conductivity of sand	250	ft/d	16.6
HK_MSand	Horizontal hydraulic conductivity of muddy sand	10	ft/d	16.6
HK_Clay	Horizontal hydraulic conductivity of clay	Tied to VK_Clay	ft/d	N/A
HK_Mix	Horizontal hydraulic conductivity of mixed material	50	ft/d	16.6
HK_Fhill	Horizontal hydraulic conductivity of foothills	250	ft/d	16.6
VK_Gravel	Vertical hydraulic conductivity of gravel	250	ft/d	16.6
VK_Sand	Vertical hydraulic conductivity of sand	25	ft/d	16.6
VK_MSand	Vertical hydraulic conductivity of muddy sand	0.1	ft/d	16.6
VK_Clay	Vertical hydraulic conductivity of clay	0.01	ft/d	16.6
VK_Mix	Vertical hydraulic conductivity of mixed material	0.1	ft/d	16.6
VK_Fhill	Vertical hydraulic conductivity of foothills	1	ft/d	16.6
SS_Gravel	Specific storage of gravel	0.000001	1/ft	16.6
SS_Sand	Specific storage of sand	0.000002	1/ft	16.6
SS_MSand	Specific storage of muddy sand	0.000003	1/ft	16.6
SS_Clay	Specific storage of clay	0.000004	1/ft	16.6
SS_Mix	Specific storage of mixed material	0.0000025	1/ft	16.6
SS_Fhill	Specific storage of foothills	0.0000025	1/ft	16.6
SY_ESDIS	Specific yield – east side distal	0.2	Unitless	16.6
SY_ESPRO	Specific yield – east side proximal	0.2	Unitless	16.6
SY_SJ	Specific yield – San Joaquin River	0.2	Unitless	16.6
SY_WEST	Specific yield – westside	0.2	Unitless	16.6
K_BYPASS	Riverbed hydraulic conductivity for bypasses	0.5	ft/d	16.6
K_SO_RIV	Riverbed hydraulic conductivity for Kings River	0.5	ft/d	16.6
K_TRIB_SW	Riverbed hydraulic conductivity for western tributaries	0.5	ft/d	16.6
K_SJRIV	Riverbed hydraulic conductivity for the San Joaquin River	0.5	ft/d	16.6
K_TRIB_SE	Riverbed hydraulic conductivity for eastern tributaries	0.5	ft/d	16.6
GHBCONDH1	General-head boundary section 1 K_h / L	None	1/d	N/A
GHBCONDH2	General-head boundary section 2 K_h / L	None	1/d	N/A
GHBCONDH3	General-head boundary section 3 K_h / L	None	1/d	N/A

Table 11. Prior information used for calibration of the San Joaquin River Restoration Program groundwater flow model (SJRRPGW) model, San Joaquin Valley, California.—Continued

[**Abbreviations**: ft/d, feet per day; N/A, not available; 1/d, 1 per day; 1/ft, 1 per foot]

Parameter name	Description	Prior information value	Units	Weight
	Direct parameter values—Continued			
GHBCONDV1	General-head boundary section 1 K_v	None	ft/d	N/A
GHBCONDV2	General-head boundary section 2 K_v	None	ft/d	N/A
KC_01	Crop coefficient scale factor for water	1	Unitless	100
KC_02	Crop coefficient scale factor for urban	1	Unitless	100
KC_03	Crop coefficient scale factor for native vegetation	1	Unitless	100
KC_04	Crop coefficient scale factor for generic orchards	1	Unitless	100
KC_05	Crop coefficient scale factor for generic pasture	1	Unitless	100
KC_06	Crop coefficient scale factor for generic row crops	1	Unitless	100
KC_07	Crop coefficient scale factor for generic small grains	1	Unitless	100
KC_08	Crop coefficient scale factor for idle	1	Unitless	100
KC_09	Crop coefficient scale factor for truck crops	1	Unitless	100
KC_10	Crop coefficient scale factor for citrus	1	Unitless	100
KC_11	Crop coefficient scale factor for field crops	1	Unitless	100
KC_12	Crop coefficient scale factor for vineyards	1	Unitless	100
KC_13	Crop coefficient scale factor for pasture	1	Unitless	100
KC_14	Crop coefficient scale factor for grain	1	Unitless	100
KC_15	Crop coefficient scale factor for dairies	1	Unitless	100
KC_16	Crop coefficient scale factor for orchards	1	Unitless	100
KC_17	Crop coefficient scale factor for rice	1	Unitless	100
KC_18	Crop coefficient scale factor for cotton	1	Unitless	100
KC_19	Crop coefficient scale factor for generic developed	1	Unitless	100
KC_20	Crop coefficient scale factor for generic cropland	1	Unitless	100
KC_23	Crop coefficient scale factor for irrigated native vegetation	1	Unitless	100
IEF_1	Irrigation efficiency scale factor for subregion 1	1	Unitless	100
IEF_2	Irrigation efficiency scale factor for subregion 2	1	Unitless	100
IEF_3	Irrigation efficiency scale factor for subregion 3	1	Unitless	100
IEF_4	Irrigation efficiency scale factor for subregion 4	1	Unitless	100
IEF_5	Irrigation efficiency scale factor for subregion 5	1	Unitless	100
IEF_6	Irrigation efficiency scale factor for subregion 6	1	Unitless	100
IEF_7	Irrigation efficiency scale factor for subregion 7	1	Unitless	100

Table 11. Prior information used for calibration of the San Joaquin River Restoration Program groundwater flow model (SJRRPGW) model, San Joaquin Valley, California.—Continued

[**Abbreviations**: ft/d, feet per day; N/A, not available; 1/d, 1 per day; 1/ft, 1 per foot]

Parameter name	Description	Prior information value	Units	Weight
	Direct parameter values—Continued			
IEF_8	Irrigation efficiency scale factor for subregion 8	1	Unitless	100
IEF_9	Irrigation efficiency scale factor for subregion 9	1	Unitless	100
IEF_10	Irrigation efficiency scale factor for subregion 10	1	Unitless	100
IEF_11	Irrigation efficiency scale factor for subregion 11	1	Unitless	100
IEF_12	Irrigation efficiency scale factor for subregion 12	1	Unitless	100
IEF_13	Irrigation efficiency scale factor for subregion 13	1	Unitless	100
IEF_14	Irrigation efficiency scale factor for subregion 14	1	Unitless	100
IEF_15	Irrigation efficiency scale factor for subregion 15	1	Unitless	100
IEF_16	Irrigation efficiency scale factor for subregion 16	1	Unitless	100
IEF_17	Irrigation efficiency scale factor for subregion 17	1	Unitless	100
IEF_18	Irrigation efficiency scale factor for subregion 18	1	Unitless	100
IEF_19	Irrigation efficiency scale factor for subregion 19	1	Unitless	100
IEF_20	Irrigation efficiency scale factor for subregion 20	1	Unitless	100
IEF_21	Irrigation efficiency scale factor for subregion 21	1	Unitless	100
IEF_22	Irrigation efficiency scale factor for subregion 22	1	Unitless	100
IEF_23	Irrigation efficiency scale factor for subregion 23	1	Unitless	100
IEF_24	Irrigation efficiency scale factor for subregion 24	1	Unitless	100
IEF_25	Irrigation efficiency scale factor for subregion 25	1	Unitless	100
IEF_26	Irrigation efficiency scale factor for subregion 26	1	Unitless	100
IEF_27	Irrigation efficiency scale factor for subregion 27	1	Unitless	100
IEF_28	Irrigation efficiency scale factor for subregion 28	1	Unitless	100
	Parameter relations			
HK_Gravel, HK_Sand	HK_Gravel / HK_Sand	2	—	50
HK_MSand, HK_Sand	HK_MSand / HK_Sand	0.04	—	50
VK_Clay, HK_Sand	VK_Clay / HK_Sand	0.00004	—	75
HK_Mix, HK_Sand	HK_Mix / HK_Sand	0.2	—	50
HK_Fhill, HK_Sand	HK_Fhill / HK_Sand	1	—	50
VK_Gravel, VK_Sand	VK_Gravel / VK_Sand	10	—	50
VK_MSand, VK_Sand	VK_MSand / VK_Sand	0.004	—	50
VK_Clay, VK_Sand	VK_Clay / VK_Sand	0.0004	—	75

Table 11. Prior information used for calibration of the San Joaquin River Restoration Program groundwater flow model (SJRRPGW) model, San Joaquin Valley, California.—Continued

[**Abbreviations**: ft/d, feet per day; N/A, not available; 1/d, 1 per day; 1/ft, 1 per foot]

Parameter name	Description	Prior information value	Units	Weight
	Parameter relations—Continued			
VK_Mix, VK_Sand	VK_Mix / VK_Sand	0.004	—	50
VK_Fhill, VK_Sand	VK_Fhill / VK_Sand	0.04	—	50
SS_Gravel, SS_Sand	SS_Gravel / SS_Sand	0.5	—	50
SS_MSand, SS_Sand	SS_MSand / SS_Sand	1.5	—	50
SS_Clay, SS_Sand	SS_Clay / SS_Sand	2	—	50
SS_Mix, SS_Sand	SS_Mix / SS_Sand	1.25	—	50
SS_Fhill, SS_Sand	SS_Fhill / SS_Sand	1.25	—	50
HK_Gravel, VK_Gravel	HK_Gravel / VK_Gravel	2	—	50
HK_Sand, VK_Sand	HK_Sand / VK_Sand	10	—	50
HK_MSand, VK_MSand	HK_MSand / VK_MSand	100	—	50
HK_Mix, VK_Mix	HK_Mix / VK_Mix	500	—	50
HK_Fhill, VK_Fhill	HK_Fhill / VK_Fhill	250	—	50
GHBCONDV1, VK_Clay	GHBCONDV1 / VK_Clay	0.01	—	25
GHBCONDV2, VK_Clay	GHBCONDV2 / VK_Clay	0.01	—	25

Table 12. San Joaquin River Restoration Program groundwater flow model (SJRRPGW) final parameter values, San Joaquin Valley, California.

[**Abbreviations**: ft/d, feet per day; 1/ft, 1 per foot; 1/d, 1 per day]

Parameter name	Description	Final estimated value	Units	Standard error (as a percentage of parameter value)	95-percent confidence interval lower limit	95-percent confidence interval upper limit
HK_Gravel	Horizontal hydraulic conductivity of gravel	846	ft/d	17.65	553	1,139
HK_Sand	Horizontal hydraulic conductivity of sand	448	ft/d	5.18	403	494
HK_MSand	Horizontal hydraulic conductivity of muddy sand	20	ft/d	18.72	13	27
HK_Clay	Horizontal hydraulic conductivity of clay	0.028	ft/d	20.70	0.017	0.040
HK_Mix	Horizontal hydraulic conductivity of mixed material	86	ft/d	20.00	52	120
HK_Fhill	Horizontal hydraulic conductivity of foothills	387	ft/d	10.74	305	468
VK_Gravel	Vertical hydraulic conductivity of gravel	454	ft/d	21.19	265	643
VK_Sand	Vertical hydraulic conductivity of sand	53	ft/d	21.65	31	76
VK_MSand	Vertical hydraulic conductivity of muddy sand	0.24	ft/d	18.50	0.15	0.33
VK_Clay	Vertical hydraulic conductivity of clay	0.028	ft/d	6.08	0.025	0.032
VK_Mix	Vertical hydraulic conductivity of mixed material	0.21	ft/d	18.80	0.13	0.28
VK_Fhill	Vertical hydraulic conductivity of foothills	1.7	ft/d	23.05	0.9	2.4
SS_Gravel	Specific storage of gravel	1.0E-06	1/ft	21.51	5.8E-07	1.4E-06
SS_Sand	Specific storage of sand	1.8E-06	1/ft	21.08	1.1E-06	2.5E-06
SS_MSand	Specific storage of muddy sand	2.6E-06	1/ft	23.12	1.4E-06	3.8E-06
SS_Clay	Specific storage of clay	3.6E-06	1/ft	19.23	2.3E-06	5.0E-06
SS_Mix	Specific storage of mixed material	2.1E-06	1/ft	21.33	1.2E-06	3.0E-06
SS_Fhill	Specific storage of foothills	2.2E-06	1/ft	21.78	1.3E-06	3.1E-06
SY_ESDIS	Specific yield – east side distal	0.35	Unitless	3.58	0.33	0.37
SY_ESPRO	Specific yield – east side proximal	0.20	Unitless	4.59	0.18	0.21
SY_SJ	Specific yield – San Joaquin River	0.35	Unitless	5.47	0.31	0.39
SY_WEST	Specific yield – westside	0.12	Unitless	7.23	0.10	0.14
K_BYPASS	Riverbed hydraulic conductivity for bypasses	0.118	ft/d	12.38	0.090	0.147
K_SO_RIV	Riverbed hydraulic conductivity for Kings River	0.42	ft/d	20.60	0.25	0.59
K_TRIB_SW	Riverbed hydraulic conductivity for western tributaries	0.29	ft/d	21.78	0.17	0.41
K_SJRIV	Riverbed hydraulic conductivity for the San Joaquin River	1.62	ft/d	14.81	1.15	2.09
K_TRIB_SE	Riverbed hydraulic conductivity for eastern tributaries	0.47	ft/d	3.21	0.44	0.50
GHBCONDH1	General-head boundary section 1 K_h / L	2.5E-02	1/d	5.60	2.2E-02	2.8E-02
GHBCONDH2	General-head boundary section 2 K_h / L	1.4E-04	1/d	24.25	7.3E-05	2.0E-04
GHBCONDH3	General-head boundary section 3 K_h / L	7.5E-05	1/d	20.77	4.5E-05	1.1E-04
GHBCONDV1	General-head boundary section 1 K_v	2.2E-03	ft/d	2.69	2.1E-03	2.3E-03

Table 12. San Joaquin River Restoration Program groundwater flow model (SJRRPGW) final parameter values, San Joaquin Valley, California.—Continued

[**Abbreviations**: ft/d, feet per day; 1/ft, 1 per foot; 1/d, 1 per day]

Parameter name	Description	Final estimated value	Units	Standard error (as a percentage of parameter value)	95-percent confidence interval lower limit	95-percent confidence interval upper limit
GHBCONDV2	General-head boundary section 2 K_v	4.7E-05	ft/d	5.63	4.2E-05	5.2E-05
KC_01	Crop coefficient scale factor for water	1.02	Unitless	2.29	0.97	1.06
KC_02	Crop coefficient scale factor for urban	0.98	Unitless	2.20	0.94	1.03
KC_03	Crop coefficient scale factor for native vegetation	1.01	Unitless	2.27	0.96	1.05
KC_04	Crop coefficient scale factor for generic orchards	1.02	Unitless	2.36	0.97	1.06
KC_05	Crop coefficient scale factor for generic pasture	0.98	Unitless	1.85	0.94	1.02
KC_06	Crop coefficient scale factor for generic row crops	1.01	Unitless	1.57	0.97	1.04
KC_07	Crop coefficient scale factor for generic small grains	1.00	Unitless	2.43	0.96	1.05
KC_08	Crop coefficient scale factor for idle	1.01	Unitless	2.17	0.96	1.05
KC_09	Crop coefficient scale factor for truck crops	1.00	Unitless	2.00	0.96	1.04
KC_10	Crop coefficient scale factor for citrus	1.01	Unitless	2.32	0.97	1.06
KC_11	Crop coefficient scale factor for field crops	1.00	Unitless	2.09	0.96	1.04
KC_12	Crop coefficient scale factor for vineyards	1.01	Unitless	1.92	0.97	1.04
KC_13	Crop coefficient scale factor for pasture	1.05	Unitless	1.74	1.01	1.08
KC_14	Crop coefficient scale factor for grain	0.98	Unitless	2.57	0.93	1.03
KC_15	Crop coefficient scale factor for dairies	1.00	Unitless	3.22	0.94	1.07
KC_16	Crop coefficient scale factor for orchards	1.07	Unitless	1.96	1.03	1.11
KC_17	Crop coefficient scale factor for rice	1.00	Unitless	2.16	0.96	1.04
KC_18	Crop coefficient scale factor for cotton	1.10	Unitless	1.75	1.06	1.14
KC_19	Crop coefficient scale factor for generic developed	0.92	Unitless	1.98	0.88	0.95
KC_20	Crop coefficient scale factor for generic cropland	1.00	Unitless	2.44	0.95	1.04
KC_23	Crop coefficient scale factor for irrigated native vegetation	0.93	Unitless	2.20	0.89	0.97
IEF_1	Irrigation efficiency scale factor for subregion 1	0.99	Unitless	2.31	0.94	1.03
IEF_2	Irrigation efficiency scale factor for subregion 2	1.01	Unitless	2.34	0.97	1.06
IEF_3	Irrigation efficiency scale factor for subregion 3	0.98	Unitless	2.13	0.94	1.02
IEF_4	Irrigation efficiency scale factor for subregion 4	0.99	Unitless	2.17	0.95	1.04
IEF_5	Irrigation efficiency scale factor for subregion 5	0.98	Unitless	2.31	0.94	1.03
IEF_6	Irrigation efficiency scale factor for subregion 6	0.99	Unitless	2.03	0.95	1.03
IEF_7	Irrigation efficiency scale factor for subregion 7	0.99	Unitless	2.18	0.95	1.04
IEF_8	Irrigation efficiency scale factor for subregion 8	1.00	Unitless	2.17	0.96	1.04
IEF_9	Irrigation efficiency scale factor for subregion 9	0.97	Unitless	2.18	0.93	1.02

Table 12. San Joaquin River Restoration Program groundwater flow model (SJRRPGW) final parameter values, San Joaquin Valley, California.—Continued

[**Abbreviations**: ft/d, feet per day; 1/ft, 1 per foot; 1/d, 1 per day]

Parameter name	Description	Final estimated value	Units	Standard error (as a percentage of parameter value)	95-percent confidence interval lower limit	95-percent confidence interval upper limit
IEF_10	Irrigation efficiency scale factor for subregion 10	1.01	Unitless	2.43	0.96	1.06
IEF_11	Irrigation efficiency scale factor for subregion 11	0.98	Unitless	2.20	0.94	1.02
IEF_12	Irrigation efficiency scale factor for subregion 12	1.00	Unitless	2.22	0.95	1.04
IEF_13	Irrigation efficiency scale factor for subregion 13	1.01	Unitless	1.97	0.97	1.05
IEF_14	Irrigation efficiency scale factor for subregion 14	1.00	Unitless	2.29	0.96	1.05
IEF_15	Irrigation efficiency scale factor for subregion 15	0.97	Unitless	1.84	0.93	1.00
IEF_16	Irrigation efficiency scale factor for subregion 16	1.00	Unitless	2.06	0.96	1.04
IEF_17	Irrigation efficiency scale factor for subregion 17	1.00	Unitless	1.85	0.96	1.03
IEF_18	Irrigation efficiency scale factor for subregion 18	0.98	Unitless	2.05	0.94	1.02
IEF_19	Irrigation efficiency scale factor for subregion 19	1.01	Unitless	2.28	0.96	1.06
IEF_20	Irrigation efficiency scale factor for subregion 20	0.97	Unitless	1.98	0.94	1.01
IEF_21	Irrigation efficiency scale factor for subregion 21	1.01	Unitless	2.41	0.96	1.06
IEF_22	Irrigation efficiency scale factor for subregion 22	1.10	Unitless	1.89	1.06	1.14
IEF_23	Irrigation efficiency scale factor for subregion 23	1.02	Unitless	2.37	0.98	1.07
IEF_24	Irrigation efficiency scale factor for subregion 24	1.00	Unitless	1.96	0.96	1.04
IEF_25	Irrigation efficiency scale factor for subregion 25	0.98	Unitless	2.05	0.94	1.02
IEF_26	Irrigation efficiency scale factor for subregion 26	1.01	Unitless	2.12	0.97	1.05
IEF_27	Irrigation efficiency scale factor for subregion 27	1.00	Unitless	1.91	0.96	1.04
IEF_28	Irrigation efficiency scale factor for subregion 28	0.99	Unitless	2.12	0.95	1.04

Calibration Results

Calibration of the SJRRPGW model using the procedure described above resulted in a set of parameter estimates that lie within the range of reasonable values (table 12). The estimated horizontal and vertical hydraulic conductivities are generally consistent with parameters from similar studies in the greater San Joaquin region (Phillips and others, 2007; Burow and others, 2008) (table 13). Differences between the three studies can be explained by how each study defines the texture groups. In Phillips and others (2007), sand and gravel are lumped into the most coarse category (resulting in 21 percent of Pleistocene deposits and 31 percent of Holocene deposits classified as the most coarse) leading to a lower calibrated hydraulic conductivity value of 260 ft/d for this category. In Burow and others (2008), the most coarse category only includes cobbles and pebbles (resulting in only 1 percent of the deposits being classified as the most coarse) leading to a higher calibrated hydraulic conductivity value of 2,600 ft/d for this category. In this study, the definition of the most coarse category takes a moderate approach (resulting in 4 percent of the deposits being classified as the most coarse) leading to a calibrated hydraulic conductivity value of 840 ft/d that lies between the values from the previous two studies. A similar pattern is also seen with the other aquifer texture categories across the three studies.

The general-head boundary hydraulic conductivity values are highest along the western boundary of the model (GHBCONDH1) and lowest in the Fresno area (GHBCONDH3), which is rooted in the local performance of the CVHM in these areas. Higher conductance values result in a stronger connection between the CVHM and SJRRPGW where the boundary heads in the CVHM matched observed values, and lower conductance values result in a weaker connection where the match between observed heads and the CVHM simulated heads was poor. The calibrated scale factors on the crop coefficients and irrigation efficiencies are between 0.92 and 1.10, resulting in parameter values that are less than 10 percent different than those used in the CVHM.

Model Fit to Observations of Groundwater Elevations

To quantify the model fit between the simulated and observed groundwater elevations for all 10,118 observations at the 133 calibration target wells, the histogram of residuals was examined (fig. 30*A*). The residuals (fig. 30*A*) range from −56 to 91 ft and have a mean of −0.6 ft, an absolute mean of 9.0 ft, a standard deviation of 12 ft, a skewness of 0.5, and an excess kurtosis of 3.0. The mean value of −0.6 ft indicates very little bias, or preferentially high or low simulated heads, and the absolute mean of 9.0 ft indicates good model fit for a region of this scale. The relatively low absolute values of skewness and excess kurtosis indicate the residuals are normally distributed around zero. Approximately 64 percent of the SJRRPGW simulated values fall within 10 ft of the observed values and about 92 percent fall within 20 ft. These residuals are within the calibration targets for a regional model of this scale.

The relation between observed and simulated groundwater elevations provides another means to quantify the model fit (fig. 30*B*). Points that plot above and below the 1-to-1 correlation line represent observations where the SJRRPGW is simulating groundwater elevations too high and too low, respectively. Most of the points are very close to the 1-to-1 correlation line, indicating a good model fit. Outliers removed early in the calibration process also are shown on figure 30*B*; these outliers are not included in the model-fit or other statistics presented in this report. The correlation at some individual wells can be seen in figure 30*B*. For example, the points from the Madera dataset that have an observed value near 100 ft and a simulated value close to 180 ft are from calibration well 94, where the long-term declining groundwater levels are not being simulated well by the SJRRPGW model because of the effects of boundary conditions.

The relation between residual and observed groundwater elevations is a third method for quantifying the model fit (fig. 30*C*). This figure shows the model generally simulates lower groundwater elevations too high and higher groundwater elevations too low.

Table 13. Comparison of San Joaquin River Restoration Program groundwater flow model (SJRRPGW) parameter values to values in similar studies, San Joaquin Valley, California.

[**Abbreviations**: ft/d, feet per day]

Source	Horizontal hydraulic conductivity				Vertical hydraulic conductivity			
	Gravel/ sand (ft/d)	Sand/silty sand (ft/d)	Muddy sand/silt (ft/d)	Clay (ft/d)	Gravel/ sand (ft/d)	Sand/silty sand (ft/d)	Muddy sand/silt (ft/d)	Clay (ft/d)
SJRRPGW simulated values	840	450	20	0.028	450	53	0.24	0.028
Burrow and others, 2008	2,600	320	7.2	0.0033	2,400	150	3.6	0.010
Phillips and others, 2007	260	98	26	0.98	130	20	3.3	0.49

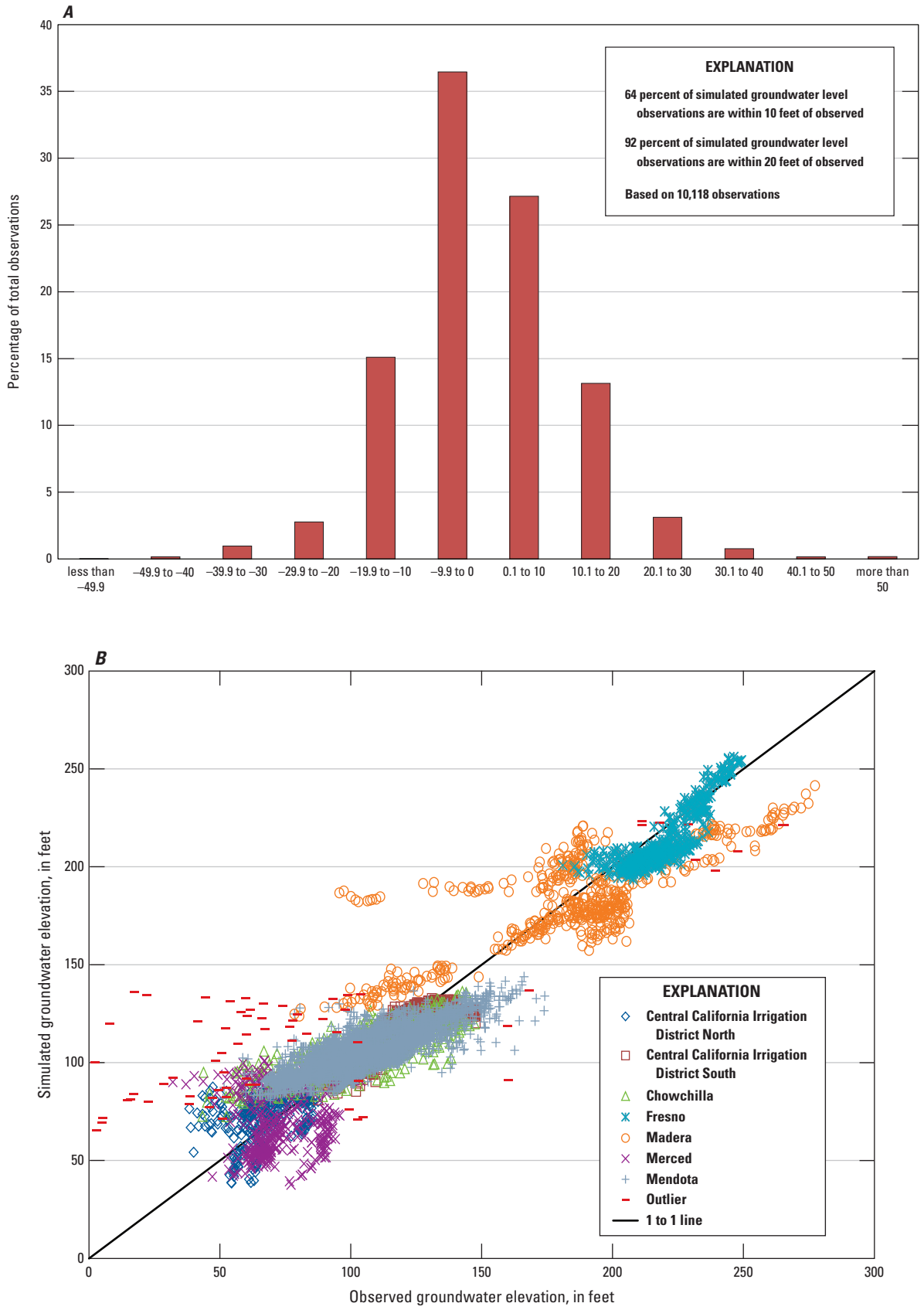

Figure 30. Relation between simulated and observed groundwater elevations: *A*, Histogram of residual groundwater elevations; *B*, Simulated and observed groundwater elevations; *C*, Residual and observed groundwater elevations.

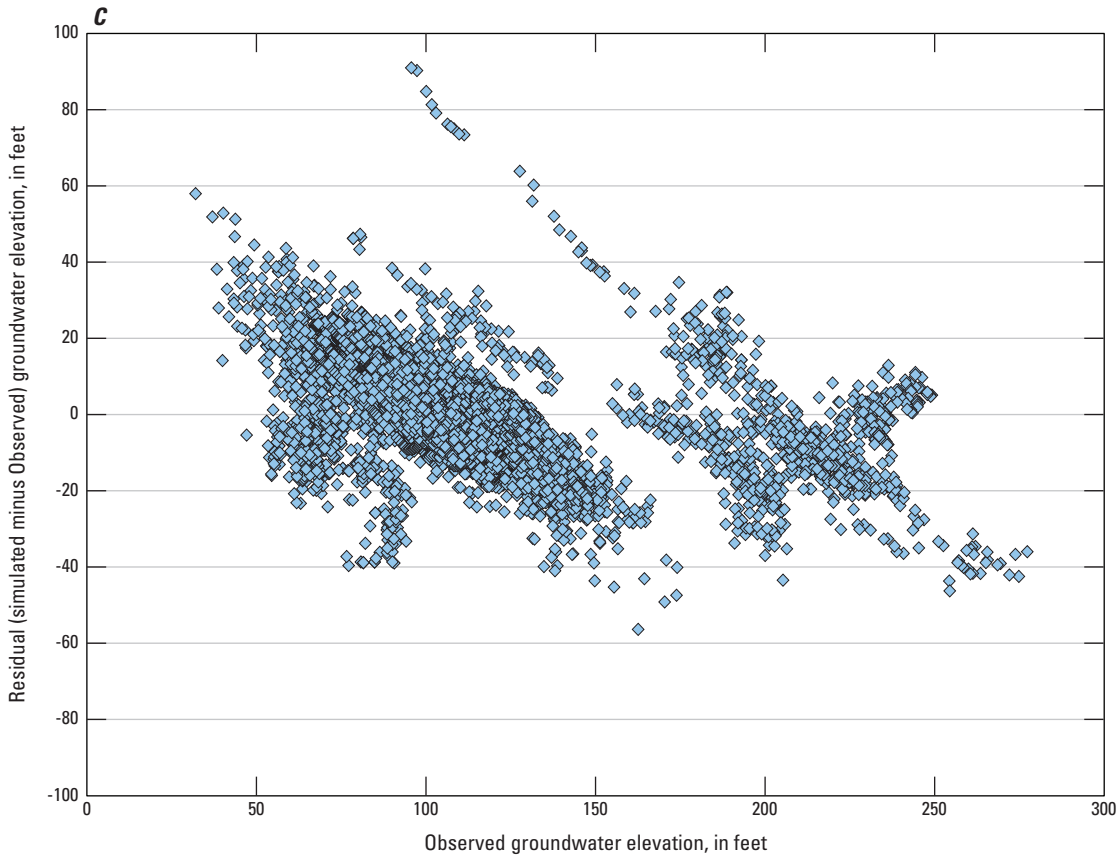

Figure 30. —Continued

It is important that there is no spatial bias in the residuals that might indicate local processes not being simulated correctly. Average residuals for each observation well show the high and low residuals are not spatially clustered (fig. 31). Plots comparing the simulated and observed time series of groundwater elevations at eight representative calibration wells are presented in the next section of this report. The relations between simulated and observed groundwater elevations at all 133 calibration wells are presented in appendix C.

Groundwater Elevations at Representative Calibration Wells

A total of eight representative calibration wells are presented in this section of the report (fig. 32*A–H*). One well was selected for each of the seven calibration well groups; two wells were selected for CCID South (one deep well and one shallow well). The hydrographs for these wells (fig. 32) show the observed groundwater elevations with points and the simulated groundwater elevations with lines. Simulated groundwater elevations are shown for model layers that correspond to where the wells are screened.

The hydrograph for calibration well 84 (13S20E17F001M) is representative of the Fresno calibration well group (fig. 32*A*). Although the SJRRPGW simulates groundwater elevation on average 6 ft too high in the Fresno area, the model reasonably simulates the decline in groundwater elevations over time caused by municipal pumping. The Fresno area has a total of 501 observations; 98 percent of them are simulated within ± 20 ft.

The hydrograph for calibration well 91 (12S18E19H001M) is representative of the Madera calibration well group (fig. 32*B*). Although the simulation at well 91 tends to underestimate the groundwater elevation, the SJRRPGW simulates groundwater elevation on average 1 ft too high in the Madera area; however, there is a large range in the residuals. Only 54 percent of the 514 observations were simulated within ± 20 ft. The relatively poor performance of the model in the Madera area is partly because of the influence of the CVHM-based boundary condition to the north and also to a large variation in groundwater levels and trends at neighboring wells. Despite the enhanced refinement of this model, the local variability in conditions and site-specific response to real pumping cannot be captured because the model distributes pumping evenly throughout each subregion. At calibration well 91, the observed seasonal variability and overall trend are well simulated. Simulated heads also respond to drought conditions in 1976–77 and 1987–92, although the recovery during wet conditions is less than observed.

The hydrograph for calibration well 63 (14S16E04A001M) is representative of the Mendota calibration well group (fig. 32*C*). The Mendota area had the most data (4,602 observations) of any of the calibration areas. On average, the SJRRPGW simulates groundwater elevations 1ft too high; 93 percent of the simulated values were within ± 20 ft of the observations. Wells in the Mendota area show a larger seasonal fluctuation in groundwater elevations than wells in the rest of the study area, but the SJRRPGW simulates these seasonal and longer-term fluctuations reasonably well.

The hydrograph for calibration well 95 (11S15E29H001M) is representative of the Chowchilla calibration well group (fig. 32*D*). Many wells in the Chowchilla area show a long-term decline in groundwater elevation with episodic recovery during wetter periods in the early 1980s and mid-1990s. Although the model reasonably matches the shape and timing of these trends, it does not reach the same magnitude in either the observed decline or the maximum recovery. It is possible some of the observations represent pumping conditions, which are not fully captured at the temporal and spatial scale of the SJRRPGW. Despite this limitation, the model performs acceptably well in the Chowchilla area; the average residual is 1 ft. The Chowchilla area has a total of 591 observations, 85 percent of which are simulated within ± 20 ft.

For the CCID South calibration well group, two wells are presented—the hydrograph for calibration well 19 (CCID140), which is representative of the water table (fig. 32*E*), and the hydrograph for calibration well 105 (10S12E13L001M), which is representative of deeper conditions (fig. 32*F*). The SJRRPGW performs exceptionally well in the CCID South area, which is attributed to accurate CVHM boundary conditions to the west and a large set of calibration wells from the CCID monitoring wells program. This area also has a comparatively small range of fluctuations in the observed groundwater elevations compared to other regions. The performance of the SJRRPGW in this area is relatively important because the CCID South calibration area is adjacent to SJRRP management Reaches 3 and 4a, which are areas underlain by a shallow water table. The CCID South area has a total of 3,200 observations. The average residual is −2 ft, and 96 percent of the observations are simulated within ± 10 ft (99 percent within ± 20 ft).

The hydrograph for calibration well 130 (07S10E07L001M) is representative of the Merced calibration well group (fig. 32*G*). On average, the SJRRPGW simulates groundwater elevations 5 ft too low in the Merced area. One difficulty in calibration of the Merced area is that most observation wells had only sparse data. Despite this limitation, the model simulates groundwater elevations in this area reasonably well; 70 percent of the 365 observations are simulated within ± 20 ft.

The hydrograph for calibration well 122 (07S08E23R001M) is representative of the CCID North calibration well group (fig. 32*H*). This area includes many of the wildlife management areas (fig. 19) in the study area, which do not have any observation wells to use for calibration. Thus, this calibration area has only 345 observations, the least of any area. Despite this lack of data, the SJRRPGW reasonably matches the groundwater elevations, although it overestimates groundwater elevations after 1980. On average, the SJRRPGW simulates groundwater elevations in the CCID North area 5 ft too high, and 89 percent of the observations are simulated within ± 20 ft.

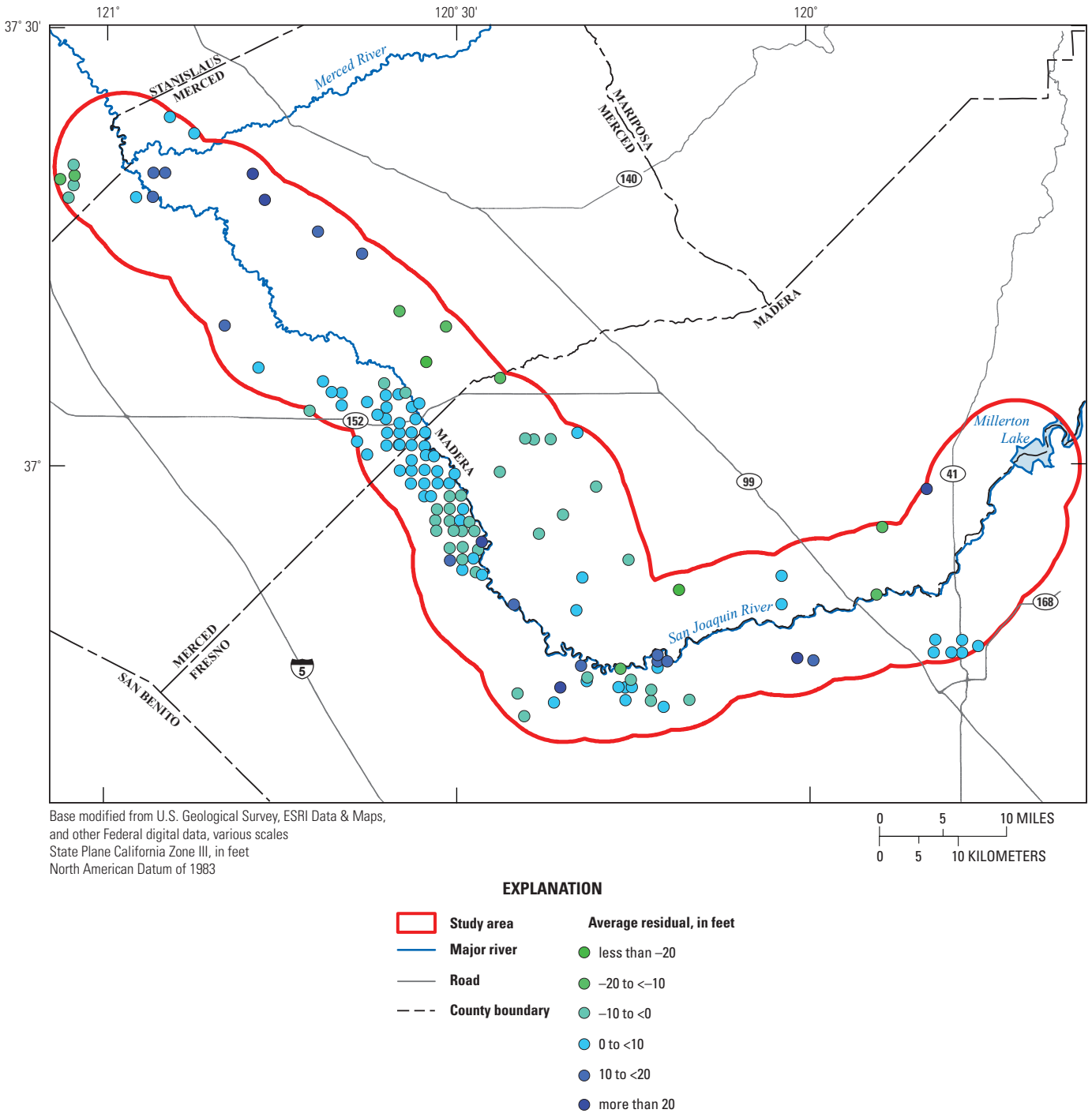

Figure 31. Average residual (simulated – observed) groundwater elevation at observation wells used in the San Joaquin River Restoration Program groundwater flow model (SJRRPGW) calibration, San Joaquin Valley, California.

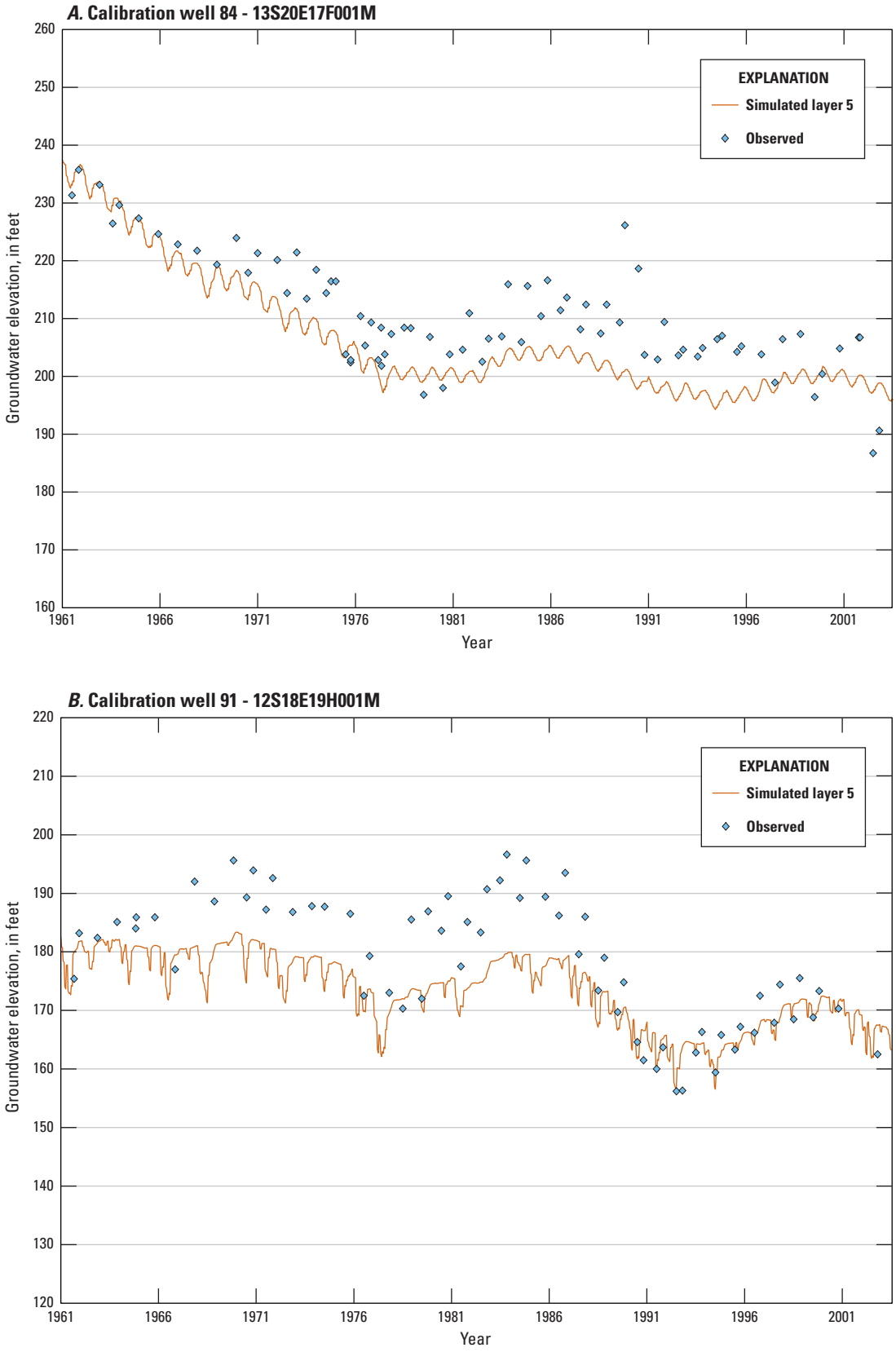

Figure 32. Representative hydrographs for each San Joaquin River Restoration Program groundwater flow model (SJRRPGW) calibration area comparing simulated and observed groundwater elevations, San Joaquin Valley, California: *A*, Fresno; *B*, Madera Area; *C*, Mendota; *D*, Chowchilla; *E*, Central California Irrigation District (CCID) South – shallow; *F*, CCID South – deep; *G*, Merced; *H*, CCID North.

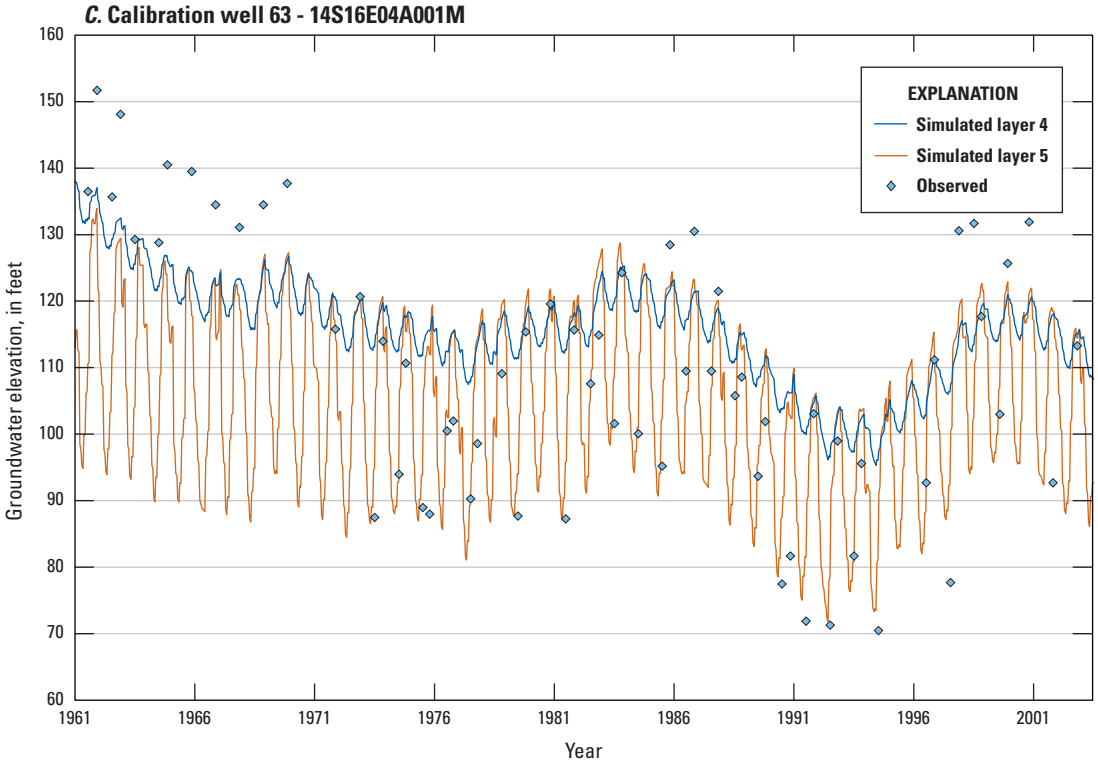

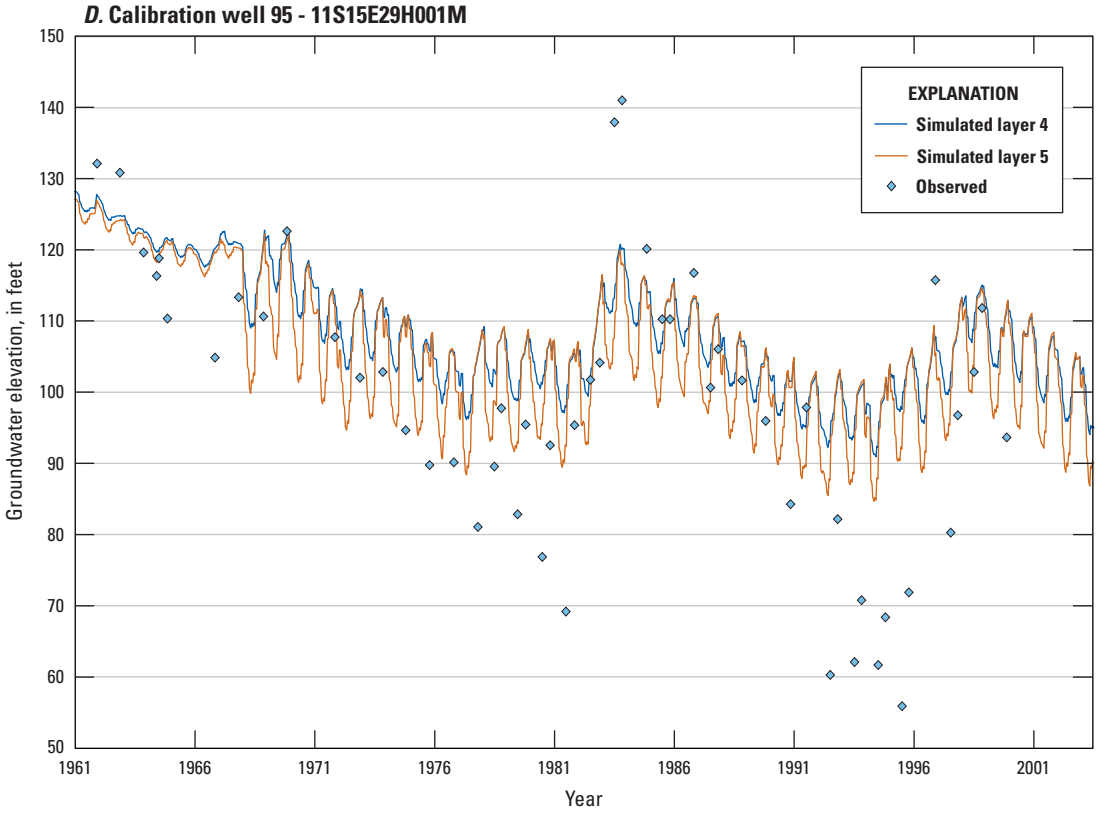

Figure 32. —Continued.

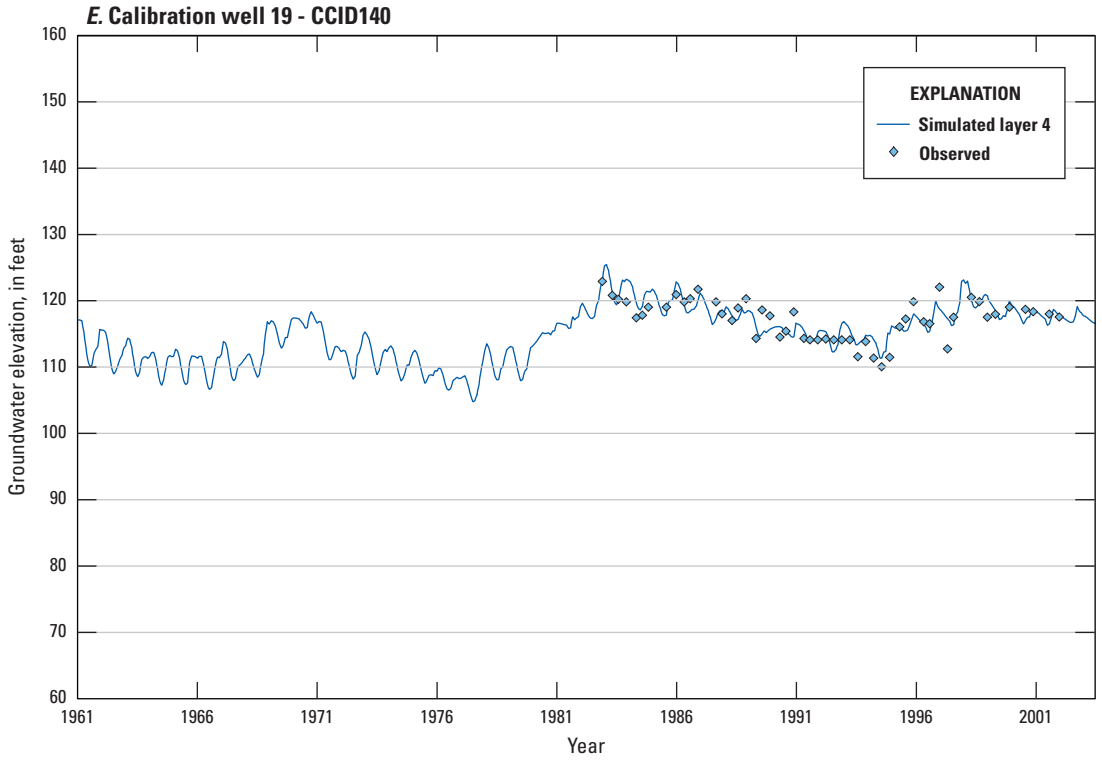

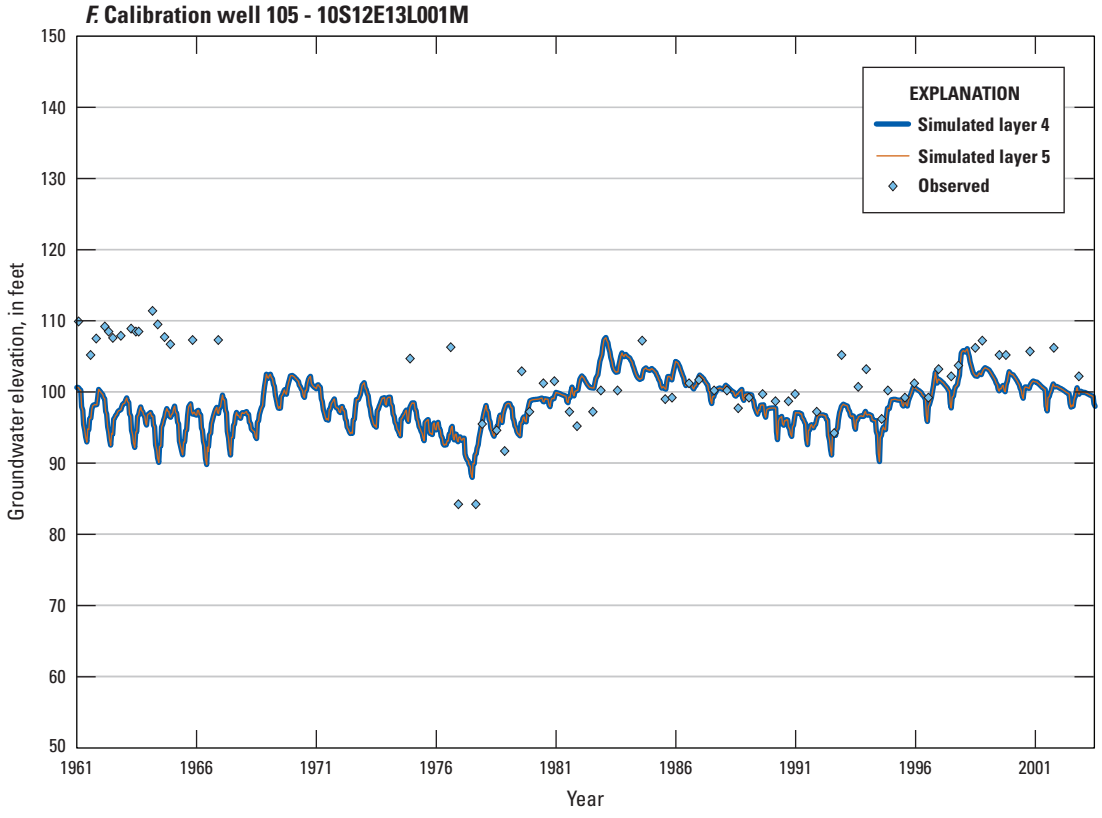

Figure 32. —Continued.

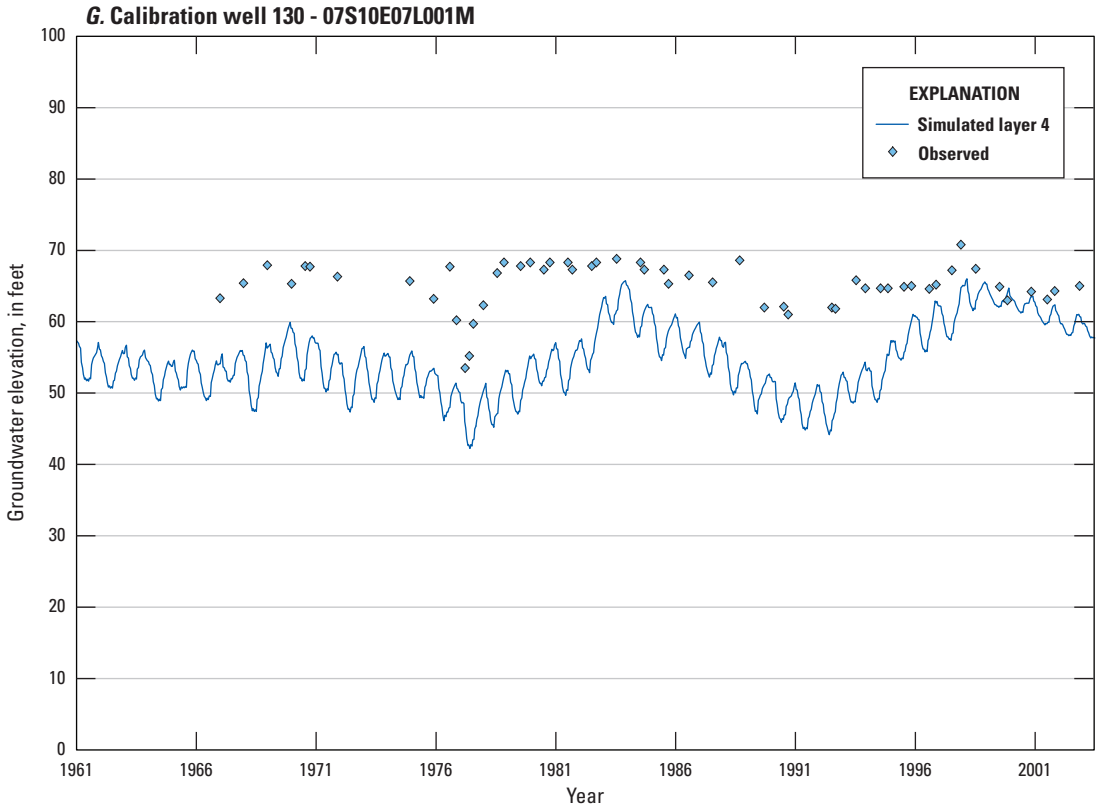

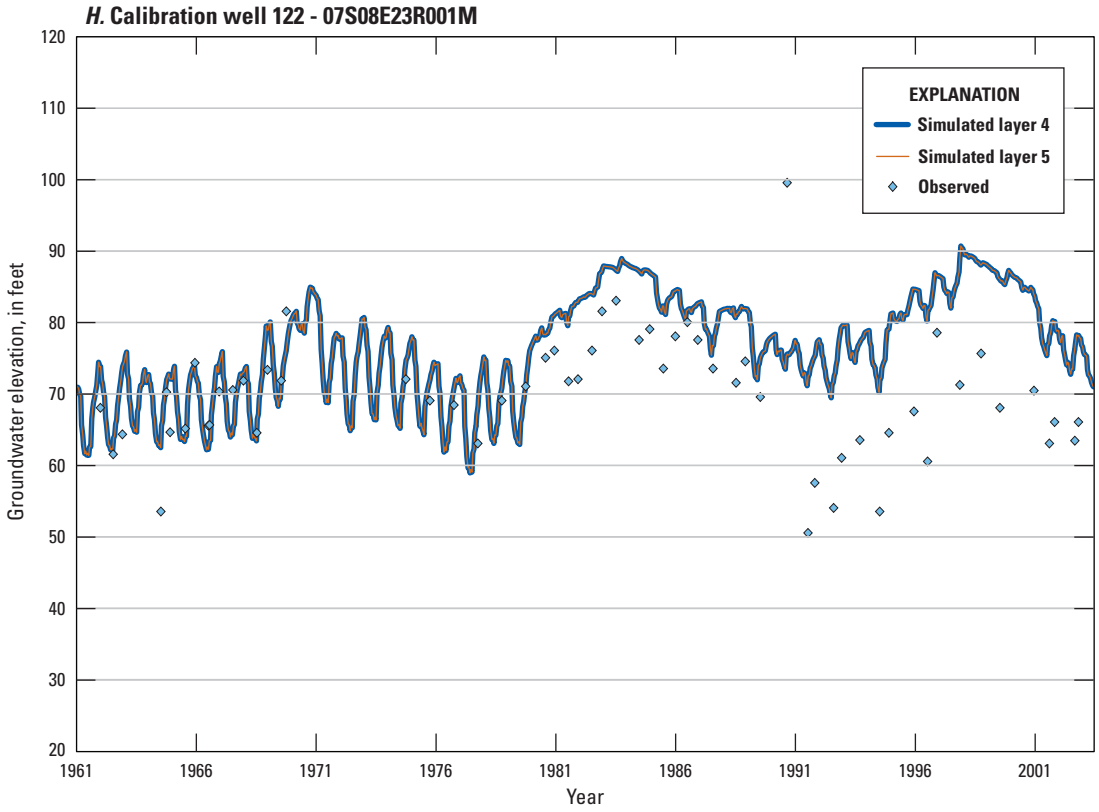

Figure 32. —Continued.

Model Fit to Streamflow Observations

A histogram of residuals between the simulated and observed streamflow for all 4,695 observations at the 19 streamgages is shown in figure 33*A*. The residuals range from −8,464 to 6,818 ft^3/s and have a mean of −111 ft^3/s, an absolute mean of 234 ft^3/s, a standard deviation of 571 ft^3/s, a skewness of −2.6, and an excess kurtosis of 46. The mean value of −111 ft^3/s indicates the simulated streamflows are biased slightly low. The higher value of excess kurtosis indicates more of the variance is associated with a small number of large-value residuals rather than with a larger number of small-value residuals. Approximately 77 percent of the values simulated by the SJRRPGW are within 250 ft^3/s of the observed values, and about 89 percent are within 500 ft^3/s (observed flows range from 0 to 24,200 ft^3/s). Plots comparing the simulated and observed streamflow at all 19 calibration streamgages are shown in appendix C.

The relation between observed and simulated streamflows provides a means to quantify the model fit (fig. 33*B*). Many of the points plot below the 1-to-1 correlation line, indicating the SJRRPGW generally simulates streamflows too low or is biased low. The greater deviation from the 1-to-1 correlation line for low streamflows indicates the model more accurately simulates high streamflows than low. The relation between residual and observed streamflow also quantifies the model fit (fig. 33*C*). This figure, like the previous ones, indicates the model generally simulates high streamflows too low.

The relation between the simulated and observed streamflow at the streamgage at San Joaquin River near Newman, Calif., is shown in figure 34. The model matches the temporal trends in streamflow well; however, the simulated streamflow is on average approximately 500 ft^3/s less than the observed streamflow. Because this streamgage is near the downstream (northwest) side of the model, it represents the total cumulative underestimation of streamflow in the SJRRPGW.

There are several reasons why the SJRRPGW underestimates streamflow by an average of 111 ft^3/s and cumulatively by approximately 500 ft^3/s. Although stream inflow to the model is specified at the locations where major streams enter the model boundary, local runoff to minor streams and drains outside the model boundary that contribute to streams within the model domain is not accounted for in the model. The routing of runoff is simulated by the FMP2 for lands within the study area; however, for lands outside of the study area, these flows are not accounted for. This discrepancy is especially evident for the streamgages on Mud Slough and Salt Slough, where the simulated values are lower than the observed flows by a factor of about 10.

In addition, there are times where surface-water deliveries to a subregion exceed the irrigation demand in that subregion as calculated by the FMP2. An option to return this surplus water to the stream system currently is not available in FMP2, so this excess water is not accounted for in the SJRRPGW streamflow network. This excess surface water not being returned to the stream network averages approximately 350 ft^3/s.

Correlation Coefficient

The *correlation coefficient* (R) is a measure of model fit that explains how well the trends in the simulated values match the trends of the observed values (Doherty, 2005). R is defined as:

$$R = \frac{\sum_m \left(w_m \times h_m^{obs} - \bar{h}^{obs}\right)\left(w_m \times \bar{h}_m^{sim}\right)}{\sqrt{\sum_m \left(w_m \times h_m^{obs} - \bar{h}^{obs}\right)^2 \times \sum_m \left(w_m \times h_m^{sim} - \bar{h}^{sim}\right)^2}} \quad (3)$$

where

R is the correlation coefficient,

h_m^{obs} is the value of observation m,

$\bar{h}^{obs}$ is the mean of the weighted observed values,

h_m^{sim} is the imulated value corresponding to observation m,

$\bar{h}^{sim}$ is the mean of the weighted simulated values, and

W_m is the weight of the m^{th} observation.

Generally, a value of R greater than 0.9 indicates the fit between the simulated and observed trends is acceptable (Hill and Tiedeman, 2007). The weighted R for groundwater elevations is 0.98, indicating an acceptable fit to observed trends. The weighted R for streamflow is 0.16, which is artificially low because of the method used to weight the streamflow observations; the unweighted R for streamflow is 0.96, indicating an acceptable fit to observed trends.

Sensitivity Analysis and Parameter Uncertainty

The final calibrated parameters represent the set of parameters that minimizes the sum of the squared residuals between each observation and its corresponding simulated value while obeying the prior information constraints placed on the parameters. However, it is possible with a complex hydrologic model to vary the values in the parameter set, sometimes by large amounts, and generate many alternate models with only slightly higher error. In a sense, the final calibrated parameter set can be viewed as a single set of parameters from an entire range of parameter sets that also would calibrate the model. Sensitivity tests and uncertainty analysis are, therefore, important steps in judging the performance of a complex hydrologic model (Hill and Tiedeman, 2007).

A sensitivity analysis is performed on the model parameters to test the robustness of the parameter values estimated during the calibration process. The sensitivity of each parameter is a measure of how much the simulated values (each corresponding to an observation) change with respect to a change in the parameter value. The parameter sensitivities give a sense of the tolerance within which model parameters can vary without substantially changing the model calibration. More sensitive parameters are more robust because they can only change a small amount before the model is out of calibration. Less sensitive parameters are less robust because they can change a large amount and still result in a calibrated model.

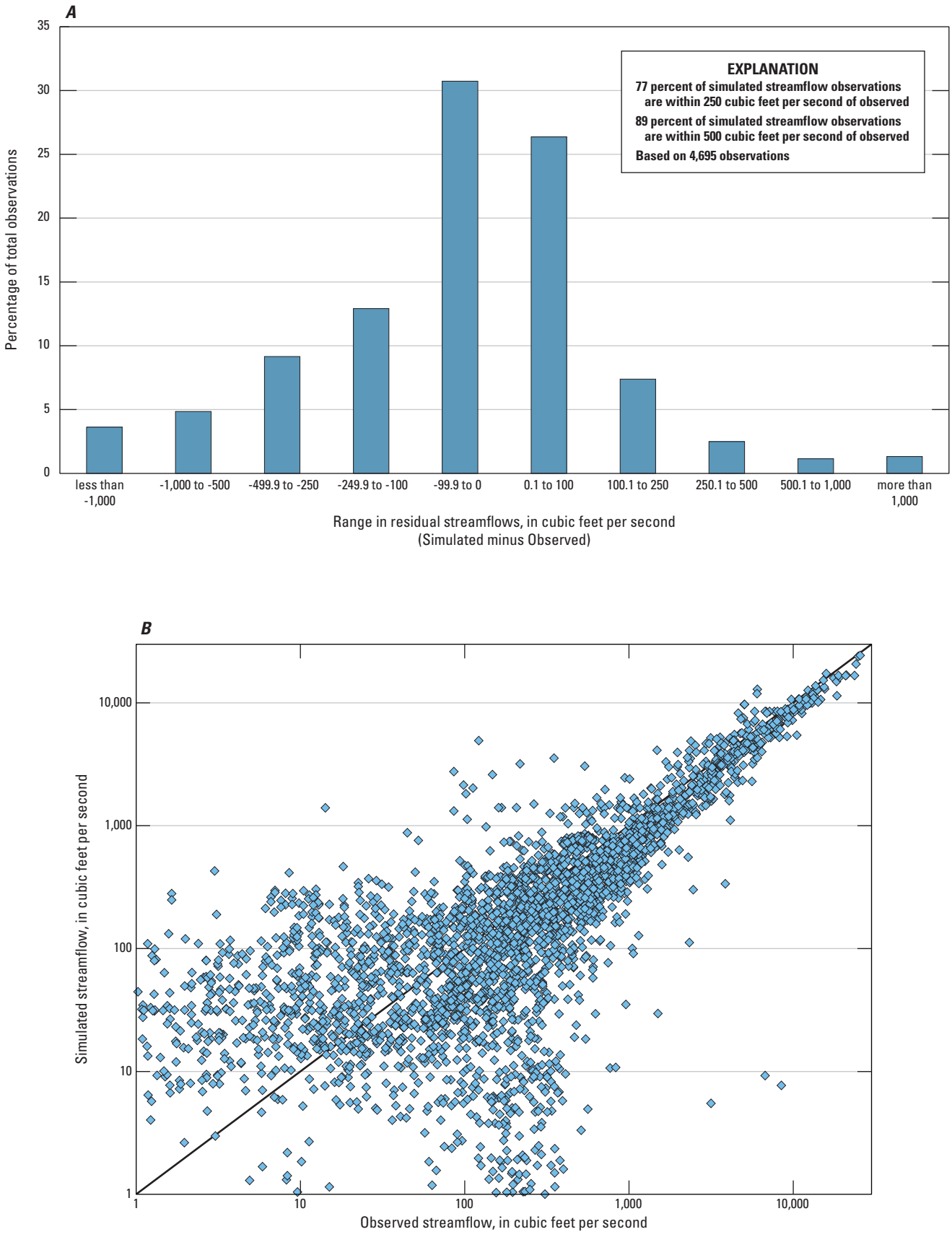

Figure 33. Relation between simulated and observed streamflows: *A*, histogram of residuals between simulated and observed streamflows; *B*, simulated and observed streamflows; *C*, residual and observed streamflows.

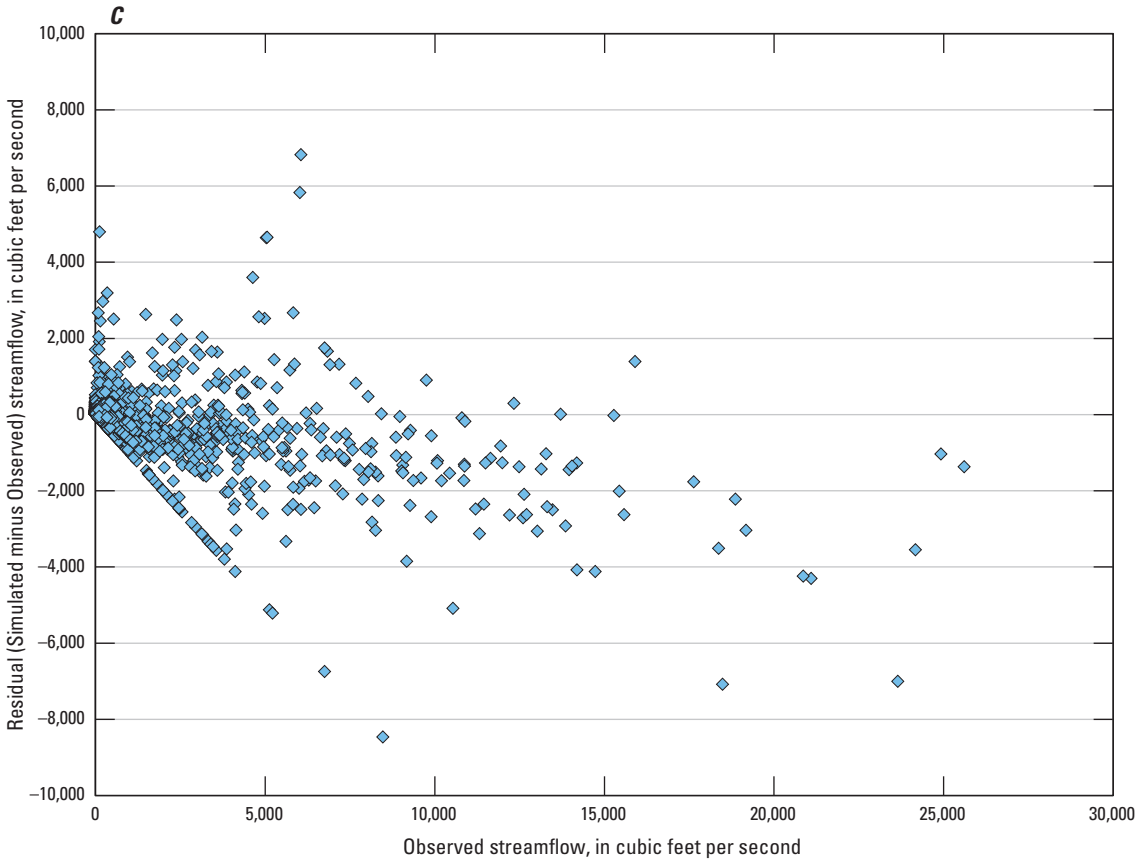

Figure 33. —Continued.

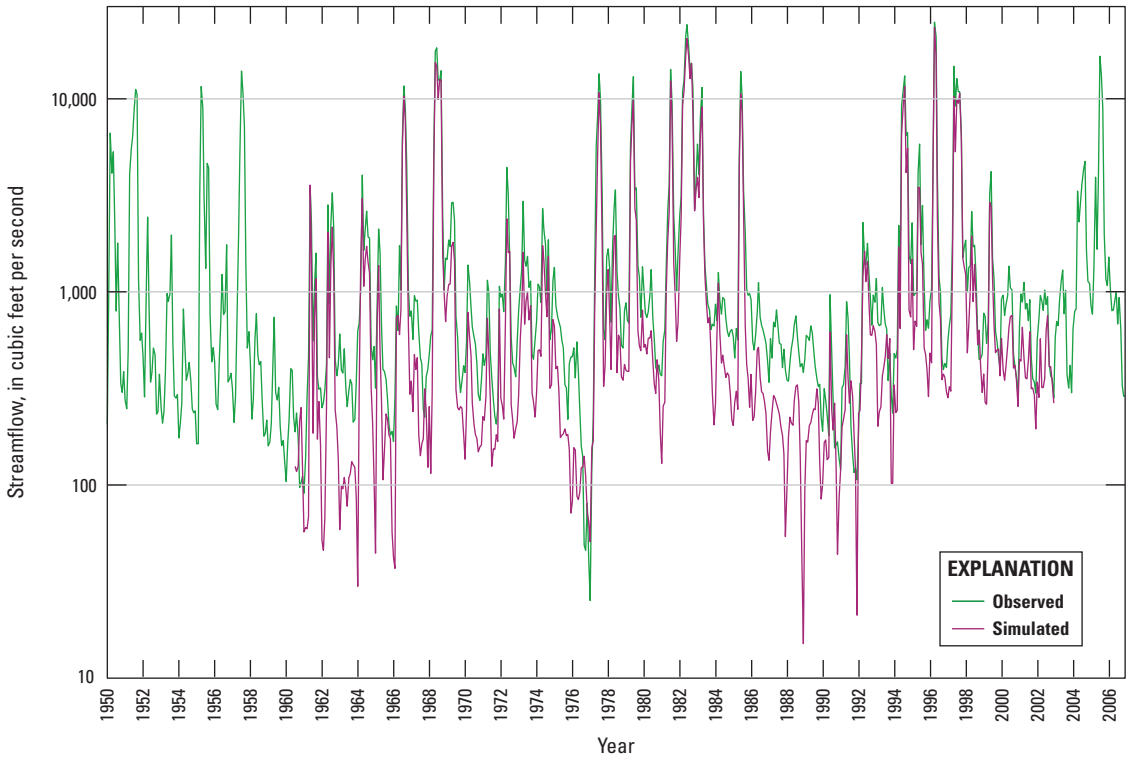

Figure 34. Simulated and observed streamflow downstream from San Joaquin River Reach 5 (San Joaquin River near Newman, California, streamgage), San Joaquin Valley, California.

It is important to discuss some limitations to the analysis performed in this section of the report. First, the calculations presented in this section assume the SJRRPGW model results vary linearly with changes in parameter values. In reality, the model sensitivity may be greater because of the non-linear response of the model. Also, a "sensitivity analysis" only measures the variability of simulated values that correspond to an observation. One of the main purposes of the model is to estimate the groundwater and surface-water interaction associated with SJRRP flows. However, because no model observations correspond to the groundwater and surface-water interaction, it is possible some parameters (such as streambed conductivities) may be insensitive to calibration observations but very sensitive to the simulated groundwater and surface-water interaction. For the analysis in this section, all prior information was removed from the objective function. Values for the 32 hydraulic parameters, which were log-transformed for the calibration, were not transformed for this analysis.

Composite Sensitivity

The *composite sensitivity* of a model parameter (Doherty, 2005) is defined as:

$$s_n = \frac{\sqrt{\sum_m \left(J_{mn} \times w_m\right)^2}}{z} \quad (4)$$

where

S_n is the composite sensitivity of the n^{th} parameter,

J_{mn} is the change in the simulated value for the m^{th} observation with respect to a change in the n^{th} parameter value (the m-by-n matrix of all these changes is known as the Jacobian matrix),

w_m is the weight of the m^{th} observation (same as used during calibration), and

z is the normalization factor (set to the number of observations by PEST).

Multiplying the composite sensitivity by the parameter value (P_n) results in the *relative composite sensitivity* (fig. 35*A–C*), which allows for better comparison of the composite sensitivities of parameters of different magnitudes. The figures show how much of the composite sensitivity of each parameter is attributed to each of the observation types (groundwater elevations, groundwater drawdowns, and streamflows), which is useful for determining parameter sensitivity to data types.

It is important to note that even with *relative composite sensitivity,* caution must be taken when comparing the sensitivities of different parameter types. For example, the crop-coefficient scale factor for pasture (KC_13) is the most sensitive parameter (fig. 35*A–C*). In contrast, the river-bed hydraulic conductivity for eastern tributaries (K_Trib_SE) is less than half as sensitive. This means that if KC_13 were doubled, it would result in roughly twice as much change in the simulated results than if K_Tribe_SE were doubled. However, doubling KC_13 would lead to a parameter value that does not make physical sense, whereas doubling K_Trib_SE would still be a plausible parameter value.

Thus, comparisons of *relative composite sensitivity* should be limited to parameters of the same type. For example, the horizontal hydraulic conductivity of sand (HK_Sand) is over five times as sensitive as the vertical hydraulic conductivity of sand (VK_Sand), indicating the estimate of HK_Sand is more robust. This relation makes physical sense because HK_Sand is much more likely to influence groundwater flow through the aquifer than VK_Sand. A similar relation is seen between the vertical hydraulic conductivity of clay (VK_Clay) and the horizontal hydraulic conductivity of clay (HK_Clay). When comparing the sensitivity of crop coefficients, the most sensitive values generally are for crops that have the most acreage in the study area (such as pasture, cotton, vineyards, and orchards). Similarly, the most sensitive irrigation efficiencies are for those subregions with high agricultural groundwater pumping and many calibration wells (such as Westlands Water District).

Confidence Limits

Another useful measure of parameter robustness is the 95-percent confidence limit for the estimated value of each parameter (table 12). As part of the parameter estimation process, PEST calculates the covariance between all parameter pairs (Doherty, 2005) as follows:

$$C = \frac{\Phi}{m-n} \times \left(J^t \times Q \times J\right)^{-1} \quad (5)$$

where

C is the covariance matrix for each parameter (n-by-n Matrix),

Φ is the objective function,

m is the total number of observations,

n is the total number of parameters,

J is the Jacobian matrix (m-by-n matrix of the change in the simulated value for the m^{th} observation with respect to a change in the n^{th} parameter value), and

Q is the m-by-m diagonal matrix whose diagonal elements are w_m (weight of the m^{th} observation).

The variance of each parameter value (P_n) is the diagonal element of the covariance matrix for that parameter. The standard error of each parameter is the square root of the variance. The 95-percent confidence interval in each direction around the estimated parameter value is 1.96 times the standard error.

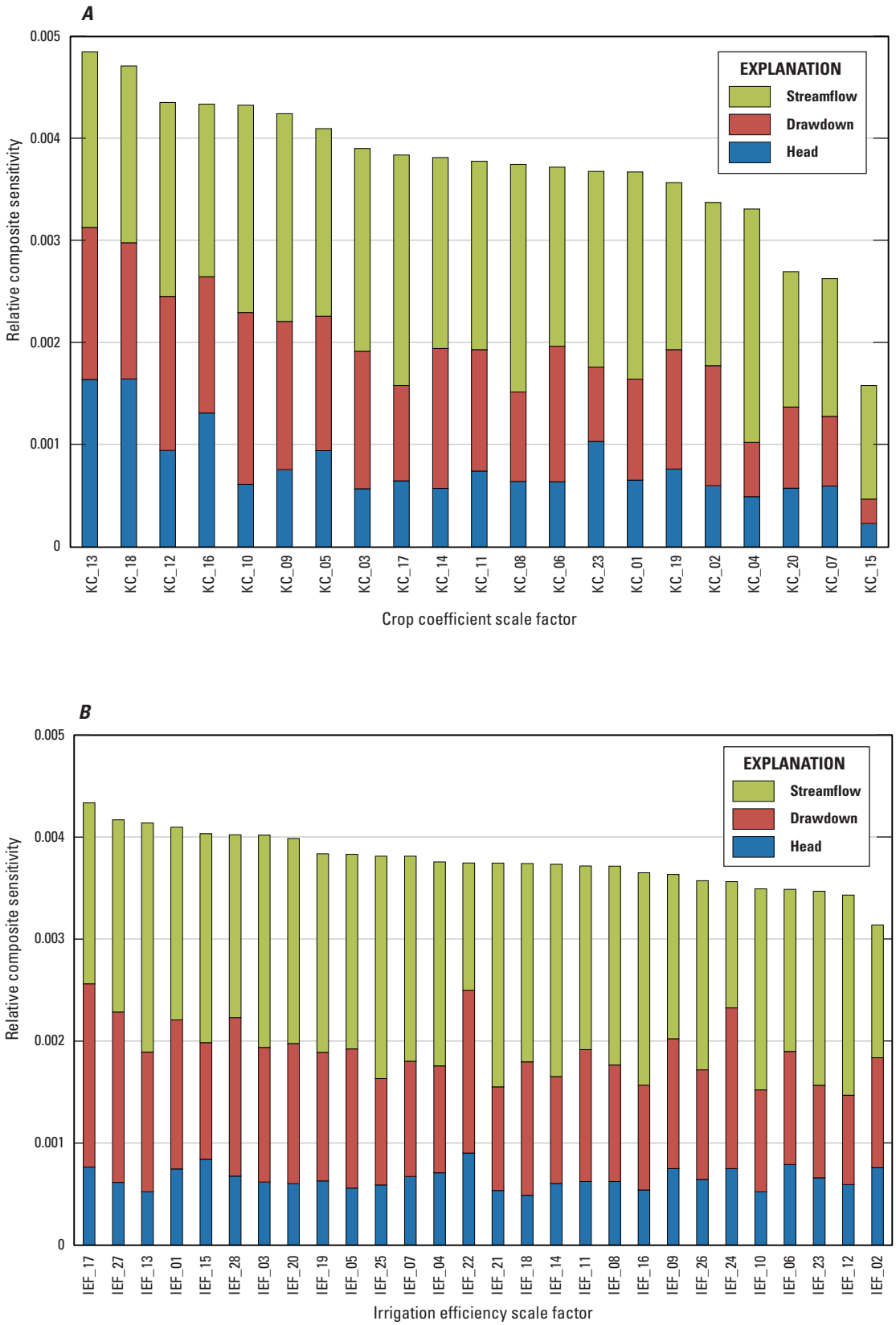

Figure 35. Relative composite sensitivities of San Joaquin River Restoration Program groundwater flow model (SJRRPGW) model parameters, San Joaquin Valley, California: *A*, sensitivity to crop coefficients for each crop type; *B*, sensitivity to irrigation efficiencies for each subregion; *C*, sensitivity to hydraulic parameters. [Hydraulic parameters are defined in table 11.]

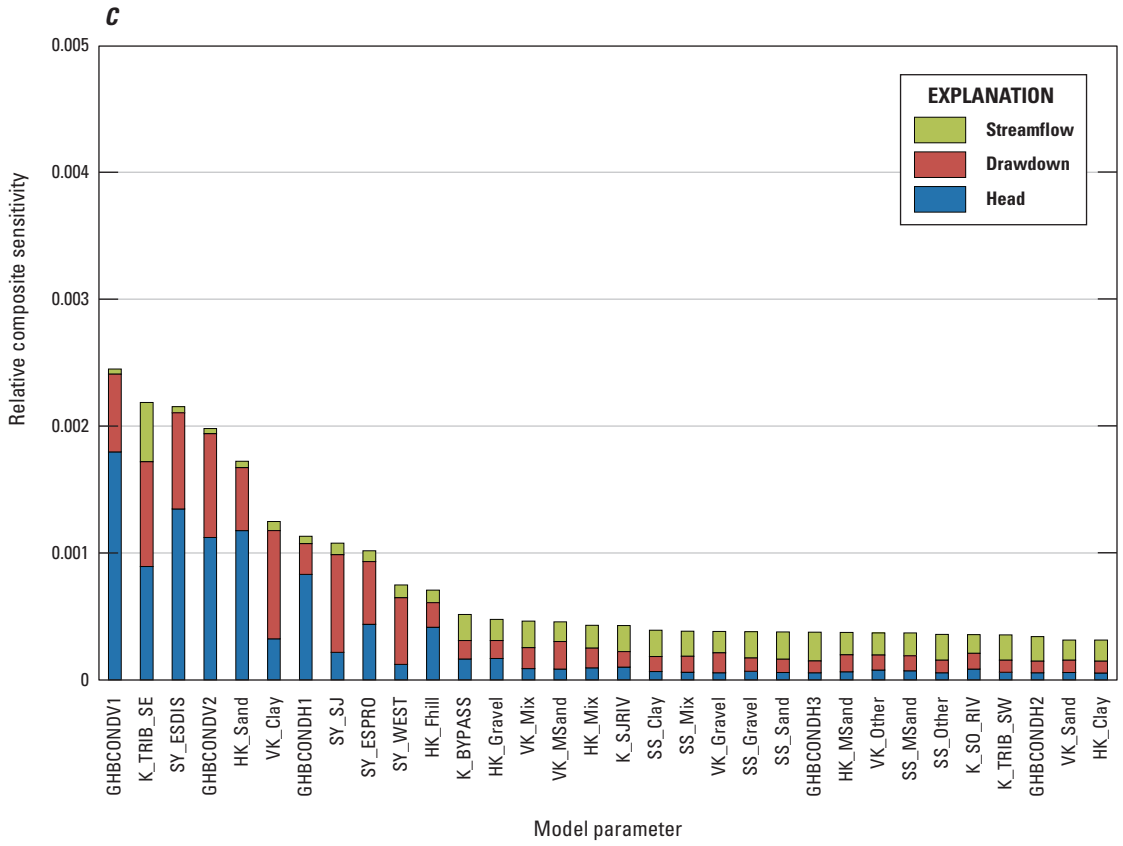

Figure 35. —Continued.

One advantage of using confidence limits is that they provide a range of sensitivity in units of actual parameter values; the traditionally used composite sensitivity method provides only a relative indicator of sensitivity. For determining the robustness of the parameter values, the confidence limits take into account the correlation between parameters. Generally, sensitive parameters are more robust (changing the parameter values by a small amount causes a large change in the simulation results), and insensitive parameters are less robust. However, in some cases, two sensitive parameters may be correlated such that a change in one parameter "cancels out" a change in the other. In these cases, the simulation results are insensitive to both parameters if they are varied together. The values of these parameters are more uncertain than is suggested by their individual sensitivities.

As an example, the lower general-head boundary conductance in the Fresno area (GHBCONDV2) is almost twice as sensitive as the lateral general-head boundary conductance for the western model boundary (GHBCONDH1) (fig. 35*C*). Looking only at the sensitivities suggests the parameter estimate for GHBCONDV2 is more robust than that for GHBCONDH1. However, GHBCONDV2 is moderately correlated to other parameters. Because of this correlation, considering the standard error (table 12), GHBCONDV2 has a percent standard error similar to that of GHBCONDH1, revealing the parameter estimate for GHBCONDV2 is no more robust than that for GHBCONDH1.

Model Results

Model results presented in this section include simulated hydrologic budgets, groundwater-elevation maps, and maps showing the interaction of surface water and groundwater.

Simulated Hydrologic Budgets

Budgets presented include the overall volumetric groundwater budget, the detailed farm budget from the FMP2, and the streamflow budget from the SFR2. The key components for each of these water budgets are shown in table 14. Some budget components are reported in more than one budget (such as groundwater pumping), and slight differences in values are possible for the same component in two budgets. These differences are primarily because of the fact that groundwater budget information was obtained from the second time step of each stress period; the rates for that time step were assumed to represent the entire stress period. This approximation was used (rather than averaging both time steps) because the model output file is extremely large when both time steps are saved and the large file size was beyond the ability of available tools to process. Slight differences are also possible because of the methods used for averaging and rounding the budget values in the tables.

Groundwater Budget

The groundwater budget provides information about the balance of flows into and out of the aquifer system in the SJRRPGW. This section presents three different ways of summarizing the groundwater budget—annual average by subregion, annual total model-wide, and monthly average model-wide.

The annual average groundwater budget for the entire simulation period for each subregion is useful for understanding the spatial distribution of the components of recharge and discharge (table 15). For example, the study area has experienced a net decline in storage over the simulation period, and this loss of storage is mostly in subregions that rely on groundwater pumping to meet demands.

Table 14. Components of San Joaquin River Restoration Program groundwater flow model (SJRRPGW) simulated hydrologic budgets, San Joaquin Valley, California.

Groundwater budget
Municipal groundwater pumping
Agricultural groundwater pumping
Net percolation to groundwater[1]
Net stream seepage to groundwater
Net subsurface boundary flow
Net inter-subregion flow
Convergence discrepancy
Change in groundwater storage
Farm budget
Precipitation
Surface-water delivery
Agricultural groundwater pumping
Groundwater uptake by plants
Crop consumptive use
Runoff to streams[2]
Percolation to groundwater[2]
Unused surface water
Streamflow budget
San Joaquin River inflow
Merced River inflow
Kings River inflow
Other streams inflow
Runoff to streams[2]
Net diversions
Net stream seepage to groundwater
San Joaquin River outflow

[1]From both precipitation and irrigation.

[2]Net percolation to groundwater is the difference between percolation to groundwater and groundwater uptake by plants.

The annual groundwater budget for the SJRRPGW from 1962 to 2003 is useful for understanding how the components of the groundwater budget change through time during the simulation period (table 16 and fig. 36). Many of the groundwater-budget components are dependent on hydrology, such as net stream seepage. Some components are dependent on land use, such as municipal pumping. Other components are more complex, depending on a variety of factors. Agricultural pumping, for example, is dependent on hydrology because dry years require more pumping due to decreased rainfall and associated surface-water deliveries, but agricultural pumping generally decreases over time due to increased irrigation efficiencies, increased surface-water availability, and changing crop types. The cumulative annual change in aquifer storage between 1962 and 2003 shows an increase in groundwater storage during wet years and a decrease in groundwater storage during dry years (fig. 36).

The monthly average groundwater budget for the SJRRPGW is useful for understanding how the components of the groundwater budget vary by month (table 17). Agricultural pumping shows a seasonal pattern; most of the pumping occurs during the growing season. Groundwater recharge by net percolation shows a bimodal distribution; most recharge occurs during January and February, when precipitation is greatest, and during July, when irrigation is greatest. On average, the aquifer loses storage during the growing season and gains storage during the rainy season.

Farm Budget

The farm budget provides information about the water demand of crops and other plants in the study area and the various water supplies that meet this demand. This section presents three different ways of summarizing the farm budget—annual average by subregion, annual total model-wide, and monthly average model-wide.

The annual average farm budget for the entire simulation period for each subregion is useful for understanding the spatial distribution of supply and demand (table 18). For example, subregions on the west side of the San Joaquin River, such as Grasslands Water District (5) and San Luis Canal Company (9), receive predominantly surface water; subregions on the east side of the San Joaquin River, such as unorganized Madera County (12), rely predominantly on groundwater. Groundwater uptake by plants occurs in subregions where the water table is shallow. The annual average farm budgets for agricultural water supply and demand for each subregion are shown in figures 37 and 38, respectively.

The annual farm budget for the SJRRPGW from 1962 to 2003 is useful for understanding how the components of the farm budget change through time during the simulation period (table 19 and fig. 39). Many of the farm-budget components are dependent on hydrology, such as surface-water delivery; the minimum surface-water delivery (415,000 acre-ft/yr) was in 1977, a critically dry year. Groundwater uptake by plants is greatest in years with above-average precipitation, runoff, and

Table 15. San Joaquin River Restoration Program groundwater flow model (SJRRPGW) annual average groundwater budget by subregion, San Joaquin Valley, California.

[All groundwater budget terms are in units of acre-feet per year. **Abbreviations**: I.D., Irrigation District; W.D., Water District]

Subregion	Name	Municipal pumping	Agricultural pumping	Net percolation to groundwater	Net stream seepage to groundwater	Net subsurface boundary flow	Net inter-subregion flow	Convergence discrepancy	Change in groundwater storage
		–	–	+	+	+	+	+	=
1	Turlock I.D.	0	13,200	6,800	1,900	6,700	–1,700	0	500
2	Central California I.D. North	300	40,200	20,400	–1,600	44,700	–22,300	0	700
3	City of Newman	700	1,600	1,300	0	700	300	0	100
4	Stevenson W.D.	100	97,700	33,500	22,100	37,800	2,300	100	–2,100
5	Grasslands W.D.	0	53,100	17,100	1,100	32,600	2,500	200	600
6	Wildlife Refuges	0	115,200	31,700	24,200	19,600	39,600	400	400
7	Unorganized Merced County	0	38,600	13,200	11,500	14,400	–3,500	100	–3,000
8	Turner Island W.D.	0	48,400	14,800	13,500	8,300	10,800	100	–1,000
9	San Luis Canal Company	100	8,200	12,800	8,400	10,900	–23,800	200	100
10	El Nido I.D.	0	7,400	8,500	2,700	1,600	–4,400	0	1,000
11	Chowchilla W.D.	0	38,800	24,900	1,700	13,400	–600	0	700
12	Unorganized Madera County	0	67,200	24,600	11,100	16,800	14,000	0	–700
13	Sierra W.D.	0	27,000	9,600	12,500	1,700	3,100	0	–100
14	Clayton W.D.	0	6,100	2,300	1,600	100	1,900	0	–100
15	Central California I.D. South	900	56,100	27,600	43,200	11,100	–24,600	100	400
16	Firebaugh Canal Company	100	23,300	16,800	600	–7,900	13,900	0	0
17	Westlands W.D.	300	17,500	23,000	100	50,800	–56,200	100	0
18	Columbia Canal Company	100	41,400	14,800	47,300	–9,200	–13,200	0	–1,800
19	New Stone W.D.	0	52,200	19,800	4,200	–1,400	26,800	0	–2,900
20	Farmers W.D.	0	2,700	1,800	2,600	–1,600	–300	0	–200
21	Allso W.D.	0	76,900	26,800	20,700	8,000	15,000	0	–6,500
22	Mendota Wildlife Area	100	132,800	34,200	16,300	12,800	64,900	0	–4,700
23	Gravelly Ford W.D.	0	200	4,800	0	–2,000	–3,400	0	–800
24	Madera I.D.	100	21,200	32,300	9,900	–16,900	–10,000	–100	–6,000
25	Fresno I.D.	100	16,300	30,000	19,200	–15,600	–25,500	–100	–8,500
26	Bonadelle Ranchos	1,400	69,000	24,800	46,600	–17,600	5,600	0	–11,200
27	City of Fresno	24,800	27,000	25,400	22,200	–18,600	7,900	0	–14,900
28	Foothills	400	8,700	4,600	23,100	–3,600	–18,700	0	–3,600
Total		29,600	1,108,100	508,100	366,700	197,900	0	1,200	–63,800

Table 16. San Joaquin River Restoration Program groundwater flow model (SJRRPGW) annual groundwater budget, San Joaquin Valley, California.

[All groundwater budget terms are in acre-feet per year.]

Water year	Municipal pumping	Agricultural pumping	Net percolation to groundwater	Net stream seepage to groundwater	Net subsurface boundary flow	Net inter-subregion flow	Convergence discrepancy	Change in groundwater storage
	–	–	+	+	+	+	+	=
1962	19,000	1,391,000	706,000	276,000	198,000	0	2,000	–228,000
1963	19,000	1,154,000	501,000	274,000	196,000	0	2,000	–201,000
1964	19,000	1,377,000	470,000	222,000	227,000	0	1,000	–476,000
1965	19,000	1,199,000	548,000	297,000	227,000	0	2,000	–143,000
1966	19,000	1,504,000	657,000	264,000	247,000	0	2,000	–353,000
1967	19,000	1,193,000	700,000	609,000	227,000	0	2,000	327,000
1968	19,000	1,473,000	480,000	219,000	243,000	0	2,000	–548,000
1969	19,000	1,138,000	961,000	775,000	203,000	0	1,000	783,000
1970	19,000	1,222,000	577,000	238,000	206,000	0	1,000	–219,000
1971	19,000	1,341,000	523,000	203,000	222,000	0	1,000	–411,000
1972	19,000	1,588,000	516,000	239,000	269,000	0	2,000	–582,000
1973	19,000	1,256,000	815,000	380,000	254,000	0	–1,000	172,000
1974	19,000	1,266,000	555,000	313,000	278,000	0	1,000	–139,000
1975	19,000	1,240,000	494,000	250,000	301,000	0	2,000	–213,000
1976	19,000	1,439,000	460,000	238,000	323,000	0	1,000	–436,000
1977	19,000	1,692,000	460,000	236,000	358,000	0	1,000	–657,000
1978	28,000	1,126,000	850,000	741,000	276,000	0	0	713,000
1979	32,000	1,241,000	624,000	322,000	286,000	0	1,000	–40,000
1980	32,000	974,000	584,000	682,000	248,000	0	2,000	509,000
1981	32,000	1,169,000	472,000	251,000	234,000	0	1,000	–244,000
1982	32,000	826,000	492,000	509,000	197,000	0	1,000	340,000
1983	32,000	699,000	735,000	903,000	152,000	0	–2,000	1,057,000
1984	32,000	989,000	352,000	344,000	174,000	0	1,000	–149,000
1985	32,000	1,035,000	322,000	166,000	169,000	0	2,000	–408,000
1986	32,000	881,000	468,000	468,000	157,000	0	3,000	183,000
1987	32,000	1,115,000	345,000	187,000	171,000	0	2,000	–442,000
1988	32,000	1,115,000	356,000	193,000	166,000	0	1,000	–431,000
1989	32,000	1,164,000	378,000	216,000	173,000	0	1,000	–428,000
1990	32,000	1,170,000	345,000	222,000	176,000	0	1,000	–459,000
1991	32,000	1,261,000	510,000	264,000	187,000	0	1,000	–330,000

Table 16. San Joaquin River Restoration Program groundwater flow model (SJRRPGW) annual groundwater budget, San Joaquin Valley, California.—Continued

[All groundwater budget terms are in acre-feet per year.]

Water year	Municipal pumping	Agricultural pumping	Net percolation to groundwater	Net stream seepage to groundwater	Net subsurface boundary flow	Net inter-subregion flow	Convergence discrepancy	Change in groundwater storage
	–	–	+	+	+	+	+	=
1992	32,000	1,247,000	490,000	289,000	170,000	0	0	–331,000
1993	38,000	911,000	731,000	447,000	137,000	0	–1,000	365,000
1994	41,000	1,057,000	351,000	328,000	162,000	0	3,000	–253,000
1995	41,000	734,000	651,000	772,000	130,000	0	1,000	780,000
1996	41,000	859,000	450,000	456,000	124,000	0	2,000	132,000
1997	41,000	863,000	562,000	610,000	113,000	0	1,000	382,000
1998	41,000	523,000	672,000	668,000	77,000	0	0	852,000
1999	43,000	696,000	118,000	285,000	121,000	0	3,000	–212,000
2000	44,000	763,000	318,000	293,000	135,000	0	2,000	–59,000
2001	44,000	843,000	195,000	250,000	139,000	0	1,000	–302,000
2002	44,000	967,000	259,000	241,000	135,000	0	2,000	–372,000
2003	44,000	838,000	289,000	260,000	122,000	0	1,000	–211,000

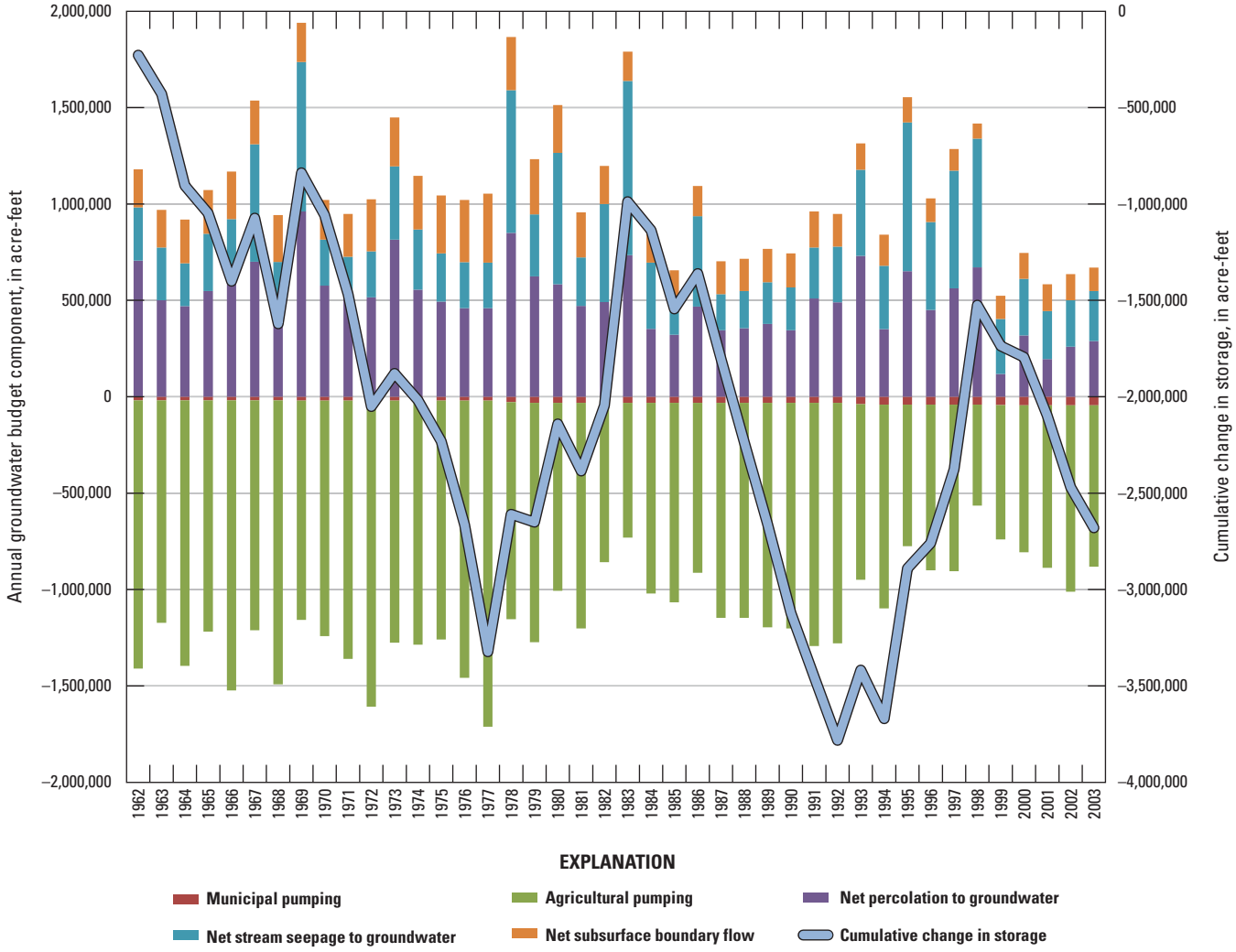

Figure 36. San Joaquin River Restoration Program groundwater flow model (SJRRPGW) annual groundwater budget and cumulative change in groundwater storage, San Joaquin Valley, California.

Table 17. San Joaquin River Restoration Program groundwater flow model (SJRRPGW) monthly average groundwater budget, San Joaquin Valley, California.

[All groundwater budget terms are in acre-feet per year.]

Month	Municipal pumping	Agricultural pumping	Net percolation to groundwater	Net stream seepage to groundwater	Net subsurface boundary flow	Net inter-subregion flow	Convergence discrepancy	Change in groundwater storage
	–	–	+	+	+	+	+	=
1	1,400	9,900	74,500	31,700	8,300	0	–100	103,300
2	1,300	20,100	61,100	41,800	9,000	0	–100	90,400
3	1,600	38,200	34,500	36,000	11,200	0	0	41,800
4	2,200	63,800	19,200	39,900	14,000	0	100	7,200
5	3,000	114,200	26,500	36,000	19,000	0	200	–35,500
6	3,500	178,500	42,000	40,300	24,200	0	300	–75,100
7	4,000	209,500	53,300	39,600	27,200	0	400	–93,100
8	3,800	207,500	51,400	31,600	26,900	0	500	–101,000
9	3,200	167,000	39,900	17,600	24,100	0	300	–88,300
10	2,500	75,000	17,900	14,800	15,300	0	0	–29,600
11	1,700	14,400	37,300	16,300	9,900	0	–100	47,200
12	1,500	10,000	50,500	21,200	8,700	0	–100	68,900

Table 18. San Joaquin River Restoration Program groundwater flow model (SJRRPGW) annual average farm budget by subregion, San Joaquin Valley, California.

[All farm budget terms are in acre-feet per year. **Abbreviations**: I.D., Irrigation District; W.D., Water District]

Subregion	Name	IN				OUT			
		Precipitation	Surface-water delivery	Agricultural groundwater pumping	Groundwater uptake by plants	Crop consumptive use	Runoff to streams	Percolation to groundwater	Unused surface water
1	Turlock I.D.	16,100	34,900	13,000	9,500	47,400	1,200	16,200	8,800
2	Central California I.D. North	24,700	42,400	40,100	5,100	76,600	2,100	25,400	8,200
3	City of Newman	1,600	6,300	1,600	300	3,900	100	1,500	4,300
4	Stevenson W.D.	51,400	17,000	97,600	8,600	129,300	3,200	42,100	0
5	Grasslands W.D.	17,200	34,900	52,600	9,100	67,600	1,400	25,900	18,900
6	Wildlife Refuges	33,800	16,500	114,500	15,900	125,600	2,700	47,200	5,100
7	Unorganized Merced County	38,400	14,500	38,600	7,700	76,000	2,200	20,900	100
8	Turner Island W.D.	35,600	13,600	48,400	6,500	80,300	2,200	21,300	200
9	San Luis Canal Company	42,000	134,800	8,000	30,100	123,600	3,700	42,400	45,300
10	El Nido I.D.	8,400	19,000	7,400	0	22,800	700	8,600	2,900
11	Chowchilla W.D.	24,200	42,300	38,800	0	70,200	2,000	25,000	8,200
12	Unorganized Madera County	30,400	4,800	67,200	0	75,900	1,900	24,700	–100
13	Sierra W.D.	13,000	3,700	27,000	800	32,700	800	10,500	400
14	Clayton W.D.	2,900	500	6,100	100	7,000	200	2,500	0
15	Central California I.D. South	48,400	91,100	55,700	20,600	127,900	4,700	47,700	35,500
16	Firebaugh Canal Company	16,100	36,400	23,300	0	50,600	1,600	16,800	6,700
17	Westlands W.D.	19,100	92,100	17,500	100	74,700	1,700	23,100	29,300
18	Columbia Canal Company	16,000	3,800	41,400	1,800	44,700	1,600	16,600	0
19	New Stone W.D.	32,300	6,400	52,200	200	69,200	1,800	20,000	0
20	Farmers W.D.	1,800	3,400	2,700	0	5,600	100	1,800	400
21	Allso W.D.	41,500	8,000	76,900	200	97,500	2,000	27,100	0
22	Mendota Wildlife Area	32,100	6,300	132,800	200	135,300	1,600	34,500	100
23	Gravelly Ford W.D.	7,600	35,600	200	0	14,600	200	4,800	24,000
24	Madera I.D.	45,300	75,000	21,200	0	84,600	700	32,300	23,800
25	Fresno I.D.	39,500	77,200	16,300	0	78,300	700	30,000	24,100
26	Bonadelle Ranchos	67,600	0	69,000	0	102,400	9,500	24,800	0
27	City of Fresno	48,600	36,500	27,000	0	75,600	1,500	25,400	9,700
28	Foothills	30,000	0	8,700	0	27,900	6,300	4,600	0
Total		785,800	857,000	1,105,800	117,000	1,927,700	58,400	623,500	255,900

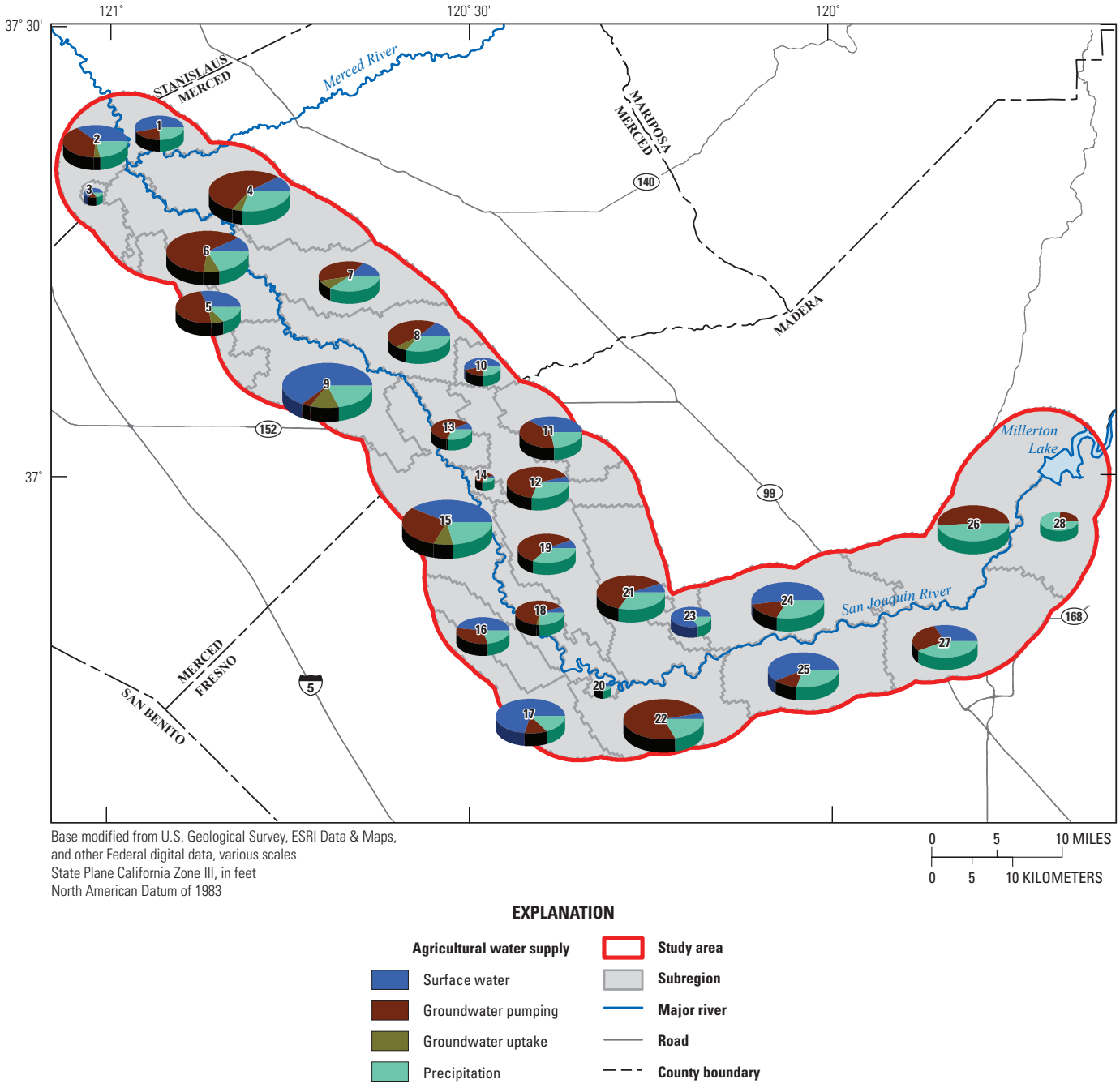

Figure 37. San Joaquin River Restoration Program groundwater flow model (SJRRPGW) agricultural water supply by subregion, San Joaquin Valley, California.

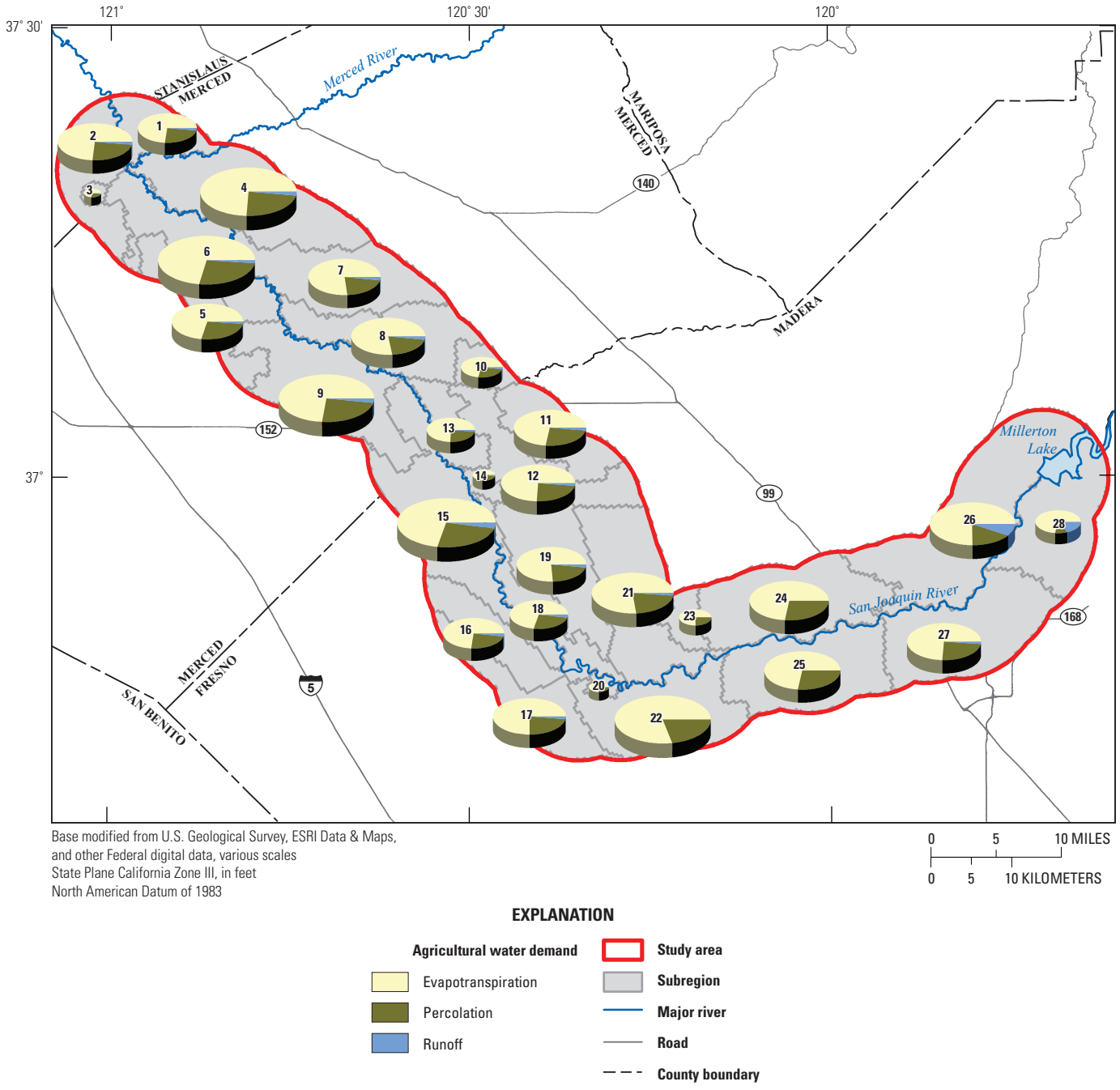

Figure 38. San Joaquin River Restoration Program groundwater flow model (SJRRPGW) agricultural water demand by subregion, San Joaquin Valley, California.

Table 19. San Joaquin River Restoration Program groundwater flow model (SJRRPGW) annual average farm budget, San Joaquin Valley, California.

[All farm budget terms are in acre-feet per year.]

Water year	IN				OUT			
	Precipitation	Surface-water delivery	Agricultural groundwater pumping	Groundwater uptake by plants	Crop consumptive use	Runoff to streams	Percolation to groundwater	Unused surface water
1962	816,000	726,000	1,387,000	142,000	1,991,000	102,000	845,000	134,000
1963	841,000	765,000	1,151,000	121,000	2,027,000	55,000	620,000	176,000
1964	510,000	671,000	1,375,000	96,000	1,926,000	39,000	565,000	123,000
1965	794,000	792,000	1,197,000	99,000	1,989,000	65,000	646,000	180,000
1966	613,000	686,000	1,501,000	102,000	1,967,000	73,000	756,000	107,000
1967	1,054,000	826,000	1,189,000	117,000	2,037,000	114,000	815,000	220,000
1968	505,000	677,000	1,471,000	90,000	2,026,000	32,000	569,000	116,000
1969	1,332,000	805,000	1,134,000	154,000	1,990,000	118,000	1,112,000	206,000
1970	792,000	873,000	1,219,000	157,000	2,044,000	57,000	732,000	208,000
1971	641,000	685,000	1,337,000	128,000	1,943,000	50,000	648,000	150,000
1972	329,000	647,000	1,586,000	91,000	1,904,000	38,000	605,000	106,000
1973	1,033,000	723,000	1,253,000	104,000	1,963,000	85,000	917,000	148,000
1974	767,000	789,000	1,264,000	93,000	2,005,000	49,000	648,000	211,000
1975	690,000	800,000	1,238,000	81,000	1,974,000	38,000	576,000	221,000
1976	502,000	623,000	1,437,000	56,000	1,944,000	29,000	516,000	129,000
1977	353,000	415,000	1,691,000	34,000	1,924,000	25,000	494,000	50,000
1978	1,286,000	691,000	1,124,000	58,000	1,983,000	88,000	906,000	182,000
1979	762,000	800,000	1,240,000	60,000	1,927,000	48,000	684,000	203,000
1980	832,000	1,014,000	973,000	82,000	1,857,000	52,000	665,000	327,000
1981	569,000	962,000	1,168,000	87,000	1,930,000	33,000	559,000	265,000
1982	1,006,000	1,022,000	825,000	109,000	1,916,000	48,000	599,000	399,000
1983	1,460,000	985,000	696,000	184,000	1,867,000	96,000	915,000	448,000
1984	553,000	1,282,000	985,000	207,000	1,845,000	43,000	554,000	585,000
1985	564,000	943,000	1,031,000	156,000	1,852,000	30,000	475,000	339,000
1986	906,000	996,000	878,000	152,000	1,884,000	48,000	617,000	383,000
1987	516,000	861,000	1,112,000	130,000	1,857,000	25,000	473,000	264,000
1988	586,000	879,000	1,114,000	106,000	1,917,000	29,000	460,000	279,000
1989	561,000	766,000	1,162,000	79,000	1,881,000	28,000	456,000	204,000
1990	520,000	755,000	1,169,000	58,000	1,883,000	20,000	403,000	197,000
1991	577,000	676,000	1,260,000	49,000	1,836,000	42,000	558,000	126,000

Table 19. San Joaquin River Restoration Program groundwater flow model (SJRRPGW) annual average farm budget, San Joaquin Valley, California.—Continued

[All farm budget terms are in acre-feet per year.]

Water year	IN				OUT			
	Precipitation	Surface-water delivery	Agricultural groundwater pumping	Groundwater uptake by plants	Crop consumptive use	Runoff to streams	Percolation to groundwater	Unused surface water
1992	671,000	640,000	1,246,000	46,000	1,907,000	37,000	536,000	123,000
1993	1,093,000	912,000	910,000	63,000	1,888,000	78,000	794,000	217,000
1994	664,000	814,000	1,055,000	60,000	1,983,000	27,000	411,000	172,000
1995	1,265,000	982,000	732,000	105,000	1,919,000	127,000	755,000	283,000
1996	883,000	1,042,000	856,000	139,000	1,958,000	75,000	588,000	300,000
1997	958,000	1,011,000	859,000	181,000	1,868,000	127,000	740,000	275,000
1998	1,651,000	934,000	522,000	221,000	1,877,000	147,000	890,000	413,000
1999	586,000	1,040,000	694,000	217,000	1,772,000	33,000	333,000	399,000
2000	859,000	1,041,000	759,000	209,000	1,905,000	82,000	525,000	356,000
2001	741,000	1,103,000	841,000	184,000	1,951,000	38,000	379,000	501,000
2002	600,000	1,057,000	964,000	161,000	1,911,000	44,000	419,000	407,000
2003	762,000	1,281,000	836,000	145,000	1,935,000	43,000	432,000	614,000

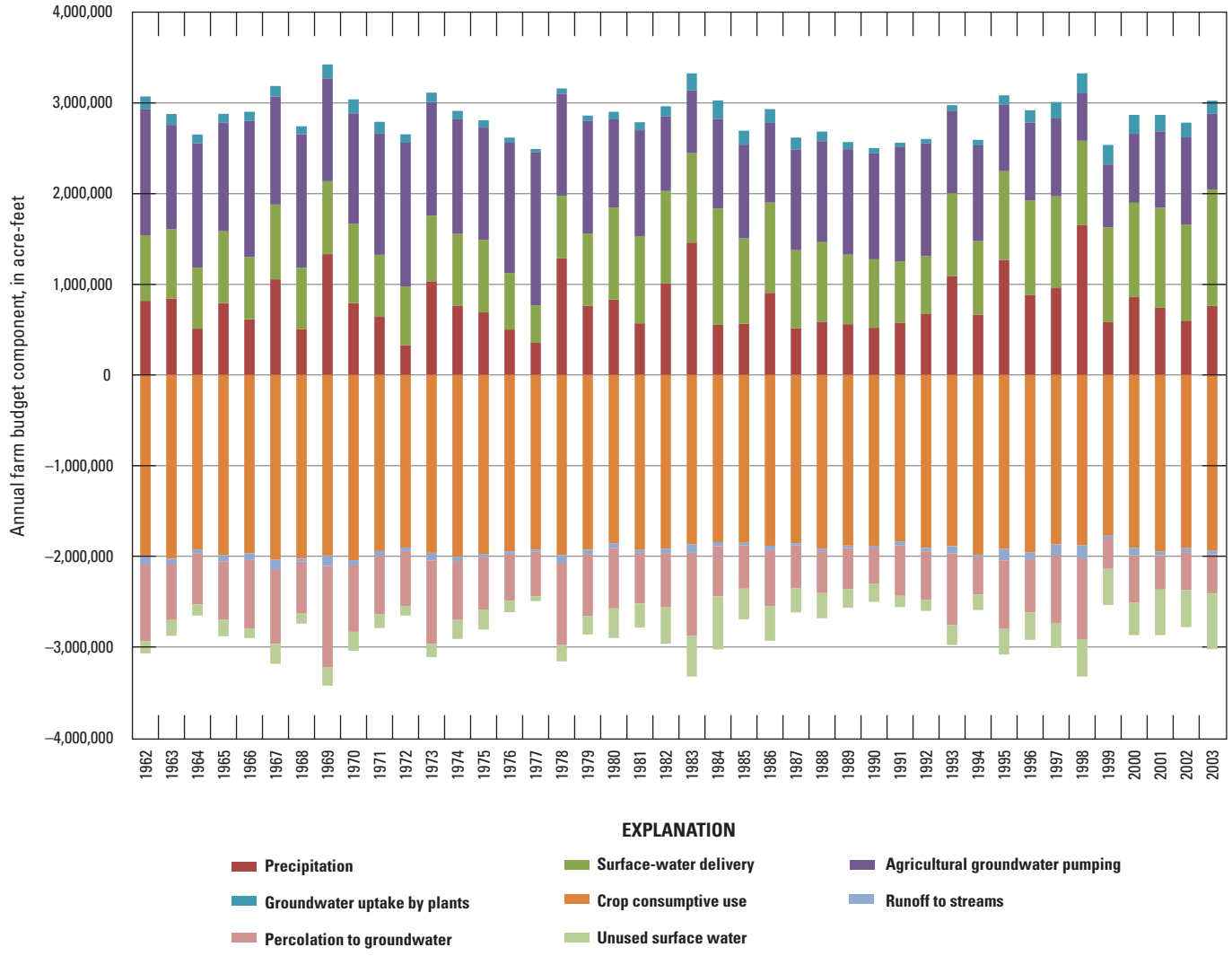

Figure 39. San Joaquin River Restoration Program groundwater flow model (SJRRPGW) annual average farm budget, San Joaquin Valley, California.

associated water-table elevation, such as 1984 and 1998. Crop consumptive use shows a slight decline over time as land use shifts from crops with higher consumptive use to ones with lower consumptive use. Groundwater recharge by percolation of applied water below the root zone decreases through time because of increases in irrigation efficiencies and declines in consumptive use.

The monthly average farm budget for the SJRRPGW is useful for understanding how the components of the farm budget vary by month (table 20). Most crop consumptive use occurs during the growing season, whereas most precipitation occurs in the rainy season. The larger quantities of unused surface water in March, April, and May are likely pre-irrigation deliveries; this process is not simulated by the FMP2.

Streamflow Budget

The streamflow budget provides information about the inflows and outflows to the stream network in the study area. This section presents two ways of summarizing the streamflow budget as well as the annual groundwater and surface-water interaction for each of the management reaches along the San Joaquin River. Note, seepage rates are highly dependent on flow in the river, so seepage rates that will occur under restoration flows are likely to be different than historical seepage rates because of the differences in the timing and magnitude of streamflow.

The annual streamflow budget for the SJRRPGW from 1962 to 2003 is useful for understanding how the components of the streamflow budget change through time during the simulation period (table 21). The average annual net groundwater recharge attributed to stream seepage is 367,000 acre-ft/yr (510 ft^3/s), which includes the seepage from the main San Joaquin River channel, the San Joaquin River flood-control bypass system, and the major San Joaquin River tributaries. The median stream seepage rate was 281,000 acre-ft/yr; the annual stream seepage ranged from 903000 acre-ft in 1983 to 166,000 acre-ft in 1985. San Joaquin River releases from Friant Dam are small except during flood-release periods. Flow from the Kings River Basin is limited to flood releases only. Inflow from the Merced River and from other streams is more steady but is still heavily dependent on hydrology. Net diversions represent the difference between CVP water that flows into the San Joaquin River from the Delta Mendota Canal and Mendota pool and the CVP water diverted from the San Joaquin River between Mendota Pool and Sack Dam. Negative net diversion indicates the Delta Mendota inflow is greater than what is diverted off the river.

Table 20. San Joaquin River Restoration Program groundwater flow model (SJRRPGW) monthly average farm budget, San Joaquin Valley, California.

[All farm budget terms are in acre-feet per month.]

Month	IN				OUT			
	Precipitation	Surface-water delivery	Agricultural groundwater pumping	Groundwater uptake by plants	Crop consumptive use	Runoff to streams	Percolation to groundwater	Unused surface water
1	150,700	13,400	9,900	3,400	76,400	12,600	77,900	10,400
2	145,300	26,900	20,100	4,700	102,800	9,600	65,700	18,900
3	126,700	56,900	38,200	8,600	145,000	4,400	43,800	37,200
4	64,400	75,300	63,700	9,600	142,400	1,900	28,700	40,100
5	24,400	107,800	113,900	14,000	183,800	1,500	40,200	34,500
6	6,400	139,400	178,000	18,200	252,700	2,800	59,700	27,000
7	1,300	159,200	208,900	18,900	289,000	3,600	71,500	24,100
8	2,100	127,700	207,000	16,900	267,800	3,700	67,700	14,400
9	13,300	75,200	166,600	10,900	200,400	2,800	50,400	12,400
10	41,100	48,400	75,000	5,700	127,600	900	24,000	17,800
11	98,800	16,700	14,400	3,100	75,600	5,300	40,400	11,700
12	111,400	10,000	10,000	2,900	64,000	9,400	53,400	7,500

Table 21. San Joaquin River Restoration Program groundwater flow model (SJRRPGW) annual average streamflow budget, San Joaquin Valley, California.

[All streamflow budget terms are in acre-feet per year.]

Year	San Joaquin River inflow	Merced River inflow	Kings River inflow	Other streams inflow	Runoff to streams	Net diversions	Net stream seepage to groundwater	San Joaquin River outflow
	+	+	+	+	+	–	–	=
1962	75,000	238,000	0	249,000	102,000	–115,000	276,000	504,000
1963	83,000	352,000	0	184,000	56,000	–116,000	274,000	517,000
1964	70,000	53,000	0	23,000	39,000	–115,000	222,000	77,000
1965	63,000	539,000	0	266,000	66,000	–115,000	297,000	752,000
1966	62,000	166,000	0	92,000	73,000	–122,000	264,000	251,000
1967	1,272,000	572,000	483,000	400,000	114,000	361,000	609,000	1,871,000
1968	58,000	181,000	0	26,000	32,000	–125,000	219,000	203,000
1969	2,233,000	1,039,000	1,562,000	797,000	118,000	460,000	775,000	4,514,000
1970	89,000	392,000	62,000	156,000	57,000	–91,000	238,000	609,000
1971	48,000	154,000	0	57,000	50,000	–121,000	203,000	228,000
1972	68,000	219,000	0	24,000	38,000	–129,000	239,000	240,000
1973	292,000	134,000	0	311,000	85,000	–85,000	380,000	527,000
1974	137,000	389,000	87,000	164,000	49,000	–5,000	313,000	517,000
1975	54,000	449,000	0	183,000	38,000	–120,000	250,000	593,000
1976	80,000	193,000	0	9,000	30,000	–119,000	238,000	193,000
1977	91,000	83,000	0	1,000	25,000	–118,000	236,000	81,000
1978	1,354,000	448,000	550,000	465,000	88,000	307,000	741,000	1,857,000
1979	108,000	471,000	12,000	210,000	48,000	–92,000	322,000	619,000
1980	979,000	840,000	578,000	421,000	52,000	268,000	682,000	1,920,000
1981	69,000	206,000	0	155,000	33,000	–127,000	251,000	339,000
1982	823,000	821,000	452,000	468,000	48,000	223,000	509,000	1,880,000
1983	3,187,000	1,945,000	2,319,000	1,360,000	96,000	634,000	903,000	7,369,000
1984	609,000	618,000	563,000	352,000	43,000	31,000	344,000	1,810,000
1985	64,000	245,000	0	66,000	30,000	–114,000	166,000	353,000
1986	989,000	483,000	667,000	377,000	48,000	286,000	468,000	1,809,000
1987	67,000	135,000	1,000	98,000	25,000	–104,000	187,000	242,000
1988	79,000	114,000	0	35,000	29,000	–95,000	193,000	160,000
1989	84,000	120,000	0	27,000	28,000	–105,000	216,000	148,000
1990	99,000	140,000	0	17,000	20,000	–97,000	222,000	150,000
1991	104,000	102,000	0	55,000	42,000	–108,000	264,000	147,000
1992	122,000	139,000	0	66,000	37,000	–116,000	289,000	192,000
1993	322,000	315,000	0	365,000	78,000	–7,000	447,000	640,000
1994	120,000	166,000	0	148,000	27,000	–137,000	328,000	269,000
1995	1,658,000	939,000	584,000	457,000	127,000	421,000	772,000	2,571,000
1996	395,000	619,000	73,000	299,000	75,000	53,000	456,000	951,000
1997	1,205,000	1,094,000	453,000	922,000	127,000	33,000	610,000	3,157,000
1998	1,617,000	1,089,000	985,000	819,000	147,000	448,000	668,000	3,541,000
1999	224,000	440,000	20,000	122,000	33,000	–104,000	285,000	657,000
2000	176,000	404,000	0	208,000	82,000	–106,000	293,000	684,000
2001	132,000	251,000	0	93,000	38,000	–109,000	250,000	373,000
2002	114,000	226,000	0	60,000	44,000	–110,000	241,000	311,000
2003	121,000	230,000	0	69,000	43,000	–117,000	260,000	321,000
Average	467,000	423,000	225,000	254,000	59,000	9,000	367,000	1,051,000

The monthly average streamflow budget for the SJRRPGW is useful for understanding how the components of the streamflow budget vary by month (table 22). All stream inflows to the model are greatest during April and May when runoff from the Sierra Nevada is greatest. Runoff to streams is greatest during January, when rainfall is greatest, but it also has a secondary peak during August because of runoff of irrigation water.

The highest seepage rates are in Reaches 1 and 3 (fig. 40*A* and fig. 40*C*) because these reaches always have flow in them. Reach 1 has flow from Friant Dam releases, and Reach 3 has flow from CVP water released from Mendota Pool. Reach 5 has negative seepage rates (where there is a net groundwater discharge to the stream) between 1999 and 2002 (fig. 40*E*).

Maps of Water-Table Elevation

Maps of depth to the water table were developed for fall 1981, 1983, 1988, 1991, and 2006 (fig. 8*A–E*). Maps of the SJRRPGW-simulated water-table elevation and depth to the water table for fall of these same years, except for 2006, which is beyond the simulation period, are presented in figures 41*A–H*.

The 1981 simulated water-table elevation map (fig. 41*A*) represents a Normal-Dry year. The elevation of the water table generally decreases down the axis of the San Joaquin River. The gradient of the water table is away from Reaches 1 and 2, indicating a losing stream. The simulated water table is flatter in the lower reaches. A notable groundwater depression is to the east of Reach 4A and is primarily caused by agricultural pumping. A depth to groundwater of between 5–15 ft is simulated west of Reaches 3, 4A, and 4B1 (fig. 41*B*). The model results generally match the map of observed depth to water (fig. 8*A*) for this area. The model simulates greater depth to water than observed west of Reaches 2B and 4B2; however, these areas are relatively poorly constrained by observation wells.

The 1983 simulated water-table elevation map (fig. 41*C*) represents a Wet year preceded by a Wet year. The simulated water table rose by around 5–10 ft in most areas relative to 1981. The water table also partially recovered in the groundwater depression east of Reach 4A. A water-table rise associated with seepage from the Chowchilla and Eastside bypasses and from other streams in the study area also is evident. The 1983 map of simulated depth to the water table (fig. 41*D*) shows a depth of 0–10 ft west of Reaches 3, 4A, and 4B1. The model results generally match the observed map of depth to water (fig. 8*B*) for these areas. However, as in 1981, the model simulates deeper water levels west of Reaches 2B and 4B2 in the areas poorly constrained by observation wells.

The 1988 simulated water-table elevation map (fig. 41*E*) represents a Dry year preceded by a Dry year. The simulated water table declined relative to 1983 and is similar to that for 1981. A depth to water of 5–15 ft is simulated west of Reaches 3, 4A, and 4B1 (fig. 41*F*). The model results generally match the observed map of depth to water (fig. 8*C*) for these areas. As for 1981 and 1983, the model simulates deeper water levels west of Reaches 2B and 4B2 in the areas poorly constrained by observation wells.

The 1991 simulated water-table elevation map (fig. 41*G*) represents conditions near the end of a multi-year drought. The simulated water table declined by 10–20 ft relative to 1988 in most areas and by about 5 ft in the shallow groundwater areas (west of Reaches 3, 4A, and 4B1). It is likely that groundwater levels remained relatively high in these areas because the local irrigation districts have firm surface-water rights and do not need to rely as much on groundwater pumping to meet agricultural demands. The simulated depth to water west of Reaches 3, 4A, and 4B1 is 10–20 ft (fig. 41*H*). The model results generally match the observed map of depth to water (fig. 8*D*) in these areas.

Comparison between the simulated and observed maps of depth to water for these 4 years demonstrates the model reasonably matches observed values in most areas where data are present. The SJRRPGW matches the observed depth to water table particularly well in the shallow groundwater areas west of Reaches 3, 4A, and 4B1. The simulated and observed 1983 and 1991 maps of depth to the water table show a shallower water table in 1983 (wet conditions) and a deeper water table in 1991 (dry conditions).

An interactive animation displaying the simulated elevation of the water table for 1961–2003 is available (*http://pubs.usgs.gov/sir/2014/5148/downloads/sir2014-5148_GWE.swf*). A similar interactive animation displaying the simulated depth to the water table is available (*http://pubs.usgs.gov/sir/2014/5148/downloads/sir2014-5148_D2GW.swf*). These animations show how the water-table elevation and depth to the water table change during the simulation period throughout the study area. Seasonal fluctuations, particularly in areas dependent on agricultural groundwater pumping, are clearly evident in the water-table elevation animation. In the animation of depth to the water table, the effects of stream seepage are evident, such as during April 1983 and January 1997, where the depth to water decreases in response to increased streamflow. During dry periods, such as November 1977 or October 1992, the water table drops to more than 10 ft below land surface throughout most of the study area.

Maps of Groundwater and Surface-Water Interaction

The average simulated interaction of groundwater and surface water for the SJRRPGW simulation period (1961–2003) is shown in figure 42. The largest amounts of stream seepage occur in Reaches 1, 2A, and 3, which are sections of the San Joaquin River that have flow most of the time. At the downstream end of Reach 5, the San Joaquin River, as simulated, transitions from a stream that on average loses water (recharges groundwater) to a stream that on average gains

Table 22. San Joaquin River Restoration Program groundwater flow model (SJRRPGW) monthly average streamflow budget, San Joaquin Valley, California.

[All streamflow budget terms are in acre-feet per month.]

Year	San Joaquin River inflow	Merced River inflow	Kings River inflow	Other streams inflow	Runoff to streams	Net diversions	Net stream seepage to groundwater	San Joaquin River outflow
	+	+	+	+	+	–	–	=
1	34,100	37,100	16,900	48,600	12,600	–600	31,700	118,300
2	55,200	52,100	20,200	71,800	9,600	500	41,800	166,700
3	63,500	50,800	30,600	51,500	4,400	8,800	36,000	156,100
4	79,500	50,700	40,300	32,200	1,900	8,800	39,900	155,900
5	74,700	54,700	47,400	9,700	1,500	14,400	36,000	137,600
6	64,400	45,600	33,300	6,100	2,800	10,700	40,300	101,100
7	37,300	27,700	16,000	5,200	3,600	–2,700	39,600	53,000
8	12,800	15,400	1,800	3,600	3,700	–18,600	31,600	24,200
9	11,900	18,600	1,200	1,700	2,800	–5,400	17,600	24,000
10	8,700	25,000	2,500	1,900	900	–4,100	14,800	28,300
11	9,500	18,800	5,700	3,200	5,300	–2,100	16,300	28,300
12	14,900	26,100	9,000	18,700	9,400	–600	21,200	57,700

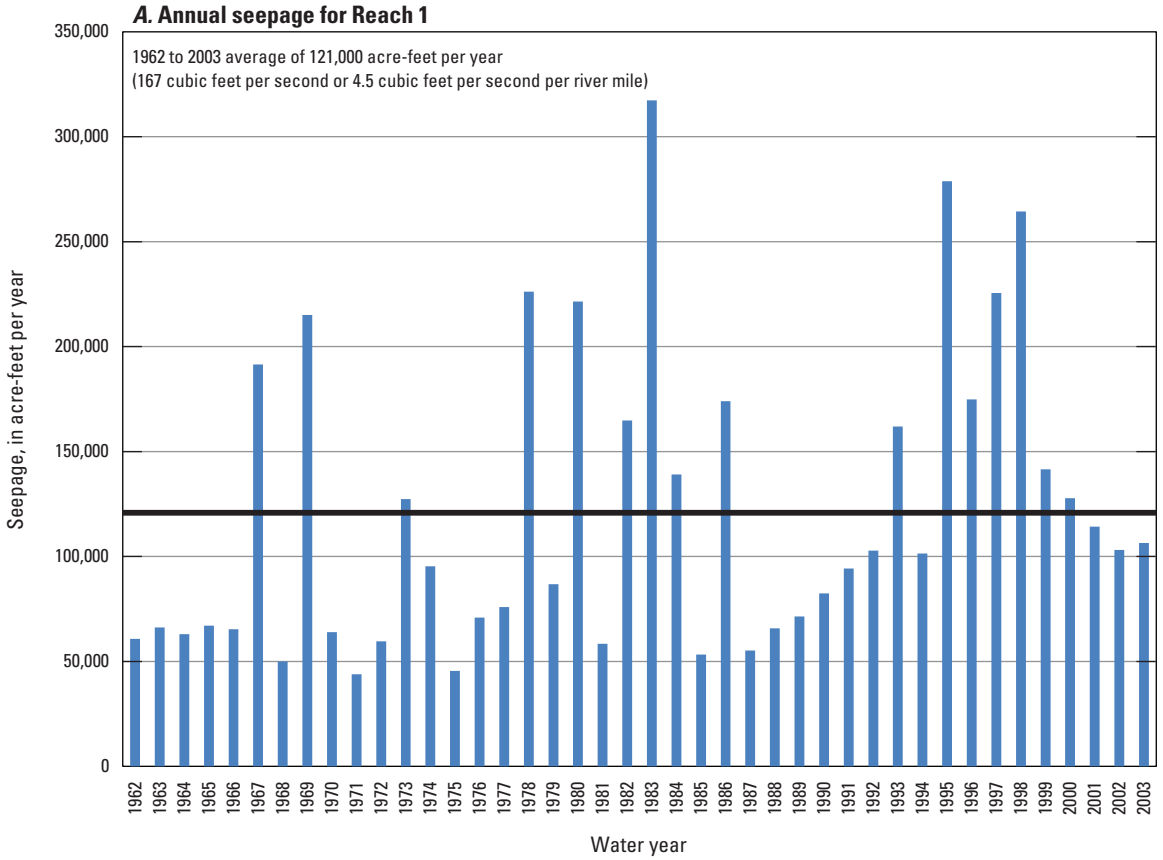

Figure 40. San Joaquin River Restoration Program groundwater flow model (SJRRPGW) annual seepage for San Joaquin River Management Reaches, San Joaquin Valley, California: *A*, Reach 1; *B*, Reach 2; *C*, Reach 3; *D*, Reach 4; *E*, Reach 5.

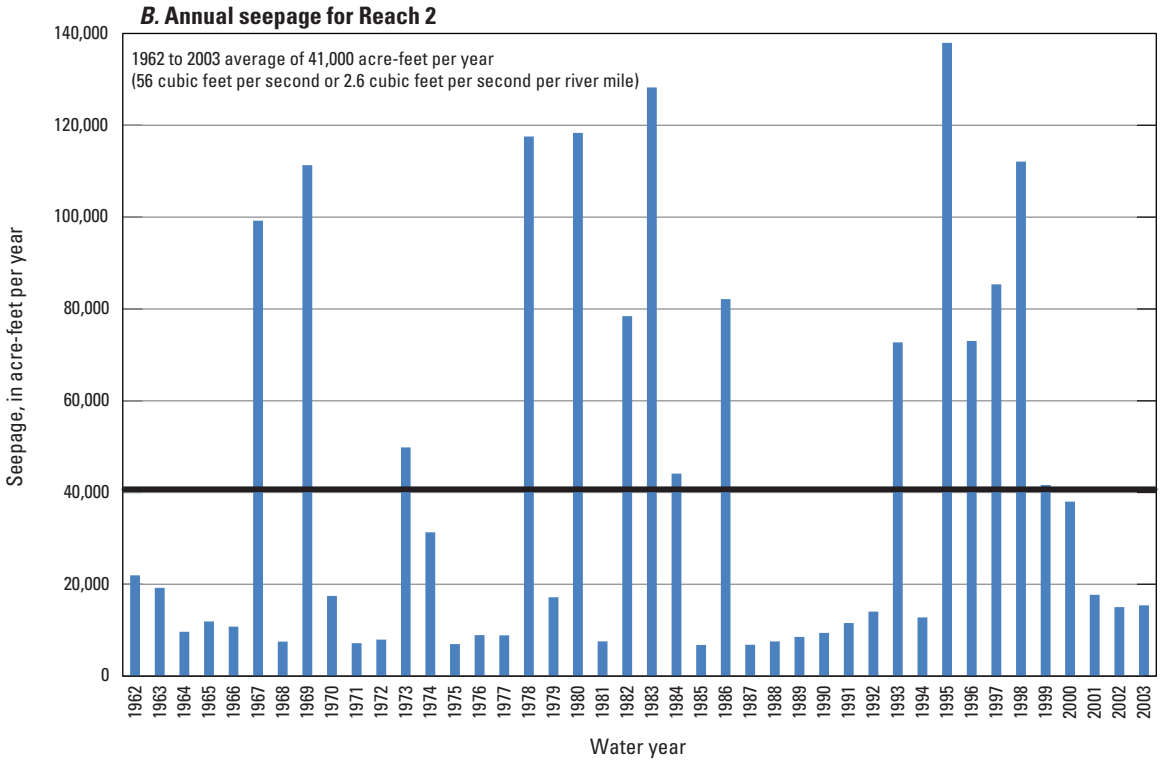

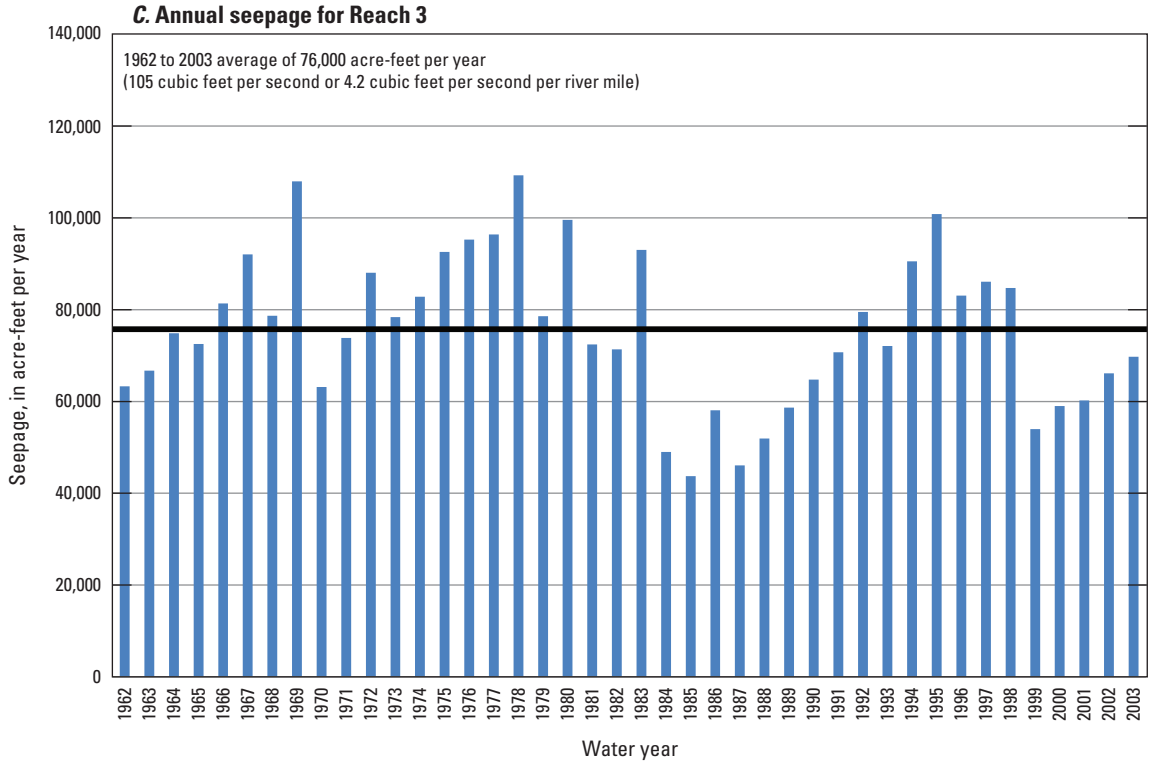

Figure 40. —Continued

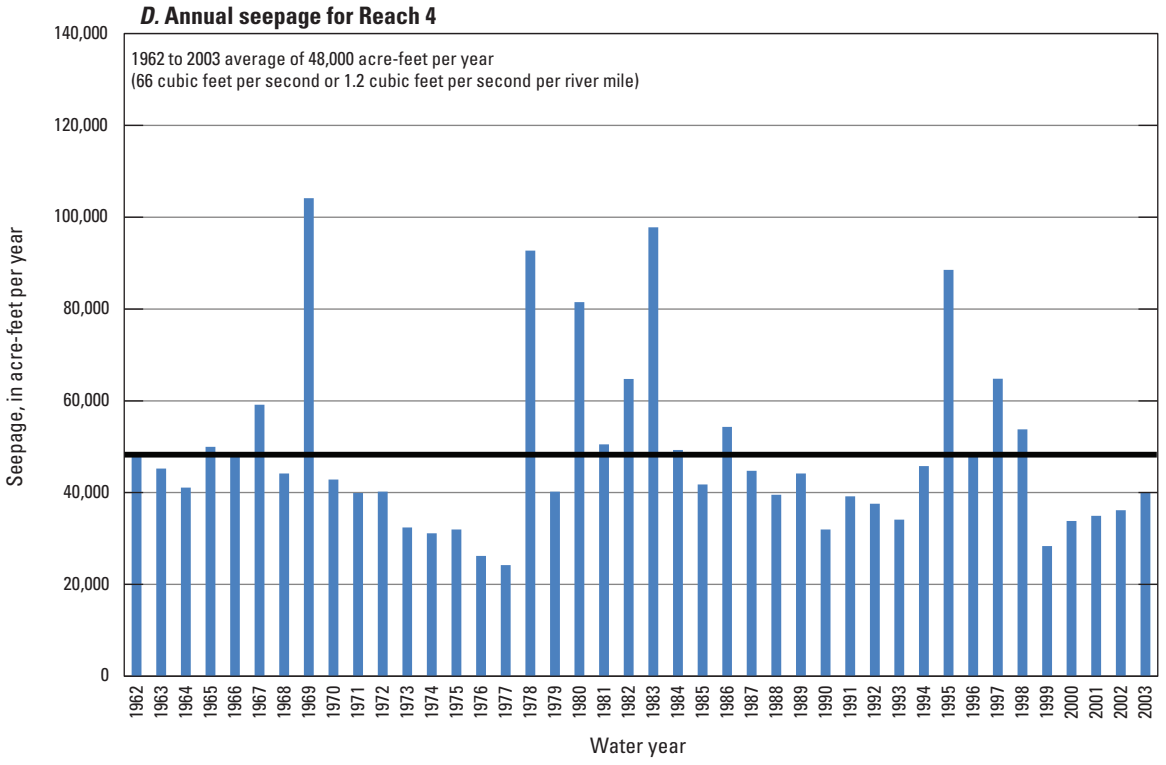

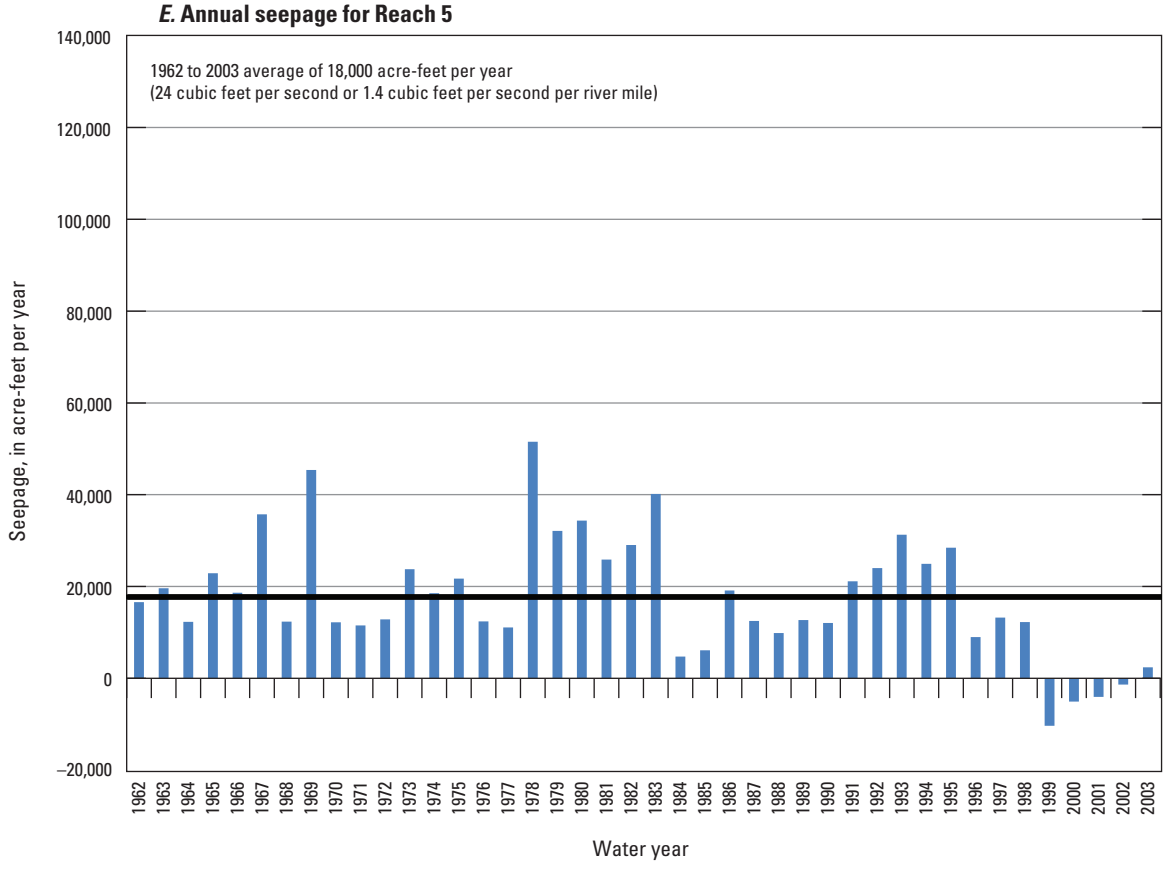

Figure 40. —Continued

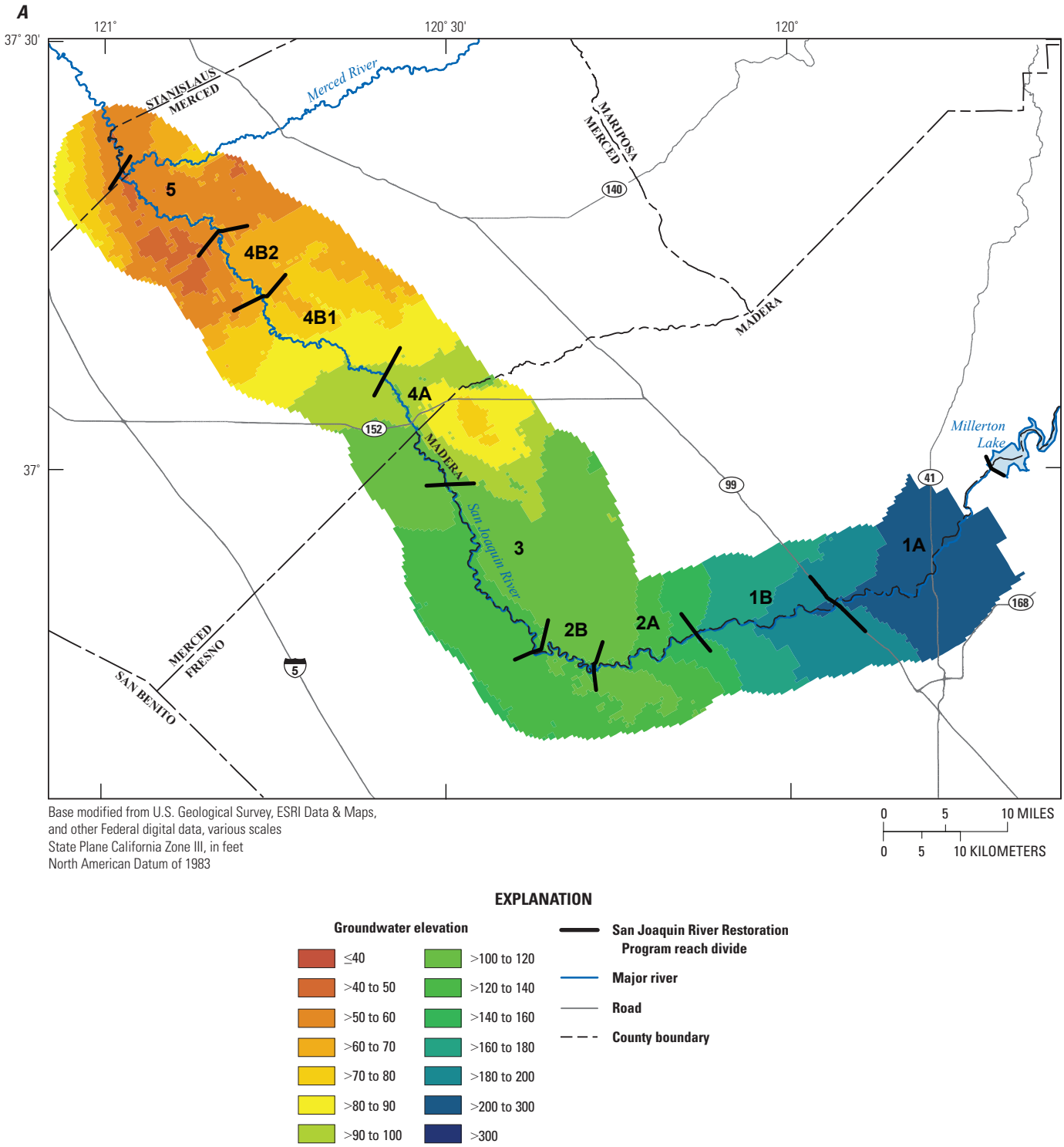

Figure 41. San Joaquin River Restoration Program groundwater flow model (SJRRPGW)-simulated groundwater elevation and depth to water table, San Joaquin Valley, California: *A*, Fall 1981 simulated groundwater elevation; *B*, Fall 1981 simulated depth to water table; *C*, Fall 1983 simulated groundwater elevation; *D*, Fall 1983 simulated depth to water table; *E*, Fall 1988 simulated groundwater elevation; *F*, Fall 1988 simulated depth to water table; *G*, Fall 1991 simulated groundwater elevation; *H*, Fall 1991 simulated depth to water table.

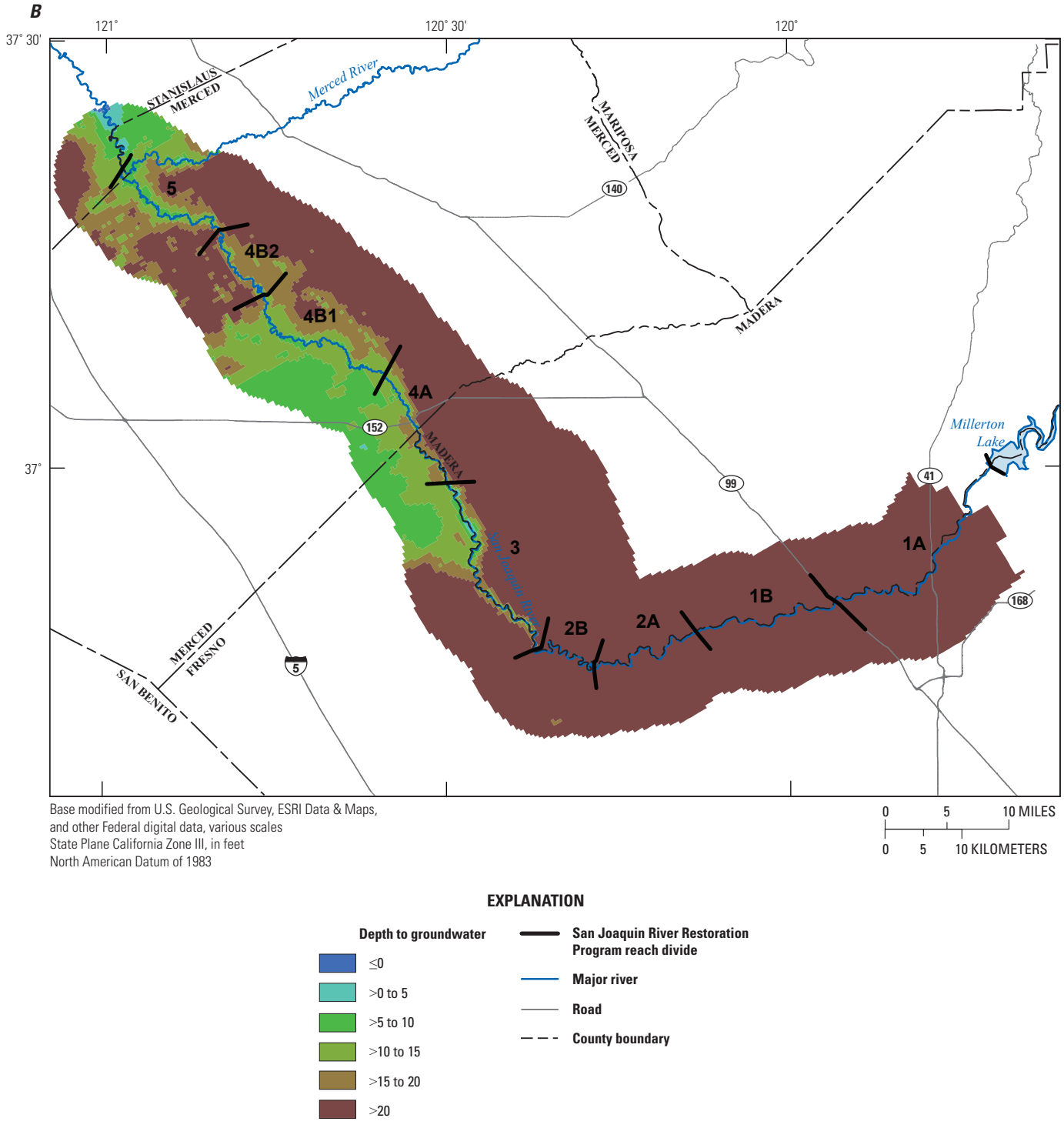

Figure 41. —Continued

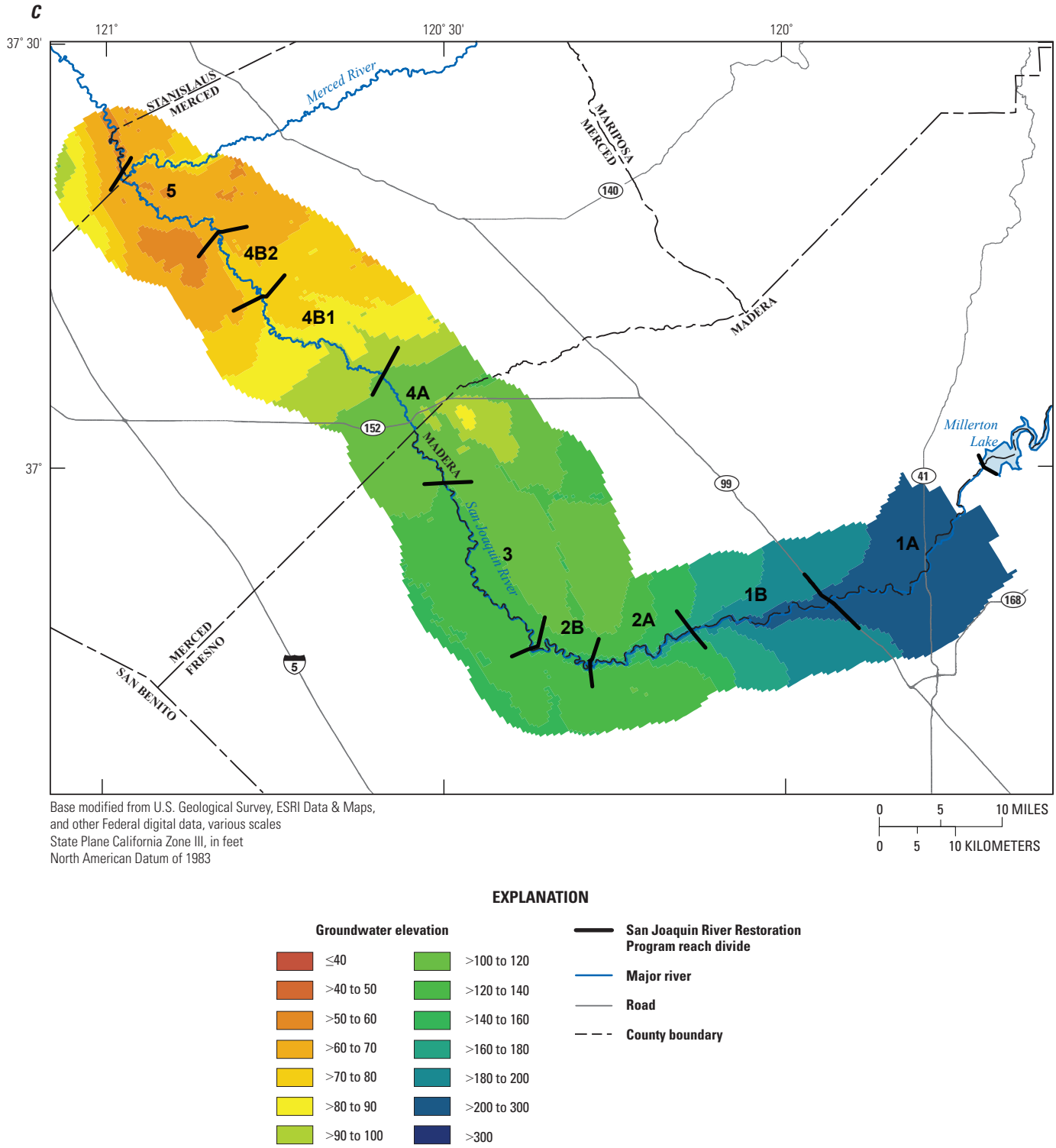

Figure 41. —Continued

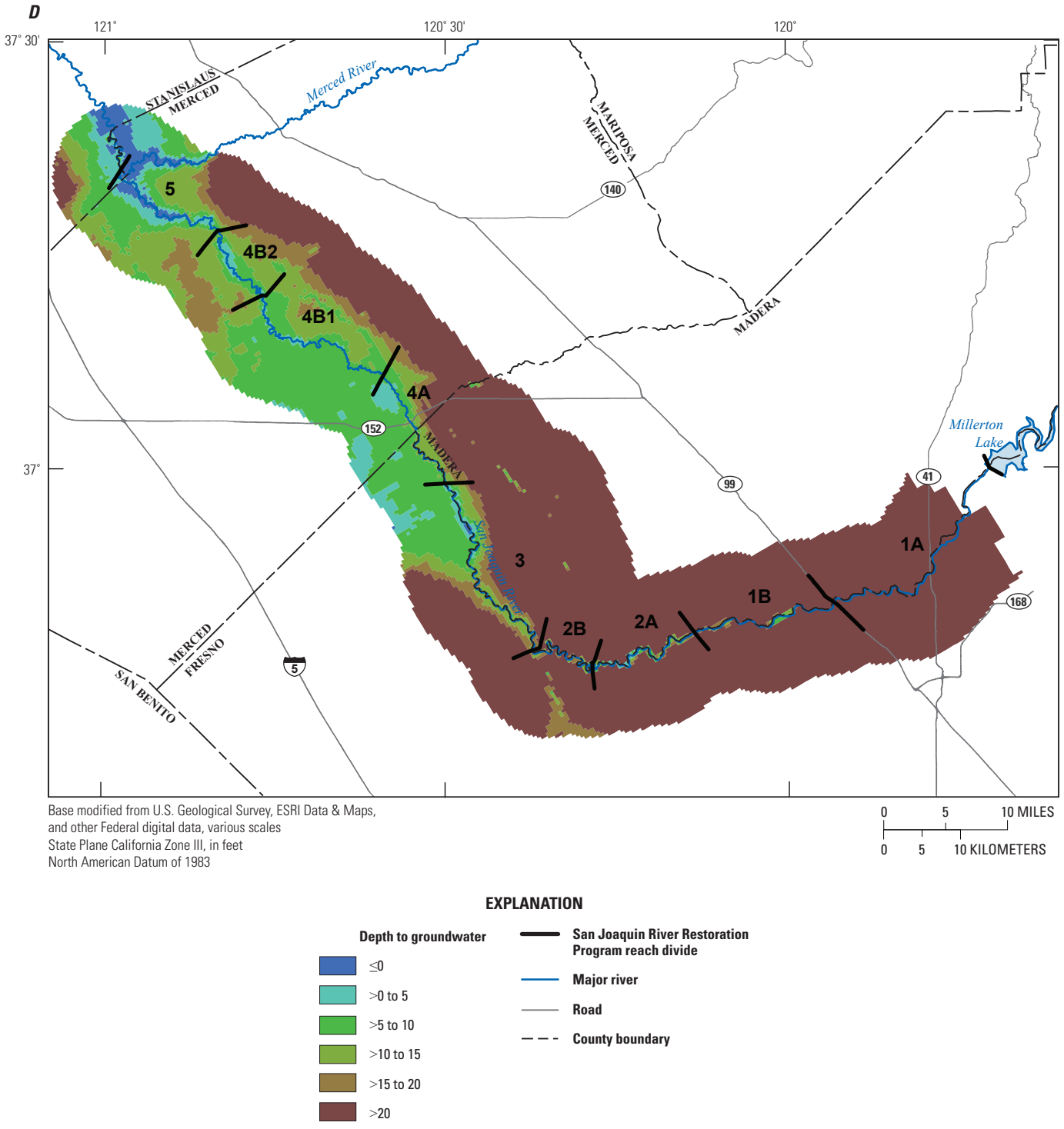

Figure 41. —Continued

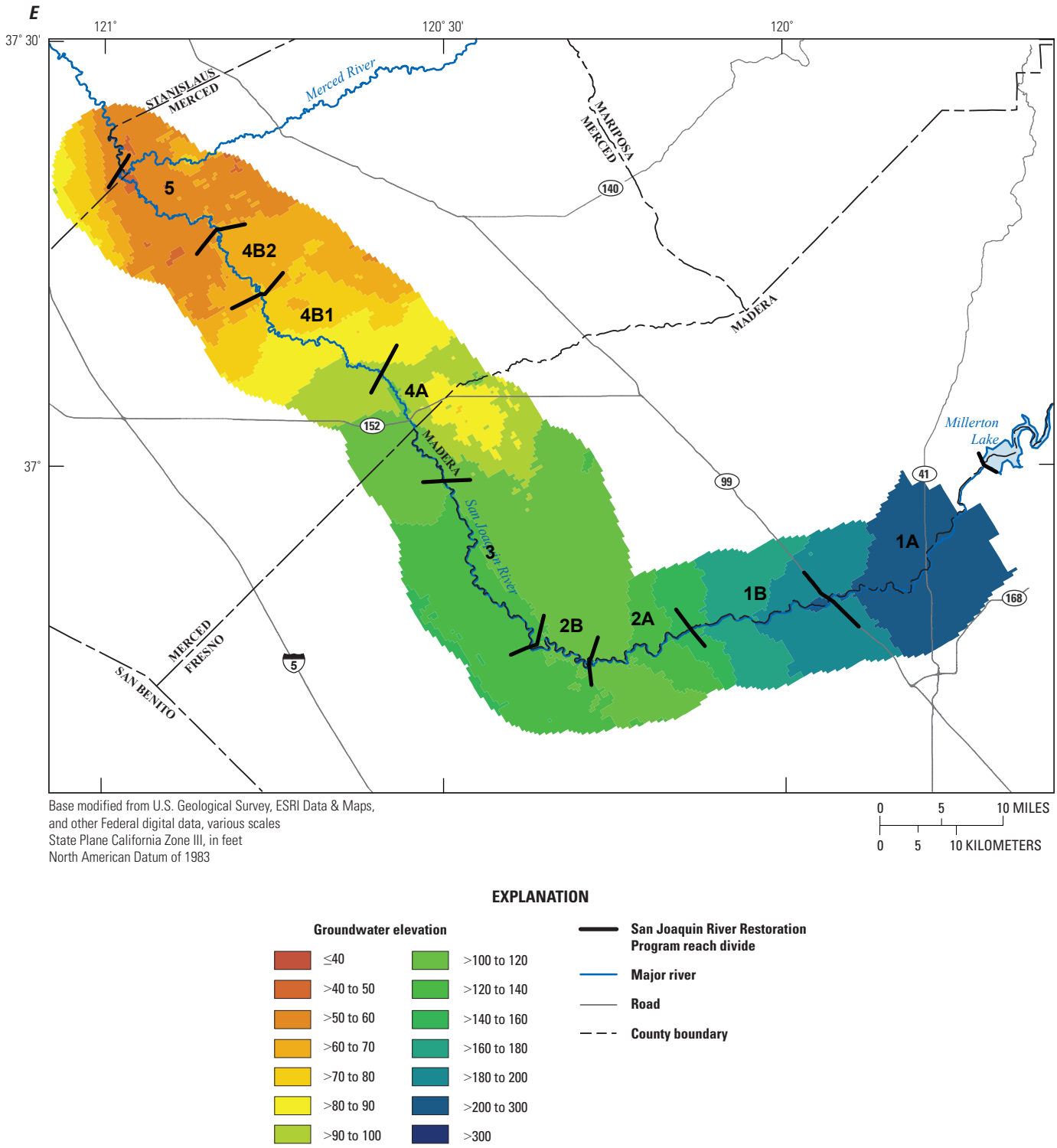

Figure 41. —Continued

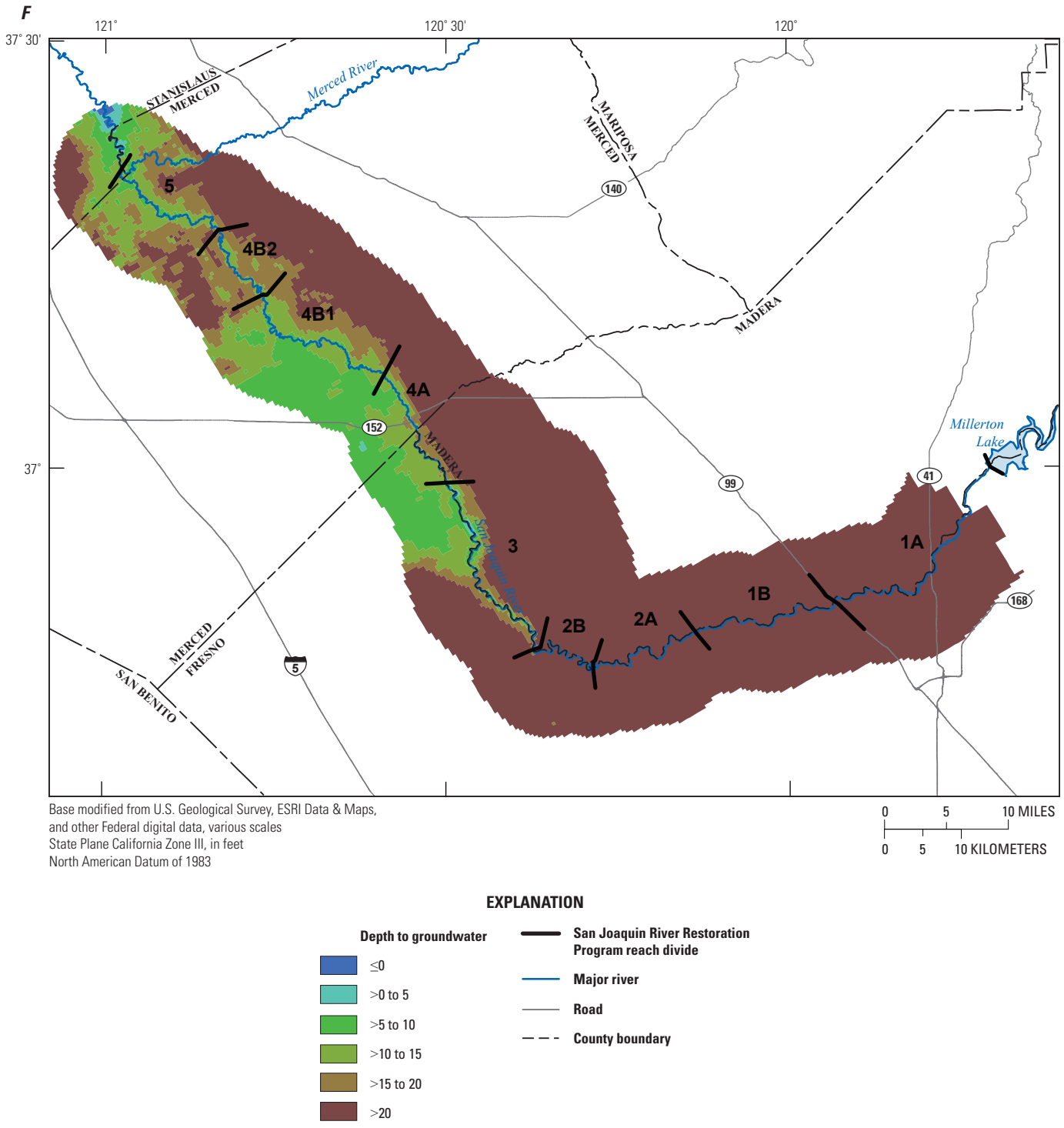

Figure 41. —Continued

G

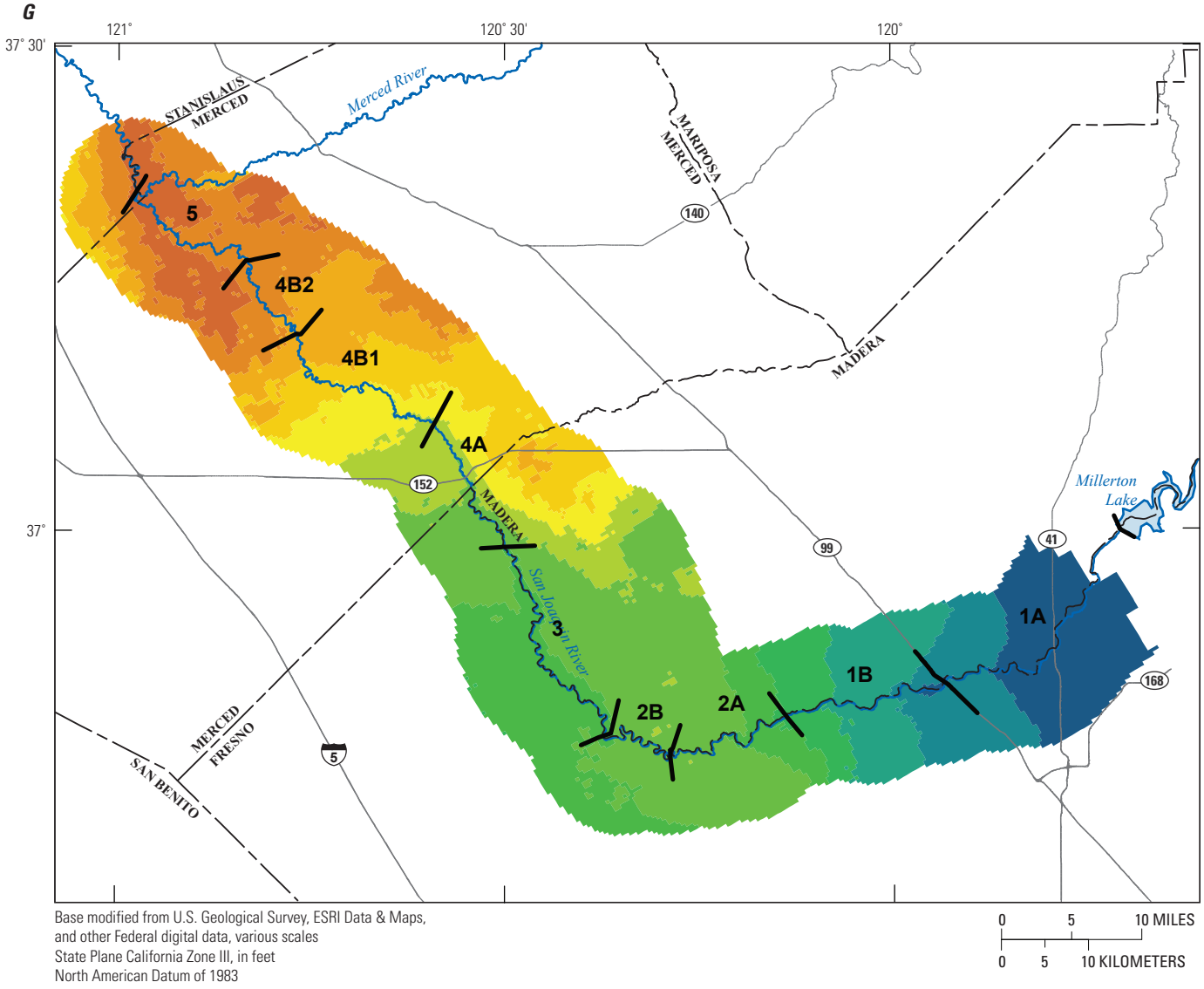

Figure 41. —Continued

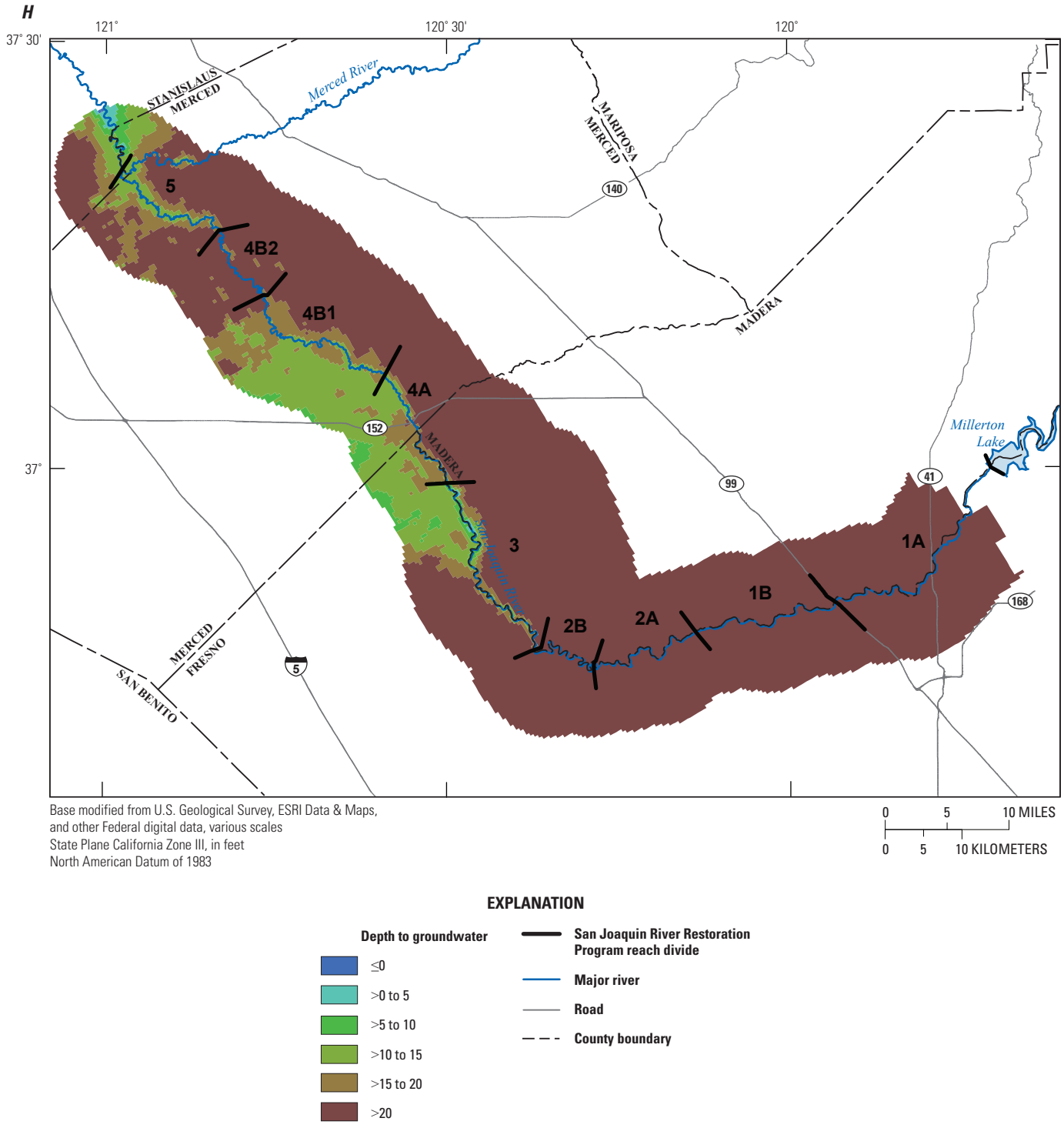

Figure 41. —Continued

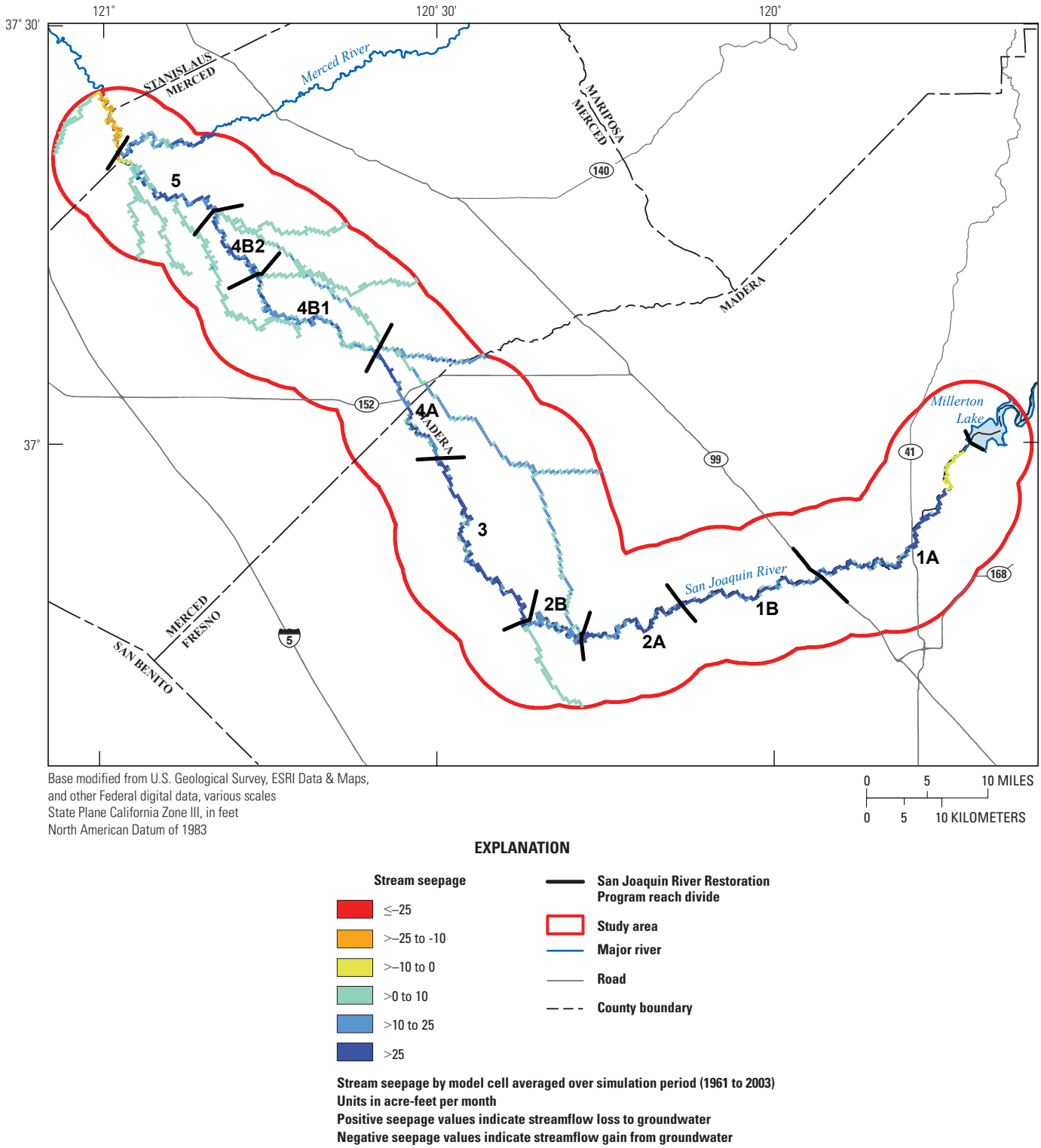

Figure 42. San Joaquin River Restoration Program groundwater flow model (SJRRPGW) average groundwater and surface-water interaction, San Joaquin Valley, California.

water from groundwater inflow. The upper section of Reach 1A has zero simulated groundwater seepage because the model cells below the stream are outside the groundwater basin and are, therefore, not active for the simulation of groundwater. The simulated gaining and losing segments generally are consistent with previous studies.

An interactive animation displaying the simulated groundwater and surface-water interactions for all 510 stress periods is available (*http://pubs.usgs.gov/sir/2014/5148/downloads/sir2014-5148_StreamSeepage.swf*). This animation shows how the interaction of groundwater and surface water changes throughout the simulation period. For example, although most simulated streams lose flow to groundwater on average (fig. 42), many simulated streams gain flow from the aquifer system during some months. For example, 1984 was a Normal-Wet year and 1997 was a Wet year; however, February 1984 and March 1997 were relatively dry months within these years. During these months, although streamflows were reduced, groundwater elevations remained high, and Reaches 3, 4, and 5 of the San Joaquin River switched from being losing to gaining. These simulated results are consistent with previous studies that indicate there can be a net river loss or gain in Reaches 3, 4, and 5 depending on the local and regional hydraulic gradients (Deverel, 2005). A primary purpose of the model is to estimate river seepage in areas with existing irrigation drainage problems (between Mendota Pool and the confluence with the Merced River—Reaches 3, 4, and 5); therefore, the performance of the SJRRPGW in this area is particularly important.

Model Limitations and Appropriate Use

The SJRRPGW is an approximate mathematical representation of the physical conditions in the field. These approximations and associated assumptions contribute to the inability of the model to fully replicate the historical observations at all locations at all times. It is important to understand these limitations before SJRRPGW is applied to the evaluation of SJRRP water-management alternatives or to other uses.

The SJRRPGW represents the physical system by a series of mathematical approximations. Because the physical system is inherently complex, it is not possible to develop a complete mathematical model of the system without introducing certain simplifying assumptions. As with most groundwater models, the SJRRPGW solves for average conditions within each model cell, which for SJRRPGW are 0.25-mi by 0.25-mi laterally. Therefore, the SJRRPGW is best used for simulating hydrologic responses on a regional scale and not as well suited for the evaluation of effects over areas smaller than a few square miles.

The input data used in the SJRRPGW represent the best information available during the study period at the time of the study. The input data for each model component are not equally available, and assumptions were made during the model-development process regarding missing data. For example, agricultural pumping data, one of the most critical stresses affecting groundwater elevations in the study area, are not available and were estimated using the FMP2. Likewise, urban pumping data also were estimated and were done so on the basis of land use, which was temporally updated only five times during the simulation period. All pumping was simulated using virtual wells because data on the location and properties of the production wells are not available.

The general-head boundary conditions are estimated from the CVHM. Care should be exercised when using the SJRRPGW to estimate the hydrologic effects of projects that extend beyond the model boundary.

For some months of the simulation, excess surface water was delivered to some subregions beyond what the FMP2 estimated for agricultural demand. This excess surface water is likely due to errors in the FMP2 estimation of agricultural demand, errors in the surface-water delivery data (either in raw data or in how it was incorporated into the model), pre-irrigation not simulated by FMP2, or actual deliveries made to irrigation canals that are not then diverted to the fields. This excess water is currently not accounted for in the SJRRPGW and could lead to an underestimation of streamflow, stream seepage to groundwater, and percolation to groundwater.

The accuracy of the model is dependent on the spatial and temporal availability of observation data. Most notably, quantitative data on groundwater and surface-water interaction are not available (although the model was consistent with qualitative studies). In addition, groundwater elevation and streamflow data are not available for all locations and all periods. On the basis of these limitations, the SJRRP is best suited for estimating the hydraulic response to restoration flows and seepage management actions in areas where the model simulates the groundwater levels and trends reasonably well. For example, SJRRPGW performance is best in the CCID South area, to the west of Reaches 3 and 4A; for this area, the model is expected to predict future system behavior reasonably well.

Though unconfined groundwater flow occurs in the water table, confined groundwater flow is simulated in all the layers in the model to avoid numerical instability and long model execution times. The model properly represents unconfined aquifer storage by using a value of specific yield for the uppermost active cells. However, by simulating confined flow in all layers, the saturated thickness and transmissivity are fixed and are not a function of groundwater head. Model cells where the simulated groundwater elevation is always below the cell bottom were made inactive during calibration to avoid overestimation of saturated thickness of the aquifer. However, it is possible that with SJRRP flow releases, the water table in some areas may rise above the highest active model cells. In

these cases, the SJRRPGW may underestimate the transmissivity of the aquifer.

Future Work

To support planned future work, the SJRRPGW can be used to provide preliminary evaluations of the potential effects of SJRRP restoration flows on agricultural lands with existing drainage problems. Planned future work includes the development of an "existing conditions" baseline by using the SJRRPGW to represent what conditions would be without the SJRRP. Plans include the simulation of several different scenarios of SJRRP flow-release alternatives to determine the effects of the SJRRP. Also, development of a "future conditions" baseline is planned in order to estimate water-table conditions during future conditions (such as those that may result from climate change or future land use).

The model is expected to be used as a decision support tool in the evaluation of several proposed seepage mitigation projects. Potential projects to be simulated include construction of slurry walls to block subsurface water movement, installation of drainage ditches or interceptor lines to capture shallow groundwater, and installation and pumping of groundwater wells or increased pumping of existing agricultural groundwater wells to lower the regional groundwater table.

Model Enhancements

Several future model enhancements planned for the SJRRPGW are discussed in this section. In addition to the enhancements discussed below, the model would be updated with any new input data that become available. These enhancements will improve the capability of the SJRRPGW to accurately simulate the hydrologic system.

The simulation period for the SJRRPGW is from April 1961 to September 2003, coinciding with the CVHM simulation period. A planned future enhancement to the model would be to extend the period to the 2013. The extended model would include the interim flows released for the project starting in 2009. Inclusion of these flows would allow calibration of the model under a set of stresses similar to those the model would operate under when used to make future predictions. Over 200 SJRRP observation wells were installed and monitored by Reclamation beginning in the spring of 2008, and extending the model would allow for use of these high-frequency, high-quality data in model calibration.

The SJRRPGW currently uses monthly stress periods. When using the model to simulate the SJRRP surface-water releases, it would be necessary to average the releases over these monthly time steps. A planned future enhancement would be to subdivide the stress periods into semi-monthly or weekly stress periods to allow for more accurate simulation of the SJRRP surface-water releases.

Confined groundwater flow is simulated in all layers in the SJRRPGW. A planned future enchantment would be to simulate all the model layers as convertible between confined and unconfined groundwater flow. The associated numerical instabilities could be mitigated by using the Newton (NWT) Solver Package in MODFLOW-NWT (Niswonger and others, 2011). NWT was developed for solving models that would otherwise fail to converge because of the drying and rewetting of unconfined model cells. The USGS is currently revising NWT for broader compatibility with other MODFLOW packages and processes, including those used in the SJRRPGW.

The SJRRPGW uses heads extracted from the CVHM as general heads along the model boundary. The drawback to this approach is that the model cannot correctly simulate water-management scenarios if the effect of the scenario extends beyond the model boundary (more than 5 mi from the San Joaquin River and bypass system). A planned future enhancement would be to embed the SJRRPGW within an updated version of the CVHM using MODFLOW-LGR (Mehl and Hill, 2005). Local Grid Refinement (LGR) allows two models to be coupled together and run simultaneously such that heads and flows are balanced at the interface between the two models. The USGS is revising MODFLOW-LGR for broader compatibility with other MODFLOW packages and processes, including those used in the SJRRPGW.

Investigate Predictive Uncertainty of Simulated Stream Seepage

The final calibrated parameter set represents just one of many parameter sets that could result in a reasonably calibrated model. Each such parameter set could lead to differences in the simulated seepage along the San Joaquin River. Planned future work involves investigating this uncertainty by using linear predictive uncertainty concepts and non-linear Pareto concepts. The uncertainty analysis would be used to determine which observation types and specific sites are most sensitive to changes in parameter values that influence stream seepage. Thus, this work could potentially identify areas where adding new observation data to the calibration dataset could help to narrow the predictive uncertainty range.

Sensitivity to Transition-Probability Geostatistical Software Texture Realizations

There were 100 equally probable realizations of the sediment-texture distribution developed for the study area. The first texture model was chosen arbitrarily for use in the SJRRPGW. The model could also be calibrated by using any of the other 99 realizations. Each realization would likely lead to a different parameter set and a different estimated seepage rate along the San Joaquin River. Evaluating the other texture realizations would help to address model uncertainty by providing a range of simulated seepage rates and the sensitivity of calibrated parameters to changes in the texture distribution. These simulations would also provide more information regarding the uncertainty of calibrated parameters compared to the simple linear confidence limits. By more fully exploring

the range of calibration values for different sediment-texture distributions, uncertainty in aquifer properties and the resulting effects on other parameters of the model could be assessed.

Summary and Conclusions

The San Joaquin River Restoration Program (SJRRP) has a dual goal to restore the natural ecology along the San Joaquin River to a degree that restores and maintains native fish populations while avoiding reductions in surface water deliveries. Increased flows in the river, particularly during the spring salmon run, are a key component of the settlement agreement and the restoration effort. One potential consequence of these increased river flows, however, is the exacerbation of existing irrigation drainage problems through increased seepage from the river along losing reaches or reduced groundwater discharge to the river along gaining reaches.

The San Joaquin River Restoration Program groundwater flow model (SJRRPGW) is a hydrologic model developed as an analytical tool for use by the SJRRP and others to help evaluate potential water-management decisions. In addition to providing quantitative budget information about the groundwater flow system, the model can be used in many ways, including the following:

- To evaluate the potential effects of restoration flows on existing drainage problems.
- To compare the potential effectiveness of proposed seepage mitigation projects.
- To determine areas most susceptible to developing high water-table conditions during restoration flows.
- To evaluate the groundwater elevation thresholds developed as part of the SJRRP seepage management plan.
- To evaluate the spatial adequacy of the groundwater monitoring network and guide the SJRRP monitoring program in the location of future monitoring sites.

The SJRRPGW simulates a 1,300-square mile ($mi^{2)}$ area within the San Joaquin Valley along a 150-mile (mi) reach of the San Joaquin River. The model simulates 42.5 years of historical hydrology from April 1961 to September 2003 on a monthly basis and utilizes datasets and hydrologic investigations from Federal (U.S. Geological Survey and U.S. Bureau of Reclamation), State (California Department of Water Resources), and local agencies (Central California Irrigation District). These datasets include ground-surface elevation, land-use and crop-related data, water supply and demand, well logs, groundwater levels, streamflows, and climate, soils, and aquifer properties.

The SJRRPGW is an integrated hydrologic model that simulates the surface-water hydrologic system, the groundwater aquifer system, and land-surface processes in a single model that uses the MODFLOW Farm Process. Simulated land-surface processes include precipitation, surface-water delivery, pumping of groundwater, plant uptake of shallow groundwater, plant evapotranspiration, on-farm efficiencies, precipitation and irrigation runoff, and percolation to groundwater. The MODFLOW SFR2 Package is used to simulate the surface-water system, which includes streamflow for the San Joaquin River, the San Joaquin River flood-control bypass system, and eight major tributaries. The MODFLOW HUF Package is used to represent a multi-layered aquifer system above the Corcoran Clay with properties defined by using a sediment-texture model developed using transition-probability geostatistics.

The SJRRPGW was calibrated against historically observed groundwater levels at 133 monitoring wells and historically observed streamflows at 19 streamgages. Calibration of 81 model parameters was accomplished in a semi-automated manner by using the software PEST. Final estimated parameter values generally were consistent with parameter estimates from previous studies. About 92 percent of simulated groundwater levels were within 20 feet (ft) vertically of observed values, and 89 percent of simulated streamflows were within 500 ft^3/s of observed values, indicating a well-calibrated model. The correlation coefficients of 0.98 for groundwater levels and 0.96 for streamflows indicated a good match between the trends of the simulated and observed values. A sensitivity analysis was performed to test the robustness of the calibrated parameter values.

The model generated monthly water budgets for agricultural water use, groundwater flow, and streamflow from 1962 to 2003. The groundwater flow budget showed the change in aquifer storage varies with hydrologic conditions; the average annual change in storage from 1962 to 2003 was a depletion of 64,000 acre-feet per year (acre-ft/yr). This storage loss occurs mostly in subregions that rely on groundwater pumping to meet demands. As indicated in the farm budget, the model estimated an average agricultural groundwater pumping of 1,110,000 acre-ft/yr. The streamflow budget showed an average annual net stream seepage to groundwater of 367,000 acre-ft/yr (510 cubic-feet per second), which included seepage from the main San Joaquin River channel, the San Joaquin River flood-control bypass system, and the major San Joaquin River tributaries. The median seepage rate was 280,000 acre-ft/yr; the annual stream seepage ranged from 903,000 acre-feet (acre-ft) in 1983 to 166,000 acre-ft in 1985.

Understanding the limitations of the SJRRPGW is important before it is applied to various problems. Future enhancements to SJRRPGW are planned to address some of these limitations, including extending the calibration period to

the 2013, subdividing the monthly stress periods, utilizing a more robust solver (such as NWT), and embedding the model within the Central Valley Hydrologic Model by using Local Grid Refinement. The predictive uncertainty of simulated stream seepage will also be further investigated by evaluating the sensitivity of seepage rates to estimated parameter values and alternate sediment-texture distributions.

References Cited

Anderman, E.R., and Hill, M.C., 2000, MODFLOW-2000, the U.S. Geological Survey modular ground-water model—Documentation of the Hydrogeologic-Unit Flow (HUF) Package: U.S. Geological Survey Open-File Report 00–342, 89 p., *http://pubs.usgs.gov/of/2000/0342/report.pdf*.

Anderman, E.R., and Hill, M.C., 2003, MODFLOW-2000, the U.S. Geological Survey modular ground-water model—Three additions to the Hydrogeologic-Unit Flow (HUF) Package—Alternative storage for the uppermost active cells, flows in hydrogeologic units, and the hydraulic-conductivity depth-dependence (KDEP) capability: U.S. Geological Survey Open-File Report 2003–347, 36 p., *http://pubs.usgs.gov/of/2003/0347/report.pdf*.

Bartow, J.A., 1991, The Cenozoic evolution of the San Joaquin Valley, California: U.S. Geological Survey Professional Paper 1501, 40 p, 2 pls., *http://pubs.usgs.gov/pp/1501/report.pdf*.

Belitz, K.R., and Heimes, F.J., 1990, Character and evolution of the ground-water flow system in the central part of the western San Joaquin Valley, California: U.S. Geological Survey Water-Supply Paper 2348, 28 p., *http://pubs.usgs.gov/wsp/2348/report.pdf*.

Belitz, K., and Phillips, S.P., 1995, Alternative to agricultural drains in California's San Joaquin Valley—Results of a regional-scale hydrogeologic approach: Water Resources Research, v. 31, no. 8, p. 1845–1862, *http://onlinelibrary.wiley.com/doi/10.1029/95WR01328/pdf*.

Bertoldi, G.L., Johnston, R.H., and Evenson, K.D., 1991, Ground water in the Central Valley, California—A summary report: U.S. Geological Survey Professional Paper 1401-A, 44 p., *http://pubs.usgs.gov/pp/1401a/report.pdf*.

Burow, K.R., Jurgens, B.C., Kauffman, L.J., Phillips, S.P., Dalgish, B.A., and Shelton, J.L., 2008, Simulations of ground-water flow and particle pathline analysis in the zone of contribution of a public-supply well in Modesto, eastern San Joaquin Valley, California: U.S. Geological Survey Scientific Investigations Report 2008–5035, 41 p., *http://pubs.usgs.gov/sir/2008/5035*.

Burow, K.R., Shelton, J.L., Hevesi, J.A., and Weissmann, G.S., 2004, Hydrogeologic characterization of the Modesto area, San Joaquin Valley California: U.S. Geological Survey Scientific Investigations Report 2004–5232, 62 p., *http://pubs.water.usgs.gov/sir20045232*.

California Department of Water Resources, 2011a, Water Resource Integrated Modeling System 2 (WRIMS 2): Sacramento, Calif, Department of Water Resources, accessed June 1, 2011, at *http://baydeltaoffice.water.ca.gov/modeling/hydrology/WRIMS2/index.cfm*.

California Department of Water Resources, 2011b, California Land & Water Use, accessed June 1, 2011, at *http://www.water.ca.gov/landwateruse/*.

California State University Chico, 2003, The Central Valley Historical Vegetation Mapping Project: California State University , Chico, Department of Geography and Planning and Geographic Information Center, 25 p.

Carle, S.F., 1999, TPROGS—Transition probability geostatistical software, version 2.1, user manual: Davis, Calif., Hydrologic Sciences Graduate Group, University of California.

Carle, S.F., and Fogg, G.E., 1996, Transition probability-based indicator geostatistics: Mathematical Geology, v. 28, no. 4, p. 453–476, *http://dx.doi.org/10.1007/BF02083656*.

Carle, S.F., and Fogg, G.E., 1997, Modeling spatial variability with one and multidimensional continuous-lag Markov chains: Mathematical Geology, v. 29, no. 7, p. 891–918, *http://dx.doi.org/ 10.1023/A:1022303706942*.

Climate Source, 2006, Parameter-Elevation Regressions on Independent Slopes Model (PRISM) Data, accessed June 1, 2011, at *http://www.prism.oregonstate.edu/*.

Croft, M.G., 1972, Subsurface geology of the late Tertiary and Quaternary water-bearing deposits of the southern part of the San Joaquin Valley, California: U.S. Geological Survey Water-Supply Paper 1999-H, 29 p., *http://pubs.usgs.gov/wsp/1999h/report.pdf*.

Doherty, John, 2005, PEST model-independent parameter estimation user manual, 5th edition: Watermark Numerical Computing, variously paged, accessed June 1, 2011, at *http://www.pesthomepage.org/Downloads.php*.

Deverel, S.J., 2005, Expert report of Dr. Steven J. Deverel, PH.D—Qualifications and experience: E.D. Cal. No. Civ. 88-1658 LKK.

Faunt, C.C., ed., 2009, Groundwater availability of the Central Valley aquifer, California: U.S. Geological Survey Professional Paper 1766, 225 p., *http://pubs.usgs.gov/pp/1766/*.

Fleckenstein, J.H., Niswonger, R.G., and Fogg, G.E., 2006, River-aquifer interactions, geologic heterogeneity, and low-flow management: Ground Water, v. 44, no. 6, p. 837–852, *http://dx.doi.org/10.1111/j.1745-6584.2006.00190.x*.

Fogg, G.E., Noyes, C.D., and Carle, S.F., 1998, Geologically based model of heterogeneous hydraulic conductivity in an alluvial setting: Hydrogeology Journal, v. 6, no. 1, p. 131–143, *http://dx.doi.org/10.1007/s100400050139*.

Gesch, Dean, Evans, Gayla, Mauck, James, Hutchinson, John, and Carswell, W.J., Jr., 2009, The National Map—Elevation: U.S. Geological Survey Fact Sheet 2009–3053, 4 p., *http://pubs.usgs.gov/fs/2009/3053/pdf/fs2009_3053.pdf*.

Hanson, R.T., and Leake, S.A., 1999, Documentation for HYDMOD: a program for extracting and processing time-series data from the U.S. Geological Survey's modular three-dimensional finite-difference ground-water flow model: U.S. Geological Survey Open-File Report 98–564, 57 p., *http://pubs.usgs.gov/of/1998/0564/report.pdf*.

Harbaugh, A.W., 2005, MODFLOW-2005, the U.S. Geological Survey modular ground-water model—The ground-water flow process: U.S. Geological Survey Techniques and Methods book 6, chap. A16, variously paged, *http://pubs.er.usgs.gov/publication/tm6A16*.

Hargreaves, G.H., and Samani, Z.A., 1982, Estimating potential evapotranspiration: Journal of the Irrigation and Drainage Division, v. 108, no. 3, p. 225–230.

Hill, M.C., and Tiedeman, C.R., 2007, Effective groundwater model calibration—With analysis of data, sensitivities, predictions, and uncertainty: Hoboken, N.J., John Wiley and Sons, Inc., 480 p.

Hill, M.C., Banta, E.R., Harbaugh, A.W., and Anderman, E.R., 2000, MODFLOW-2000, the U.S. Geological Survey modular ground-water model; user guide to the observation, sensitivity, and parameter-estimation processes and three post-processing programs: U.S. Geological Survey Open-File Report 2000–184, 209 p., *http://pubs.usgs.gov/of/2000/0184/report.pdf*.

Isaaks, E.H., and Srivastava, R.M., 1989, An introduction to applied geostatistics: New York, N.Y., Oxford University Press, 592 p.

Kings River Water Association, (1961–2003). Annual Watermaster Reports from 1961 through 2003, Kings River Water Association. Fresno, Calif., variously paged.

Lee, Si-Yong, Carle, S.F., and Fogg, G.E., 2007, Geologic heterogeneity and a comparison of two geostatistical models—Sequential Gaussian and transition probability-based geostatistical simulation: Advances in Water Resources, v. 30, no. 9, p. 1914–1932, *http://dx.doi.org/10.1016/j.advwatres.2007.03.005*.

Marchand, D.E., and Allwardt, Alan, 1981, Late Cenozoic stratigraphic units, northeastern San Joaquin Valley, California: U.S. Geological Survey Bulletin 1470, 70 p., *http://pubs.usgs.gov/bul/1470/report.pdf*.

McBain and Trush, Inc., ed., 2002, San Joaquin River restoration study background report: Arcata, Calif., prepared for Friant Water Users Authority, Lindsay, Calif., and Natural Resources Defense Council, San Francisco, Calif., variously paged, *http://www.waterboards.ca.gov/waterrights/water_issues/programs/bay_delta/bay_delta_plan/water_quality_control_planning/docs/sjrf_spprtinfo/mcbainandtrush_2002.pdf*.

Mehl, S.W., and Hill, M.C., 2005, MODFLOW-2005, the U.S. Geological Survey modular ground-water model—Documentation of shared node local grid refinement (LGR) and the boundary flow and head (BFH) package: U.S. Geological Survey Techniques and Methods, book 6, chap. A12, 68 p., *http://pubs.water.usgs.gov/tm6a12*.

National Historical Geographic Information System, 2011, National historical geographic information system: Twin Cities, Minn., University of Minnesota database, *https://www.nhgis.org/*.

Natural Resources Defense Council versus Kirk Rodgers, Stipulation of Settlement, 2006, CIV S-88-1658 LKK/GGH (United States District Court Easter District of California, September 13, 2006), *http://www.restoresjr.net/program_library/06-Settlement_Related/index.html*.

Niswonger, R.G., Panday, Sorab, and Ibaraki, Motomu, 2011, MODFLOW-NWT, A Newton formulation for MODFLOW-2005: U.S. Geological Survey Techniques and Methods, book 6, chap. A37, 44 p., *http://pubs.usgs.gov/tm/tm6a37/pdf/tm6a37.pdf*.

Niswonger, R.G., and Prudic, D.E., 2005, Documentation of the Streamflow-Routing (SFR2) Package to include unsaturated flow beneath streams—A modification to SFR1: U.S. Geological Survey Techniques and Methods, book 6, chap. A13, 50 p., *http://pubs.usgs.gov/tm/2006/tm6A13/pdf/tm6a13.pdf*.

Page, R.W., 1986, Geology of the fresh ground-water basin of the Central Valley, California, with texture maps and sections: U.S. Geological Survey Professional Paper 1401-C, 54 p., 5 pls., *http://pubs.er.usgs.gov/publication/pp1401C*.

Phillips, S.P., Green, C.T., Burow, K.R., Shelton, J.L., and Rewis, D.L., 2007, Simulation of multiscale ground-water flow in part of the northeastern San Joaquin Valley, California: U.S. Geological Survey Scientific-Investigations Report 2007–5009, 43 p., *http://pubs.water.usgs.gov/sir20075009*.

Ritzi, R.W., Jr., Dominic, D.F., Brown, N.R., Kausch, K.W., McAlenney, P.J., and Basial, M.J., 1995, Hydrofacies distribution and correlation in the Miami Valley aquifer system: Water Resources Research, v. 31, no. 12, p. 3271–3281, *http://dx.doi.org/10.1029/95WR02564*.

Ritzi, R.W., Jr., Dominic, D.F., Slesers, A.J., Greer, C.B., Reboulet, E.C., Telford, J.A., Masters, R.W., Klohe, C.A., Bogle, J.L., and Means, B.P., 2000, Comparing statistical models of physical heterogeneity in buried-valley aquifers: Water Resources Research, v. 36, no. 11, p. 3179–3192, *http://dx.doi.org/10.1029/2000WR900143*.

Schmid, Wolfgang, and Hanson, R.T., 2009, The Farm Process Version 2 (FMP2) for MODFLOW-2005—Modifications and upgrades to FMP1: U.S. Geological Survey Techniques and Methods, book 6, chap. A32, 102 p., *http://pubs.usgs.gov/tm/tm6a32/pdf/tm6a32.pdf*.

San Joaquin River Restoration Program, 2012, San Joaquin River Restoration Program—Background and History, accessed June 1, 2011, at *http://www.restoresjr.net/background.html*.

Tetra Tech, 2010, Draft San Joaquin River Interim Flow Unsteady Modeling Analysis. California. Sacramento, California: U.S. Bureau of Reclamation, Mid-Pacific Region, 35 p, *http://www.usbr.gov/mp/nepa/documentShow.cfm?Doc_ID=5861*.

U.S. Bureau of Reclamation, 1962, Definite plan report, San Luis Unit, Central Valley Project, California. Sacramento, California: U.S. Bureau of Reclamation, Mid-Pacific Region, 331 p.

U.S. Bureau of Reclamation, Central Valley Operations Office, 2011, Report of Operations Monthly Delivery Tables: Sacramento, Calif., accessed June 1, 2011, at *http://www.usbr.gov/mp/cvo/deliv.html*.

U.S. Department of Agriculture, Natural Resource Conservation Service, 2005, State Soil Geographic Database (STATSGO), accessed June 1, 2011, at *http://datagateway.nrcs.usda.gov/*.

U.S. Geologic Survey, 1990, Land use and land cover digital data 1:250,000- and 1:100,000-scale maps—Data users guide 4: U.S. Geological Survey, accessed June 1, 2011, at *http://vterrain.org/Culture/LULC/Data_Users_Guide_4.html*.

U.S. Geologic Survey, 1999, National land cover dataset 1992 (NLCD 1992): U.S. Geological Survey database, accessed June 1, 2011, at *http://landcover.usgs.gov/natllandcover.php*.

U.S. Geologic Survey, 2011, Hydrography—National hydrography dataset: U.S. Geological Survey database, accessed June 1, 2011, at *http://nhd.usgs.gov/index.html*.

Weissmann, G.S., Bennett, G.L., and Lansdale, A.L., 2005, Factors controlling sequence development on Quaternary fluvial fans, San Joaquin Basin, California, USA: Geological Society, London, Special Publications, v. 251, p. 169–186, *http://dx.doi.org/10.1144/GSL.SP.2005.251.01.12*.

Weissmann, G.S., Carle, S.F., and Fogg, G.E., 1999, Three-dimensional hydrofacies modeling based on soil surveys and transition probability geostatistics: Water Resources Research, v. 35, no., 6, p. 1761–1770, *http://dx.doi.org/10.1029/1999WR900048*.

Weissmann, G.S., and Fogg, G.E., 1999, Multi-scale alluvial fan heterogeneity modeled with transition probability geostatistics in a sequence stratigraphic framework: Journal of Hydrology, v. 226, no. 1–2, p. 48–65, *http://dx.doi.org/10.1016/S0022-1694(99)00160-2*.

Appendix A. Crop-Related Data Utilized from the Central Valley Hydrologic Model (CVHM)

This appendix provides values for crop-related datasets utilized in the San Joaquin River Restoration Program Groundwater flow model (SJRRPGW) by the Farm Process (FMP2) (table A-1, A-2, A-3, fig. A-1).

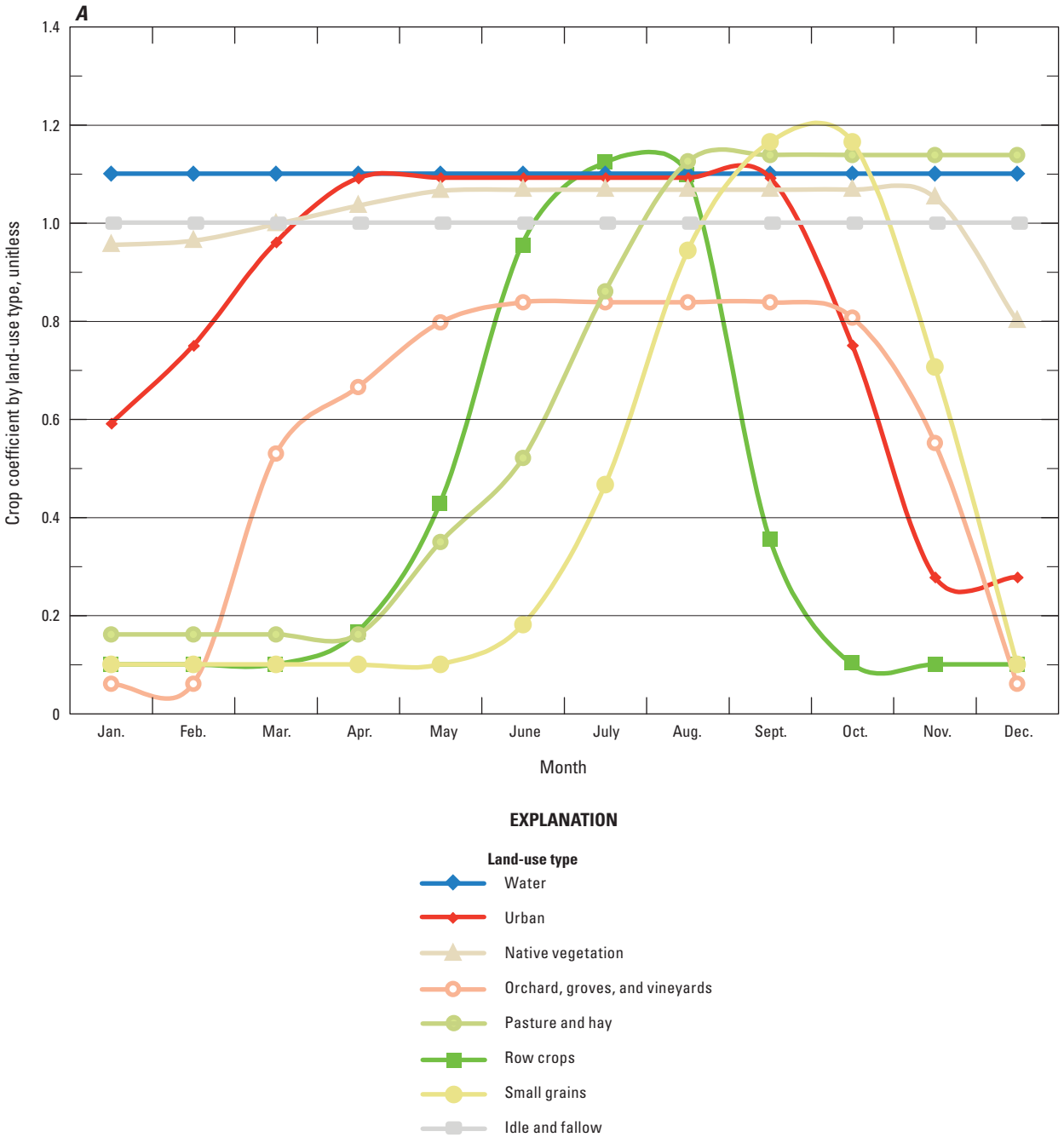

Figure A-1. Monthly crop coefficients for each crop utilized in the San Joaquin River Restoration Program groundwater flow model (SJRRPGW) by different land-use types: A, agricultural, undeveloped, and other uses; B, agricultural uses; C, agricultural and other developed uses.

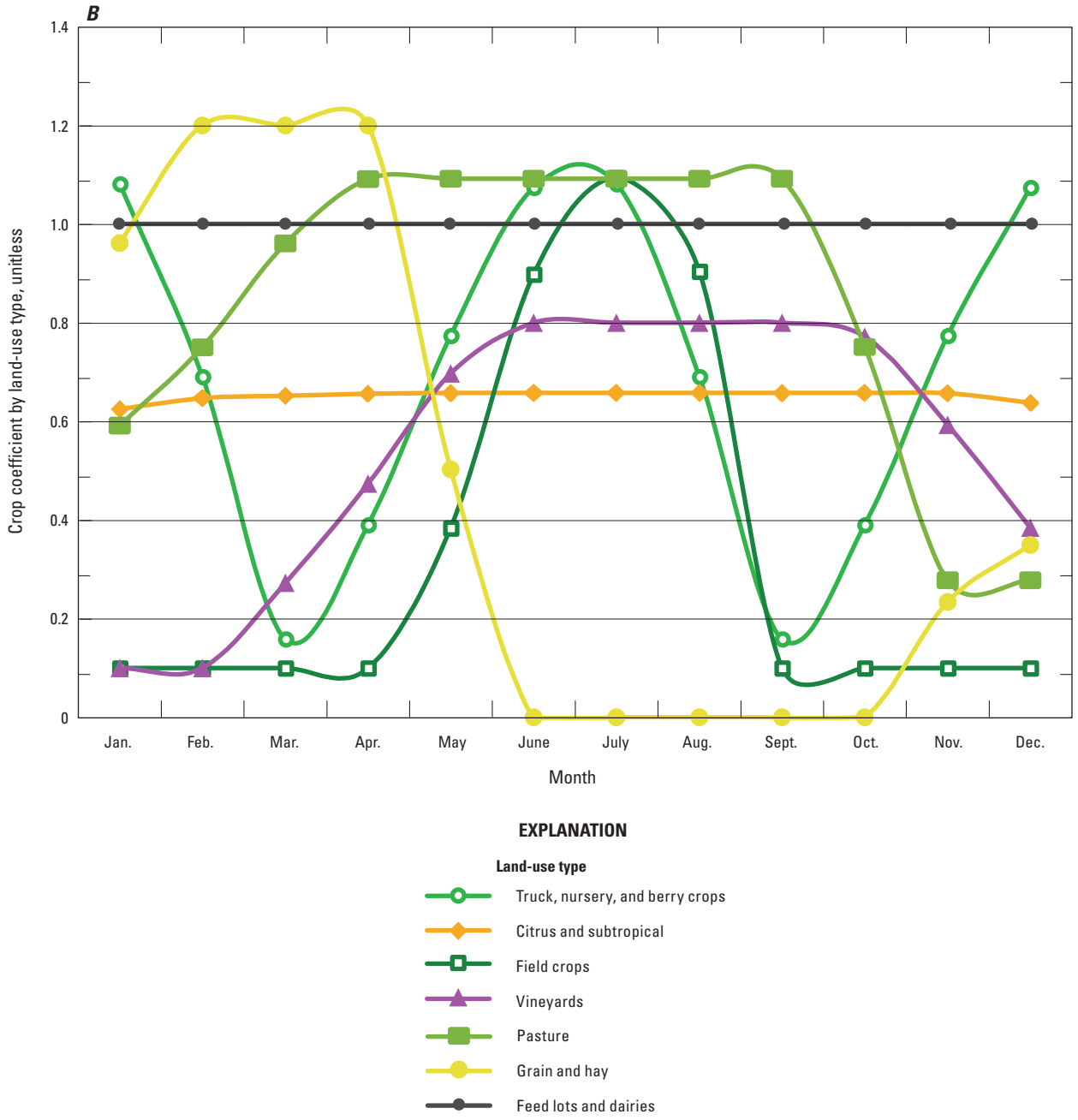

Figure A-1. —Continued

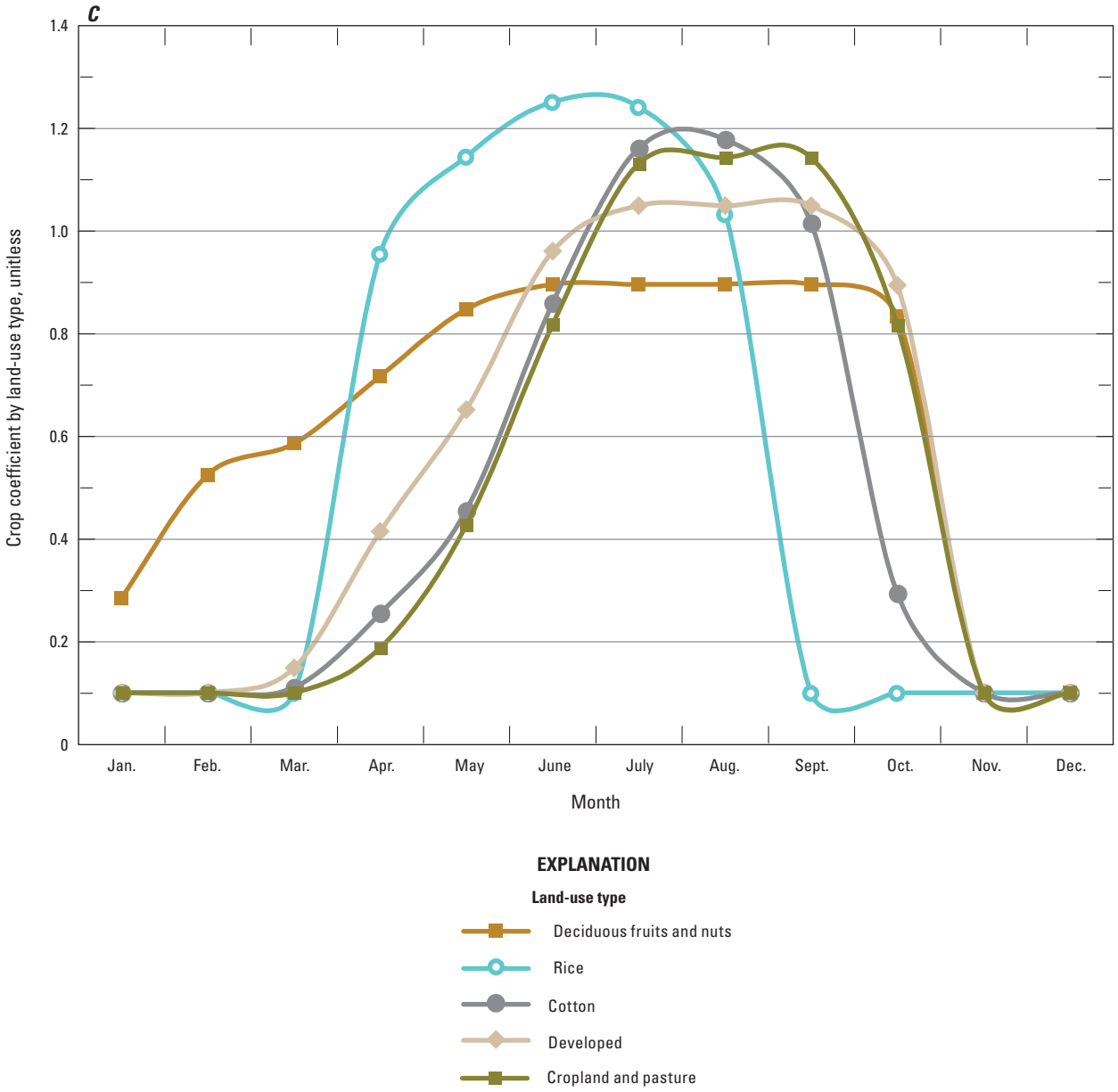

Figure A-1. —Continued

Table A-1. Non-time varying crop-related data in study area for each crop type.

Virtual-crop crop category (number)	Root depth (in feet)	Root uptake pressure heads (in feet)				Fraction of surface-water runoff from precipitation / irrigation (dimensionless)
		Anoxia	Lower optimal range	Upper optimal range	Wilting	
Water (1)	3.6	1.6	0.3	–1.0	–1.3	0.05/0.01
Urban (2)	2.0	–0.4	–0.9	–37.4	–262.5	0.01/0.01
Native classes (3, 23)	10.6	1.6	0.4	–27.1	–377.3	0.21/0.01
Orchards, groves, and vineyards (4)	6.0	–0.4	–0.9	–22.8	–291.4	0.10/0.01
Pasture/hay (5)	5.3	–0.4	–0.9	–37.4	–262.5	0.10/0.02
Row crops (6)	8.3	–0.5	–1.0	–17.9	–262.5	0.10/0.06
Small grains (7)	4.0	–0.4	–0.9	–37.4	–262.5	0.10/0.04
Idle/fallow (8)	5.3	–0.2	–0.7	–27.1	–377.3	0.06/0.01
Truck, nursery, and berry crops (9)	6.3	–0.5	–1.0	–17.9	–262.5	0.10/0.10
Citrus and subtropical (10)	4.0	–0.5	–1.0	–19.7	–262.5	0.10/0.01
Field crops (11)	4.0	–0.5	–1.0	–98.4	–405.9	0.10/0.08
Vineyards (12)	5.0	–0.5	–1.0	–23.8	–262.5	0.01/0.01
Pasture (13)	5.3	0.0	–0.9	–37.4	–262.5	0.10/0.02
Grain and hay crops (14)	4.0	–0.5	–1.0	–170.9	–525.3	0.10/0.04
Semi-agricultural (livestock feedlots, dairies, poultry farms) (15)	3.6	–0.2	–0.7	–27.1	–377.3	0.32/0.35
Deciduous fruits and nuts (16)	6.0	–0.4	–0.9	–22.8	–377.3	0.11/0.05
Rice (17)	5.3	1.6	0.4	–5.8	–525.0	0.01/0.03
Cotton (18)	9.3	–0.2	–0.9	–91.3	–503.0	0.10/0.10
Developed (19)	5.3	–0.4	–0.9	–37.4	–262.5	0.10/0.08
Cropland and pasture (20)	4.9	–0.4	–0.9	–37.4	–262.5	0.10/0.08

Table A-2. Fractions of transportation and evaporation of consumptive use for each crop type.

[**Abbreviations**: Fei, Evaporative fraction of consumptive use related to irrigation; Fep, Evaporative fraction of consumptive use related to precipitation; Ftr, Transpiratory fraction of consumptive use]

Virtual-crop crop category (number)	January (Ftr/Fep/Fei)	February (Ftr/Fep/Fei)	March (Ftr/Fep/Fei)	April (Ftr/Fep/Fei)	May (Ftr/Fep/Fei)	June (Ftr/Fep/Fei)
Water (1)	0.00/1.00/1.00	0.00/1.00/1.00	0.00/1.00/1.00	0.00/1.00/1.00	0.00/1.00/1.00	0.00/1.00/1.00
Urban (2)	0.25/0.75/0.02	0.25/0.75/0.02	0.25/0.75/0.02	0.25/0.75/0.02	0.25/0.75/0.02	0.25/0.75/0.02
Native classes (3 and 23)	0.28/0.72/0.72	0.28/0.72/0.72	0.66/0.34/0.34	0.66/0.34/0.34	0.66/0.34/0.34	0.66/0.34/0.34
Orchards, groves, and vineyards (4)	0.20/0.80/0.80	0.20/0.80/0.80	0.37/0.63/0.63	0.23/0.77/0.77	0.46/0.54/0.54	0.47/0.53/0.53
Pasture/hay (5)	0.50/0.50/0.50	0.50/0.50/0.50	0.50/0.50/0.50	0.50/0.50/0.50	0.72/0.28/0.28	0.88/0.12/0.12
Row crops (6)	0.11/0.89/0.89	0.11/0.89/0.89	0.11/0.89/0.89	0.09/0.91/0.91	0.36/0.64/0.64	0.46/0.54/0.54
Small grains (7)	0.00/1.00/1.00	0.00/1.00/1.00	0.00/1.00/1.00	0.00/1.00/1.00	0.00/1.00/1.00	0.00/1.00/1.00
Idle/fallow (8)	0.00/1.00/0.00	0.00/1.00/0.00	0.00/1.00/0.00	0.00/1.00/0.00	0.00/1.00/0.00	0.00/1.00/0.00
Truck, nursery, and berry crops (9)	0.80/0.20/0.18	0.80/0.20/0.18	0.39/0.61/0.61	0.44/0.56/0.36	0.42/0.58/0.38	0.80/0.20/0.18
Citrus and subtropical (10)	0.27/0.73/0.73	0.27/0.73/0.73	0.46/0.54/0.14	0.46/0.54/0.14	0.46/0.54/0.14	0.46/0.54/0.14
Field crops (11)	0.01/0.99/0.99	0.01/0.99/0.99	0.01/0.99/0.99	0.15/0.85/0.85	0.15/0.85/0.85	0.94/0.06/0.06
Vineyards (12)	0.00/1.00/0.03	0.00/1.00/0.03	0.28/0.72/0.22	0.40/0.60/0.10	0.38/0.62/0.12	0.36/0.64/0.14
Pasture (13)	0.18/0.82/0.82	0.15/0.85/0.85	0.46/0.64/0.64	0.91/0.09/0.03	0.91/0.09/0.03	0.91/0.09/0.03
Grain and hay crops (14)	0.46/0.54/0.54	0.92/0.08/0.08	0.92/0.08/0.08	0.92/0.08/0.08	0.23/0.77/0.77	0.00/1.00/1.00
Semi-agricultural (15)	0.00/1.00/1.00	0.00/1.00/1.00	0.00/1.00/1.00	0.00/1.00/1.00	0.00/1.00/1.00	0.00/1.00/1.00
Deciduous fruits and nuts (16)	0.10/0.90/0.90	0.10/0.90/0.90	0.10/0.90/0.90	0.50/0.50/0.50	0.50/0.50/0.50	0.97/0.03/0.03
Rice (17)	0.20/0.80/0.50	0.20/0.80/0.50	0.20/0.80/0.50	0.75/0.25/0.25	0.75/0.25/0.25	0.80/0.20/0.10
Cotton (18)	0.75/0.25/0.25	0.75/0.25/0.25	0.75/0.25/0.25	0.43/0.57/0.17	0.75/0.25/0.20	0.75/0.25/0.20
Developed (19)	0.30/0.70/0.67	0.30/0.70/0.67	0.22/0.78/0.78	0.16/0.84/0.84	0.42/0.58/0.38	0.85/0.15/0.15
Cropland and pasture (20)	0.00/1.00/1.00	0.00/1.00/1.00	0.00/1.00/1.00	0.00/1.00/1.00	0.20/0.80/0.80	0.30/0.70/0.70

Virtual-crop crop category (number)	July (Ftr/Fep/Fei)	August (Ftr/Fep/Fei)	September (Ftr/Fep/Fei)	October (Ftr/Fep/Fei)	November (Ftr/Fep/Fei)	December (Ftr/Fep/Fei)
Water (1)	0.00/1.00/1.00	0.00/1.00/1.00	0.00/1.00/1.00	0.00/1.00/1.00	0.00/1.00/1.00	0.00/1.00/1.00
Urban (2)	0.25/0.75/0.02	0.25/0.75/0.02	0.25/0.75/0.02	0.25/0.75/0.02	0.25/0.75/0.02	0.25/0.75/0.02
Native classes (3)	0.66/0.34/0.34	0.66/0.34/0.34	0.66/0.34/0.34	0.66/0.34/0.34	0.66/0.34/0.34	0.28/0.72/0.72
Orchards, groves, and vineyards (4)	0.47/0.53/0.53	0.47/0.53/0.53	0.47/0.53/0.53	0.47/0.53/0.53	0.45/0.55/0.55	0.20/0.80/0.80
Pasture/Hay (5)	0.95/0.05/0.05	0.96/0.04/0.04	0.96/0.04/0.04	0.96/0.04/0.04	0.96/0.04/0.04	0.96/0.04/0.04
Row Crops (6)	0.95/0.05/0.05	0.87/0.13/0.13	0.12/0.88/0.88	0.11/0.89/0.89	0.11/0.89/0.89	0.11/0.89/0.89
Small Grains (7)	0.20/0.80/0.80	0.50/0.50/0.50	0.90/0.10/0.10	0.90/0.10/0.10	0.00/1.00/1.00	0.50/0.50/0.50
Idle/fallow (8)	0.00/1.00/0.00	0.00/1.00/0.00	0.00/1.00/0.00	0.00/1.00/0.00	0.00/1.00/0.00	0.00/1.00/0.00
Truck, nursery, and berry crops (9)	0.80/0.20/0.18	0.80/0.20/0.18	0.80/0.20/0.18	0.80/0.20/0.18	0.80/0.20/0.18	0.80/0.20/0.18
Citrus and subtropical (10)	0.46/0.54/0.14	0.46/0.54/0.14	0.46/0.54/0.14	0.46/0.54/0.14	0.46/0.54/0.14	0.46/0.54/0.14
Field crops (11)	0.94/0.06/0.06	0.94/0.06/0.06	0.90/0.10/0.10	0.01/0.99/0.99	0.01/0.99/0.99	0.01/0.99/0.99
Vineyards (12)	0.36/0.64/0.14	0.36/0.64/0.14	0.36/0.64/0.14	0.36/0.64/0.14	0.36/0.64/0.14	0.38/0.62/0.12
Pasture (13)	0.96/0.04/0.04	0.91/0.09/0.03	0.91/0.09/0.03	0.46/0.64/0.64	0.15/0.85/0.85	0.15/0.85/0.85
Grain and hay crops (14)	0.00/1.00/1.00	0.00/1.00/1.00	0.00/1.00/1.00	0.00/1.00/1.00	0.16/0.84/0.84	0.35/0.65/0.65
Semi-agricultural (15)	0.00/1.00/1.00	0.00/1.00/1.00	0.00/1.00/1.00	0.00/1.00/1.00	0.00/1.00/1.00	0.00/1.00/1.00
Deciduous fruits and nuts (16)	0.97/0.03/0.03	0.97/0.03/0.03	0.97/0.03/0.03	0.10/0.90/0.90	0.10/0.90/0.90	0.10/0.90/0.90
Rice (17)	0.75/0.25/0.25	0.60/0.40/0.27	0.20/0.80/0.50	0.20/0.80/0.50	0.20/0.80/0.50	0.20/0.80/0.50
Cotton (18)	0.75/0.25/0.20	0.75/0.25/0.20	0.47/0.53/0.33	0.36/0.64/0.44	0.75/0.25/0.25	0.75/0.25/0.25
Developed (19)	0.90/0.10/0.10	0.90/0.10/0.10	0.90/0.10/0.10	0.50/0.50/0.50	0.30/0.70/0.70	0.30/0.70/0.67
Cropland and pasture (20)	0.85/0.15/0.15	0.95/0.05/0.05	0.90/0.10/0.10	0.50/0.50/0.50	0.00/1.00/1.00	0.00/1.00/1.00

Table A-3. Irrigation efficiencies through the simulation period averaged by San Joaquin River Restoration Program groundwater flow model (SJRRPGW) subregion, San Joaquin Valley, California

[Efficiency values are percentages.]

Subregions	1960s	1970s	1980s	1990s	2000s
2, 3, 5, 6, 9, 15, 16	69	72	78	80	79
1	71	70	74	77	76
4, 7, 8, 10, 11, 12, 13, 14 ,18 ,19, 20, 21, 23, 24, 26	71	72	77	80	79
17, 22	67	69	75	76	76
25, 27, 28	72	72	78	79	81

This page intentionally left blank.

Appendix B. Information for San Joaquin River Restoration Program Groundwater Model Calibration Wells

This appendix provides well construction and other information for the 133 wells used for the calibration of the San Joaquin River Restoration Program groundwater flow model (SJRRPGW). Fifty-five wells are from the Central California Irrigation District (CCID) monitoring program (table B-1) and seventy eight wells are from California Department of Water Resources (DWR) or U.S. Geological Survey (USGS) databases (table B-2).

Table B-1. Well information for selected Central California Irrigation District (CCID) monitoring wells used in model calibration for the San Joaquin River Restoration Project area, Fresno, Madera, and Merced Counties, California.

[See figure 28 for locations [San Joaquin River Restoration Program groundwater flow model (SJRRPGW) identification numbers] of wells. U.S. Geological Survey (USGS) identification number: the unique number for each site in USGS National Water Information System (NWIS) database. Depths in feet below land surface. Land-surface elevation in feet above sea level, which refers to the National American Vertical Datum of 1988 (NAVD 88); measured by U.S. Bureau of Reclamation (USBR) using a Real Time Kinematic Global Positioning System (RTK GPS). **Abbreviations**: —, no data]

SJRRPGW identification number	Well group	State well number	USGS site identification number	Local identification number	Depth drilled	Depth completed	Depth of top perforation	Depth of bottom perforation	Land-surface elevation	Total number of measurements available[2]	Total number of measurements used for model calibration[3]	Observation site weight for calibration
1	CCID South	10S/13E-30D2	—	CCID 110	—	—	7.0	16.0	111.9	52	52	0.139
2	CCID South	10S/13E-31D1	—	CCID 111	—	—	8.9	17.9	113.0	52	52	0.139
3	CCID South	10S/13E-20N1	—	CCID 118	—	—	7.8	16.8	114.3	52	52	0.139
4	CCID South	10S/13E-30R1	—	CCID 119	—	—	7.0	16.0	113.6	52	52	0.139
5	CCID South	11S/13E-05M1	—	CCID 120	—	—	8.1	17.1	117.6	52	52	0.139
6	CCID South	11S/13E-08D2	—	CCID 121	—	—	8.6	17.7	116.7	53	53	0.137
7	CCID South	11S/13E-17A1	—	CCID 126	—	—	8.3	17.3	118.3	51	51	0.140
8	CCID South	11S/13E-09D1	365945120334201	CCID 127	—	—	8.3	17.3	117.5	52	52	0.139
9	CCID South	11S/13E-04D1	—	CCID 128	—	—	8.6	17.6	115.9	51	51	0.140
10	CCID South	10S/13E-32A2	—	CCID 129	—	—	8.2	17.2	114.9	50	50	0.141
11	CCID South	10S/13E-28D2	—	CCID 130	—	—	8.6	17.6	114.8	51	51	0.140
12	CCID South	10S/13E-22N2	—	CCID 131	—	—	8.7	17.7	115.3	52	52	0.139
13	CCID South	10S/13E-33A1	—	CCID 132	—	—	7.8	16.8	118.0	50	50	0.141
14	CCID South	10S/13E-34N1	—	CCID 133	—	—	9.5	18.5	117.0	51	51	0.140
15	CCID South	11S/13E-03N1	—	CCID 134	—	—	8.2	17.2	117.6	51	51	0.140

Table B1. Well information for selected Central California Irrigation District (CCID) monitoring wells used in model calibration for the San Joaquin River Restoration Project area, Fresno, Madera, and Merced Counties, Calif.—Continued.

[See figure 28 for locations [San Joaquin River Restoration Program groundwater flow model (SJRRPGW) identification numbers] of wells. U.S. Geological Survey (USGS) identification number: the unique number for each site in USGS National Water Information System (NWIS) database. Depths in feet below land surface. Land-surface elevation in feet above sea level, which refers to the National American Vertical Datum of 1988 (NAVD 88); measured by U.S. Bureau of Reclamation (USBR) using a Real Time Kinematic Global Positioning System (RTK GPS). **Abbreviations**: —, no data]

SJRRPGW identification number	Well group	State well number	USGS site identification number	Local identification number	Depth drilled	Depth completed	Depth of top perforation	Depth of bottom perforation	Land-surface elevation	Total number of measurements available[2]	Total number of measurements used for model calibration[3]	Observation site weight for calibration
16	CCID South	11S/13E-16A2	—	CCID 135	—	—	8.4	17.4	120.1	53	53	0.137
17	CCID South	11S/13E-21A1	—	CCID 136	—	—	7.7	16.7	121.2	53	53	0.137
18	CCID South	11S/13E-27R2	—	CCID 139	—	—	7.0	16.0	125.6	50	50	0.141
19	CCID South	11S/13E-26D2	—	CCID 140	—	—	7.3	16.3	124.1	52	52	0.139
20	CCID South	11S/13E-23D1	—	CCID 141	—	—	8.3	17.3	120.0	47	47	0.146
21	CCID South	11S/13E-14D1	—	CCID 142	—	—	7.0	16.0	121.8	53	53	0.137
22	CCID South	11S/13E-11D3	—	CCID 143	—	—	8.1	17.1	119.5	52	51	0.140
23	CCID South	11S/13E-02D1	—	CCID 144A	—	—	7.1	16.1	121.3	49	49	0.143
24	CCID South	11S/13E-14A1	—	CCID 145	—	—	7.3	16.3	123.3	53	53	0.137
25	CCID South	11S/13E-23A1	—	CCID 146	—	—	8.6	17.6	124.5	53	53	0.137
26	CCID South	11S/13E-23R1	—	CCID 147	—	—	9.6	18.6	126.7	53	53	0.137
27	CCID South	11S/13E-25N1	—	CCID 148	—	—	6.9	15.9	129.1	49	49	0.143
28	CCID South	11S/13E-13R2	—	CCID 151	—	—	7.5	16.5	127.9	53	53	0.137
29	CCID South	11S/13E-25A1	—	CCID 152	—	—	4.4	13.4	130.8	52	52	0.139
30	CCID South	11S/13E-25R1	—	CCID 153	—	—	4.7	13.7	131.4	35	35	0.169

Table B1. Well information for selected Central California Irrigation District (CCID) monitoring wells used in model calibration for the San Joaquin River Restoration Project area, Fresno, Madera, and Merced Counties, Calif.—Continued.

[See figure 28 for locations [San Joaquin River Restoration Program groundwater flow model (SJRRPGW) identification numbers] of wells. U.S. Geological Survey (USGS) identification number: the unique number for each site in USGS National Water Information System (NWIS) database. Depths in feet below land surface. Land-surface elevation in feet above sea level, which refers to the National American Vertical Datum of 1988 (NAVD 88); measured by U.S. Bureau of Reclamation (USBR) using a Real Time Kinematic Global Positioning System (RTK GPS). **Abbreviations**: —, no data]

SJRRPGW identification number	Well group	State well number	USGS site identification number	Local identification number	Depth drilled	Depth completed	Depth of top perforation	Depth of bottom perforation	Land-surface elevation	Total number of measurements available[2]	Total number of measurements used for model calibration[3]	Observation site weight for calibration
31	CCID South	11S/14E-31C 1	—	CCID 154	—	—	8.6	17.6	130.4	49	49	0.143
32	CCID South	11S/14E-31J 1	—	CCID 155	—	—	7.1	16.1	132.9	48	48	0.144
33	CCID South	12S/14E-07A1	—	CCID 156	—	—	7.0	16.0	135.7	48	48	0.144
34	CCID South	12S/14E-17D1	—	CCID 157	—	—	5.3	14.3	137.8	51	51	0.140
35	CCID South	12S/14E-17N1	—	CCID 158	—	—	7.1	16.1	139.4	51	51	0.140
36	CCID South	12S/14E-20Q1	—	CCID 159	—	—	9.0	18.0	140.5	50	50	0.141
37	CCID South	12S/14E-18M2	—	CCID 161	—	—	6.6	15.6	142.8	48	48	0.144
38	CCID South	12S/13E-12R1	—	CCID 162	—	—	8.4	17.4	134.3	46	46	0.147
39	CCID South	12S/14E-07D2	—	CCID 163	—	—	7.8	16.8	132.5	48	48	0.144
40	CCID South	11S/13E-36R1	365539120292401	CCID 164	—	—	8.4	17.4	129.9	49	49	0.143
41	CCID South	11S/13E-36M [1]	—	CCID 165A	—	—	6.8	15.8	127.4	40	40	0.158
42	CCID South	12S/13E-11A2	—	CCID 166A	—	—	6.8	15.8	132.5	53	53	0.137
43	CCID South	12S/13E-13D1	—	CCID 167	—	—	6.9	15.9	140.8	52	52	0.139
44	CCID South	11S/13E-34J2	—	CCID 169	—	—	8.8	17.8	127.7	51	51	0.140
45	CCID South	10S/12E-13R1	—	CCID 181	—	—	9.2	18.2	114.4	49	49	0.143

Table B1. Well information for selected Central California Irrigation District (CCID) monitoring wells used in model calibration for the San Joaquin River Restoration Project area, Fresno, Madera, and Merced Counties, Calif.—Continued.

[See figure 28 for locations [San Joaquin River Restoration Program groundwater flow model (SJRRPGW) identification numbers] of wells. U.S. Geological Survey (USGS) identification number: the unique number for each site in USGS National Water Information System (NWIS) database. Depths in feet below land surface. Land-surface elevation in feet above sea level, which refers to the National American Vertical Datum of 1988 (NAVD 88); measured by U.S. Bureau of Reclamation (USBR) using a Real Time Kinematic Global Positioning System (RTK GPS). **Abbreviations**: —, no data]

SJRRPGW identification number	Well group	State well number	USGS site identification number	Local identification number	Depth drilled	Depth completed	Depth of top perforation	Depth of bottom perforation	Land-surface elevation	Total number of measurements available[2]	Total number of measurements used for model calibration[3]	Observation site weight for calibration
46	CCID South	10S/12E-12R1	—	CCID 182	—	—	6.1	15.1	110.6	45	45	0.149
47	CCID South	10S/13E-07D1	—	CCID 183	—	—	7.4	16.4	107.8	49	49	0.143
48	CCID South	10S/12E-01A1	—	CCID 184	—	—	6.7	15.7	104.2	44	44	0.143
49	CCID South	10S/13E-07A1	—	CCID 186A	—	—	9.0	18.0	108.0	53	53	0.137
50	CCID South	10S/13E-19A1	—	CCID 188A	—	—	9.1	18.1	112.4	49	49	0.143
51	CCID South	10S/13E-21D1	—	CCID 189	—	—	7.0	16.0	115.3	44	44	0.151
52	CCID South	10S/13E-16D3	—	CCID 190	—	—	9.1	18.1	113.3	46	46	0.147
53	CCID South	10S/13E-05E1	—	CCID 191	—	—	7.9	16.9	110.9	49	49	0.143
54	CCID South	11S/13E-12F2	—	CCID 350	—	—	6.6	15.6	125.9	33	33	0.174
55	CCID South	12S/14E-05K [1]	—	CCID 351	—	—	7.8	16.8	135.4	34	34	0.171

[1]Unofficial number or uncertain location.

[2]From 4/1961 to 9/2003.

[3]Excludes measurements identified as outliers.

Table B-2. Well information for selected wells from the California Department of Water Resources (CDWR) and U.S. Geological Survey (USGS) databases used in model calibration for the San Joaquin River Restoration Project area, Fresno, Madera, and Merced Counties, California.

[See figure 28 for locations [San Joaquin River Restoration Program groundwater flow model (SJRRPGW) identification numbers] of wells. U.S. Geological Survey (USGS) identification number: the unique number for each site in USGS NWIS (National Water Information System) database. Depths in feet below land surface. Land-surface elevation in feet above sea level, which refers to the National American Vertical Datum of 1988 (NAVD 88); obtained from California Department of Water Resources (DWR) and USGS databases unless otherwise noted. **Abbreviations**: —, no data.]

SJRRPGW identification number	Calibration well group	State well number	USGS site identification number	Depth drilled	Depth completed	Depth of top perforation	Depth of bottom perforation	Land-surface elevation	Total number of measurements available[1]	Total number of measurements used for model calibration[2]	Observation site weight for calibration
56	Mendota	14S/14E-13E3	364257120240902	—	499	312	380	193.5	18	0	0.000
57	Mendota	14S/16E-10J1	364335120113001	—	72	60	—	182.5	43	43	0.152
58	Mendota	14S/15E-08C4	364355120213702	—	174	100	174	[3]163.4	35	34	0.171
59	Mendota	14S/16E-09A1	364357120123201	—	240	75	240	[4]176.5	30	30	0.183
60	Mendota	14S/16E-08D1	364403120143601	157	156	72	156	167.5	102	101	0.100
61	Mendota	14S/16E-12A1	364403120092001	260	260	84	260	[4]192.5	44	39	0.160
62	Mendota	14S/14E-02G2	364431120244201	459	445	175	445	[4]191.4	20	17	0.243
63	Mendota	14S/16E-04A1	364446120123001	305	300	116	300	[4]176.5	65	65	0.124
64	Mendota	14S/16E-06A1	364456120143801	278	278	154	260	172.4	63	61	0.128
65	Mendota	14S/15E-05A2	364456120210501	—	276	77	275	[4]161.9	35	35	0.169
66	Mendota	14S/16E-06C1	364459120151001	325	38	116	38	172.4	29	29	0.186
67	Mendota	14S/16E-05C1	364457120140501	325	38	136	38	[4]170.4	25	25	0.200
68	Mendota	13S/15E-34J2	364521120184902	—	282	140	280	[4]166.4	32	32	0.177
69	Mendota	13S/16E-32F1	364528120150201	378	368	116	368	177.4	50	49	0.143
70	Mendota	13S/15E-35D5	364536120184301	—	433	373	433	[4]168.4	3,665	3,664	0.017
71	Mendota	13S/16E-30L1	364616120150301	—	300	70	300	177.4	64	64	0.125
72	Mendota	13S/16E-27F1	364618120115801	300	300	18	300	[4]185.9	70	70	0.120
73	Mendota	13S/15E-27F1	364624120192001	302	301	136	300	167.4	45	45	0.149
74	Mendota	13S/16E-27C1	364644120115801	320	256	132	316	[4]188.4	71	71	0.119
75	Mendota	13S/16E-23N1	364646120111201	245	245	96	245	[4]192.9	60	60	0.129
76	Madera	13S/18E-27A1	364641119590301	345	340	140	340	257.5	36	36	0.167
77	Madera	13S/18E-21P1	364645120005301	180	180	140	180	[3]246.0	67	67	0.122
78	Mendota	13S/16E-22F1	364713120115801	315	312	91	312	[4]189.4	68	68	0.121
79	Fresno	13S/20E-22L1	364707119463701	293	280	199	29	[4]315.3	72	71	0.119
80	Fresno	13S/20E-21K1	364712119474601	436	420	180	420	[4]309.5	56	56	0.134
81	Fresno	13S/20E-20E1	364710119490101	540	296	140	283	[4]306.5	80	79	0.113
82	Fresno	13S/20E-23B1	364733119452101	290	268	195	28	327.5	146	145	0.083
83	Fresno	13S/20E-15L1	364758119463801	288	236	205	214	[4]318.1	71	71	0.119

Table B-2. Well information for selected wells from the California Department of Water Resources (CDWR) and U.S. Geological Survey (USGS) databases used in model calibration for the San Joaquin River Restoration Project area, Fresno, Madera, and Merced Counties, California.—Continued

[See figure 28 for locations [San Joaquin River Restoration Program groundwater flow model (SJRRPGW) identification numbers] of wells. U.S. Geological Survey (USGS) identification number: the unique number for each site in USGS NWIS (National Water Information System) database. Depths in feet below land surface. Land-surface elevation in feet above sea level, which refers to the National American Vertical Datum of 1988 (NAVD 88); obtained from California Department of Water Resources (DWR) and USGS databases unless otherwise noted. **Abbreviations**: —, no data.]

SJRRPGW identification number	Calibration well group	State well number	USGS site identification number	Depth drilled	Depth completed	Depth of top perforation	Depth of bottom perforation	Land-surface elevation	Total number of measurements available[1]	Total number of measurements used for model calibration[2]	Observation site weight for calibration
84	Fresno	13S/20E-17F1	364802119485101	38	280	205	257	[4]321.5	79	79	0.113
85	Chowchilla	12S/15E-33R1	365012120194301	38	38	170	296	[4]162.4	63	63	0.126
86	Madera	12S/18E-31J1	365032120021201	—	252	144	252	[4]256.4	70	70	0.120
87	Chowchilla	12S/14E-34J3	365037120250201	248	248	80	248	152.3	34	33	0.174
88	Madera	12S/19E-28P1	365112119540801	299	299	8	299	[4]307.5	79	79	0.113
89	Madera	12S/16E-26H1	365135120105501	330	314	130	298	[4]202.4	74	73	0.117
90	Chowchilla	12S/15E-22F1	365224120190901	—	350	100	350	[4]165.3	20	20	0.224
91	Madera	12S/18E-19H1	365230120021201	652	530	274	492	253.4	67	67	0.122
92	Chowchilla	12S/16E-17D1	365341120151601	150	150	120	150	[3]183.3	18	18	0.236
93	Chowchilla	11S/14E-36R1	365526120225401	299	294	18	292	[3]151.3	44	44	0.151
94	Madera	11S/19E-33J1	365549119533601	451	294	192	292	[4]331.9	74	74	0.116
95	Chowchilla	11S/15E-29H1	365646120205001	—	350	100	350	[4]159.8	53	53	0.137
96	Madera	11S/20E-18L1	365826119494901	364	328	120	202	[4]391.4	55	48	0.144
97	Chowchilla	11S/15E-14G1	365840120180001	—	174	164	167	177.2	68	67	0.122
98	Chowchilla	11S/14E-09A3	365944120261201	—	243	126	239	[4]138.8	69	59	0.130
99	CCID South	10S/12E-35K1	370051120373601	28	185	75	181	112.3	40	40	0.158
100	CCID South	10S/12E-27K1	370145120382001	—	154	60	150	[4]110.8	15	15	0.258
101	Chowchilla	10S/14E-25K1	370157120231901	183	183	50	183	167.2	41	41	0.156
102	Chowchilla	10S/15E-30J1	370157120215001	418	418	130	412	169.2	31	31	0.180
103	Chowchilla	10S/14E-26H1	370158120240201	145	145	36	124	[3]162.2	39	39	0.160
104	Chowchilla	10S/15E-27D3	370223120193601	—	130	110	130	[3]185.2	123	123	0.090
105	CCID South	10S/12E-13L1	370336120364001	28	200	90	196	112.3	65	65	0.124
106	CCID South	10S/11E-13H1	370351120422801	—	168	78	—	[4]102.7	56	56	0.134
107	CCID South	10S/12E-09P1	370413120394301	180	180	40	152	[3]107.3	106	106	0.097
108	CCID South	10S/13E-09K1	370430120331301	—	178	80	178	117.3	66	65	0.124
109	CCID South	10S/12E-11L1	370428120373401	—	210	73	—	107.3	23	23	0.209
110	CCID South	10S/12E-04P1	370507120394401	219	219	86	219	105.3	26	26	0.196
111	CCID South	10S/12E-05Q1	370509120403401	210	28	60	204	[4]105.3	27	26	0.196

Table B-2. Well information for selected wells from the California Department of Water Resources (CDWR) and U.S. Geological Survey (USGS) databases used in model calibration for the San Joaquin River Restoration Project area, Fresno, Madera, and Merced Counties, California.—Continued

[See figure 28 for locations [San Joaquin River Restoration Program groundwater flow model (SJRRPGW) identification numbers] of wells. U.S. Geological Survey (USGS) identification number: the unique number for each site in USGS NWIS (National Water Information System) database. Depths in feet below land surface. Land-surface elevation in feet above sea level, which refers to the National American Vertical Datum of 1988 (NAVD 88); obtained from California Department of Water Resources (DWR) and USGS databases unless otherwise noted. **Abbreviations**: —, no data.]

SJRRPGW identification number	Calibration well group	State well number	USGS site identification number	Depth drilled	Depth completed	Depth of top perforation	Depth of bottom perforation	Land-surface elevation	Total number of measurements available[1]	Total number of measurements used for model calibration[2]	Observation site weight for calibration
112	CCID South	9S/12E-32N1	370553120411901	210	210	69	206	[4]100.3	71	71	0.119
113	Merced	9S/14E-33R1	370606120261101	—	[5]158	101	—	[4]159.7	31	30	0.183
114	CCID North	9S/11E-29R1	370650120465101	—	180	80	180	92.4	29	29	0.186
115	Merced	9S/13E-27M1	370713120322801	359	359	178	359	122.3	18	18	0.236
116	Merced	9S/13E-11K1	370939120304901	—	324	80	320	133.3	49	35	0.169
117	CCID North	9S/10E-12M1	370942120494401	160	160	45	138	[4]87.5	24	24	0.204
118	Merced	9S/13E-05M1	371043120344701	305	290	110	290	116.3	25	23	0.209
119	Merced	8S/12E-15A1	371438120375901	296	254	125	240	110.4	24	24	0.204
120	Merced	8S/12E-06G1	371607120414101	248	243	120	243	102.4	22	22	0.213
121	Merced	7S/11E-21P1	371818120462101	—	[5]185	84	—	[4]97.4	32	32	0.177
122	CCID North	7S/8E-23R1	371832121030701	350	341	90	337	108.5	59	58	0.131
123	CCID North	7S/9E-23M1	371828120572301	—	101	97	100	[4]70.8	28	28	0.189
124	CCID North	7S/9E-24L1	371829120555501	—	100	97	100	64.4	25	25	0.200
125	CCID North	7S/8E-13N2	371916121024401	—	360	85	355	109.5	40	39	0.160
126	CCID North	7S/8E-14E1	371939121035401	—	29	80	195	[4]127.7	72	72	0.118
127	CCID North	7S/8E-13D1	371958121023901	—	398	90	393	107.5	44	43	0.152
128	Merced	7S/11E-08P1	372006120472201	170	168	72	168	98.4	23	23	0.209
129	Merced	7S/9E-12K1	372008120554901	—	148	48	148	[4]67.4	38	38	0.162
130	Merced	7S/10E-07L1	372007120545101	—	124	—	—	[4]73.4	55	55	0.135
131	CCID North	7S/8E-12D1	372040121024501	429	425	100	415	108.5	27	27	0.192
132	Merced	7S/10E-04Q1	372251120522501	215	210	60	150	84.4	44	44	0.151
133	Merced	6S/10E-19G1	372358120543001	—	170	—	—	76.4	21	21	0.218

[1]From April 1961 to September 2003.

[2]Excludes measurements identified as outliers.

[3]Value from USGS NWIS database.

[4]Most recent value from DWR database converted from NGVD29 (National Geodetic Vertical Datum of 1929) to NAVD88 using difference between NGVD29 and NAVD88 land-surface elevation in USGS NWIS database.

[5]Information uncertain.

Appendix C. Calibration Results

This appendix shows the relation between the simulated and observed groundwater elevations at all 113 calibration wells (fig. C-1) and the simulated and observed streamflow at all 19 calibration streamgages (fig. C-2). Differences between observed and simulated groundwater elevations are expected in a calibrated groundwater model. Overall, the simulated groundwater-level elevations and trends and surface-water flow magnitudes and trends reasonably matched observed data for a regional model of this scale.

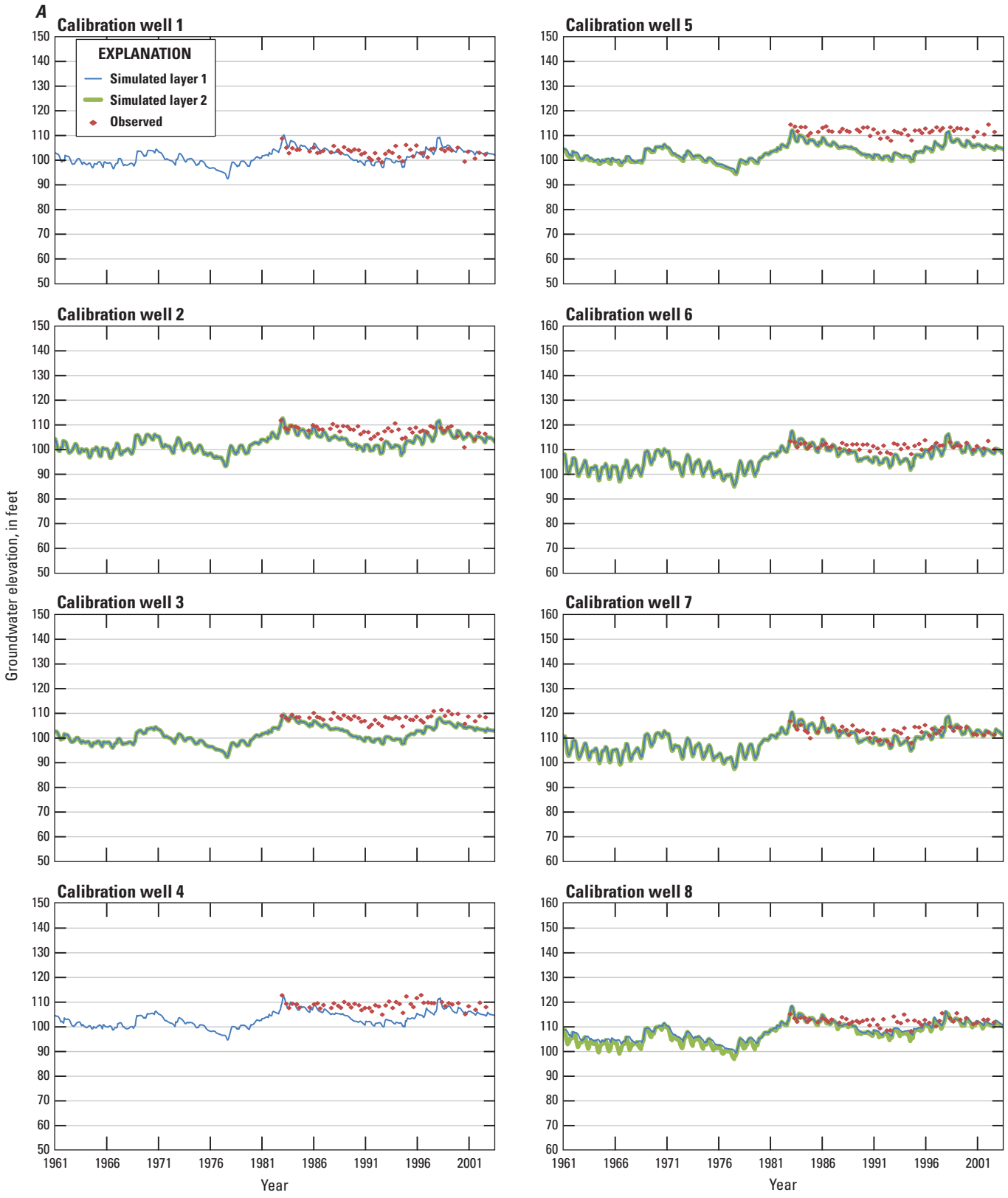

Figure C-1. Hydrographs showing simulated and observed groundwater elevations at each calibration well in the San Joaquin valley, 1961–2001: *A*, calibration wells 1–8; *B*, calibration wells 9–16; *C*, calibration wells 17–24; *D*, calibration wells 25–32; *E*, calibration wells 33–40; *F*, calibration wells 41–48; *G*, calibration wells 49–56; *H*, calibration wells 57–64; *I*, calibration wells 65–72; *J*, calibration wells 73–80; *K*, calibration wells 81–88; *L*, calibration wells 89–96; *M*, calibration wells 97–104; *N*, calibration wells 105–112; *O*, calibration wells 113–120; *P*, calibration wells 121–128; *Q*, calibration wells 129–133.

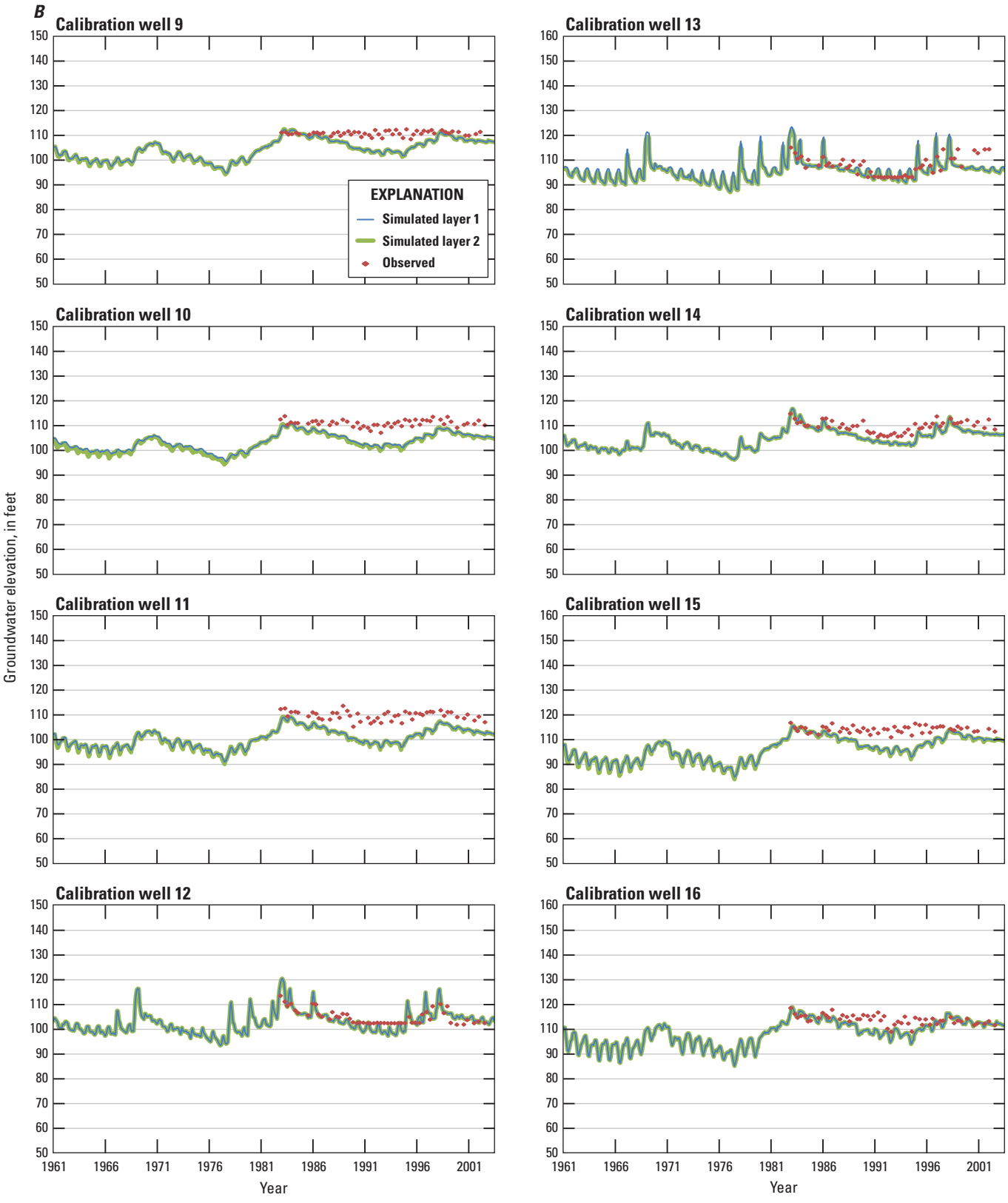

Figure C-1. —Continued

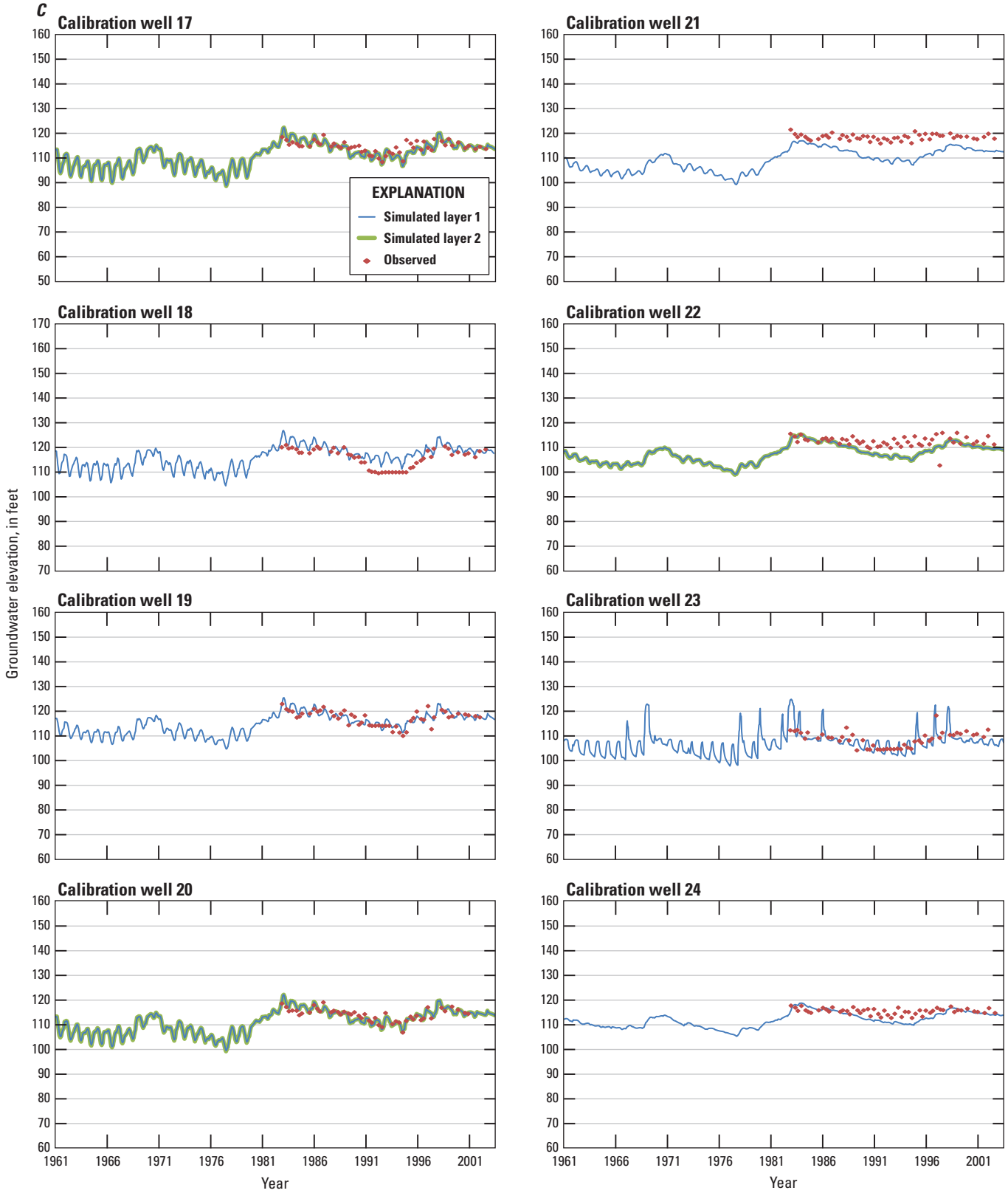

Figure C-1. —Continued

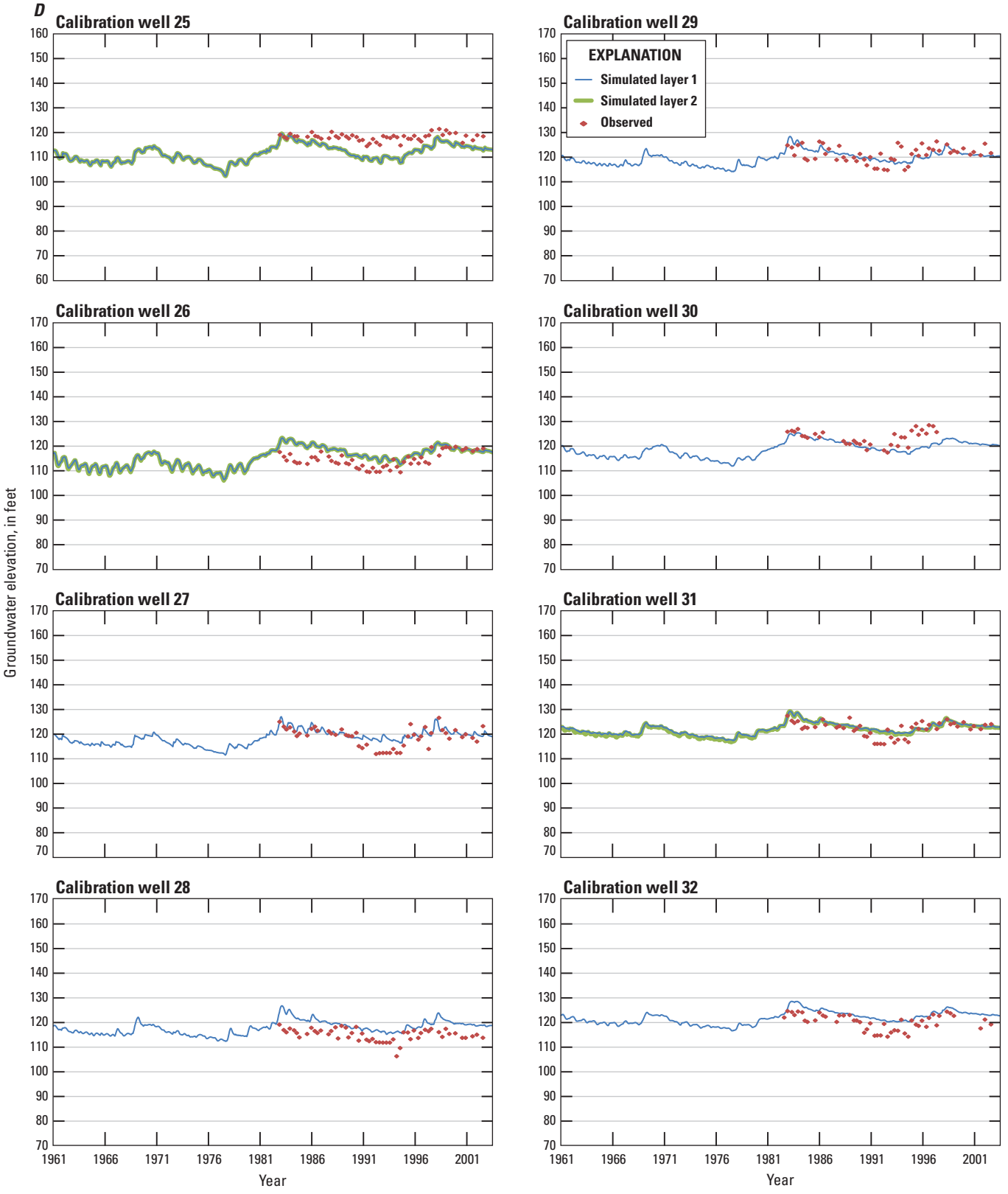

Figure C-1. —Continued

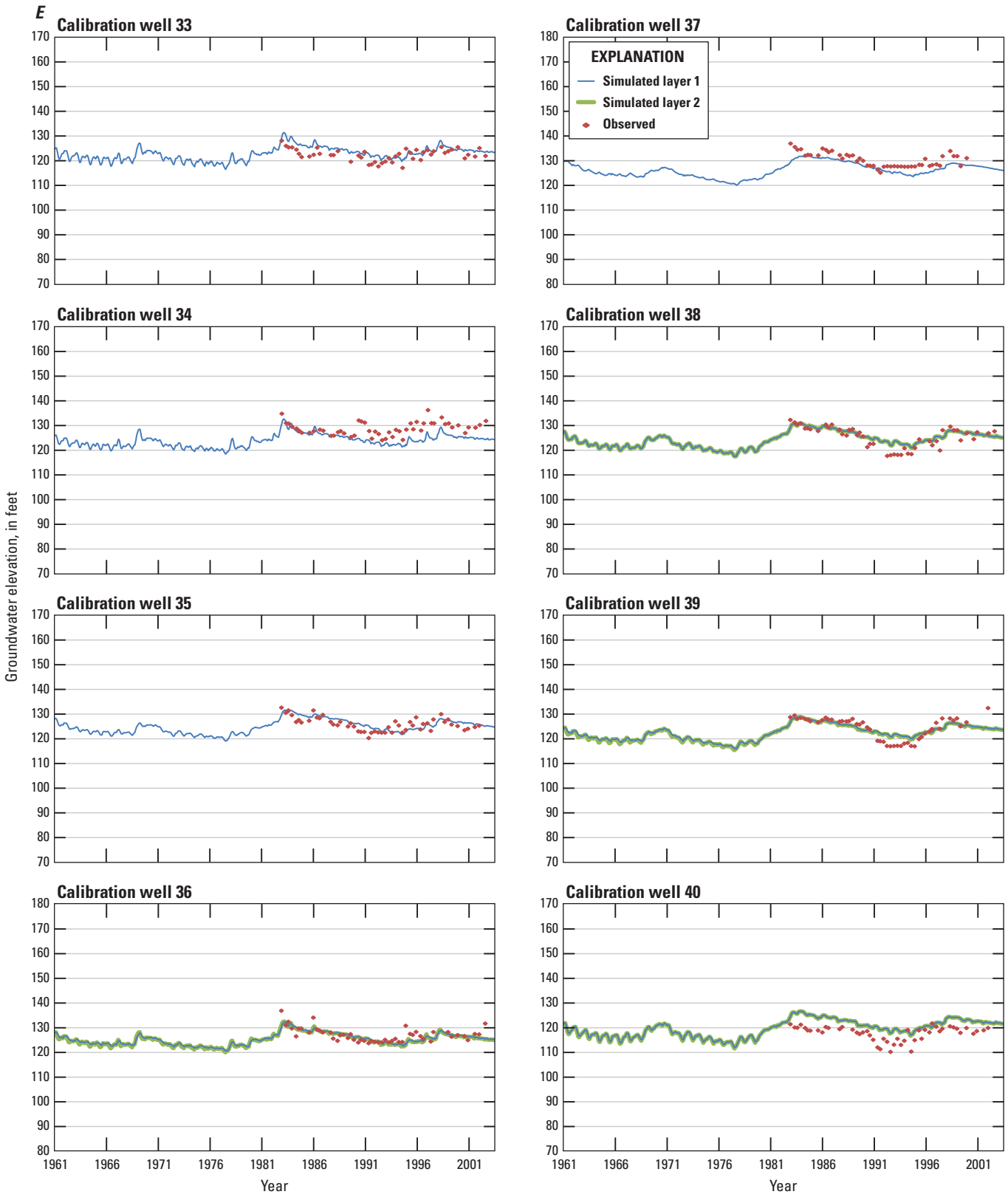

Figure C-1. —Continued

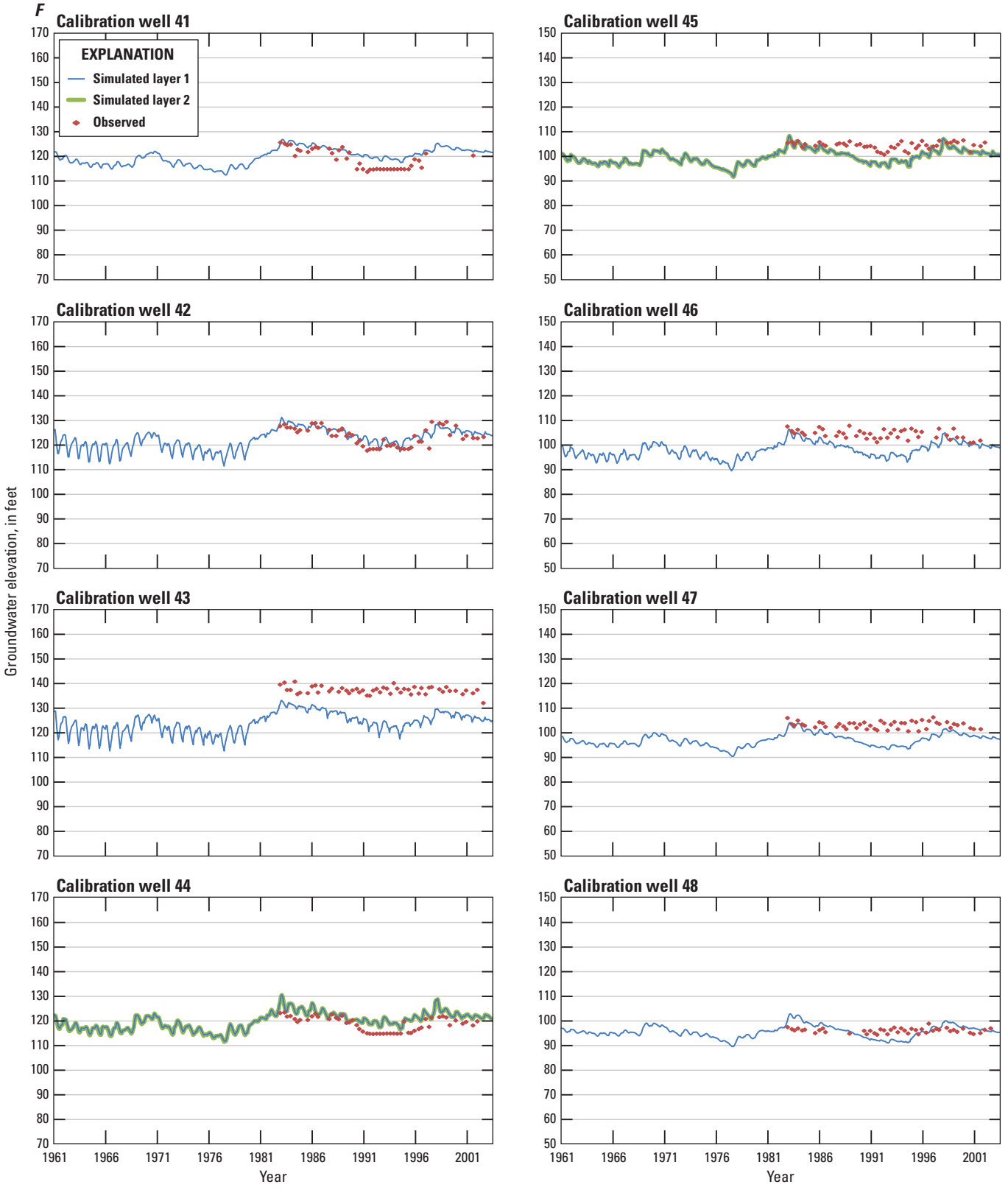

Figure C-1. —Continued

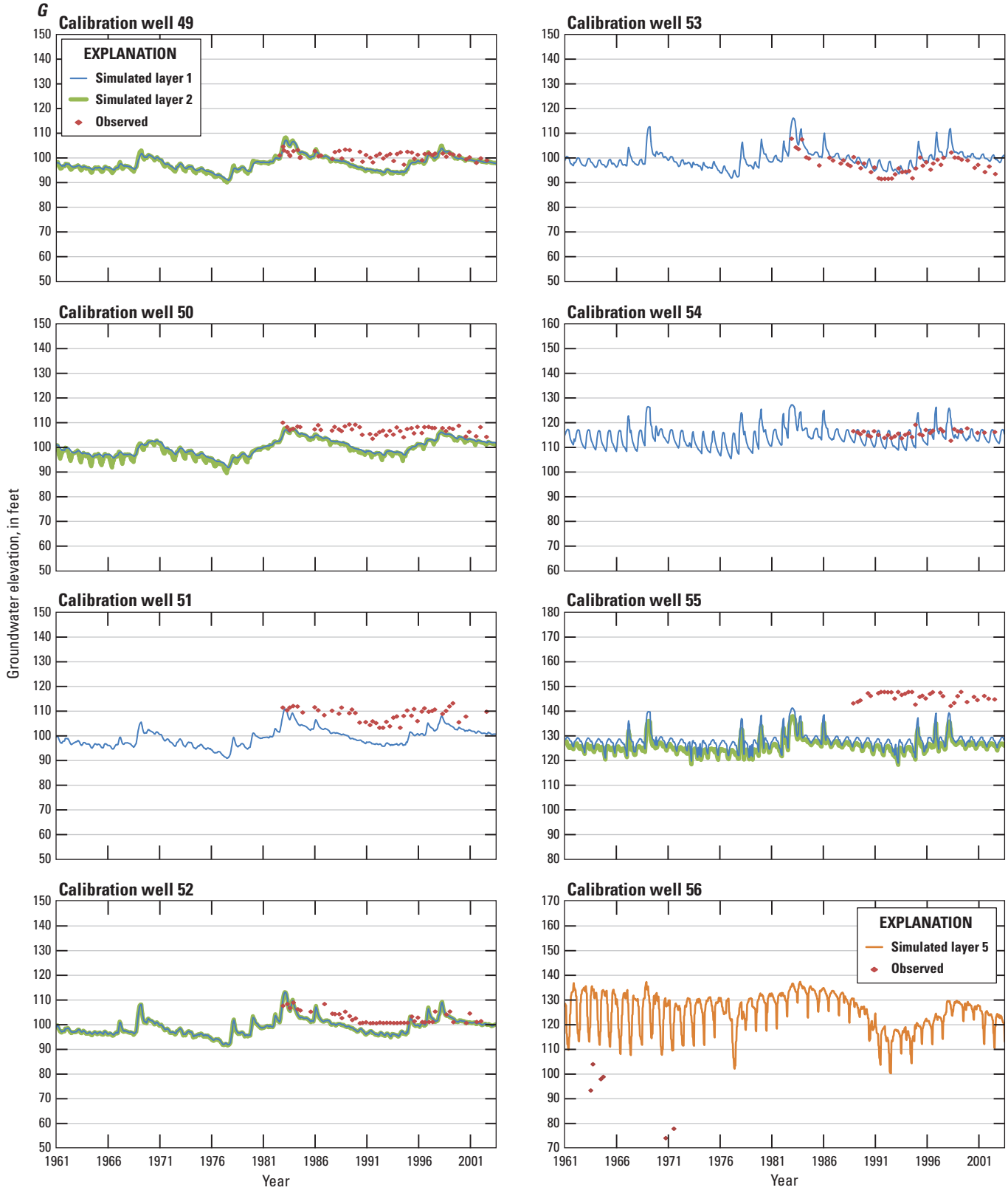

Figure C-1. —Continued

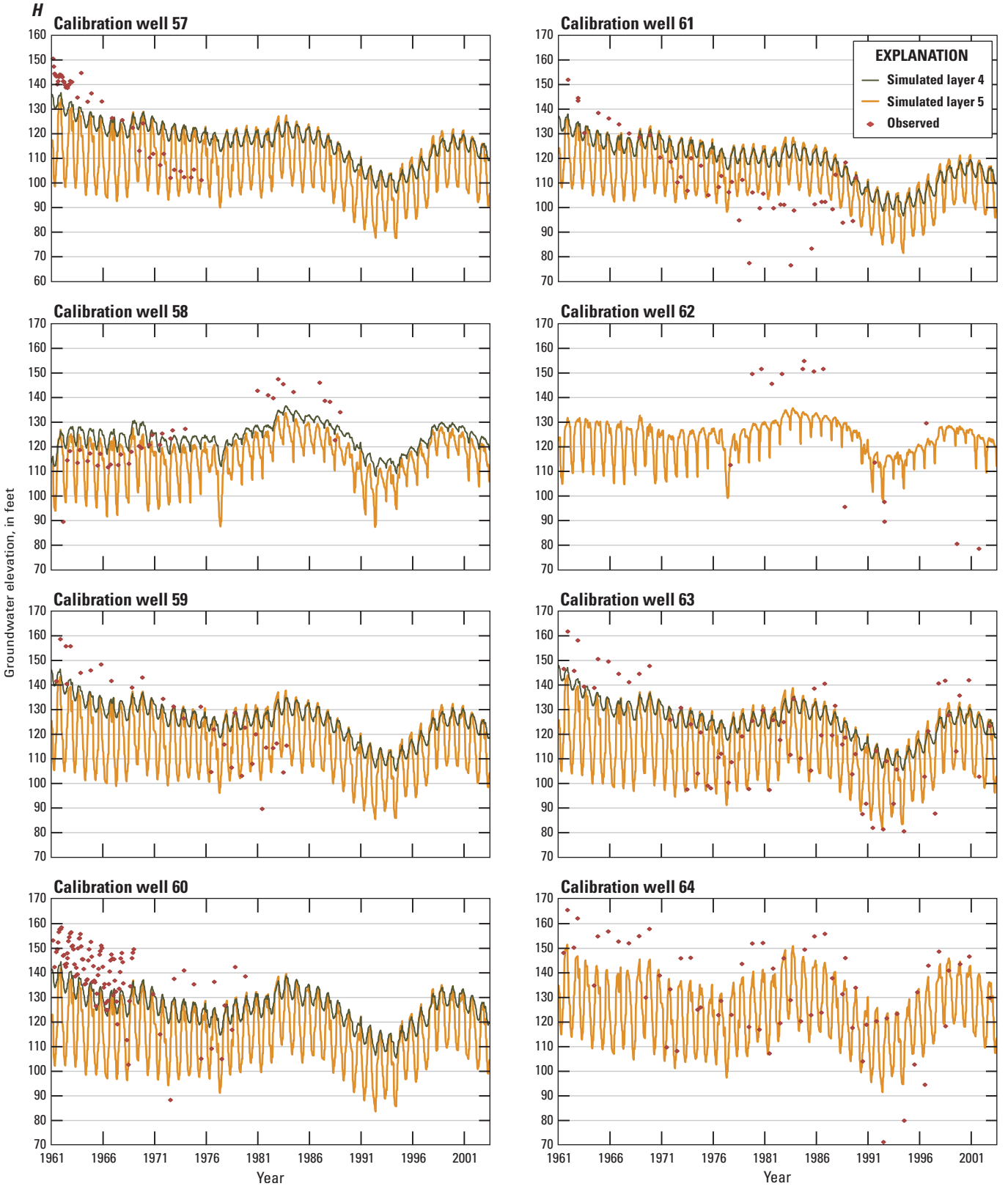

Figure C-1. —Continued

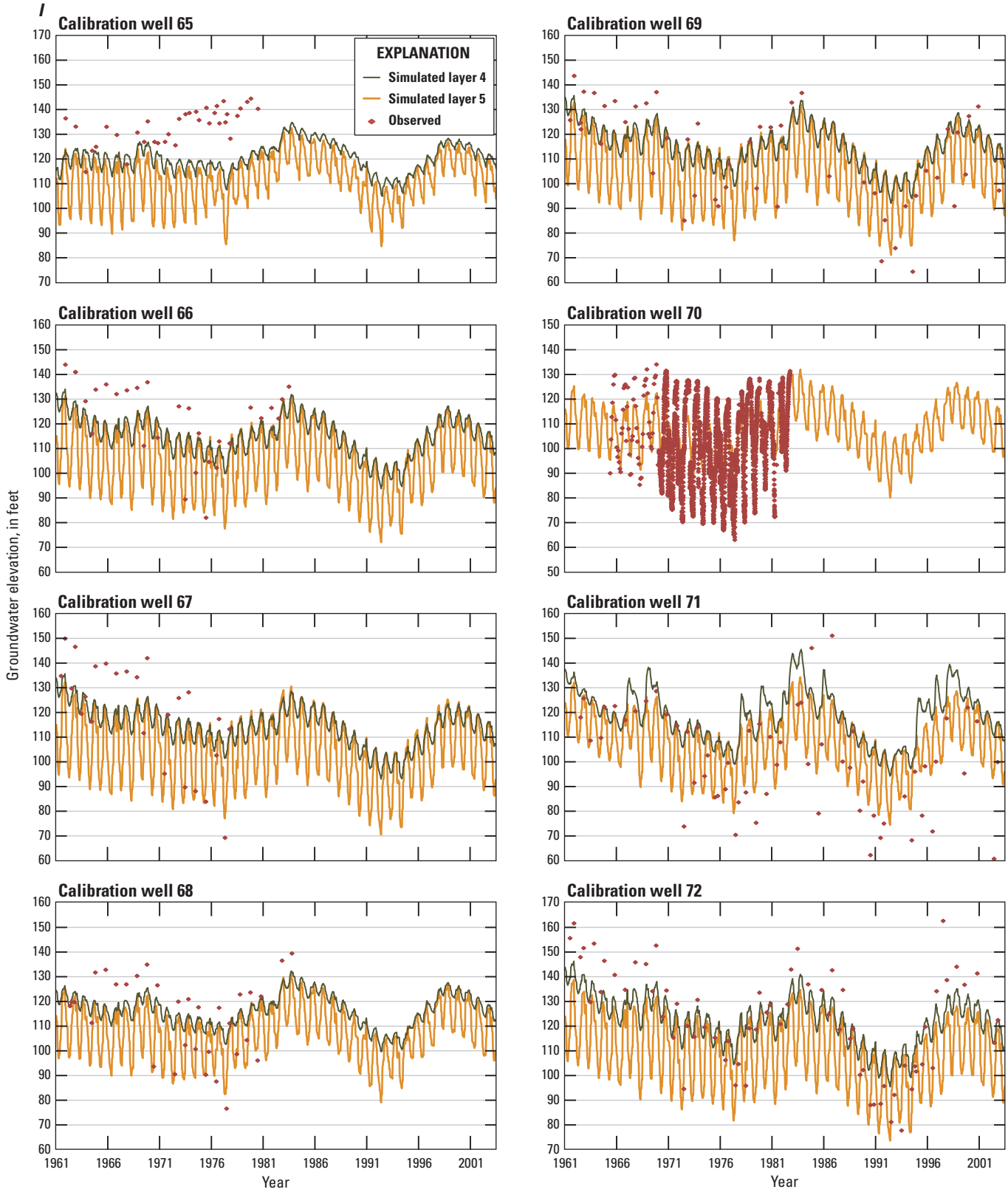

Figure C-1. —Continued

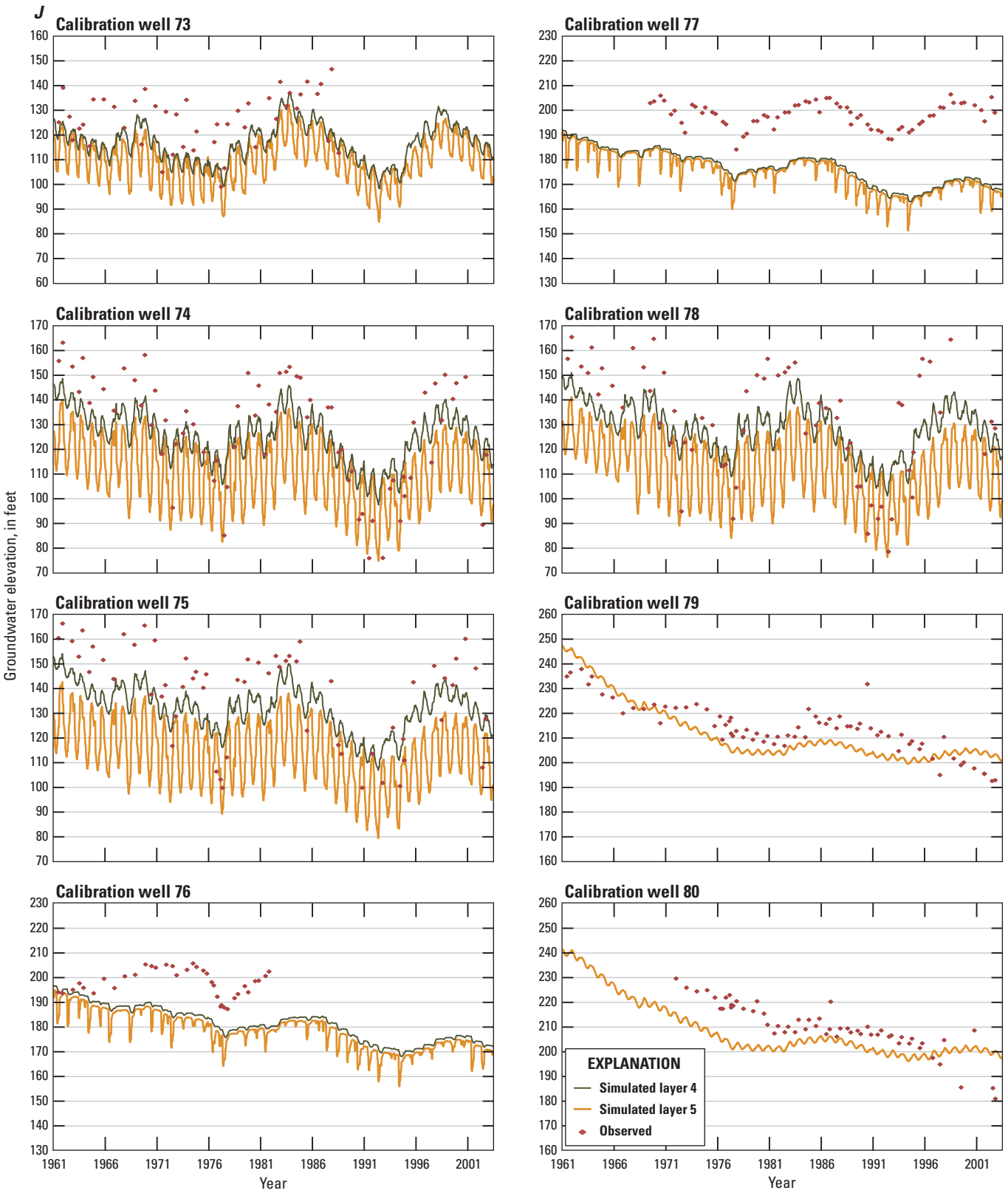

Figure C-1. —Continued

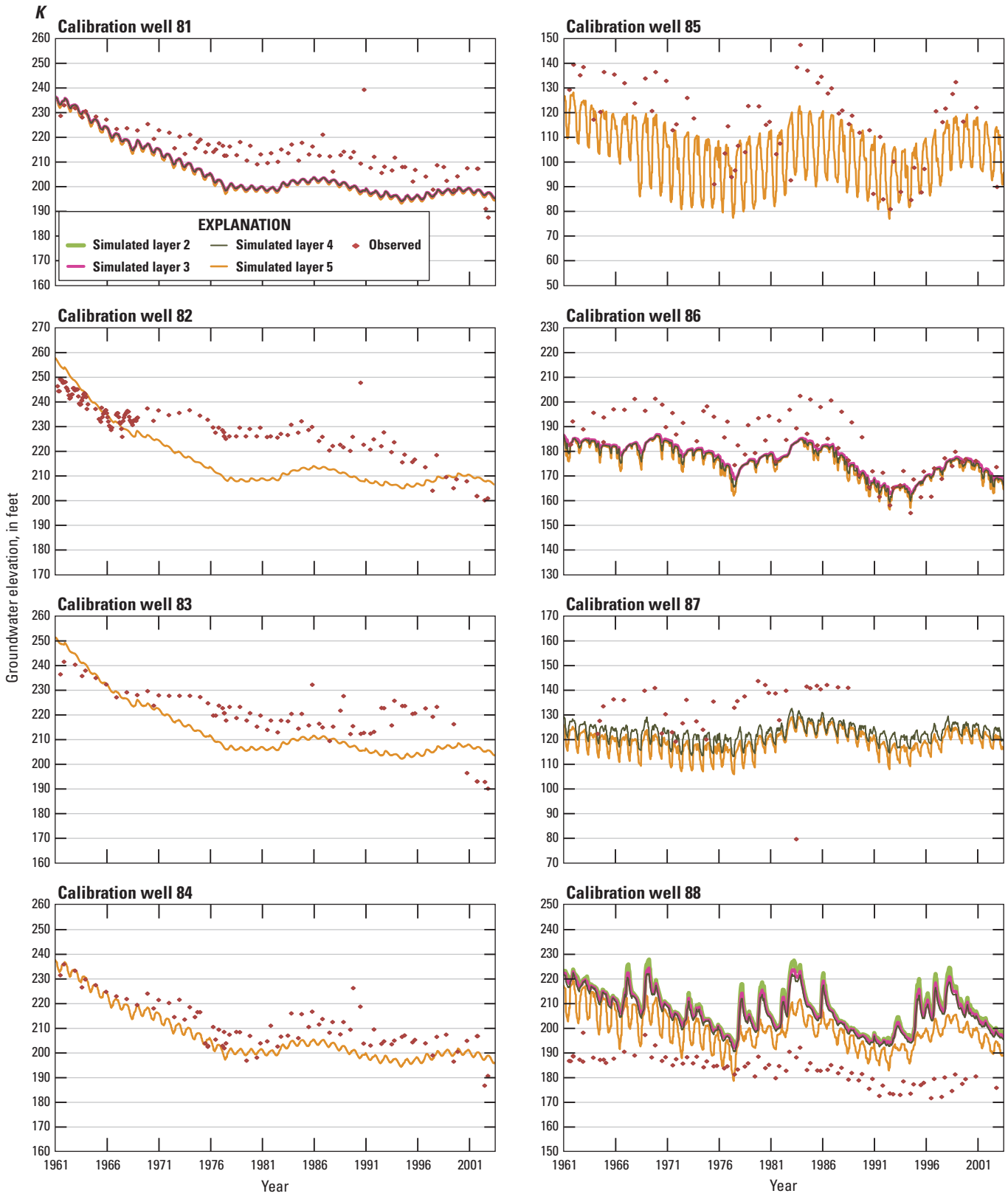

Figure C-1. —Continued

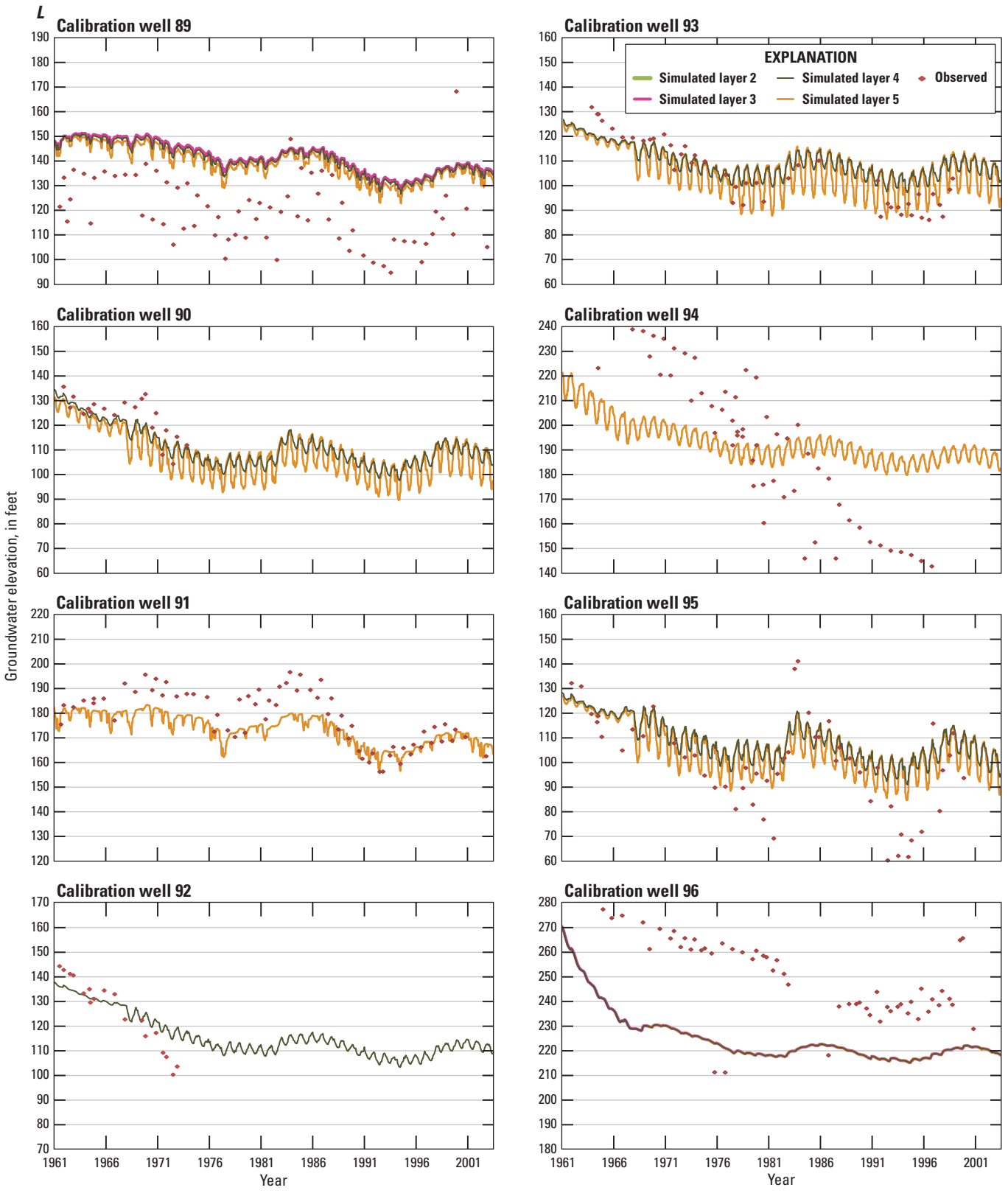

Figure C-1. —Continued

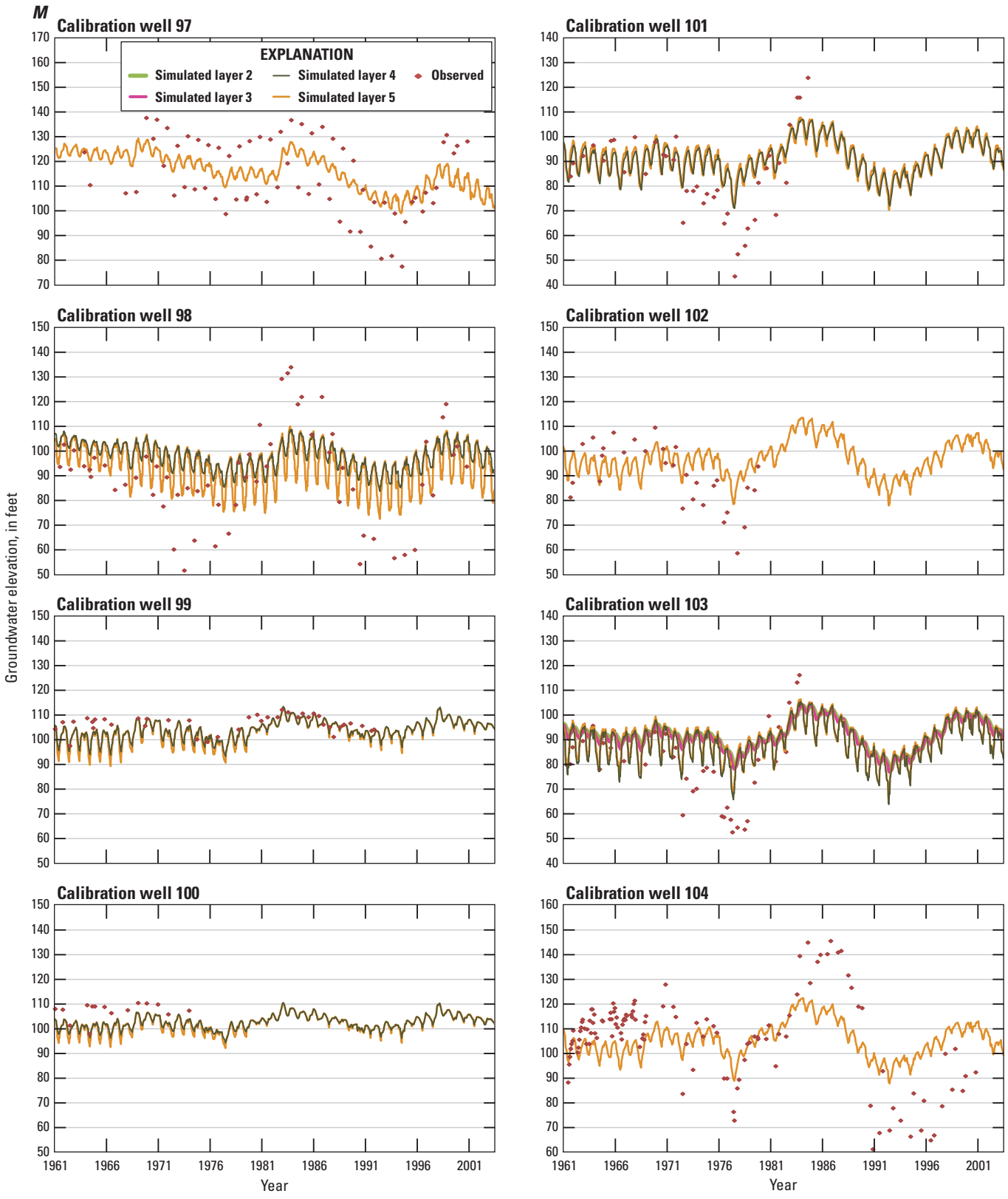

Figure C-1. —Continued

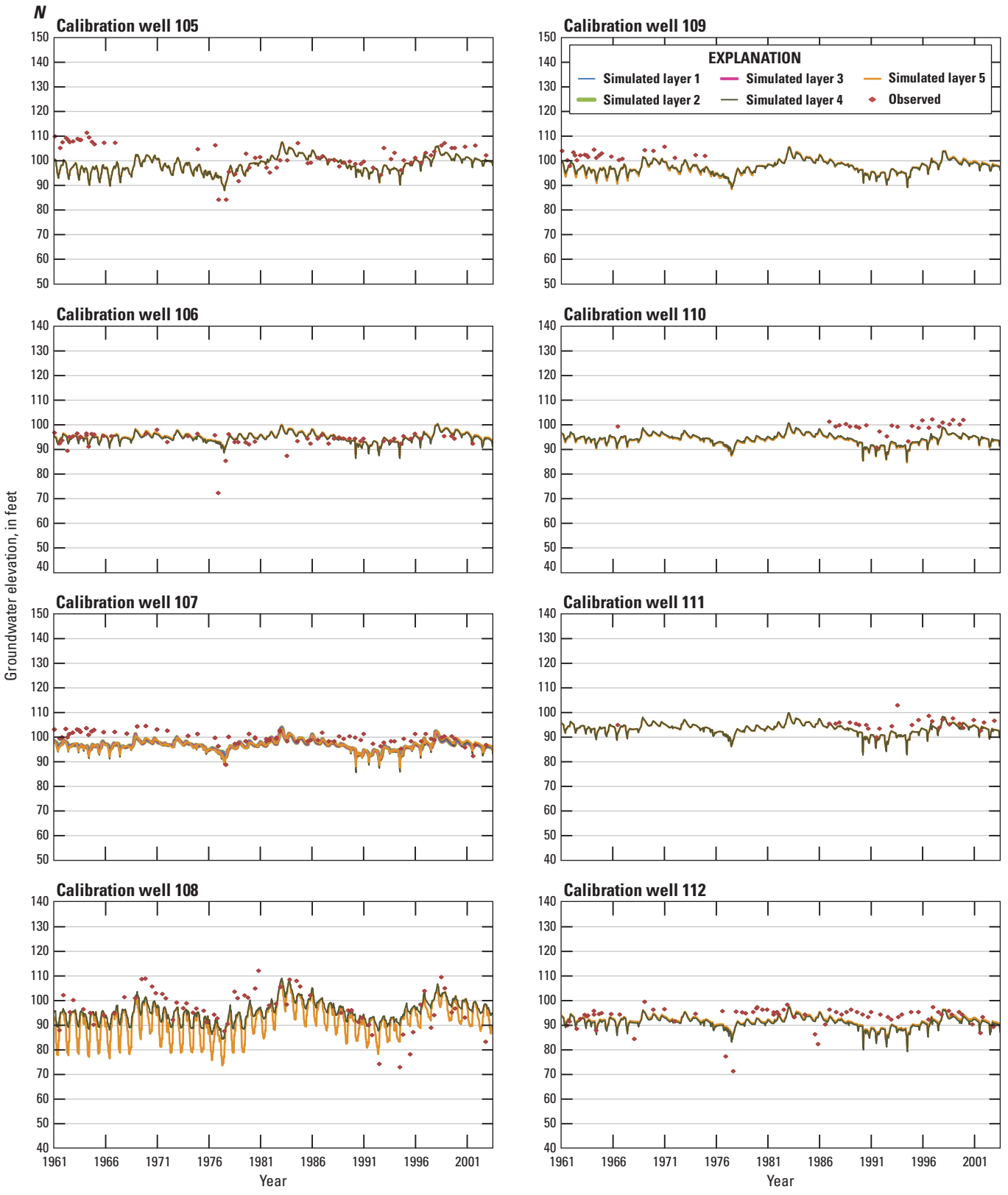

Figure C-1. —Continued

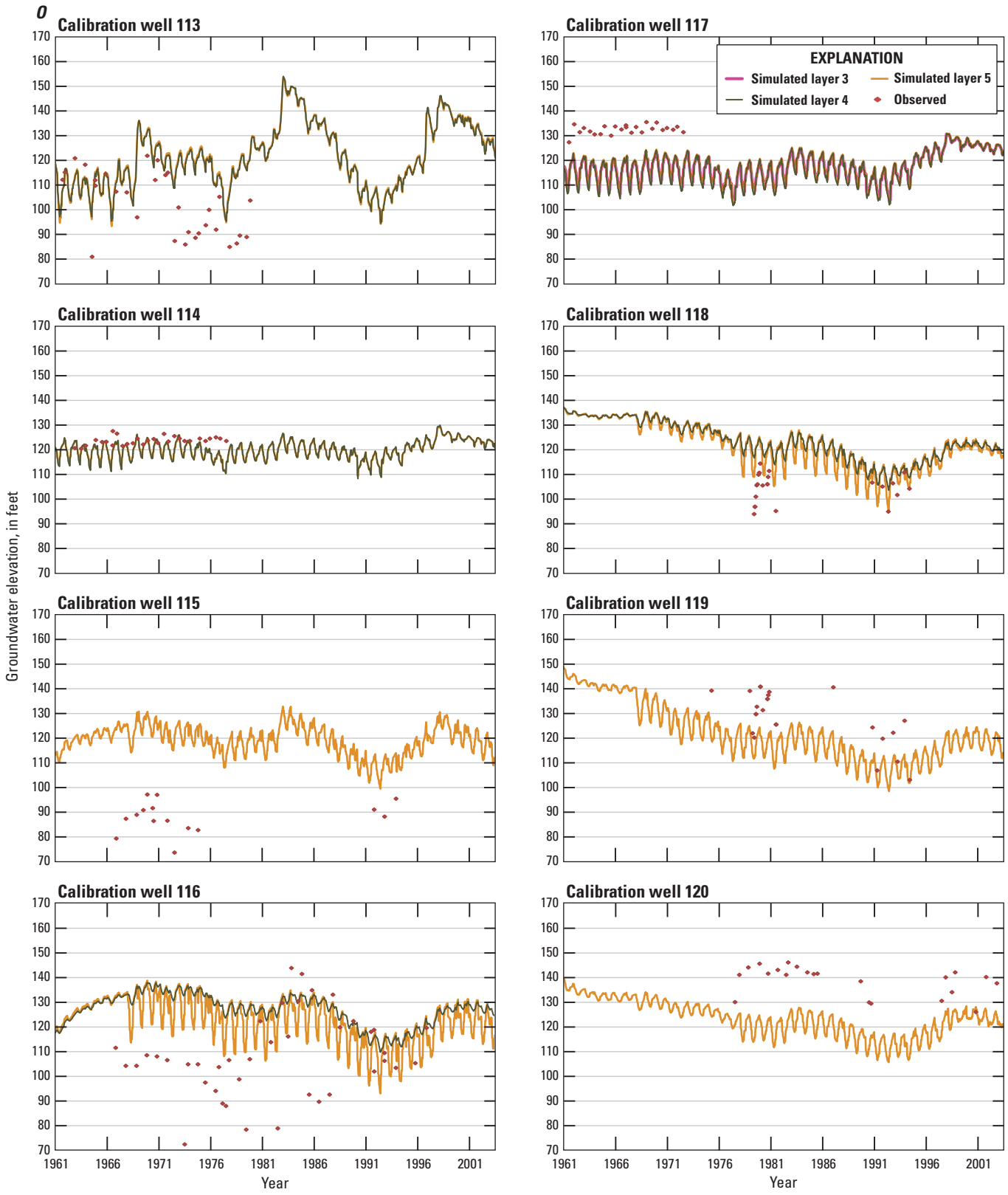

Figure C-1. —Continued

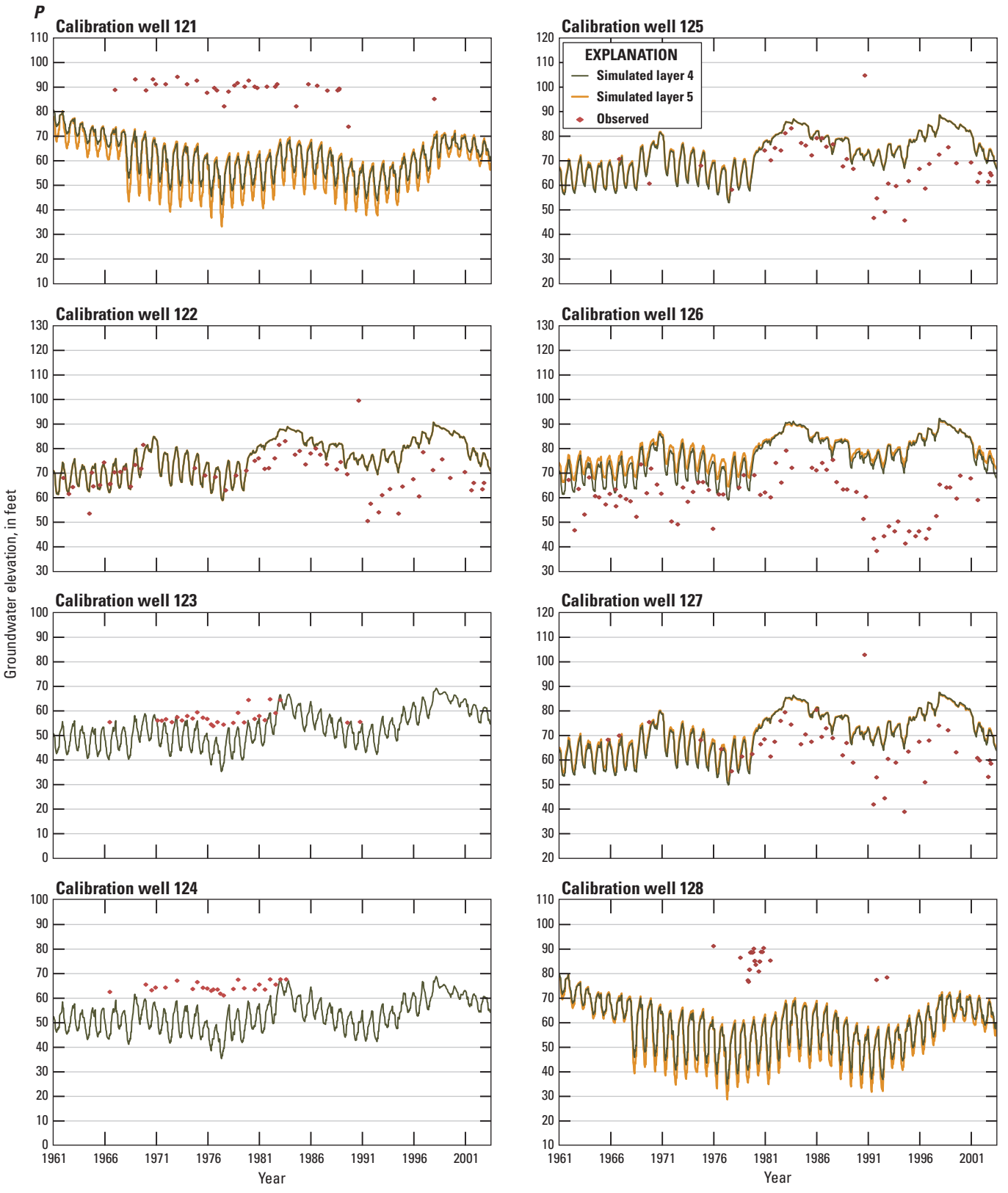

Figure C-1. —Continued

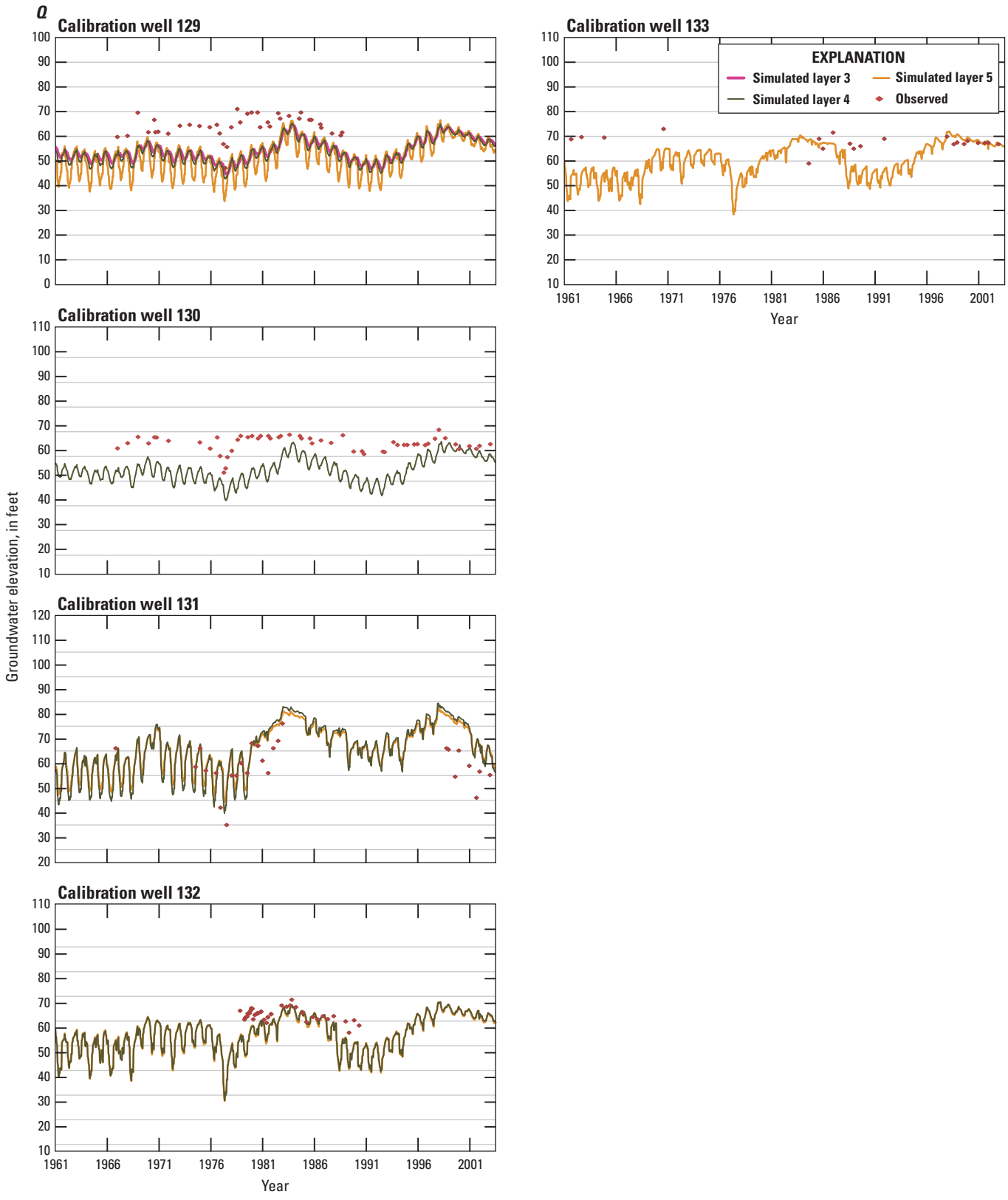

Figure C-1. —Continued

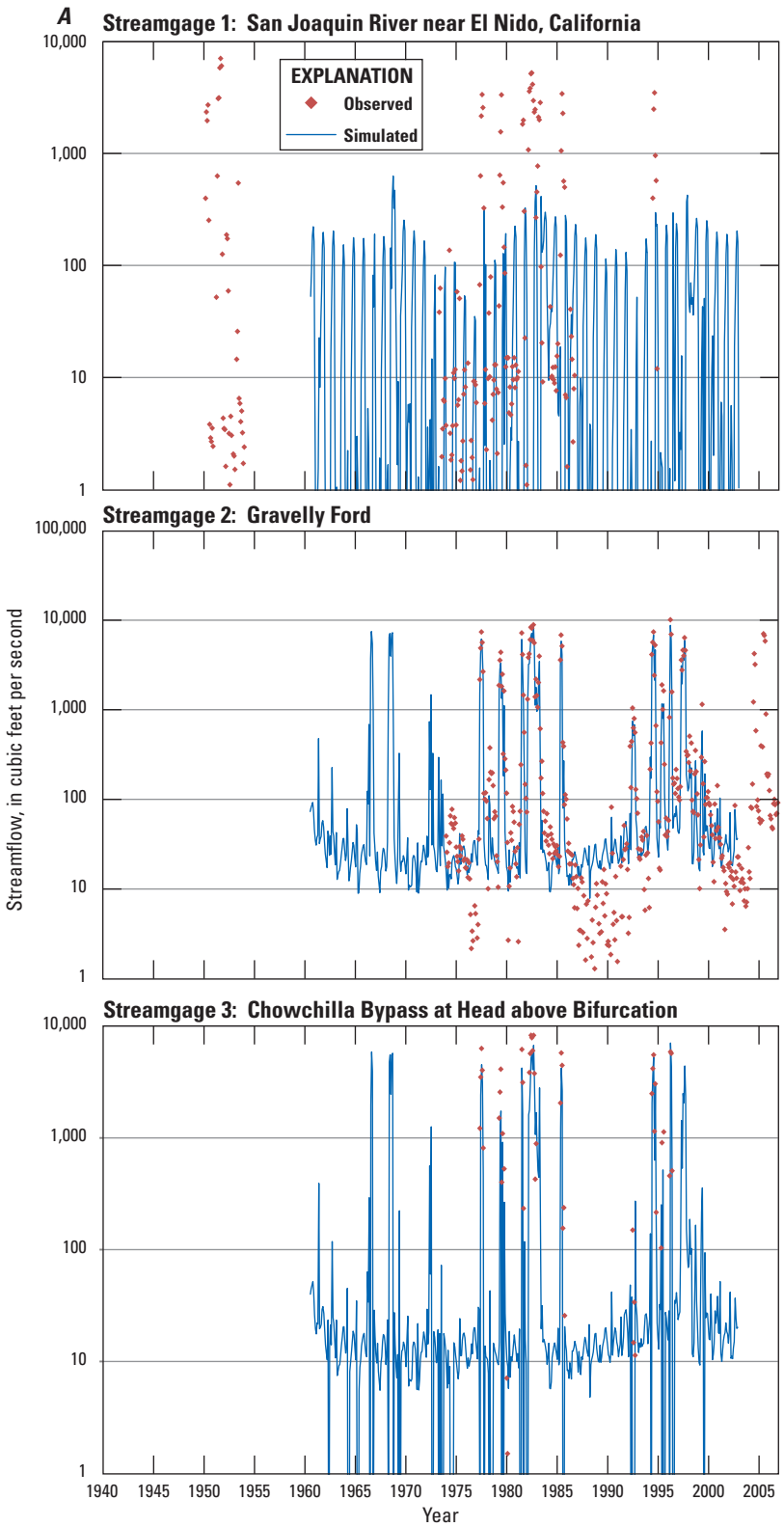

Figure C-2. Hydrographs showing differences between simulated and observed streamflow at all 19 calibration streamgages in the San Joaquin valley, 1940–2005: *A*, San Joaquin River (SJR) near El Nido, Gravelly Ford, and Chowchilla Bypass at Head above Bifurcation; *B*, SJR below Bifurcation, SJR near Mendota, and SJR near Dos Palos; *C*, Eastside bypass near El Nido, SJR near El Nido, and Eastside Bypass below Mariposa Bypass; *D*, Bear Creek below Eastside Canal, SJR near Stevinson, and Salt Slough at Highway 165 near Stevinson; *E*, SJR at Fremont Ford Bridge, Mud Slough near Gustine, and Merced River near Stevinson; *F*, SJR near Newman, Donney Bridge, and Mariposa Bypass near Crane Ranch; *G*, SJR near Crows Landing. [**Abbreviations**: USBR, U.S. Bureau of Reclamation; USGS, U.S. Geological Survey]

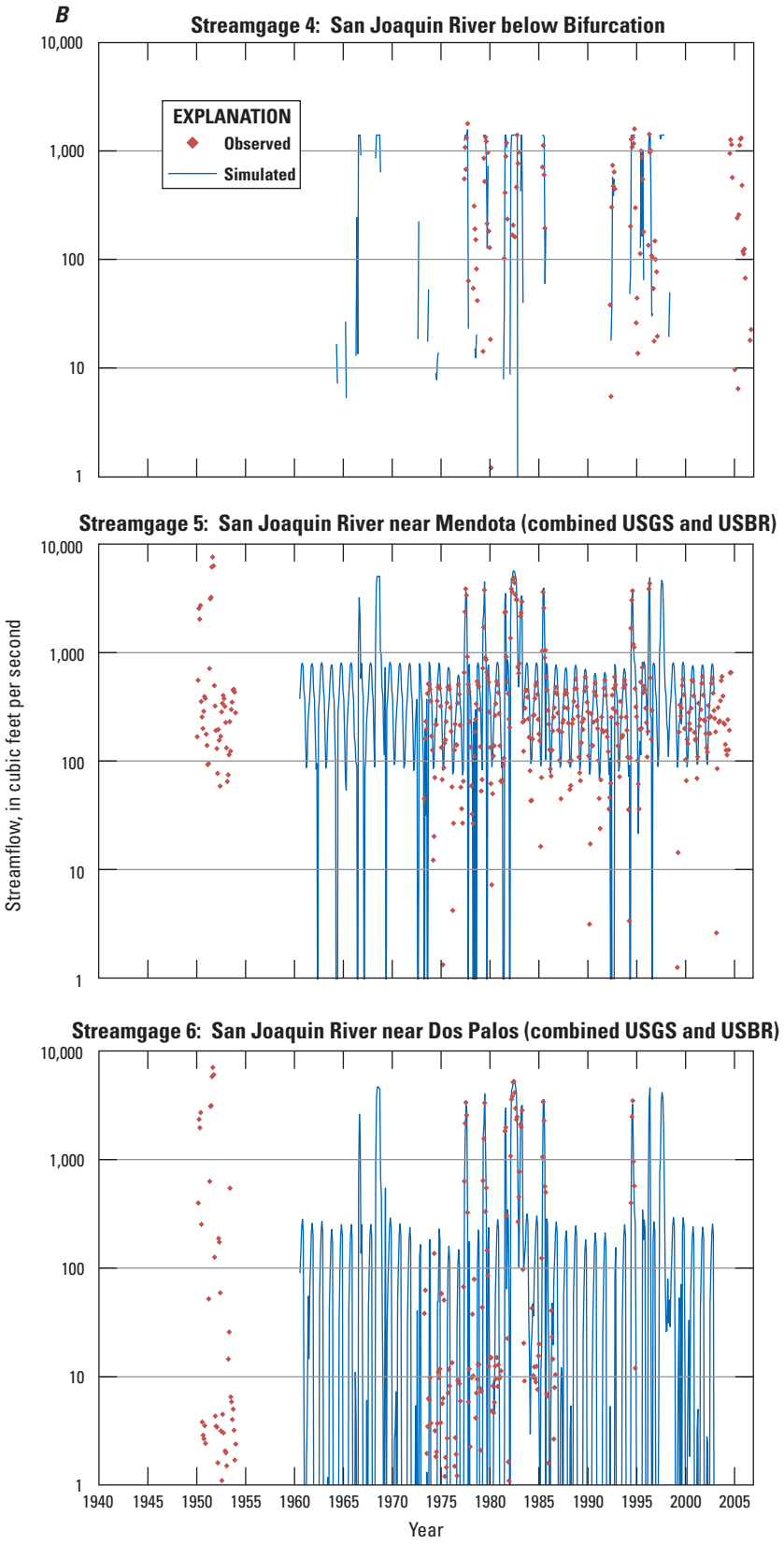

Figure C-2. —Continued

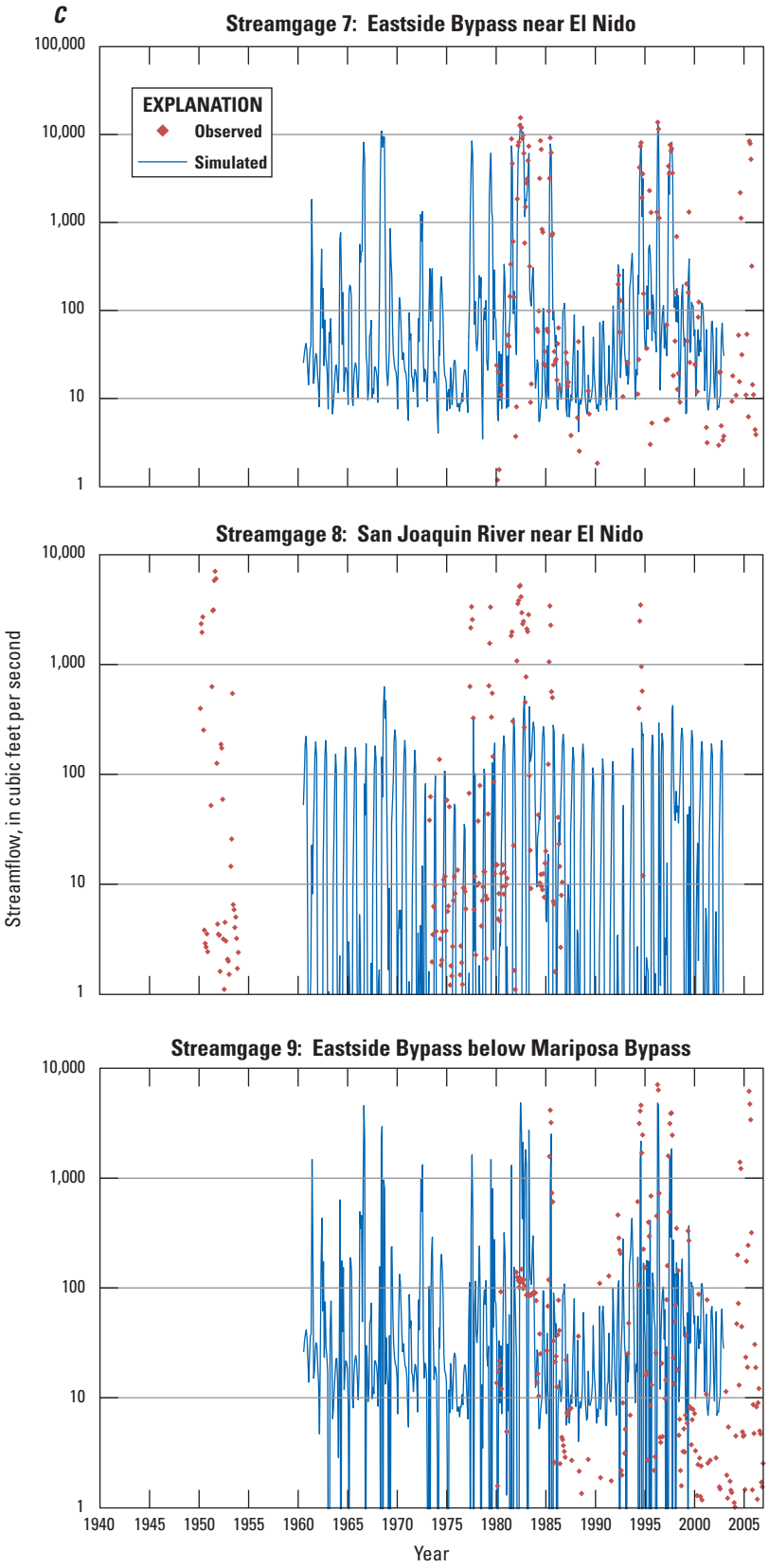

Figure C-2. —Continued

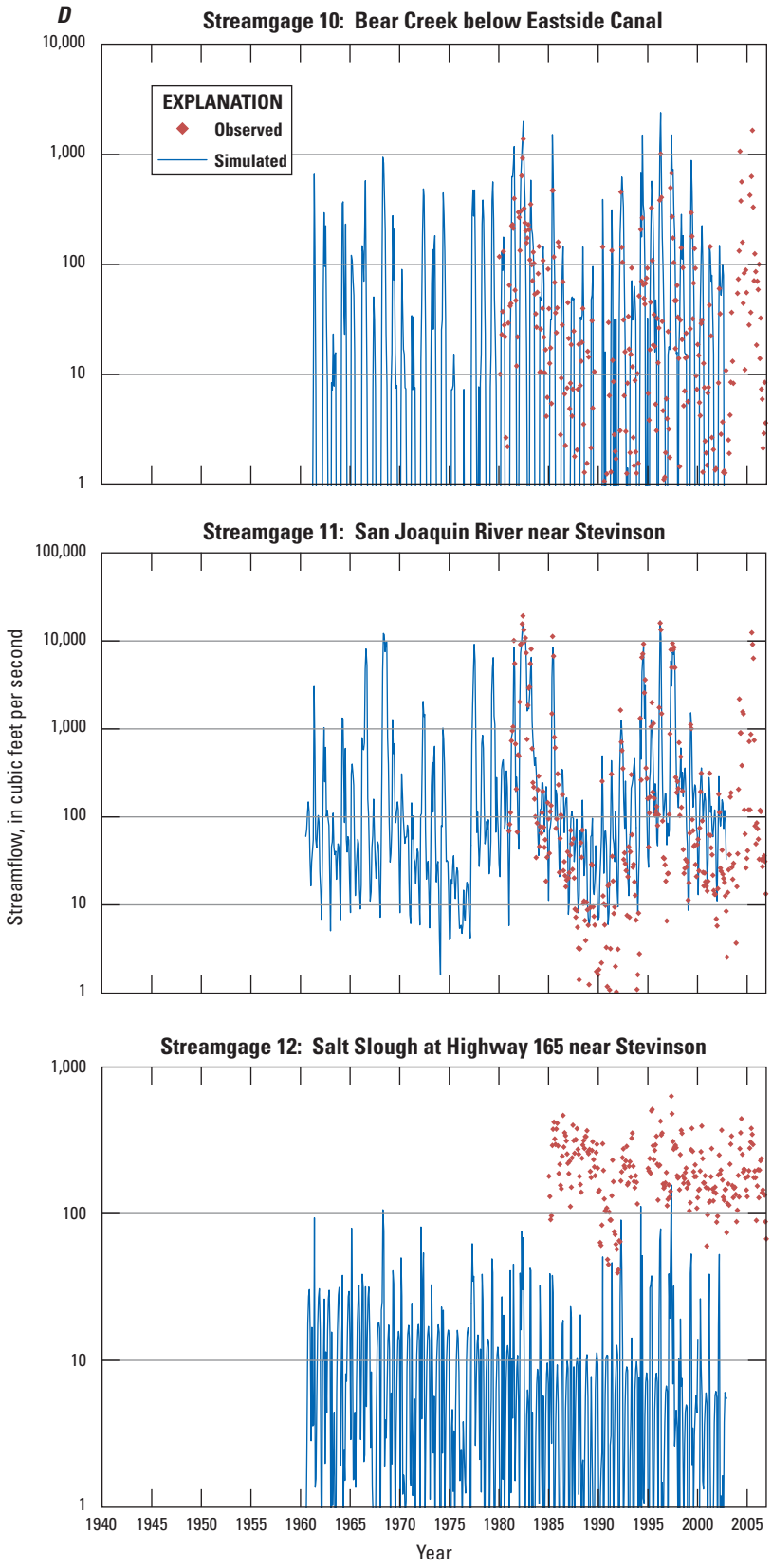

Figure C-2. —Continued

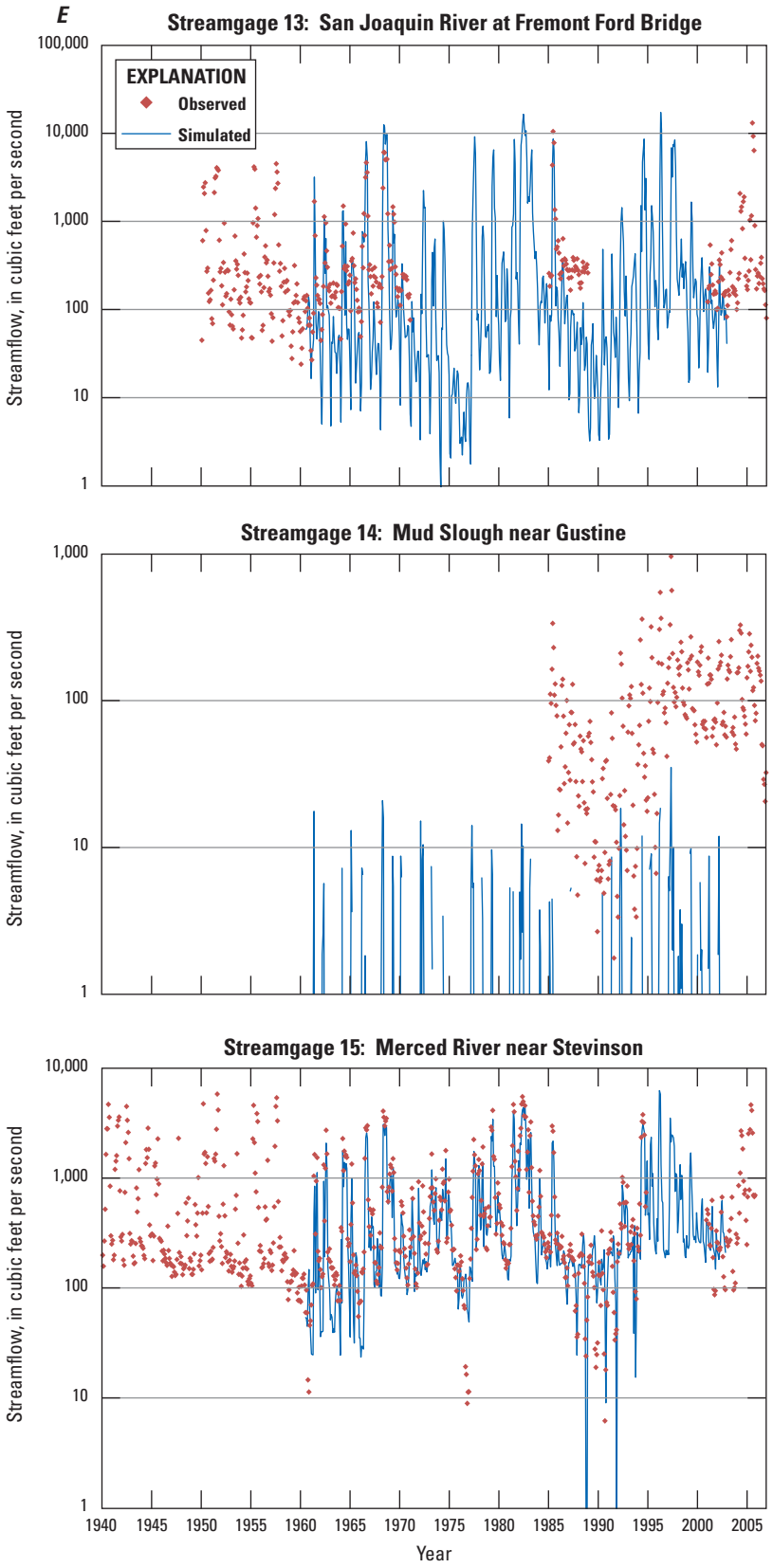

Figure C-2. —Continued

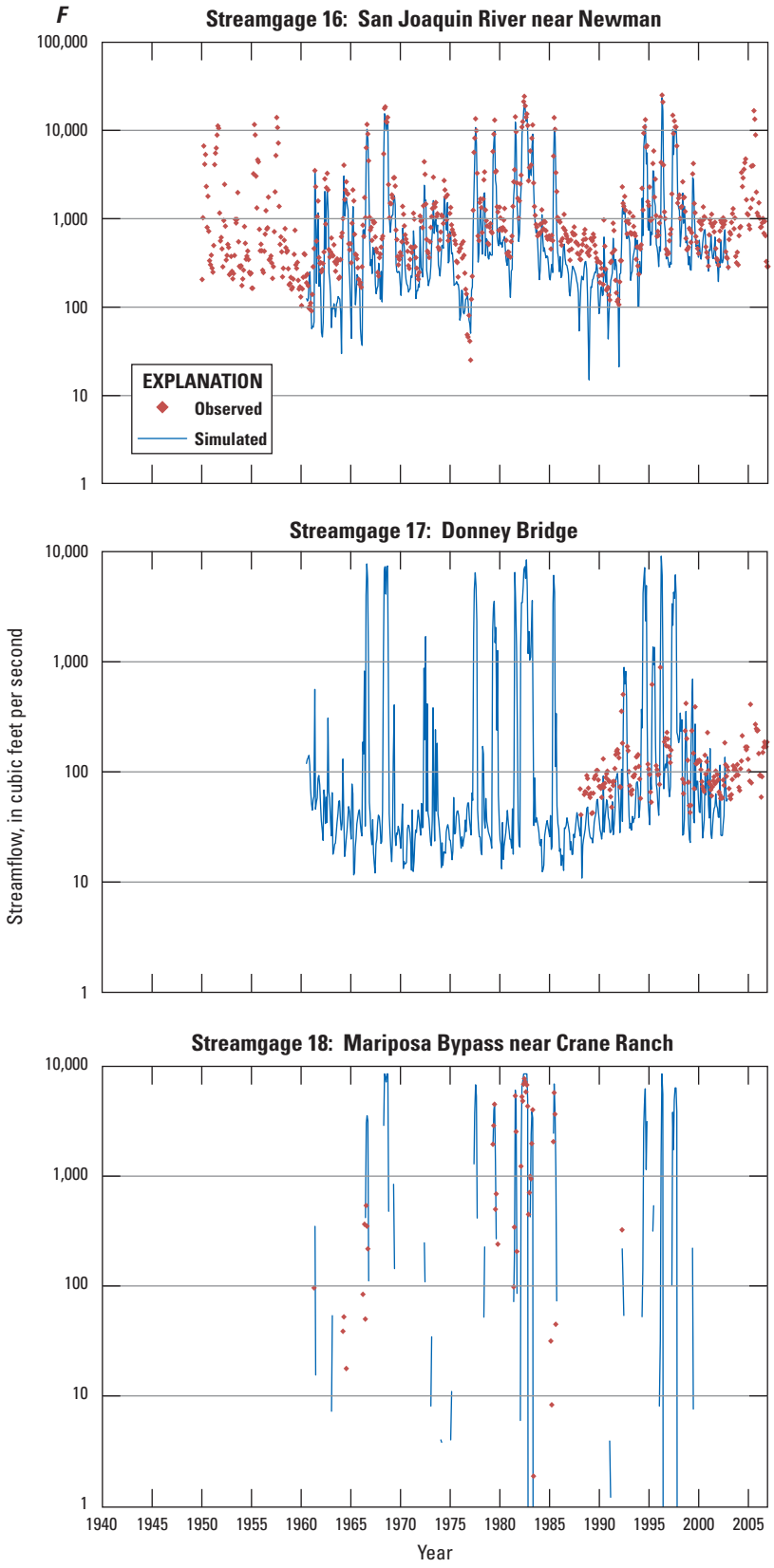

Figure C-2. —Continued

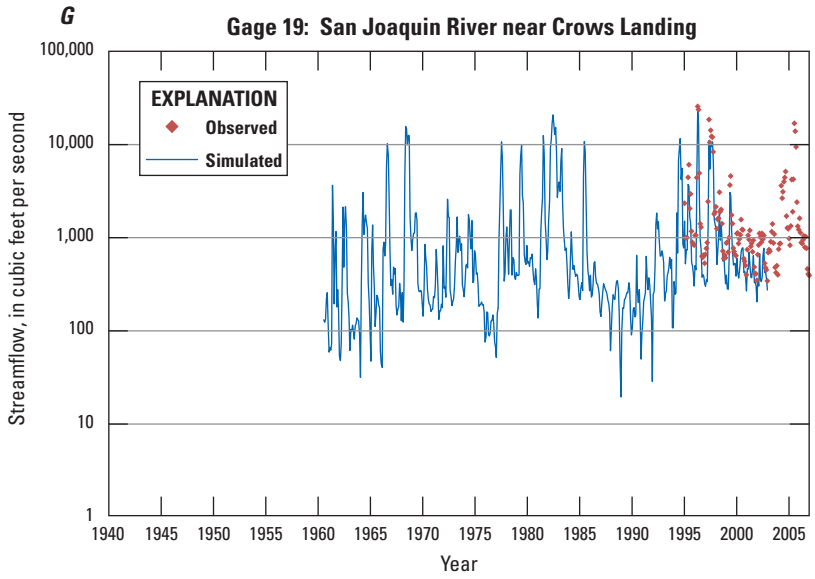

Figure C-2. —Continued

Prepared by the Sacramento Publishing Service Center.

For more information concerning this report, contact:

Director
U.S. Geological Survey
California Water Science Center
6000 J Street, Placer Hall
Sacramento, CA 95829

or visit our Web site at:
http://ca.water.usgs.gov

ISSN 2328-0328 (online)
http://dx.doi.org/10.3133/sir20145148